Public Safety and Emergency Preparedness Canada
Critical Infrastructure Protection and Emergency Preparedness

Sécurité publique et Protection civile Canada
Protection des infrastructures essentielles et Protection civile

Assessment and Prediction of Prairie Severe Thunderstorm Weather Phenomena

Acknowledgements

This publication has been prepared for:

Public Safety and Emergency
Emergency Preparedness Canada

2nd Floor, Jackson Bldg.
122 Bank St.
Ottawa, ON K1A 0W6
Tel: (613) 944-4875
Toll Free: 1-800-830-3118
Fax: (613) 998-9589
Email: communications@ocipep-bpiepc.gc.ca
Internet: www.ocipep-bpiepc.gc.ca

Authors:

G.S. Strong, Ph.D. and C.D. Smith, M.Sc.

This material is based upon work supported by the Division of Research and Development (DRD) in the Office of Critical Infrastructure Protection and Emergency Preparedness (OCIPEP), under Contract Reference No. 2000D023. OCIPEP is now a part of Public Safety and Emergency Preparedness Canada (PSEPC). Any opinions, findings, and conclusions or recommendations expressed in this material are those of the author(s) and do not necessarily reflect the views of Public Safety and Emergency Preparedness Canada.

Catalogue No.: D82-89/2003E-PDF
ISBN: 0-662-35697-7

Abstract

The goal of this study is to review our current understanding of the formation and life cycle of severe thunderstorms on the Canadian Prairies, and to identify gaps in both our scientific knowledge and our data systems. An extensive but not exhaustive literature review has been undertaken, with an emphasis on convective storm forecasting. It is not feasible to report on all facets of severe convective storms, so that references reported here have been selected to fit the theme, with an emphasis on Canadian studies as much as possible. The report includes a descriptive (rather than mathematical) review of theories concerning interactions among various scales of atmospheric motion, including mesoscale convection, climatological and kinematic studies of thunderstorms, and case studies using the lead author's own forecasting technique.

A main focus of this report is a review of a multi-scale conceptual model of Alberta thunderstorms developed by the lead author during the 1980s (Strong, 1986), and recently updated (Strong, 2000). Process and forecasting case studies of north-south similarities and differences between "lee-of-the-Rockies" thunderstorms from Alberta to west Texas are reviewed in order to test and improve on the conceptual model. These case studies include several well-documented and costly Canadian storms, including the recent Pine Lake tornado. West-east similarities and differences of storms across the Prairies are also discussed.

The study includes results of consultations with various professional meteorologists in the field, including severe weather forecasters, research scientists, private sector meteorologists involved in hail suppression, and a unique couple who devote their lives to cloud photography from "storm chases." The report is summarized, highlighting gaps in our knowledge of storms and in our data systems, and providing a list of recommendations that may alleviate these gaps.

Authors' Acknowledgments

The impetus for this study came from the lead author's (Strong) 30 years' experience in forecasting and research, first with the Meteorological Service of Canada (MSC), followed by 12 years with the Alberta Research Council Hail Project (AHP), where he headed a forecasting and research team investigating mesoscale thunderstorm systems. Much of the original research was conducted while Strong was employed by AHP. We acknowledge the financial support of that organization, including the Limestone Mountain Experiment (LIMEX) fieldwork during the 1980s, especially LIMEX-85, which remains to this day the only Canadian example of a mesoscale upper air network. This study also takes advantage of co-investigator Smith's training and experience in climatological studies and field research.

We wish to acknowledge our collaborators, in particular: our official regional (PNR) MSC contact, Mr. Brad Shannon of MSC (Calgary), Pat McCarthy of MSC (Winnipeg) and his colleagues who provided a perspective on operational forecasting from the eastern Prairies; Mr. Rick Raddatz of the same office, who has conducted extensive research on the role of local evapotranspiration in severe storm development, and kindly provided copies of a number of his publications; Mr. Bob Kochtubajda of MSC (Edmonton) who was also involved with AHP field research, and who now studies thunderstorms and lightning with MSC; forecasters Steve Knott, Bruno Larochelle, Jamie Archibald, Dan Kulak, and Neil Taylor of MSC (Edmonton), who provided operational forecasting perspectives from the western Prairies; Dr. Terry Krauss of Weather Modification Incorporated (Red Deer), who provided feedback both from his experience with the old AHP program, as well as a number of weather modification operational programs in which he has been involved, including Greece, Oklahoma, and his current programs in both Alberta and Argentina; Mr. Jim Renick, who headed the AHP for many years, and now oversees the current hail program; Mr. Julian Brimelow, who provided feedback and helpful suggestions with his hail research experience from South Africa and Alberta; Arjen and Jerrine Verkaik, who shared a wealth of knowledge and photography gained from their unique careers as "storm chasers" throughout North America; Professors Edward Lozowski and Gerhard Reuter of the University of Alberta (Edmonton), who provided unique perspectives from past thunderstorm research dealing with microscale (cloud physics) and mesoscale processes respectively. Professor Lozowski was also the lead author's supervisor for both his M.Sc. and Ph.D. degrees on thunderstorm research at the University of Alberta.

There are many others who have provided varying degrees of feedback either directly or indirectly to this study. In particular, the experience and publications of many colleagues, too numerous to mention, from the old Alberta Hail Project (including Renick and Krauss above), as well as those from similar projects visited in the United States while with AHP, are all acknowledged here. We also appreciate the immediate feedback from Canadian Meteorological and Oceanographic Society (CMOS) audiences during presentations on this study given to Manitoba, Saskatchewan and Alberta CMOS Centres during 2000. Finally, we gratefully acknowledge the funding provided by Emergency Preparedness Canada that made this study feasible.

We thank all those who participated in any way in this review and consultation process. A few have been identified in the acknowledgements preceding the review. We apologize for any we

Public Safety and Emergency Preparedness Canada
Critical Infrastructure Protection and Emergency Preparedness

Sécurité publique et Protection civile Canada
Protection des infrastructures essentielles et Protection civile

Assessment and Prediction of Prairie Severe Thunderstorm Weather Phenomena

Acknowledgements

This publication has been prepared for:

Public Safety and Emergency
Emergency Preparedness Canada

2nd Floor, Jackson Bldg.
122 Bank St.
Ottawa, ON K1A 0W6
Tel: (613) 944-4875
Toll Free: 1-800-830-3118
Fax: (613) 998-9589
Email: communications@ocipep-bpiepc.gc.ca
Internet: www.ocipep-bpiepc.gc.ca

Authors:

G.S. Strong, Ph.D. and C.D. Smith, M.Sc.

This material is based upon work supported by the Division of Research and Development (DRD) in the Office of Critical Infrastructure Protection and Emergency Preparedness (OCIPEP), under Contract Reference No. 2000D023. OCIPEP is now a part of Public Safety and Emergency Preparedness Canada (PSEPC). Any opinions, findings, and conclusions or recommendations expressed in this material are those of the author(s) and do not necessarily reflect the views of Public Safety and Emergency Preparedness Canada.

Catalogue No.: D82-89/2003E-PDF
ISBN: 0-662-35697-7

Abstract

The goal of this study is to review our current understanding of the formation and life cycle of severe thunderstorms on the Canadian Prairies, and to identify gaps in both our scientific knowledge and our data systems. An extensive but not exhaustive literature review has been undertaken, with an emphasis on convective storm forecasting. It is not feasible to report on all facets of severe convective storms, so that references reported here have been selected to fit the theme, with an emphasis on Canadian studies as much as possible. The report includes a descriptive (rather than mathematical) review of theories concerning interactions among various scales of atmospheric motion, including mesoscale convection, climatological and kinematic studies of thunderstorms, and case studies using the lead author's own forecasting technique.

A main focus of this report is a review of a multi-scale conceptual model of Alberta thunderstorms developed by the lead author during the 1980s (Strong, 1986), and recently updated (Strong, 2000). Process and forecasting case studies of north-south similarities and differences between "lee-of-the-Rockies" thunderstorms from Alberta to west Texas are reviewed in order to test and improve on the conceptual model. These case studies include several well-documented and costly Canadian storms, including the recent Pine Lake tornado. West-east similarities and differences of storms across the Prairies are also discussed.

The study includes results of consultations with various professional meteorologists in the field, including severe weather forecasters, research scientists, private sector meteorologists involved in hail suppression, and a unique couple who devote their lives to cloud photography from "storm chases." The report is summarized, highlighting gaps in our knowledge of storms and in our data systems, and providing a list of recommendations that may alleviate these gaps.

Authors' Acknowledgments

The impetus for this study came from the lead author's (Strong) 30 years' experience in forecasting and research, first with the Meteorological Service of Canada (MSC), followed by 12 years with the Alberta Research Council Hail Project (AHP), where he headed a forecasting and research team investigating mesoscale thunderstorm systems. Much of the original research was conducted while Strong was employed by AHP. We acknowledge the financial support of that organization, including the Limestone Mountain Experiment (LIMEX) fieldwork during the 1980s, especially LIMEX-85, which remains to this day the only Canadian example of a mesoscale upper air network. This study also takes advantage of co-investigator Smith's training and experience in climatological studies and field research.

We wish to acknowledge our collaborators, in particular: our official regional (PNR) MSC contact, Mr. Brad Shannon of MSC (Calgary), Pat McCarthy of MSC (Winnipeg) and his colleagues who provided a perspective on operational forecasting from the eastern Prairies; Mr. Rick Raddatz of the same office, who has conducted extensive research on the role of local evapotranspiration in severe storm development, and kindly provided copies of a number of his publications; Mr. Bob Kochtubajda of MSC (Edmonton) who was also involved with AHP field research, and who now studies thunderstorms and lightning with MSC; forecasters Steve Knott, Bruno Larochelle, Jamie Archibald, Dan Kulak, and Neil Taylor of MSC (Edmonton), who provided operational forecasting perspectives from the western Prairies; Dr. Terry Krauss of Weather Modification Incorporated (Red Deer), who provided feedback both from his experience with the old AHP program, as well as a number of weather modification operational programs in which he has been involved, including Greece, Oklahoma, and his current programs in both Alberta and Argentina; Mr. Jim Renick, who headed the AHP for many years, and now oversees the current hail program; Mr. Julian Brimelow, who provided feedback and helpful suggestions with his hail research experience from South Africa and Alberta; Arjen and Jerrine Verkaik, who shared a wealth of knowledge and photography gained from their unique careers as "storm chasers" throughout North America; Professors Edward Lozowski and Gerhard Reuter of the University of Alberta (Edmonton), who provided unique perspectives from past thunderstorm research dealing with microscale (cloud physics) and mesoscale processes respectively. Professor Lozowski was also the lead author's supervisor for both his M.Sc. and Ph.D. degrees on thunderstorm research at the University of Alberta.

There are many others who have provided varying degrees of feedback either directly or indirectly to this study. In particular, the experience and publications of many colleagues, too numerous to mention, from the old Alberta Hail Project (including Renick and Krauss above), as well as those from similar projects visited in the United States while with AHP, are all acknowledged here. We also appreciate the immediate feedback from Canadian Meteorological and Oceanographic Society (CMOS) audiences during presentations on this study given to Manitoba, Saskatchewan and Alberta CMOS Centres during 2000. Finally, we gratefully acknowledge the funding provided by Emergency Preparedness Canada that made this study feasible.

We thank all those who participated in any way in this review and consultation process. A few have been identified in the acknowledgements preceding the review. We apologize for any we

Public Safety and Emergency Preparedness Canada
Critical Infrastructure Protection and Emergency Preparedness

Sécurité publique et Protection civile Canada
Protection des infrastructures essentielles et Protection civile

Assessment and Prediction of Prairie Severe Thunderstorm Weather Phenomena

Acknowledgements

This publication has been prepared for:

Public Safety and Emergency Preparedness Canada

2nd Floor, Jackson Bldg.
122 Bank St.
Ottawa, ON K1A 0W6
Tel: (613) 944-4875
Toll Free: 1-800-830-3118
Fax: (613) 998-9589
Email: communications@ocipep-bpiepc.gc.ca
Internet: www.ocipep-bpiepc.gc.ca

Authors:

G.S. Strong, Ph.D. and C.D. Smith, M.Sc.

This material is based upon work supported by the Division of Research and Development (DRD) in the Office of Critical Infrastructure Protection and Emergency Preparedness (OCIPEP), under Contract Reference No. 2000D023. OCIPEP is now a part of Public Safety and Emergency Preparedness Canada (PSEPC). Any opinions, findings, and conclusions or recommendations expressed in this material are those of the author(s) and do not necessarily reflect the views of Public Safety and Emergency Preparedness Canada.

Catalogue No.: D82-89/2003E-PDF
ISBN: 0-662-35697-7

Abstract

The goal of this study is to review our current understanding of the formation and life cycle of severe thunderstorms on the Canadian Prairies, and to identify gaps in both our scientific knowledge and our data systems. An extensive but not exhaustive literature review has been undertaken, with an emphasis on convective storm forecasting. It is not feasible to report on all facets of severe convective storms, so that references reported here have been selected to fit the theme, with an emphasis on Canadian studies as much as possible. The report includes a descriptive (rather than mathematical) review of theories concerning interactions among various scales of atmospheric motion, including mesoscale convection, climatological and kinematic studies of thunderstorms, and case studies using the lead author's own forecasting technique.

A main focus of this report is a review of a multi-scale conceptual model of Alberta thunderstorms developed by the lead author during the 1980s (Strong, 1986), and recently updated (Strong, 2000). Process and forecasting case studies of north-south similarities and differences between "lee-of-the-Rockies" thunderstorms from Alberta to west Texas are reviewed in order to test and improve on the conceptual model. These case studies include several well-documented and costly Canadian storms, including the recent Pine Lake tornado. West-east similarities and differences of storms across the Prairies are also discussed.

The study includes results of consultations with various professional meteorologists in the field, including severe weather forecasters, research scientists, private sector meteorologists involved in hail suppression, and a unique couple who devote their lives to cloud photography from "storm chases." The report is summarized, highlighting gaps in our knowledge of storms and in our data systems, and providing a list of recommendations that may alleviate these gaps.

Authors' Acknowledgments

The impetus for this study came from the lead author's (Strong) 30 years' experience in forecasting and research, first with the Meteorological Service of Canada (MSC), followed by 12 years with the Alberta Research Council Hail Project (AHP), where he headed a forecasting and research team investigating mesoscale thunderstorm systems. Much of the original research was conducted while Strong was employed by AHP. We acknowledge the financial support of that organization, including the Limestone Mountain Experiment (LIMEX) fieldwork during the 1980s, especially LIMEX-85, which remains to this day the only Canadian example of a mesoscale upper air network. This study also takes advantage of co-investigator Smith's training and experience in climatological studies and field research.

We wish to acknowledge our collaborators, in particular: our official regional (PNR) MSC contact, Mr. Brad Shannon of MSC (Calgary), Pat McCarthy of MSC (Winnipeg) and his colleagues who provided a perspective on operational forecasting from the eastern Prairies; Mr. Rick Raddatz of the same office, who has conducted extensive research on the role of local evapotranspiration in severe storm development, and kindly provided copies of a number of his publications; Mr. Bob Kochtubajda of MSC (Edmonton) who was also involved with AHP field research, and who now studies thunderstorms and lightning with MSC; forecasters Steve Knott, Bruno Larochelle, Jamie Archibald, Dan Kulak, and Neil Taylor of MSC (Edmonton), who provided operational forecasting perspectives from the western Prairies; Dr. Terry Krauss of Weather Modification Incorporated (Red Deer), who provided feedback both from his experience with the old AHP program, as well as a number of weather modification operational programs in which he has been involved, including Greece, Oklahoma, and his current programs in both Alberta and Argentina; Mr. Jim Renick, who headed the AHP for many years, and now oversees the current hail program; Mr. Julian Brimelow, who provided feedback and helpful suggestions with his hail research experience from South Africa and Alberta; Arjen and Jerrine Verkaik, who shared a wealth of knowledge and photography gained from their unique careers as "storm chasers" throughout North America; Professors Edward Lozowski and Gerhard Reuter of the University of Alberta (Edmonton), who provided unique perspectives from past thunderstorm research dealing with microscale (cloud physics) and mesoscale processes respectively. Professor Lozowski was also the lead author's supervisor for both his M.Sc. and Ph.D. degrees on thunderstorm research at the University of Alberta.

There are many others who have provided varying degrees of feedback either directly or indirectly to this study. In particular, the experience and publications of many colleagues, too numerous to mention, from the old Alberta Hail Project (including Renick and Krauss above), as well as those from similar projects visited in the United States while with AHP, are all acknowledged here. We also appreciate the immediate feedback from Canadian Meteorological and Oceanographic Society (CMOS) audiences during presentations on this study given to Manitoba, Saskatchewan and Alberta CMOS Centres during 2000. Finally, we gratefully acknowledge the funding provided by Emergency Preparedness Canada that made this study feasible.

We thank all those who participated in any way in this review and consultation process. A few have been identified in the acknowledgements preceding the review. We apologize for any we

may have missed. And finally, if you are interested in receiving further information on a possible prairie convective processes *network*, please identify yourself as such by sending an e-mail to:

geoff.strong@shaw.ca

The authors would also appreciate any helpful (positive or negative) feedback on this report.

G.S. (Geoff) Strong, Meteorological Consultant, Ardrossan, Alberta
and
C.D. (Craig) Smith, CDS Hydromet Consulting, Warman, Saskatchewan

External Collaborators

Brad Shannon, M.Sc.
Meteorological Service of Canada
Calgary, Alberta
Phone: (403) 299-7803
e-mail: Brad.Shannon@ec.gc.ca

Patrick McCarthy, M.Sc.
Severe Weather Program Manager
Prairie Storm Prediction Centre
Meteorological Service of Canada (PNR)
Winnipeg, Manitoba
Phone: (204) 984-6389
Fax: (204) 983-0109
e-mail: Patrick.McCarthy@ec.gc.ca

Bob Kochtubajda, M.Sc.
Atmospheric and Hydrologic Sciences Division
Meteorological Service of Canada (PNR)
Edmonton, Alberta
Phone: (780) 951-8811
Fax: (780) 951-8634
e-mail: Bob.Kochtubajda@ec.gc.ca

Terry Krauss, Ph.D.
Weather Modification Inc.
P.O. Box 27177
Red Deer, Alberta
T4N 6X8
Phone & Fax: (403) 342-5685
e-mail: krausst@telusplanet.net

Prof. Edward Lozowski
Dept. Earth & Atmospheric Sciences
University of Alberta
Edmonton, Alberta
Phone: (780) 492-0348
Fax: (780) 492-2030
e-mail: Edward.Lozowski@ualberta.ca

Prof. Gerhard Reuter
Dept. Earth & Atmospheric Sciences
University of Alberta
Edmonton, Alberta
Phone: (780) 492-0358
Fax: (780) 492-7598
e-mail: Gerhard.Reuter@UAlberta.ca

Executive Summary

Meteorologists are the first to admit that their science is far from perfect. The atmospheric system is very complex and requires much more research effort to increase our understanding. In light of this complexity, this project had three main goals: to provide a review of our knowledge of and predictive capabilities for severe prairie thunderstorms and related phenomena, to identify gaps in our science and data systems, and to provide science and technology recommendations to alleviate such gaps.

In the review of our knowledge and predictive capabilities, this study considered a number of issues, including synoptic forcing, spatial/temporal characteristics of storms, atmospheric boundary layer processes, forecasting, numerical modeling, climate, data systems and communications. Several scientific research and data gaps were identified in these areas. First, there is a lack of detailed mesoscale atmospheric boundary layer (ABL) information. More information is required to validate Strong's (1986, 2000) *multiscale conceptual model* of Alberta thunderstorm formation, particularly the role of the *capping lid* and associated processes. Second, perturbations in drylines and low-level jets (LLJs) are considered to be signals for storm initiation over the U.S. Mid-West, but these have not been well quantified on the Canadian Prairies. Third, quantitative analyses of the temporal and spatial characteristics of prairie storms are required to assess similarities and differences west-east across the Prairies and north-south into the U.S. High Plains. Fourth, techniques to provide consistently accurate objective forecasts of storm formation areas and time, movement, maximum intensity and time, storm decay and time, are all lacking. Last, numerical weather prediction (NWP) and mesoscale models cannot yet accurately simulate the ABL changes in the absence of high spatial and temporal resolution radiosonde data.

The data gaps identified include the fact that forecasters have no operational radiosonde soundings over the critical Alberta foothills area. Second, severe weather reports and climatologies are often inaccurate, incomplete, and may be more dependent on population density than on actual occurrence. Third, there are too few datasets available on the capping lid for the central and eastern Prairies to make any generalizations. Fourth, accurate regional estimates of evapotranspiration, identified as a key factor in storm generation and growth, are not available. Finally, there is a need for severe storm data archives specifically tailored to case study analysis.

Operational and research meteorologists provided the following recommendations to alleviate these gaps in the future:

- Form an ad hoc Prairie Convective Processes Network.
- Create a permanent home to archive prairie convective research datasets.
- Implement new part-time summer operational sounding sites.
- Create new data systems and proxy data sources.
- Develop severe weather forecasting techniques using radar and lightning data.
- Compute atmospheric moisture and energy budgets to identify sources and sinks.
- Design and implement a field research experiment to map atmospheric boundary layer processes.

- Develop and field-test new model output statistics (MOS) forecast techniques using radar and lightning data.

This study attempted to emphasize the importance of severe prairie thunderstorms in economic, human, and scientific contexts. Understanding and predicting these systems is essential.

List of Abbreviations Used in this Report

ABL	atmospheric boundary layer
AC	altocumulus clouds
ACC	altocumulus castellanus clouds
ACSL	altocumulus standing lenticularis clouds
AES	Atmospheric Environment Service (former name for MSC)
AG	above ground
AHMP	Alberta Hail Modification Project, Olds-Didsbury Airport, Alberta, 1996–present
AHP	ARC Hail Project, Red Deer, Alberta, 1975–85
AKE	available kinetic energy
ALHAS	Alberta Hail Studies project, 1957–74
AMS	American Meteorological Society
APE	available potential energy
ARC	Alberta Research Council, Edmonton, Alberta
ASL	above sea level
AVE	Area Variability Experiment
BERMS	Boreal Ecosystem Research and Monitoring Sites
BOREAS	Boreal Ecosystem Atmosphere Study
C	degrees Celsius, preceded by the degree symbol, "°"
CAPE	Convective Available Potential Energy
CB	cumulonimbus cloud
CCOPE	Cooperative Convective Precipitation Experiment
CDC	Convective Day Category
CGU	Canadian Geophysical Union
CIS	Capping Inversion Study, 1982 (of AHP)
CISK	Conditional Instability of the Second Kind
CMC	Canadian Meteorological Centre (of MSC)
CMOS	Canadian Meteorological and Oceanographic Society
CS	cirrostratus clouds
CU	cumulus clouds
CV	Curriculum Vitae

DAY-1	first 12–24 hours of a weather forecast period
EC	Environment Canada
EPC	Emergency Preparedness Canada
FAR	False Alarm Ratio
g kg^{-1}	grams of water vapour per kilogram of dry air (mixing ratio)
hPa	hector-Pascal(s), unit of atmospheric pressure (1 hPa = 1 mb)
GEM	Global Environmental Multiscale (NWP) model (Canadian CMC model)
GEWEX	Global Energy and Water Cycle Experiment
GMT	Greenwich Mean Time, now known as UTC
GOES	Geostationary Operational Environment Satellite
hindcast	a prediction made "after the fact," based on the same available data
ICLR	Institute for Catastrophic Loss Reduction, London, ON
K	degrees Absolute
KE	kinetic energy
kft	kilofeet (1000 feet)
LHS	left hand side
LIMEX	Limestone Mountain Experiments (of AHP), 1980–85
LLJ	low-level jet (or streak)
MAGS	Mackenzie GEWEX Study
mb	millibar(s), unit of atmospheric pressure (1 hPa = 1 mb)
MCC	Mesoscale Convective Complex
METEOR	Name given to first AI convective forecast model from AHP
MOS	Model Output Statistics
m s^{-1}	meters/second
MSC	Meteorological Service Canada (formerly AES)
MSL	mean sea level
NCAR	National Center for Atmospheric Research, Boulder, Colorado
NHRE	National Hail Research Experiment of NCAR
NOAA	National Oceanic and Atmospheric Administration
N, S, E, W	north, south, east, and west directions
NSSL	National Severe Storms Laboratory, Norman, Oklahoma

NWP	Numerical Weather Prediction
NWS	National Weather Service (of NOAA)
PI	Principal Investigator
PNR	Prairie and Northern Region (of Environment Canada)
POD	Probability of Detection
PPI	Plan-Position Indicator
PYR	Pacific and Yukon Region (of Environment Canada)
QPF	Quantitative Precipitation Forecast
RDG	Regional Director General
RW	(moderate) showers (with qualifiers –, +, ++ for light, heavy, or very heavy)
SAGE	Saskatchewan GEWEX Experiment (proposed for 2002–03)
SHARP	Saskatchewan Hail Research Project, 1973–78
SESAME	Severe Environmental Storms and Mesoscale Experiment, Oklahoma, 1979
SC	stratocumulus cloud
Sc_3	Synoptic Index of Convection (3-predictor)
Sc_4	Synoptic Index of Convection (4-predictor)
Sc_{10}	Synoptic Index of Convection (10-predictor)
SHARP	Saskatchewan HAil Research Project, 1973–78
SSCC	Sub-synoptic Scale Convective Complex
SWIFT	Severe Weather Intelligent Forecast Terminal
S/W	shortwave trough or ridge (synoptic scale)
SWIFT	Severe Weather Intelligent Forecast Terminal
TCU	towering cumulus, or cumulus congestus clouds
Theta	potential temperature
Theta-E	equivalent potential temperature
Theta-W	Pseudo-adiabatic wet-bulb potential temperature
TRW	(moderate) thundershower (followed by qualifiers –, +, ++ for light, heavy, and very heavy or severe)
UJ	upper jet (or streak)
UTC	Coordinated Universal Time, formerly known as GMT or Z (Zulu)
W	watts

WATFLOOD	Hydrological model at University of Waterloo, Waterloo, ON
WMI	Weather Modification Incorporated, Bismarck, North Dakota, and Red Deer, AB
Z	(Zulu) abbreviation on maps for UTC

Table of Contents

Acknowledgements ii

Abstract iii

Authors' Acknowledgments iv

External Collaborators vi

Executive Summary vii

List of Abbreviations Used in this Report ix

1.0 Introduction 1

1.1 Impetus and Purpose of Study 1
1.2 Methodology 3
1.2.1 Consultation Process 4
1.3 Scales of Atmospheric Motion – Background 5
1.4 Summary 9

2.0 Qualitative Studies and Pattern Recognition 10

2.1 Conceptual Models of the Visible Thunderstorm 11
2.1.1 Single-Cell Thunderstorm Concept 11
2.1.2 Multicell and Supercell Storms 12
2.1.3 Tornadogenesis Conceptual Models 13
2.2 Thunderstorm Climatology 14
2.2.1 Hail Climatology, Alberta 15
2.2.2 Hail Climatology, Saskatchewan and Manitoba 19
2.2.3 Tornado Climatology 20
2.2.4 Other Thunderstorm Climatologies and Storm Characteristics 21
2.3 Storm Environment Climatology 23
2.3.1 The "Capping Lid" and Synoptic Kinematics 24
2.3.2 Synoptic Scale Climatology 26
2.4 Example Storm Environment Case Studies 27
2.5 Modification of Thunderstorms 30
2.6 Cloud Photography in Severe Storm Research 31
2.7 Summary 33

3.0 Quantitative Atmospheric Processes Research 34

3.1 Scale Interactions 34
3.2 Energetics of Scale Interactions 35
3.3 Kinematics and Scale Interactions 37
3.3.1 Observed Effects of Scale Interactions for Alberta Storm 37
3.3.2 Advection, Convergence and Related Factors 39
3.3.3 Sensible and Latent Heat Fluxes 40
3.3.4 Drylines 40
3.4 Technological Influences on Thunderstorm Research 41
3.5 Summary 43

4.0 Multi-Scale Conceptual Model of Alberta Thunderstorms 45
4.1 Background Research and the *Capping Lid* 45
4.1.1 Topography 45
4.1.2 Meso-γ (Cloud) Scale Patterns for Convective Storms 48
4.1.3 The Capping Lid and a Severe Alberta Hailstorm Example 51
4.2 Hypothesis for the Conceptual Model 52
4.3 Summary 56

5.0 Tests of the Conceptual Model 57
5.1 LIMEX-80 Results 57
5.2 SESAME-79 Tests 60
5.2.1 Synoptic Situation of 20 May 1979 and Early Pre-Storm Lid Preparation 61
5.2.2 Pre-Storm Lid Breakdown 62
5.2.3 Storm Initiation and Progression 67
5.2.4 Storm Decay 68
5.3 LIMEX-85 Tests 69
5.3.1 Synoptic Conditions and Weather on 11 July 1985 70
5.3.2 The Pre-Storm Capping Lid 71
5.3.3 Mesoscale Dynamics during Pre-Storm Lid Formation and Breakdown 72
5.3.4 Sensible and Latent Heat Fluxes 73
5.4 The Pine Lake Tornado Storm, 14 July 2000 77
5.5 Summary 83

6.0 Forecasting Convective Weather 85
6.1 Pattern Recognition – Qualitative Techniques 85
6.1.1 Necessary and Sufficient Conditions for Thunderstorms 85
6.1.2 Favourable Conditions for Thunderstorms 85
6.1.3 Composite Analyses for Forecasting Severe Thunderstorms 88
6.2 Quantitative Operational Techniques 88
6.3 Numerical Models 88
6.3.1 Synoptic Scale NWP Models 88
6.3.2 Mesoscale Models 90
6.3.3 Cloud Physics Models 90
6.4 The Synoptic Index of Convection 91
6.4.1 Convective Day Category (CDC) 91
6.4.2 Single-Valued Synoptic Index of Convection 93
6.4.3 Evaluation of Single-Valued Sc_4 94
6.5 The "Areal" Version of the Synoptic Index of Convection (Sc_4 and Sc_3) 98
6.5.1 The Calgary Hailstorm, 28 July 1981 98
6.5.2 Weak Alberta Convective Case, 7 September 1982 100
6.5.3 Small, Intense Storm Test, 17 July 1984 100
6.5.4 An "Unpredictable" Colorado Hailstorm, 30 July 1979 101
6.5.5 Oklahoma Tornadic Storm, 20 May 1979 104
6.6 Artificial Intelligence (AI) Applications: METEOR and SWIFT 105
6.6.1 Edmonton Tornadic Storm, 31 July 1987 106
6.7 Summary 107

7.0 Conclusions: Synthesis of Review and Consultations 109
7.1 Feedback from Consultations 109
7.2 Objective 1: Status of Scientific Knowledge and Forecasting Capabilities 112
7.3 Objective 2: Gaps in Our Knowledge and Data 116
7.4 Objective 3: Recommendations 117
7.4.1 Form a Prairie Convective Weather Network (R1) 117
7.4.2 Create a Permanent Home to Archive Prairie Research Datasets (R2) 118
7.4.3 Create New Part-time Summer Operational Sounding Sites (R3) 118
7.4.4 New Data Systems and Proxy Data Sources (R4) 119
7.4.5 Develop Severe Weather Predictands Based on Radar/Lightning Data (R5). 119
7.4.6 Compute Atmospheric Moisture and Energy Budgets for Sources and Sinks (R6) 119
7.4.7 Design/Implement a Field Research Experiment to Map Atmospheric Boundary Layer Processes (R7) 120
7.4.8 Develop and Field-Test New MOS Forecast Techniques Using Radar and Lightning Data (R8) 120
7.5 Relevance of Review and Closing Remarks 121
7.5.1 Relevance 121

8.0 Bibliography 122

Appendix A – Brief Descriptions of the Limestone Mountain Experiments A-1

Appendix B – Annual Alberta Hail Project (AHP) Forecast Evaluation Tables B-1

Appendix C – Non-Research Issues C-1

1.0 Introduction

1.1 Impetus and Purpose of Study

This study addresses the problems of weather prediction (in the first 12 to 24 hours; DAY-1) and early-warning (first one to three hours) of severe convective thunderstorms and related phenomena on the Canadian Prairies, and the mitigation of their damaging effects. Weather phenomena associated with these storms include large hail, heavy rainfalls, flooding, tornadoes and other damaging winds. All of these phenomena exact heavy annual tolls in crop and other property damage, and all too often in human lives. Such storms occur during summer with high frequency over the Canadian Prairies; e.g., hail occurs on almost 50% of summer days over central Alberta alone, with about one-third of these classified as severe (walnut or larger size hail). Some well-documented examples of prairie storms of the past 20 years include:

- the Calgary hailstorm of 28 July 1981 – more than $100M damage and several lives lost in flooding (Strong, 1982);
- the Edmonton tornado of 31 July 1987 – $250m million damage and 27 lives lost (Charlton et al., 1998, or Atchison, 1988);
- the Calgary hailstorms of 1991 ($400m damage) and 1996 ($150m damage);
- the Winnipeg hailstorm of 16 July 1996 – $110m damage (McCarthy et al., 2000); and
- the Pine Lake tornado of 2000 – 12 deaths, at least 140 injuries, $15m damage (Joe and Dudley, 2000).

Detailed field research programs on severe Alberta hailstorms were carried out by the combined Alberta Hail Studies (ALHAS, 1957–74; Renick, ed., 1970) initiated by McGill University (Douglas et al., 1959), and the Alberta Hail Project (AHP, 1975–85; Deibert, ed., 1985) coordinated by Alberta Research Council (ARC). This program included a major cloud-seeding effort to reduce heavy hailfall and resulting crop damage over central Alberta. The current Alberta Hail Modification Project (AHMP, 1996–present) is focused on reducing property damage from hail over major urban centeres (Krauss, 1999).

One of the technical problems with respect to prairie thunderstorms is the lack of synthesis of knowledge of storms and in related areas such as forecasting, emergency measures, communications for dissemination of warnings, and lack of coordination between agencies. Paul (1982) wrote that "Past research into prairie thunderstorms has largely been conducted by meteorologists and has been marked by fragmented studies rather than overall synthesis." Five years later following the Edmonton tornado disaster, the chair of the review team, Hage (1987) wrote as one of his recommendations, "The Government of Canada and the Governments of Provinces affected by severe summer weather should encourage and support research to improve early detection and prediction of severe local storms, including tornadoes." Since the termination of AHP research and operations in 1985 and the effective break-up of the remaining ARC research group around 1987–88, there has been little published research on Alberta thunderstorm systems, and even less for Saskatchewan and Manitoba. The few research meteorologists left in this field have been even more fragmented than at the time of Paul's statement above. Moreover, while major field meteorological research efforts have been funded by the federal government in almost every other region of Canada in the past 15 years, there has never been a similarly funded

effort on the Prairies, despite the need for one dedicated to their number one hazard, severe thunderstorms. Many of Hage's (1987) recommendations, including the quoted one, have never been carried out.

One important scientific issue, which has long been recognized but never documented in the literature, is that thunderstorms and their generation mechanisms are different from west to east across the Prairies. In contrast, storms in the lee of the Rockies from northern Alberta south to west Texas appear to exhibit many similarities in both type and formation mechanisms (Strong, 1986). The Pine Lake tornado incident in central Alberta on 14 July 2000 is a case in point for the west-east differences in storms. For example, the infrared satellite image in Figure 1.1 just one hour before tornado touchdown shows significant-looking large convective formations in North Dakota, southern and northern Saskatchewan. However, the storm which did all the damage and took 12 lives is a much smaller entity over south-central Alberta and, at this image scale, does not appear to look very significant by comparison, even though it had already dumped a swath of hail (up to golf ball size) in a west-east path across the province, and was about to become tornadic.

Figure 1.1 Colour-enhanced infrared GOES satellite image at 0000 UTC, 14 July 2000, showing thunderstorms over the Dakotas, southern and northern Saskatchewan, and a smaller but large hail-producing intense thunderstorm over south-central Alberta (which spawned the Pine Lake tornado one hour later, leaving 12 dead in its wake).

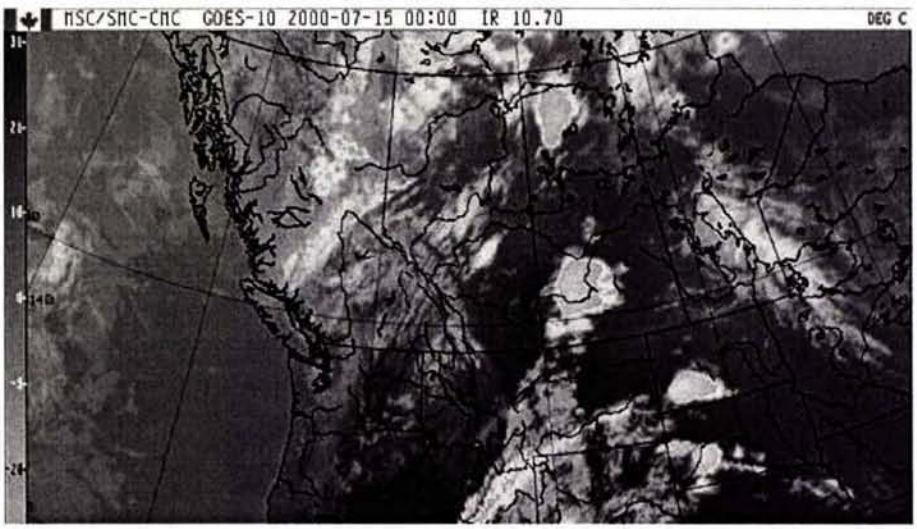

Documentation of north-south and west-east similarities and differences in characteristics between prairie convective storms is crucial to improving our understanding and prediction of these phenomena. This is all the more important since budgetary restrictions have forced the Meteorological Service of Canada (MSC) to move all of its prairie severe weather forecasting to their Winnipeg office in the past few years. Once the differences and similarities have been quantified, Canadian meteorologists might also make better use of research results coming from the United States.

Thus, the main purpose of the current study is to synthesize what is known (and unknown) about prairie thunderstorm systems. It will attempt to highlight major north-south and west-east differences and similarities in storms, identify gaps in both our knowledge base and datasets, and try to assess the accuracy of current techniques used to forecast convective weather and storms. Recommendations will focus on what steps could be taken to improve deficiencies, including the design of specific field experiments and use of new technologies where prudent. The primary objectives for this study are therefore:

1. To provide a "state-of-the-art" review of our knowledge of and predictive capabilities for severe prairie thunderstorms and related phenomena;
2. Identify gaps in our science and data collection networks; and
3. Provide recommendations for increasing our knowledge base and improving our forecasting capabilities on these storms.

The review is based on published literature, and includes some critical analysis tests of a *multi-scale conceptual model of severe thunderstorms* published by Strong (1986, 2000), with a goal to improve on this model. An accurate and comprehensive conceptual model of these storms can be used quite effectively for DAY-1 forecasting (i.e., the 12 to 24-hour period), for early-warning (one to six hours) once a storm is in progress, and for modification of such storms through cloud-seeding efforts. The report highlights where there are major gaps in our knowledge, and provides recommendations for closing these gaps leading directly to improved forecasting and early warning of these phenomena.

1.2 Methodology

The literature review part of this report (Sections 1.0 thru 3.0 and portions of the remaining sections) concentrates as much as possible on studies carried out over the Canadian Prairies, including refereed journal articles, published reports, proceedings and preprints of conferences, workshops, and symposia, and personal communications where necessary. The largest amount of research on severe prairie thunderstorms available in the literature was conducted by the ALHAS/AHP programs in central Alberta. Reviews of non-Canadian studies are included to demonstrate results that apply universally to severe convective storms, and to show where research efforts have been directed. MSC would not provide results from their in-house forecast evaluations for external publication because they deemed that these had not been peer-reviewed. In their place, severe storm forecast evaluations reported in Section 5.0 are limited to those of the Alberta Hail Project, which is in itself a substantial eight-year database. Analysis results used to test the conceptual model hypothesis in Section 6.0 include new analyses carried out specifically for this report as well as results from the PI's Ph.D thesis (Strong, 1986) and other publications.

The overall methodology used to complete this report is as follows:

1. Review and synthesize published literature on severe thunderstorms and related phenomena on the Canadian Prairies such as hail, tornadoes, heavy convective rainfall and flooding, and high winds. This stage also involves extensive consultation with

meteorologists involved in research, forecasting, numerical modeling, and weather modification.

2. Consult with other meteorological experts in severe storm research, observations, forecasting, numerical modeling, and weather modification operations, to obtain a broader perspective on the science and technological issues around convective storms, on the needs in research, and potential solutions. This consultation process is outlined below (Section 1.3.1), and results of the consultation are detailed in Section 7.1.

3. Use mesoscale surface, radiosonde, radar, Sodar, and aircraft data collected during the Limestone Mountain Experiment (LIMEX-85) to test various aspects of the multi-scale conceptual model of thunderstorms proposed by Strong (1986, 2000b), using analyses of pre-storm synoptic and mesoscale dynamics, boundary layer processes, and sensible and latent heat inputs to the storm.

4. Employ these data to test a convective forecast index (SC_{10}, SC_4) developed by Strong (1979, 1983, 1986), and still in use in Alberta, Argentina, and other countries by weather modification programs (Krauss, 1999).

5. Encourage numerical modellers at MSC/CMC (Montreal) to carry out specific model runs using the LIMEX data as further tests of the conceptual model.

6. Identify gaps in our knowledge of Canadian Prairie summer storms, as well as gaps in current data collection networks.

7. Provide recommendations for improving our knowledge base of severe prairie thunderstorms and our use of existing datasets, with the goal of improving our prediction and early-warning capabilities.

8. As necessary, design field experiments to test remaining aspects of the conceptual model.

1.2.1 Consultation Process

The consultation process[1] carried out during August 2000 for this report included in-person interviews with weather forecasters of both the Alberta and Prairie Weather Centres of MSC in Edmonton and Winnipeg, research scientists with expertise on severe thunderstorms at the University of Alberta, and key members of the current Alberta hail suppression program (AHMP) at Red Deer and Olds-Didsbury Airport. Other in-person interviews were conducted in

[1] Three formal presentations on the subject and project were given to CMOS Centres in all three Prairie provinces (including Alberta Centre where the lead author is chairperson) as follows:

- 24 August 2000 – "North-South (Alberta to Texas) and West-East (Alberta-Manitoba) Severe Thunderstorm Similarities and Differences" by G.S. Strong, to CMOS Winnipeg Centre, Winnipeg.
- 14 September 2000 – "A Multi-Scale Conceptual Model of 'Lee of the Rockies' Severe Thunderstorms" by G.S. Strong, to CMOS Alberta Centre, Edmonton.
- 14 November 2000 – "*Spatial/Temporal Variations in Severe Prairie Thunderstorms – Multi-scale* Conceptual *Model with Forecasting Applications*" by G.S. Strong, to CMOS Saskatchewan Centre, Saskatoon.

November with Arjen Verkaik, an experienced "storm chaser" and cloud photographer based in Elmwood, Ontario, and with Ray Keller, a flood forecasting expert with Alberta Environment. A number of other consultations were conducted by e-mail and phone with severe storm experts in both Canada and the U.S. Discussions during and following these presentations to "severe storm" knowledgeable audiences of 10 to 25 experts generated additional valuable feedback for the study.

1.3 Scales of Atmospheric Motion – Background

By way of background, this section includes information on virtually all spatial and temporal scales of motion in the atmosphere, including presentation of the multi-scale conceptual model in Section 4.0. One scheme for classifying the atmospheric "scales" of motion is shown in Table 1.1. These scales are not discrete physical entities, but rather, they represent the most common stratifications discussed in the literature (e.g., Orlanski, 1975). The reader is advised that many somewhat different variations of this table appear in the literature.

Examples of three of these scales of motion are revealed in the enhanced infrared satellite image of Figure 1.2. It includes a synoptic scale cyclonic system of more than 2000 km across, several sub-synoptic (or Meso-α) scale convective complexes (clusters of thunderstorms) with horizontal dimensions of 250–350 km in this case, and at least one mesoscale (Meso-β) thunderstorm complex of 50–100 km. The approximate position of the surface front is superimposed on Figure 1.2. The aerial photograph of Figure 1.3 depicts three other scales of motion from a much closer vantage point. Here the thunderstorm system is a (Meso-β) mesoscale convective complex of 50–80 km across. This complex includes cloud scale (Meso-γ) clusters of 2–10 km across, which by themselves would be identified as cumulus congestus (TCU) clouds, each of which is made up of microscale cloud turrets of the order of 1 km or less across. The precipitation patterns from these clusters have been observed on radar as "fine-scale reflectivity patterns" or FSPs (Barge and Bergwall, 1976). It has been assumed in the past that these clusters, and certainly the turrets, are a result of turbulent processes (e.g., Tennekes, 1978). Still, Barge and Bergwall have shown that the FSPs exhibit continuity in space and time, suggesting that such features have predictable qualities. This may require some re-examination of those features that we assume to be indeterminate three-dimensional turbulence – a problem that cannot be resolved in the current study.

A further clarification of the two convective complex scales is necessary here. Maddox (1980) defined but one scale of Mesoscale Convective Complex (MCC) having a quasi-elliptic shape and a total cloud shield area exceeding 100,000 km^2 (linear horizontal dimensions more than 350 km) for a period of six hours or more. Maddox did not place upper limits on his MCC definition, but his summary of 43 MCCs for 1978 ranged in diameter from 350 to 1000 km, with durations of six to 25 hours (except one >54 hours). Bosart and Sanders (1981) described the life history of a relatively small convective complex (at times, smaller than 300 km diameter), which originated over South Dakota, but caused disastrous flash floods over Pennsylvania four days later (well into the synoptic scale lifetime). The smallest entity noted in Figures 1.2 and 1.3 falls short of the minimum dimensions given by Maddox, as do two particularly severe storms to be discussed in Section 1.3. These smaller severe storms are more the "norm" for Alberta and other

High Plains[2] regions, yet many of them develop their own mesoscale circulation (Lemon and Doswell, 1979).

Since there is apparently no clear relation between complex size, intensity, and duration, it makes sense to have at least two classifications of MCC. The Maddox MCC will therefore be called a Sub-synoptic Scale Convective Complex (SSCC), if horizontal dimensions exceed 200 km. Mesoscale Convective Complexes (MCC) will be defined to range from small clusters of cumulus clouds of 20 km across, up to small thunderstorm complexes of 200 km. While satellite imagery such as Figure 1.2 provides no proof of the scale interaction concept, the fact that groups of entities at one scale tend to be organized into entities at the next larger scale, suggests a strong relation between adjacent scales. Diagnostic studies, such as the four-day storm complex documented by Bosart and Sanders (1981), provide direct evidence of the interactions between different scales of motion.

[2] The High Plains are loosely defined as the broad region in the lee of the Rocky Mountains, generally above 500 m elevation and extending from Texas northwest to Alberta.

Table 1.1 Definitions and examples of the scales of atmospheric motion discussed in this paper (Strong, 1986).

SCALE	Range of Wavelength (km)	Time Scale of Associated Weather over region	Scale Examples	Example Data Source	Mean Spacing or Data Resolution (km)	Frequency of Observation	Remarks
MACRO or Planetary	> 5000	More than one week	Longwaves, large, persistent quasi-stationary highs, lows	Global upper air network (weekly averages)	500 (land stations)	Twice daily (00Z, 12Z)	Variable density; e.g., often inadequate over oceans
SYNOPTIC (upper Meso α)	2000 – 5000	2 – 7 days	Intermediate and shortwaves, migratory lows, highs	N.A. upper air network	500	Twice daily (0Z, 12Z)	Irregular design; e.g., no sites over Sask.
SUB-SYNOPTIC (lower Meso-α)	200 – 2000	12 – 48 hours	Sub-synoptic Convective Complexes (SSCCs), or TRW clusters, hurricanes, secondary lows	N.A. surface observing network	130	Hourly plus special observations	Irregular design, sites sometimes not represent-ative
MESO (Meso-β)	20 – 200	1 – 12 hours	Large TRWs or Mesoscale Convective Complexes (MCCs), cold fronts and squall lines, cumulus clusters	NSSL (1966–67) SESAME (AVE-III/IV/V) upper air networks, Alta. Foresty reports	75	1.5 – 3 hours	Irregular design
					80	1.5 – 3 hours	Near-regular design
					30	twice daily (14Z, 19Z)	Irregular, limited area (Alta. Foothills)
CLOUD (Meso-γ) or Cumulus Scale	2 – 20	10 – 60 min.	Single-cell CU, TCU, small CB, tornado, fine-scale reflectivity patterns	GOES sat. data; ARC rain gauges; NOAA sat. data	4–16 (IR), 1–2 (vsbl)	30 minutes	Res. deteriorates N from equator
					2–10	once daily	AHP region
					1	4–8 hours	Polar-orbiting
MICRO	A few cm to 10 km	Seconds to minutes	Turbulent eddies, convective thermals, CU cloud turrets, wind gusts	Radar data; LANDSAT data; research aircraft	0.5–2.0	1 minute	Uniform grid
					0.05	1–2 weeks	Poor temporal
					< 0.01	1 second	Uniform, but 1-D unless sev. acft
VISCOUS	Molecular distances	??	Molecular motions	Electron microscope	N/A to most meteorology applications	N/A	N/A

Figure 1.2 Enhanced infrared NOAA-6 image for 0136 UTC, 15 July 1982, depicting three of the scales of atmospheric motion indicated in Table 1.1; fronts and surface and 500 mb low centres have been super-imposed.

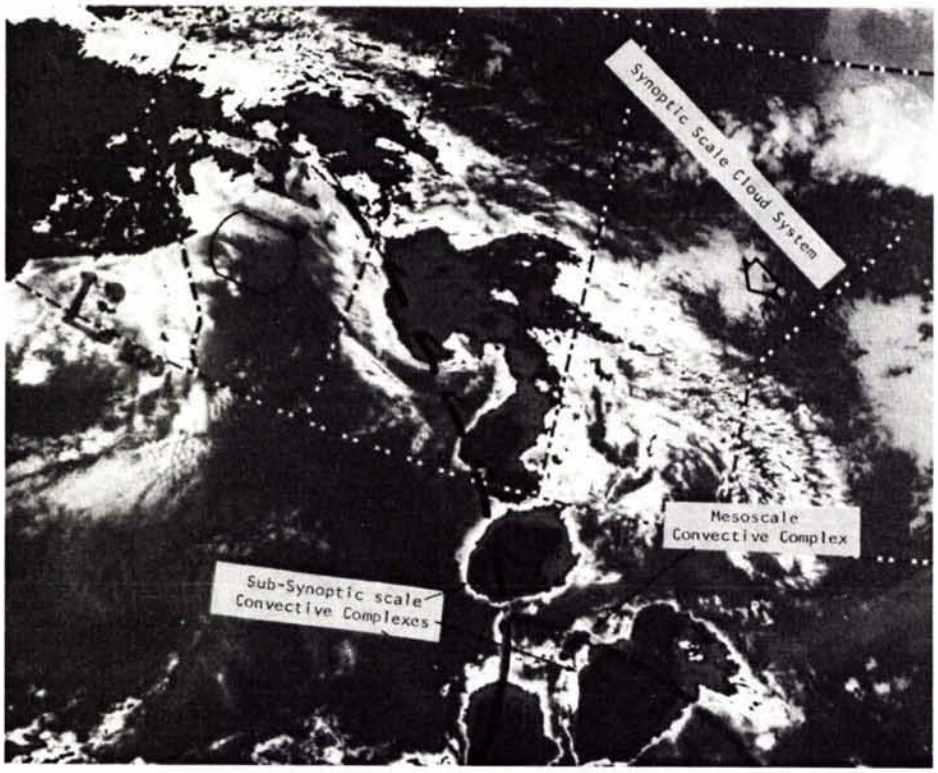

Figure 1.3 Aerial view of a mesoscale thunderstorm complex (40–80 km across), with cloud scale clusters (2–10 km across) in the "new growth zone," and individual cloud turrets with horizontal dimensions of 1 km or less – three identifiable interacting scales of motion.

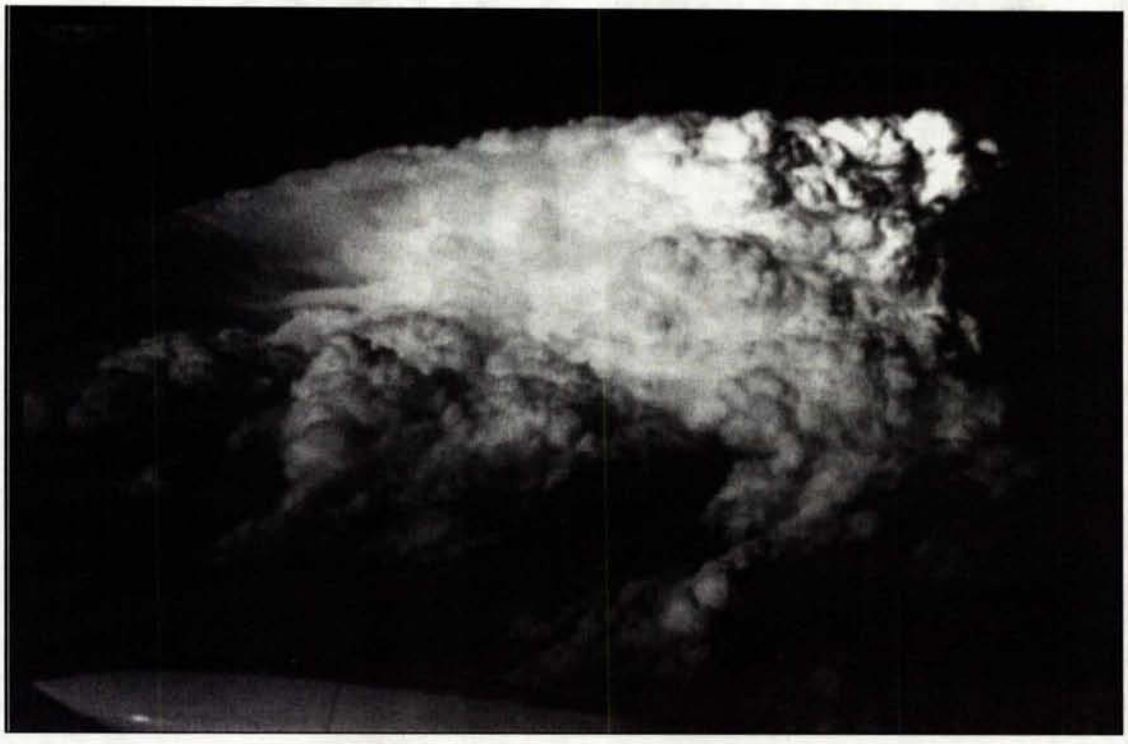

1.4 Summary

The example severe thunderstorm disasters mentioned in Section 1.1 clearly underscore the urgent need for reviews on the status of thunderstorm research in Canada, and for clear recommendations for improving the knowledge base, forecasting and mitigation of impacts of severe thunderstorm hazards. While numerical weather prediction models have made major advances in the last 10 to 15 years in forecasting major (synoptic-scale) weather systems, our weather services are still unable to predict with great confidence the initiation region, timing, and severity of mesoscale systems such as severe thunderstorms, and even less so, related phenomena such as large hail, tornadoes, heavy precipitation, and high winds. A major step to improve cloud-seeding techniques for suppressing severe hailfall, for example, is to improve the short-range DAY-1 (three to 12 hours) prediction capability and early-warning (one to three hours) of storms (Krauss, 1998, 1999). This should also be one of the primary objectives of any new severe storm research efforts, hence the desirability of close collaboration with regional MSC offices, numerical modeling communities, and user-groups such as federal and provincial environment, forestry, and emergency agencies. The current study will describe the important multi-scale processes involved in the initiation and life cycle of severe prairie thunderstorms, and provide recommendations for reaching the longer-term goal of accurate forecasts of the related phenomena.

2.0 Qualitative Studies and Pattern Recognition

Severe storm research during the 1950s and 1960s tended to follow one of two different schools of thought, which concentrated on two opposite ends of the scale spectrum. One approach was to focus attention primarily at the *visible* cloud scale, dealing with the physics of cloud and precipitation particles, and how these might be altered to change the type and amount of precipitation at the ground, virtually ignoring the larger environment outside the cloud. Out of this was born the science of weather modification. The other approach was interested in how large-scale (synoptic) processes modify the severe storm environment, *before* the storm forms, and how the effects might be predicted. For some time, these two approaches were pursued virtually independent of each other, and tended to develop slightly conflicting ideas as to cause and effect of convective storms.

This section reviews both of these approaches, including published climatologies both of visible storm features and of the storm environment, then discusses some results of case studies from both approaches. When discussing hail size, the old ALHAS/AHP definitions of: shot size (< 4 mm), pea (4–12 mm), grape (13–20 mm), walnut (21–32 mm), golf ball (33–52 mm), and larger than golf ball (> 52 mm) are commonly used in Canada. For tornadoes, the Fujita (1971) F-scale, as shown in Table 2.1, is used universally to classify tornado strength by resulting damage.

Table 2.1 The Fujita Tornado Scale (Fujita 1971) – usually referred to as the F-Scale – classifies tornadoes based on resulting damage.

F-SCALE	WINDS	TYPE OF DAMAGE	FREQUENCY
F0	64–116 km/h	MINIMAL DAMAGE: Some damage to chimneys, TV antennas, roof shingles, trees, and windows.	28%
F1	117–180 km/h	MODERATE DAMAGE: Automobiles overturned, carports destroyed, trees uprooted.	39%
F2	181–253 km/h	MAJOR DAMAGE: Roofs blown off homes, sheds and outbuildings demolished, mobile homes overturned.	24%
F3	254–332 km/h	SEVERE DAMAGE: Exterior walls and roofs blown off homes. Metal buildings collapsed or are severely damaged. Forests and farmland flattened.	6%
F4	333–418 km/h	DEVASTATING DAMAGE: Few walls, if any, standing in well-built homes. Large steel and concrete missiles thrown far distances.	2%
F5	419–512 km/h	INCREDIBLE DAMAGE: Homes levelled with all debris removed. Schools, motels, and other larger structures have considerable damage with exterior walls and roofs gone. Top stories storeys demolished.	< 1%

For example, the Barrie (May, 1985), Edmonton (July, 1987), and Pine Lake (July, 2000) tornadoes achieved maximum strengths of F4, F4, and F3 respectively. Also discussed in this

section are weather modification, especially of hail suppression, and the use of cloud photography in severe thunderstorm research.

2.1 Conceptual Models of the Visible Thunderstorm

2.1.1 Single-Cell Thunderstorm Concept

Very little research was carried out on thunderstorms until after World War II. In-flight encounters with such storms by Allied pilots during the war, frequent severe tornado-producing storms over the American Mid-West, the war-time development of radar, and availability of such radar and numerous aircraft following the war prompted a series of field experiments in Florida and Ohio during the late 1940s called the *Thunderstorm Project*. It was quite natural for this first major thunderstorm field project to concentrate on the *visible* problem: the mature thunderstorm. One of the results reported by this project (Byers and Braham, 1949) was the recognition of three main phases in the life cycle of a thunderstorm as reproduced in Figure 2.1, and summarized in the following paragraphs.

Cumulus Stage – characterized by updrafts throughout the cloud, initially very weak, but eventually attaining speeds as high as 15 m s^{-1} (55 kph), with no precipitation from the cloud. The cumulus cloud has a relatively flat base that can range from 500–2000 m above ground (AG), while tops can grow rapidly to 7000 m. This stage has a duration of only 10–15 minutes.

Mature Stage – takes over from the cumulus stage with the occurrence of rain at the ground. Updrafts reach their maximum velocity at this stage, attaining speeds of 15–30 m s^{-1} (50–110 kph). Surface precipitation rapidly becomes heavy, and hail also frequently forms during this stage as ice particles collect super-cooled water droplets through repeated traverses up and down through the cloud. Cloud tops often exceed 12,000 m and occasionally 15,000 m. The heavy precipitation at the surface usually creates a strong downdraft and outflow, leading to strong horizontal winds at the leading edges of the storm, often exceeding 50 kph. The duration of this stage is typically 15–30 minutes. During this stage of severe thunderstorms, tornadoes are also a threat, forming in response to circulations induced by the updraft-downdraft couplet, although this aspect was not elucidated in the original Byers and Braham model.

Dissipating Stage – The dissipating stage essentially begins when rainfall at the surface becomes light or ends altogether, while updrafts within the cell drop significantly and eventually all vertical motion is downward, so that the cloud begins to dissipate and only ice crystals remain in the upper part of the cloud, which give the marked "anvil" appearance as upper winds spread the crystals downstream. The remaining downdrafts are lighter than during the mature stage. There is no longer a threat of either hail or tornadoes at this stage, although both can form again if the storm regenerates from new cells. The duration of the dissipating stage cannot be specifically determined, since the cloud simply fades away gradually due to evaporation in stages, this being a function of the degree of downdrafts (subsidence and drying out, the opposite of ascent and condensation) and dryness of the environmental air around the cloud. Usually, the storm loses its distinguished (anvil) appearance within 30 minutes of this stage.

Figure 2.1 Simple three-stage conceptual model of thunderstorms, including *cumulus* stage (weak updrafts, no precipitation), *mature* stage (most intense phase with strongest updrafts *and* downdrafts, heavy precipitation at surface including hail), and *dissipating* stage (weak downdrafts, light precipitation, primarily ice crystals left in cloud, and marked *anvil* top). Reproduced from Byers and Braham, 1949.

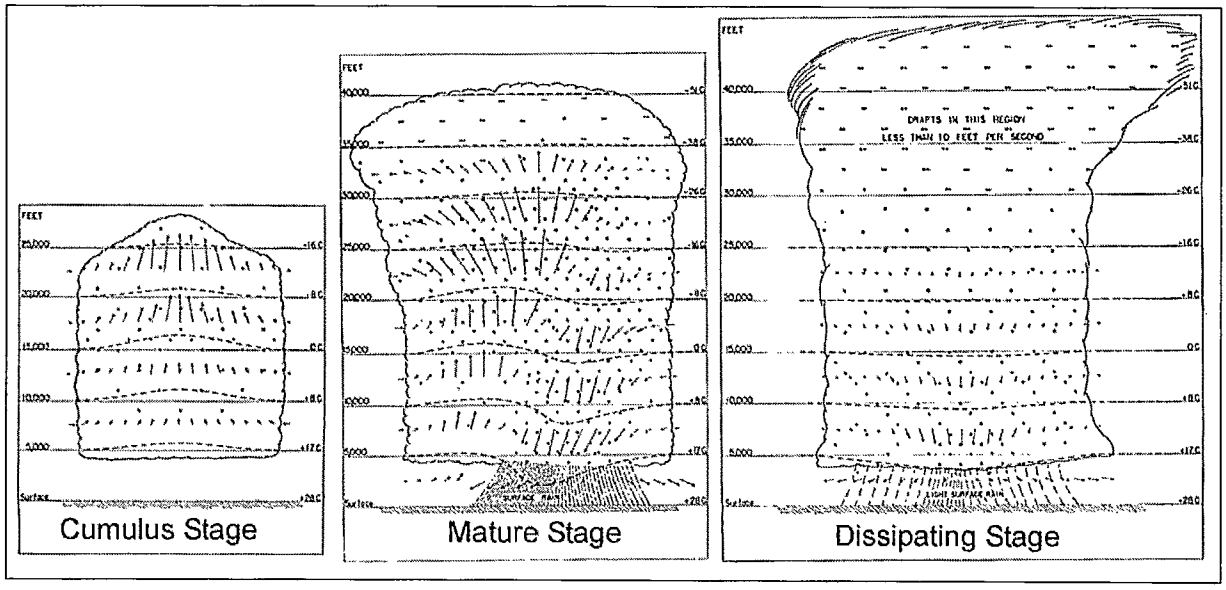

2.1.2 Multicell and Supercell Storms

The Thunderstorm Project initiated important studies in cloud physics and thunderstorm kinematics, and led into attempts in weather modification, especially hail suppression. The single-cell thunderstorm concept, while simplistic by today's definition, is still somewhat valid within the framework of *multicellular* storms, where all three stages occur simultaneously in different parts of a storm. The concept of multicell storms appears to have originated with the McGill group studying Alberta storms (Douglas and Hitschfeld, 1959), although it was not described in any detail until much later, such as shown in Figure 2.2 (Chisholm and Renick, 1972).

The definition of a *supercell* storm appeared at about this time as well. The main difference between multicell and supercell storms is in terms of the wind structure and shear, as depicted in the wind hodograph of Figure 2.3 (after Chisholm and Renick, 1972). Single-cell storms exhibit light winds with little wind shear, multicell storms have strong shear but all in one plane, while supercell storms have strong directional shear at low-levels. The effect of this is that air entering the multicell storm at low levels rises in the cell core, then leans downwind such that once heavy precipitation commences, the resulting downdraft effectively cuts off the inflow to that cell. Propagation of the storm (with new cells) requires a strong inflow of moist air so that new cells can form as shown in Figure 2.2. The strong directional shear of supercell storms (generally southeast at the surface, veering to southwest aloft) allows precipitation to occur without cutting off the inflow. The effect is often a long-lived thunderstorm, while the complex updraft-downdraft couplet is conducive to rotation of the cloud base, often leading to tornadoes.

Figure 2.2 Artistic view of a multicell storm illustrating the time variations in the lifetime of a single-cellular element. Reproduced from Chisholm and Renick, 1972.

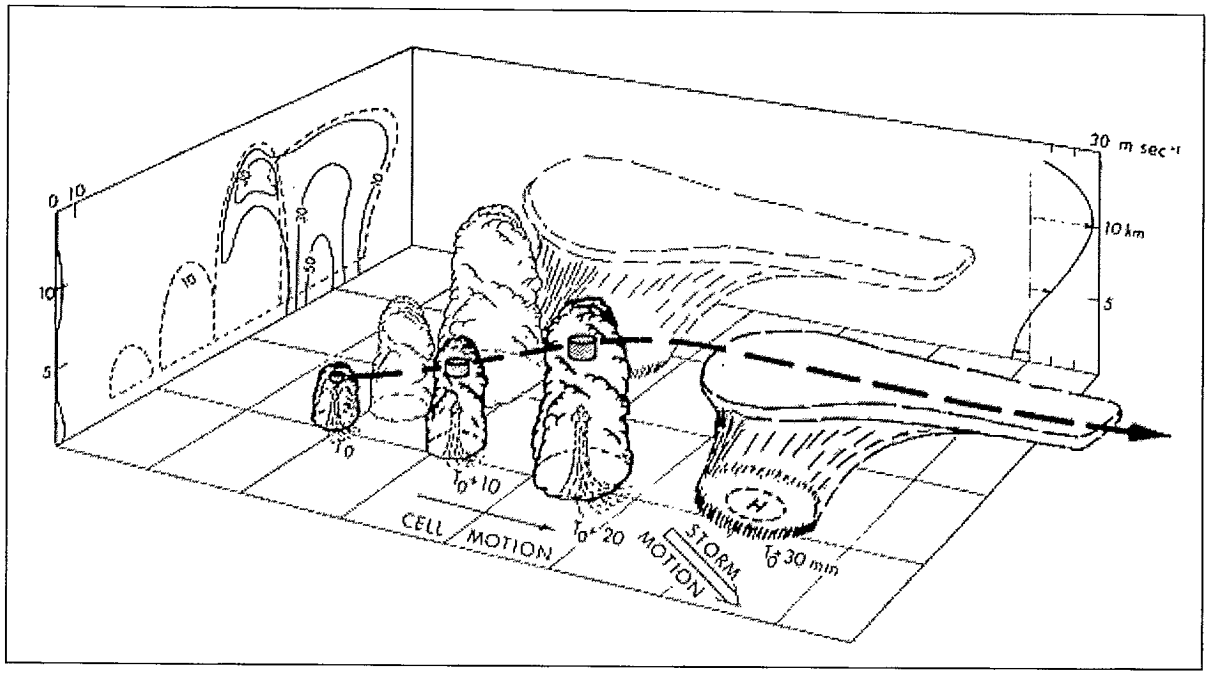

Figure 2.3 Typical wind hodographs for (a) single-cell, (b) multicell, and (c) supercell thunderstorms. Reproduced from Chisholm and Renick, 1972.

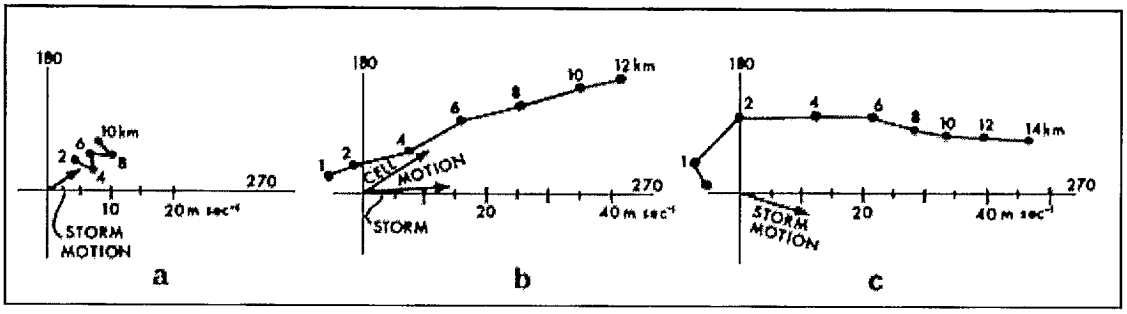

2.1.3 Tornadogenesis Conceptual Models

By the late 1970s, tornadic supercell thunderstorms were capturing most of the attention (and funding) in the U.S. The concentration of effort on the visible, most severe tornadic supercell storms, which are the exception rather than the rule, continued to provide fuel for those who still claimed that such storms reach a stage independent of the larger-scale atmospheric processes, and some claimed that they were therefore not predictable with the current observations systems. An example of this is given by Fritsch and Rodgers (1981), who describe a non-predictable storm that dropped grapefruit size hail on Fort Collins, Colorado. We will show in Section 6.0 how a simple model output statistics (MOS) forecast technique can indeed predict such storms, including this Fort Collins storm.

By this time, conceptual models of tornadic thunderstorms had evolved into complex (yet simplified from reality) systems such as depicted partially in Figure 2.4 (from Lemon and Doswell, 1979). These models now included depictions of the environmental flow around and through the storm, so that attitudes concerning the independence and non-predictability of severe storms would thankfully disappear during the 1980s with research on scale interactions.

Figure 2.4 (a) Schematic plan view of tornadic thunderstorm at the surface, showing the updraft (UD), front flank downdraft (FFD), rear flank downdraft (RFD), and tornado (T) inside the "hook"; (b) schematic 3-D depiction of the drafts, tornado, mesocyclone, and environmental flow for a supercell storm. Reproduced from Lemon and Doswell, 1979.

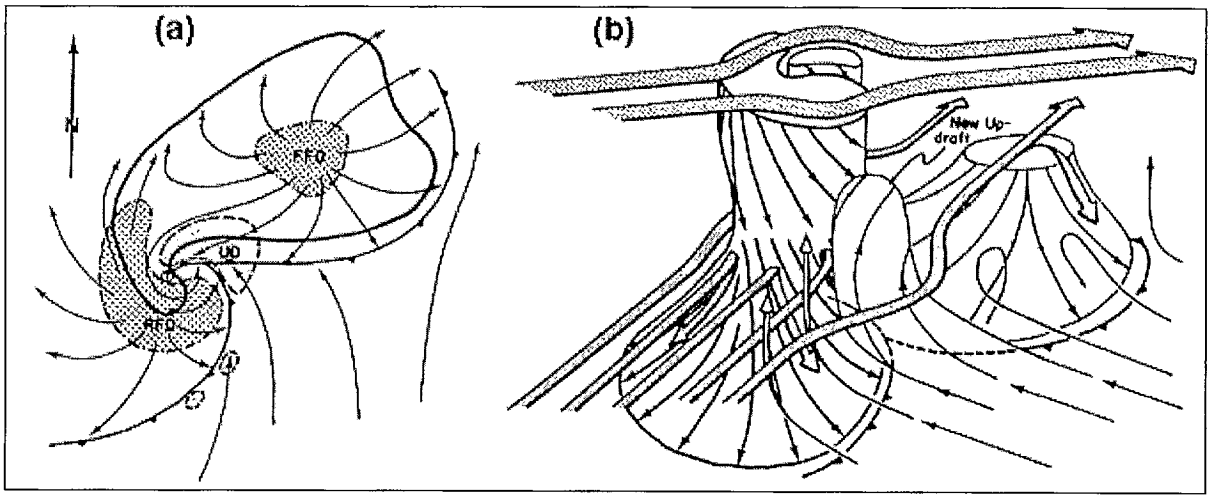

2.2 Thunderstorm Climatology

The term "climatology" is used rather loosely here, not referring to average values over standard climate periods, but rather to include analysis "averages" of many cases to highlight persistent features of a phenomenon under study. This section attempts to summarize, for each of the three Prairie provinces, climatologies of the four categories of *severe* thunderstorm events recognized by the operational forecasting community which Paruk and Blackwell (1993) list as follows: hail greater than 20 mm diameter (walnut size or larger), strong winds with gusts above 90 km hr^{-1}, heavy rain with accumulation more than 30 mm in any one-hour period, and the report of a tornado or waterspout. Other potential climatologies discussed briefly include clouds, satellite data, radar data, and lightning. The largest and most continuous prairie severe storm datasets by far were those collected over central Alberta by the ALHAS/AHP hail research programs initiated by McGill University and coordinated by Alberta Research Council during 1957–85. Climatologies of hail in Manitoba or Saskatchewan, or of other thunderstorm phenomena, are less complete, and are mostly due to the efforts of individual researchers such as Paul (1980, 1982, 1991, 1993), Hage (1987, 1994), and a few operational meteorologists such as Paruk and Blackwell (19983) and Vickers (1996).

2.2.1 Hail Climatology, Alberta

For Alberta, substantial numbers of hail reports were solicited from untrained observers in the farming community by phone and mail surveys after every hailstorm during 1957–85, primarily for the 130 km radius semi-circular area in central Alberta between Edmonton and Calgary shown in Figure 2.5, an area of almost 50,000 km^2. These volunteer hail reports were summarized by Summers and Paul (1967) in a 10-year study, and then updated for the 17-year database of 1957–73 by Wojtiw (1975), and through subsequent ALHAS/AHP annual field program reports such as Deibert (1985). The two earlier studies yielded probabilities of hail on any given day in May through September of 50%, but 60–70% for June and July. Severe hailstorms (producing walnut or larger hail) occur during 15% of the period. Later years reveal similar statistics (see Section 6.4.3 of this report). Wojtiw's (1975) chart for the seasonal distribution of hail days, reproduced in Figure 2.6, reveals that the hail day frequency picks up rapidly between mid-May and early-June, is relatively steady through July, tails off slightly in early August, and then drops rapidly in frequency in September.

Figure 2.5 AHP 130 km radius operations area with coarse topography and synoptic observing sites, including Calgary Airport (YYC), Red Deer Airport (YQF), Rocky Mountain House (YRM), and Edmonton/Stony Plain (WSE).

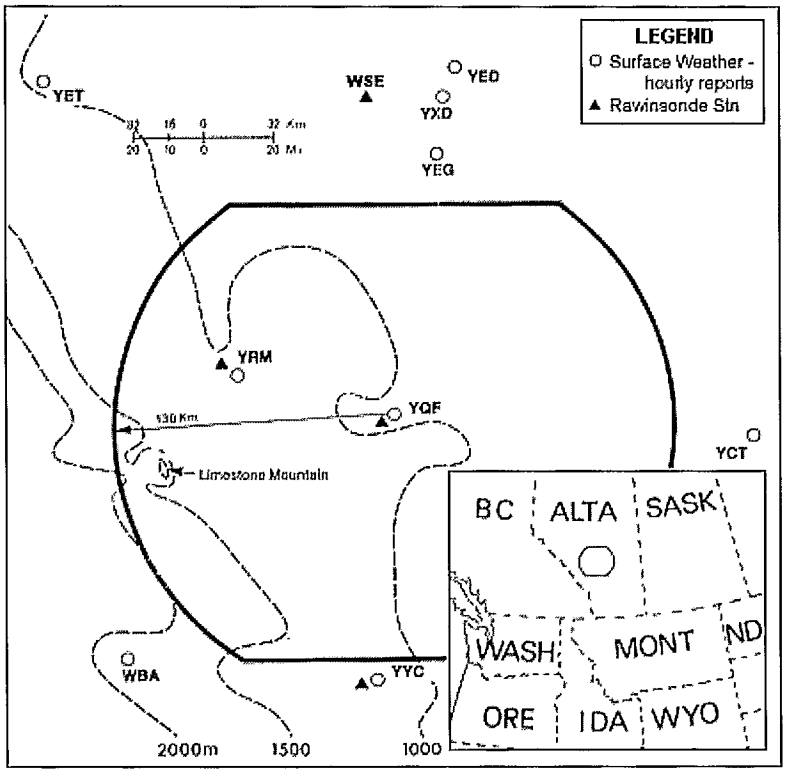

Figure 2.6 Seasonal variation of hail days, 1957–73 (reproduced from Wojtiw, 1975).

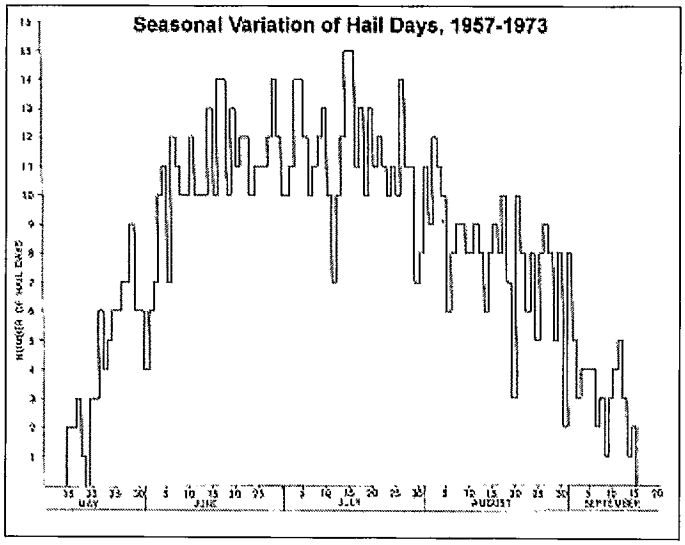

Regional soil moisture and the growing cycle of grain crops have a significant influence on convective cloud processes (and therefore thunderstorms and hail) on the Prairies due to evapotranspiration. More recently, Strong (1997) showed that during a season of high soil moisture, regional evapotranspiration rates averaged 5 mm day^{-1} during July, occasionally exceeding 10 mm. Applying such rates to a boundary layer 1 km deep would increase daily mixing ratios by more than 5 g kg^{-1}, which would increase the potential for convective clouds and thunderstorms very significantly. Similar evapotranspiration rates were given by Raddatz (1998), who also showed that the agricultural development of the Prairies, from prairie grasses with a deep root zone to grain crops with a shallow root zone, has increased the production of convective clouds and thunderstorms during the growing season due to increased evapotranspiration from crops. This would explain the drop-off in hail frequency during early August in Figure 2.6, when grain crops "head out" and transpiration virtually ceases, and a further drop-off in September as other vegetation commences dormant conditions. Related to this, hail and thunderstorm frequencies are lower overall during years of low soil moisture.

Annual *hailswath* maps were routinely produced from AHP hail survey reports (e.g., Wojtiw, 1975; Deibert, 1985). A hailswath was defined as a convective precipitation pattern observed on the surface from which at least six hail reports were obtained. An example hailswath map for 1985 appears in Figure 2.7, on which are super-imposed the discontinuities of the Rocky Mountain barrier (near the western edge of the AHP operations area) and of the foothills region (approximately the western half of the operations area). Two main patterns emerge in every annual hailswath map. One is the not-surprising general west-east direction of hail swaths, dictated primarily by the upper winds, which control storm motion. The second pattern is that the dominant genesis region for these storms is over the foothills.

Figure 2.7 Major hail swaths of 1985 (reproduced from Deibert, 1985). The super-imposed jagged lines are the approximate eastern edges of the main Rocky Mountain barrier and the foothills.

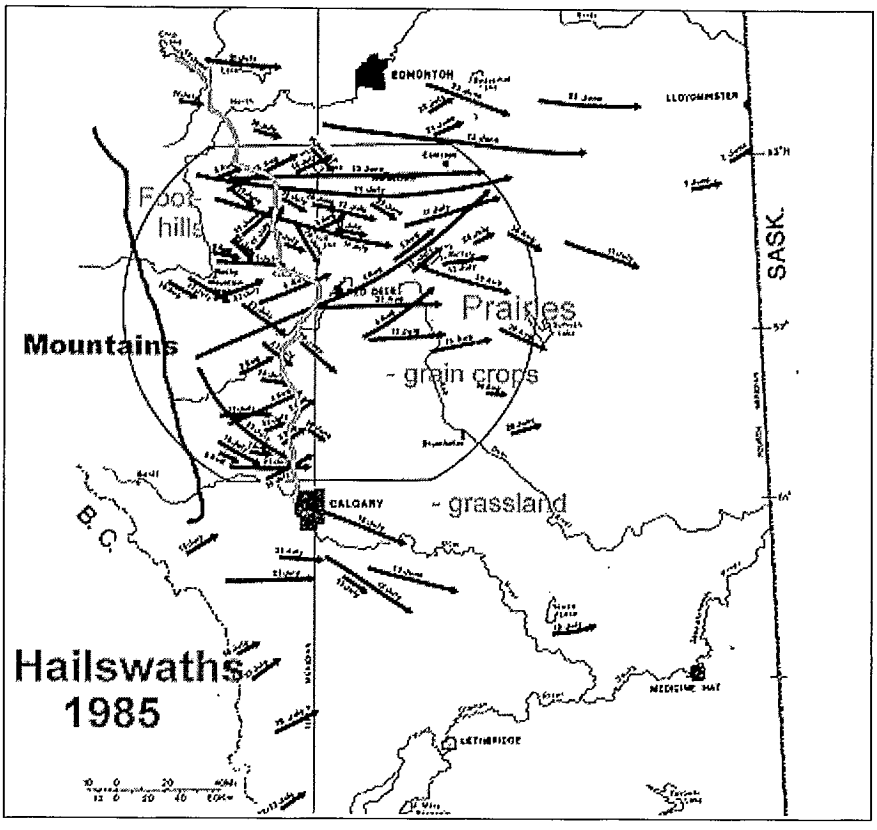

This concurs with a study by Lawford (1970) using Alberta Forestry observations of hail and lightning. He determined that there were preferred areas of storm development associated with the topography, particularly over the foothills of the Rockies west of Red Deer.

Wojtiw (1975) also provided analyses of the spatial distribution of hail day frequency during 1957–73, reproduced in Figure 2.8a. This analysis shows the highest frequency southeast of Rocky Mountain House (RM), with secondary peaks near Sundre (SU) and south of Calgary. Similar analyses using more recent data are consistent with this. Wojtiw noted that hail observing density was as high as one report per 5 km^2 in some instances, or a linear spacing of just over 2 km between reports. This raises the question of how different the pattern might look with coarser data. To test this, Figure 2.8b shows the spatial frequency of hail for the seven years, 1974–80, using only data from regular synoptic stations that have an average spacing in central Alberta of well over 100 km. The coarse pattern is similar in that the main peak shows up over the foothills "somewhere" in the vicinity of Rocky Mountain House. It should also be pointed out that the dense hail surveys on which Figure 2.8a is based would be lacking data where population density was low, that is, over or close to the mountains.

Figure 2.8 (a) Spatial distribution of hail day frequency, 1957–73 (reproduced from Wojtiw, 1975); (b) spatial distribution of hail day frequency, 1974–80 using only data from main synoptic stations as shown.

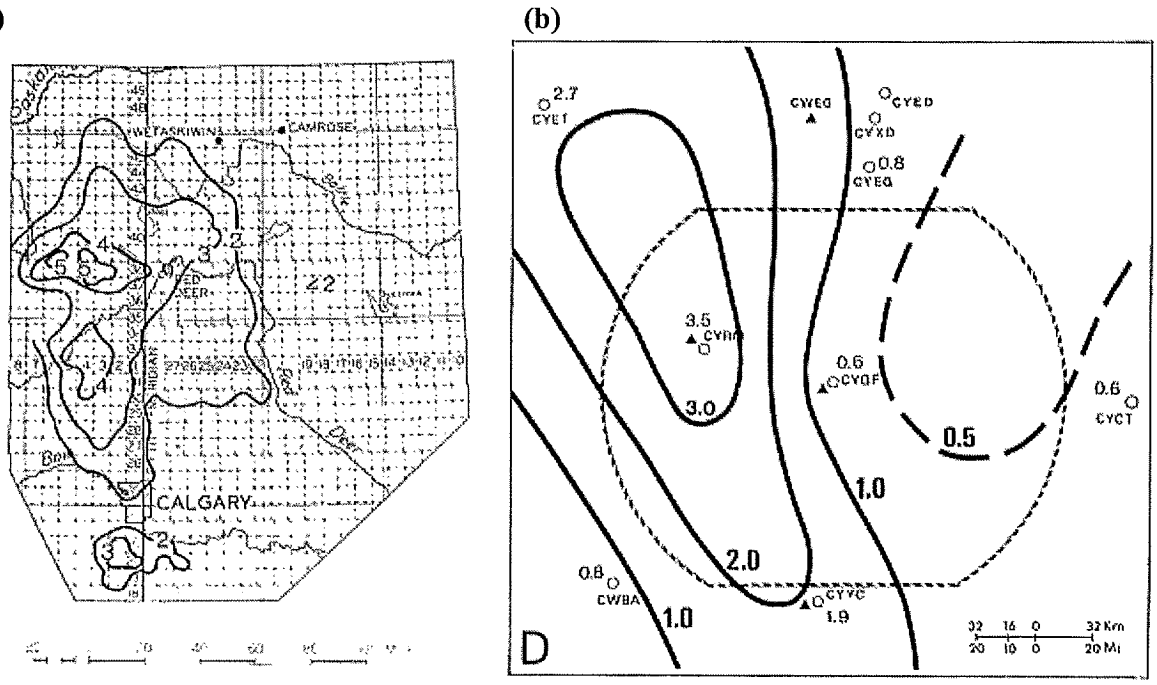

There is always an extra degree of uncertainty in using data from volunteers with little or no training. In particular, since *maximum hail size* is often used as an indicator of *storm severity*, this statistic should be examined more carefully. Figure 2.9 provides a comparison between volunteer reports of maximum hail size from mailed-in hailcards for the 1957–66 database (from Paul, 1967), the 1957–73 hailcard database (Wojtiw, 1975), and from objectively-measured hail sizes from 1973 hailpads (Strong, 1974). The hailpads were simply one foot square pieces of one-inch thick styrofoam covered in aluminum foil (to make dents stand out), and fixed to the ground. Hailpads were calibrated by measuring dents produced by steel balls dropped from a height such as to give them the same impact kinetic energy (KE = $\frac{1}{2}mv^2$) as a hailstone of the same diameter impacting at its terminal velocity. The hail diameters estimated in this objective fashion are considered to be quite accurate, except for the smallest size category (shot size, < 4 mm size), since many of those would not make a large enough dent to be detected. In this comparison, all hailpad maximum hail sizes have been grouped into the same six size categories as for the volunteer reports. The two hailcard reporting periods yield virtually the same size distribution (±1%), but the hailpad size distribution suggests that volunteer observers (mostly from the farming community) tend to over-estimate the larger hail sizes, with over 65% of pads indicating pea maximum size where hailcards suggest <40%. The tendency to over-estimate the larger hail sizes is not too surprising when their livelihood is threatened by hail damage to crops.

Figure 2.9 Comparison of maximum hail size as determined from hail cards, 1957–66 (Paul, 1967), hailcards, 1957–73 (Wojtiw, 1975), and hailpads, 1973 (Strong, 1974).

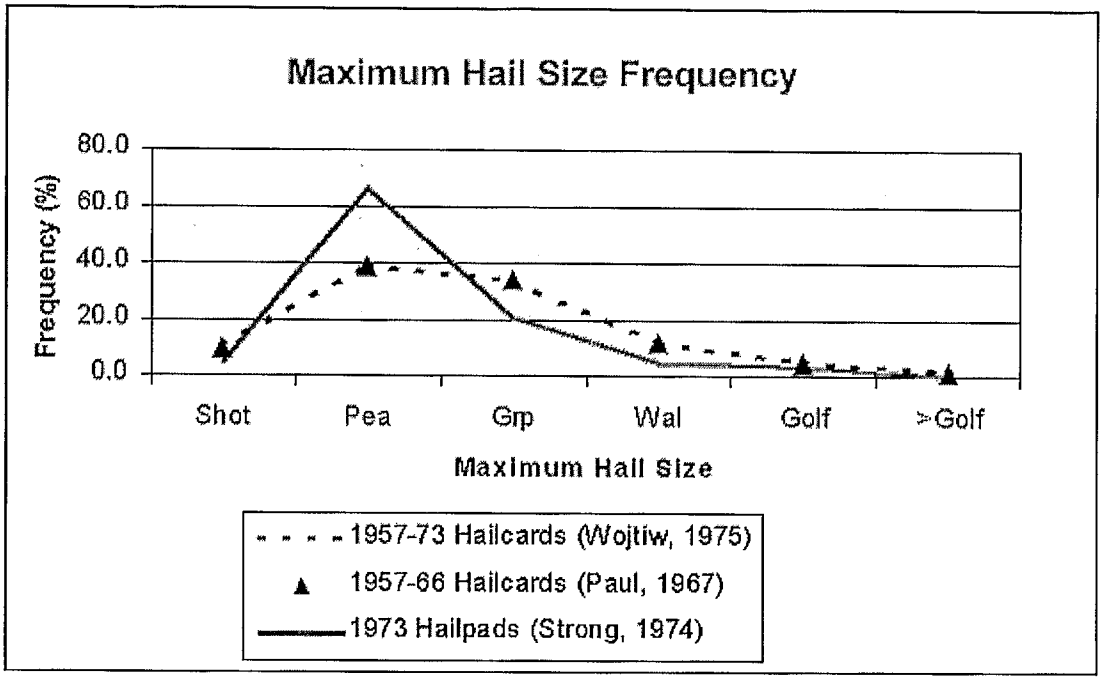

2.2.2 Hail Climatology, Saskatchewan and Manitoba

Paul (1980a) describes a five-year Saskatchewan Hail Research Project (SHARP) study of hail during 1973–77, covering an area of more than 100,000 km^2, about double the area of AHP. Approximately 50% of the days recorded at least one hail report, which translates to a point frequency of half that of central Alberta. It appears that the seasonal distribution differs from Alberta, with May being the peak hail month (July in Alberta), while August experiences just as much hail as July whereas hail tapers off during August in Alberta. Paul (1991a, b), using proxy crop insurance data, discusses Saskatchewan hailstorm durations and hailswath lengths. He observes 76 hail swaths with lengths >150 km, with some exceeding 600 km and persisting from eight to 10 hours. He suggests that such hail swaths may be longer than anywhere else in the world.

There has been no concerted field effort to collect comparable hail data in Manitoba, although LaDouchy (1985) used synoptic station data and crop hail insurance data to study 50 of the most serious hail days during the 1970s.

Etkin and Brun (1999) used synoptic station data for the 1977–93 period to develop an average hail frequency for all regions of Canada. Only the warm season of May through September was included in the analysis in an attempt to remove erroneous hail reports due to ice pellets or snow pellets in the cold season. Based on synoptic data, highest point frequencies were found in southwest Alberta and in the Williams Lake region of British Columbia. For province-wide averaging, the highest average provincial hail frequencies were Alberta (1.04 days),

Saskatchewan (0.82), and Manitoba and British Columbia (each with 0.70). However, their analysis suggests that Alberta has experienced a near doubling of hail frequency from the 1977–82 mean of 0.64 days to a 1983–93 mean of 1.25 days, with no similar increases in any other province.

2.2.3 Tornado Climatology

Tornado reports are far less frequent than hail, but attract significant attention due to their destructive potential such as described briefly in Section 1.0. It is a fact that not all tornadoes are reported – a problem due simply to our low population densities in regions where they occur. Therefore, we treat most tornado statistics as "relative." We can, however, make generalizations such as locations where they are most frequent, or when they are most frequent.

Newark (1984) provided some maps and statistics on tornado F-strength, path length/width, probability of damage, and annual frequency for the period 1950–79, including a composite North American map of annual frequency. The latter shows an extension of the U.S. Mid-West tornado frequencies into southwestern Ontario and southeastern Manitoba. The highest annual probability of tornado damage in Canada is in southwestern Ontario at 0.05–0.1% per 10,000 km^2, followed by southeastern Manitoba at 0.05%, while central Alberta was 0.02%. He points out that the tornadoes of Alberta appear to be distinct from those of the eastern Prairies.

Hage (1987a) completed a 50-year (1910–60) study of 740 Alberta and Saskatchewan tornadoes and over 1200 other destructive windstorms. By considering the total number of tornadoes reported in the seven largest urban centres along with their average areas, he extrapolates to a constant reference area of 10,000 km^2, then computes an average tornado frequency for these locations to be 13.5 per 10,000 km^2 per year – significantly higher than the comparable value for Oklahoma of 3.2 per 10,000 km^2 per year (Kessler and Lee, 1976) – emphasizing how sensitive tornado statistics are to population density. He computes two large area peaks in each of the two provinces exceeding five tornadoes per 10,000 km^2 per year. Furthermore, unlike hail, which peaks during July in Alberta, significant tornadoes appear to have a June peak. Hage (1994) has also produced a large table of tornado, windstorm, and lightning fatality records for the 1879 to1984 period. In a newspaper article, Hage (2000) confirmed popular notions that the frequency of tornadoes in Alberta has increased since the 1980s, but attributes this mainly to increased awareness on the part of both our weather services (MSC) and the general public. He points out that when one considers only tornadoes that cause death, injuries, or destruction of at least one substantial building, then the number of significant Alberta tornadoes peaked at 32 for the 10-year period ending in 1924, and have decreased steadily since then to only six for the 10-year period ending in 1984.

A climatological study of tornado days by Raddatz and Hanesiak (1991) appears to provide conflicting values of tornadoes per 10,000 km^2 per year to those of Hage (1987a). The more recent study, using weather watcher or spotter networks established by the weather service (MSC) in each province for the 1978–89 period, yields values of 0.1 to a maximum of 1.5 tornado days per 10,000 km^2 per year, where Hage's estimates were a factor of five to 10 times larger. However, they used tornado "days" where Hage used "sightings," and their weather watchers each had to cover areas of some 17,000 km^2, which may leave some doubt as to whether all tornado days were observed. The differences simply reinforce Hage's caution on

sensitivity to population density. Both studies indicate similar locations for maximum frequencies.

Cummine and Noonan (2001) suggest that the steady increase in Manitoba tornado reports by decade, from <10 in the 1860s to ~100 during the 1990s, indicates that these reports are increasing more in conjunction with population density and "awareness" than with actual occurrence. The data are thus becoming more complete with time. Manitoba tornadoes have occurred as early as April 17 and as late as October 10. Based on statistics since 1980, the highest risk months are July (33 occurrences) and August (32), and the average season-length for tornadoes is 64 days in Manitoba. The highest risk area for tornadoes in Manitoba is the Red River Valley.

2.2.4 Other Thunderstorm Climatologies and Storm Characteristics

In addition to severe hail (size >20 mm) and tornadoes, Paruk and Blackwell (1993) indicate that MSC includes heavy rain (>30 mm in any one hour) and strong wind (gusts >90 kph) as severe thunderstorm events. They note several problems in the climatology of these four types of severe events. One is that the definition of "severe" has varied over the past 15 years; e.g., heavy rain was previously defined as 25 mm in one hour, severe winds were defined as >100 kph, and prior to 1986, severe hail was 15 mm or greater. Another problem with volunteer reports in particular is the subjective nature of the observation, which can vary depending on the observer's qualitative perception of the event at the time, what other things may be occupying his time, and the intangible degree of stimulation to report the event at the time. Incorrect dates and times are another problem, although these can usually be verified through other related data.

Despite these problems, Paruk and Blackwell compiled a severe weather climatology for Alberta using a compilation of 800 summer storm events occurring between 1982 and 1991. Data were corrected for population distribution, suggesting that there were 300 events (34% of the total number) that went unobserved or unreported each year. The most active hail, rain, and wind events occur in July, while more tornadoes are reported in June. Most events occur around 17:00 local time, except for a maximum number of damaging winds reported after 19:00. There was a high correlation between population density and observations with some known storm tracks evident in the analysis, which was the impetus for correcting the number of observations by using population density. When re-mapped, the axis of maximum severe event frequency shifted away from the Edmonton-Calgary corridor to a line running from east-central Alberta (Oyen) northwest to Edmonton. More frequent events of hail and wind occurred in the foothills as opposed to tornadoes and heavy rain that were more frequent farther east. This is largely due to storm dynamics, with many storms forming over the foothills, then propagating eastward where the later stages of mature storms favour heavy rain over hail, and a few develop tornadoes. While the authors caution use of these data in decision-making, the summary presents an interesting set of severe weather climatology that is more difficult to produce than other climatic variables because of the qualitative nature of the data. Brooks (2000) recommends a similar approach to the Paruk and Blackwell study; that is, to use limited datasets of "high-end" events in which there is more confidence to build statistical models and climatologies. Brooks also discusses the problem of forecast verification using the "low-end," low confidence data. This leads to our final observations and recommendations on this topic as follows.

In a study of non-tornadic severe weather events in southern Ontario for 1980–92, Etkin and Leduc (1994) show an average 68 severe events per year with an expected summertime peak, but then suggest that, because of poor records on severe weather due to their small-scale nature along with varying population densities, that the true number could be an order of magnitude higher. Although the data magnitudes are unreliable, the study did highlight high-risk areas.

Taylor (1999) compiled a 31-year (1966–96) climatology of convective sounding parameters for central Alberta using 4743 soundings released at 0000 UTC from Stony Plain, west of Edmonton. Among the variables processed were convective available potential energy (CAPE), precipitable water, wind shear, storm relative helicity, and other parameters. He stratified some of the outputs according to large and small hail (> or < 30 mm), and severe and non-severe weather days. The CAPE outputs were compared with lightning and hail data.

There is a great need for climatologies of other forms of severe weather data only recently available, which should be more quantitative to deal with than the above studies encountered. The addition of new operational weather radars over the past 10 years now provides near-complete radar coverage of the Prairie regions. In the past five years, Environment Canada has also assembled a network of 81 lightning detector systems, which can pinpoint strikes to within a few hundred meters (Lanken, 2000), including complete coverage of the Prairies. Most strikes are detected by four to 10 stations, and their strength, location, polarity, and time are recorded. Lightning studies such as Williams et al. (1989), Reap (1993), and Moller et al. (1994) suggest techniques to use lightning data to determine the convective state of thunderstorms, detect severe thunderstorms at key surface locations, and to recognize supercell thunderstorm environments and storm structures. Closer to home, Anderson (2000) suggested a technique for predicting rainfall amounts from lightning flash density, but with mixed results. King and Burrows (2000), using 1998–99 data, show persistent lightning flash maxima along the Alberta foothills with decidedly lower counts over the mountains. This confirms inferences made from radar and hailswath data that most Alberta storms form over the foothills, and offers a valuable new dataset for studies of these phenomena. In a follow-up study, Burrows et al. (2001) use Canadian lightning data to develop potential predictors for operational lightning prediction models based on statistical methods. Figure 2.10 (reproduced from Burrows et al., 2001) updates the earlier study, providing a short period (39 month) climatology of lightning strikes across the Prairies. The peak in lightning flash density forming over the Alberta foothills confirms the high incidence of thunderstorm activity there. This analysis also reveals a hot-bed of thunderstorm activity over southern Saskatchewan and the U.S. High Plains.

Prairie-based climatologies of radar and lightning data for one, five, and 10-year periods, along with comparable synoptic surface and upper air climatologies, would provide excellent tools to begin the process of documenting severe weather events. Statistical relations between various predictor variables based on these data should be developed. A quantitative investigation of spatial/temporal similarities and differences in storm characteristics across the Prairies is crucial to investigators and forecasters alike, in order to enable them to distinguish the important characteristics of severe storm situations such as hindsight tells us about Figure 1.1 in Section 1.0 on the Pine Lake tornado case.

Finally, it is unfortunate that one major downside of automating surface observation sites has been the loss of data from a well-developed observing art form – that of cloud types and amounts. Regardless, a cloud climatology of the period prior to complete automation (~ the mid-1980s) would provide additional insight to storm characteristics. With the degree of computing power only recently available, a satellite cloud climatology is also now feasible, and could be designed in such a way as to augment the manual cloud observations since the mid-1980s.

Figure 2.10 Total flash count density (flashes per 100 km^2) for the western Canada region, May 1997 to July 2000, equal area boxes resolution 10 km by 10 km (reproduced with permission from Burrows et al., 2001).

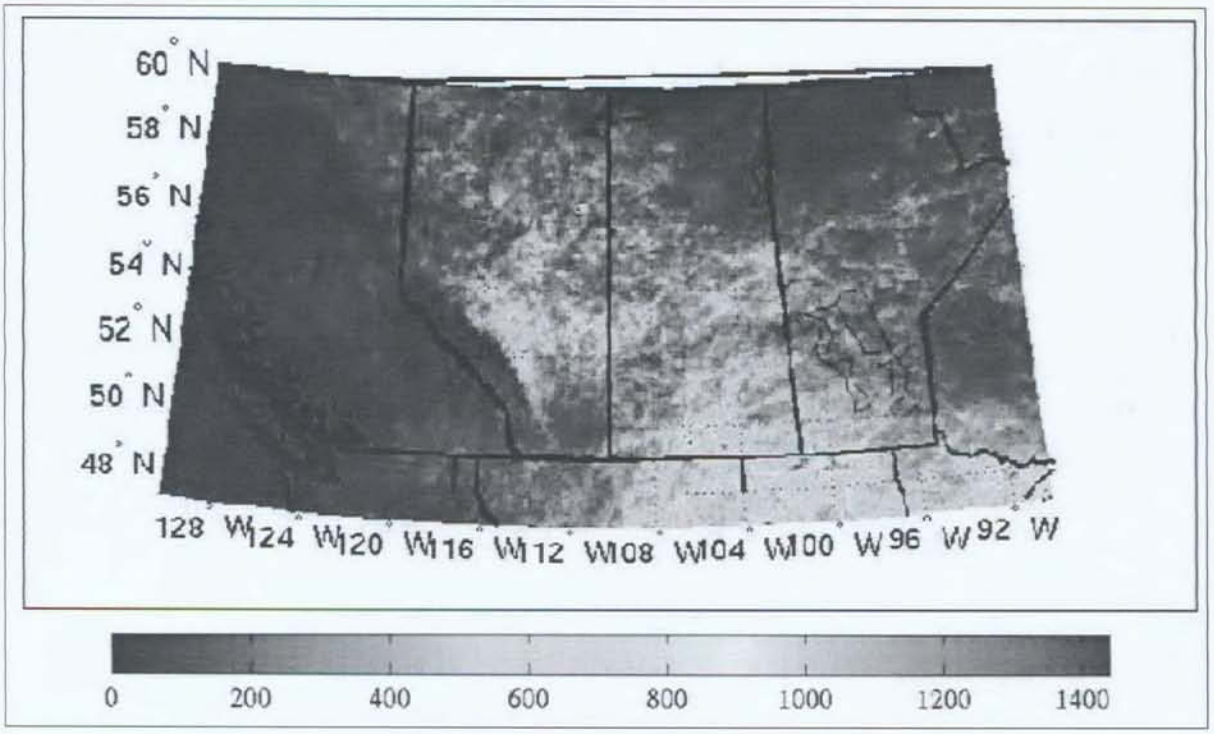

2.3 Storm Environment Climatology

After many years of severe storm research, meteorologists agree that synoptic scale processes organize the mesoscale environment so that convective storms may form (e.g., Fawbush et al., 1951; Beebe and Bates, 1955; Ogura and Chen, 1977; Doswell, 1980). Until the early 1980s, however, some investigators argued that larger thunderstorms, once formed, developed some sort of autonomous mesoscale circulation, moving quite independently of, yet feeding back energy to, the mean synoptic flow. The real mesoscale storm is now known to be far more complex and variable, being intricately tied to synoptic scale processes as well as local microscale effects such as topography and local fluxes of sensible and latent heat feeding the storm. The larger scale processes not only help to initiate the severe storm, but also continue to exert control throughout the storm's life cycle.

The motivation for research into synoptic scale influences on severe storms came not from the research community, but from severe weather forecasters, because of the necessity for improved forecasts of destructive and life-threatening storms. While the need for mesoscale predictions was recognized, progress in developing forecasting techniques was impeded by the lack of resolution of routinely available (upper air and surface) thermodynamic and wind data, which were of synoptic to sub-synoptic scale at best. Partly because of this, early research in this area concentrated on synoptic kinematics, climatological studies, and statistical forecast models, rather than on a theoretical approach.

2.3.1 The "Capping Lid" and Synoptic Kinematics

One of the earliest significant advances here was the kinematic model developed by Beebe and Bates (1955), then of the Kansas City Severe Storms Center. They described how synoptic scale ascent might change a previously stable sounding into the type observed in the vicinity of severe thunderstorms (Figure 2.11). This conceptual model partially explained the role of the *capping lid,*[3] a thermodynamic signature 0.5–1.5 km above ground, which often precedes severe thunderstorms over the High Plains. We look for four main signatures on the capping lid sounding, as indicated in the figure; a moist boundary layer of 500–1000 m deep, capped by an inversion of *potential* temperature (the *lid*), dry air above the lid and a mid-level unstable layer (usually dry adiabatic). The basic role of the lid is to *temporarily* trap moisture within the boundary layer, and to prevent convection and latent heat release. For Alberta severe storm days, early morning soundings (standard soundings are released for 1200 UTC, 0600 MDT) often exhibit only a shallow nocturnal inversion initially. If the lower few hundred meters are moist (sometimes confirmed by morning fog patches), and dry above the inversion, this can change very rapidly during late morning into the type of sounding shown in Figure 2.11. Thereafter, adiabatic cooling provided by synoptic scale ascent can partially remove the inversion, allowing sudden release of the trapped energy, and often an explosive growth of a severe thunderstorm.

[3] The *capping lid* is an important severe storm signature throughout the High Plains regions from Texas to Alberta. The creation and breakdown of the lid, including the role of topography and local fluxes of sensible and latent heat, is important to the overall understanding of severe storms, and is one of the main similarities between storms of west Texas/Oklahoma and those of Alberta.

Figure 2.11 Average pre-tornado sounding emphasizing the boundary layer with *capping lid* temperature (solid line), dew point (broken line), and mean tornado-vicinity temperature sounding (dotted line) following hypothetical profile of synoptic scale adiabatic ascent as shown. Typical upper/lower jet couplings for severe storm cases are also indicated. (After Beebe and Bates, 1955.)

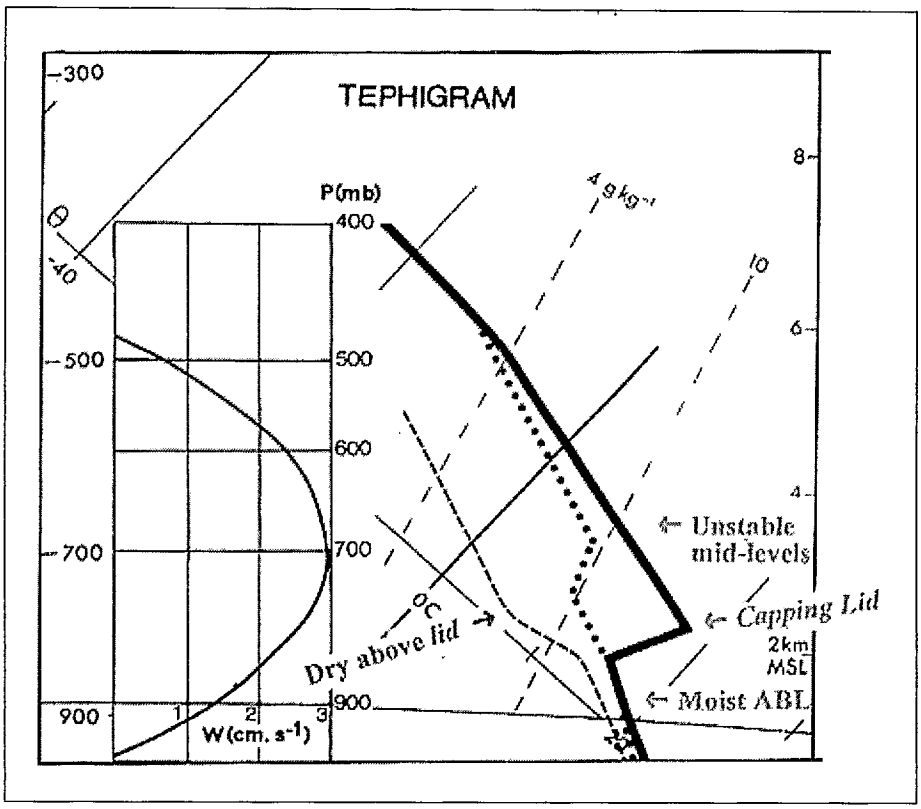

Darkow (1969) confirmed the partial or complete removal of the capping lid in advance of storms, and this has also been established by the LIMEX studies in Alberta (Strong, 1986, 2000). This is further supported by observations of low-level convergence often preceding radar echoes of convection (e.g., Doneaud et al., 1983). The important factor here is that the ascent and cooling, whether it is synoptic scale ascent or otherwise, commences *before* the storm forms.

Closely related to this adiabatic cooling was Beebe and Bates' model of upper and lower jet structures that assist in the release of convective instability. The left exit of a cyclonically curved upper jet, for example, is a preferred region for high level divergence and ascent at lower levels favourable to storm development. The left entrance region of an upper jet will favour convergence, and is therefore likely to be associated with subsidence below this level, not conducive to storms. Upper level convergence would also favour cirrus clouds at these levels, which is one way to recognize its presence in the absence of other data. Often, a low-level jet is also part of the atmospheric structure, slightly downstream from the upper jet core and oriented across it. It will have a similar structure of divergence and convergence associated with it, with low-level convergence favouring ascent aloft. The intersection region where both jet structures favour ascent is the ideal region for thunderstorm formation. In the presence of an anticylonic

curved jet, the favoured conditions for convection are slightly different. Then, divergence is most probable in the right entrance region aloft, with the lower jet beneath or upstream from the upper jet core.

Uccellini and Johnson (1979) quantified these relations between wind jets and convective storms through diagnostic and numerical model results, and provided an explanation of how the upper and lower jets are physically coupled through mass-momentum adjustments and transverse circulations within the exit region of the upper jet. Lemon and Doswell (1979) provided a model of how jet coupling assists in tornado genesis (see Figure 2.4). Thus, the Beebe and Bates models still have relevance to the understanding and forecasting of thunderstorms almost 50 years after their formulation.

Miller (1959) manually compiled synoptic charts for more than 300 tornado days in the United States, and stratified these into five major synoptic map types. The difficulty with this approach is that the types are not always mutually exclusive, while other cases would be difficult to classify at all.

2.3.2 Synoptic Scale Climatology

Synoptic climatology has been one means of investigating severe storms. In Canada for instance, Lowe and McKay (1962) produced climatological charts that imply that tornadoes over Manitoba and Saskatchewan occur primarily along a cold frontal trough, preceding an associated upper (500 hPa) shortwave trough (Figure 2.12. Note the use of *mb* for pressure units in older charts – 1 mb = 1 hPa). Slightly contrary to this, a similar investigation of severe Alberta hailstorms (Longley and Thompson, 1965) provided mean charts that suggest Alberta storms occur predominantly "behind" the low-level trough, in the cold baroclinic zone, but still preceding the upper trough (Figure 2.13).

Figure 2.12 Average 500 and 850 mb (hPa) flow patterns for Saskatchewan tornado occurrences (after Lowe and McKay, 1962).

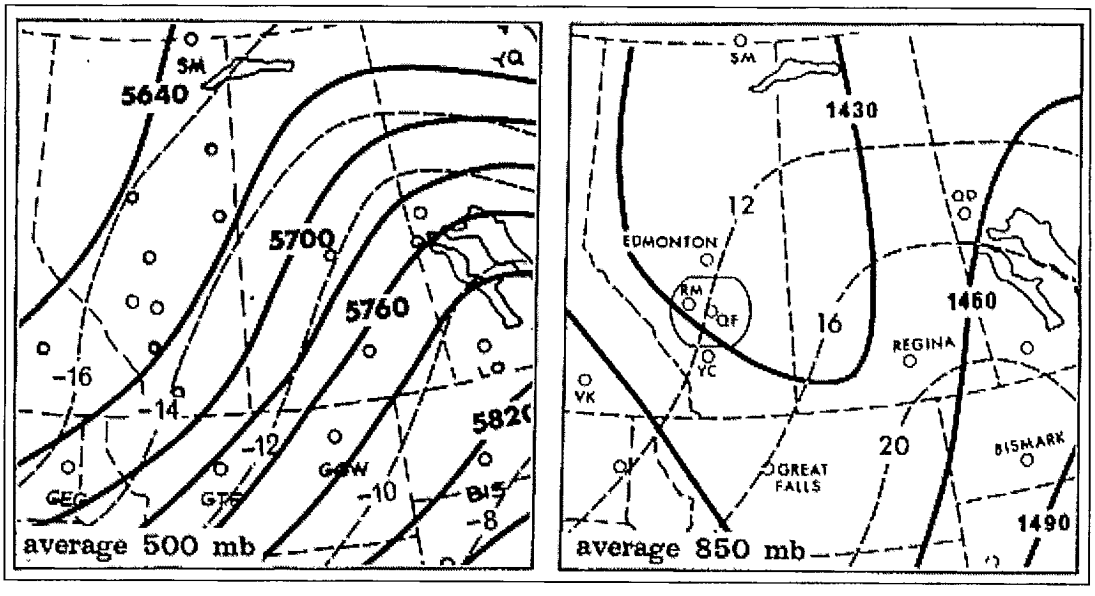

Figure 2.13 Average 500 and 850 mb (hPa) flow patterns for severe Alberta hailstorm occurrences (after Longley and Thompson, 1965).

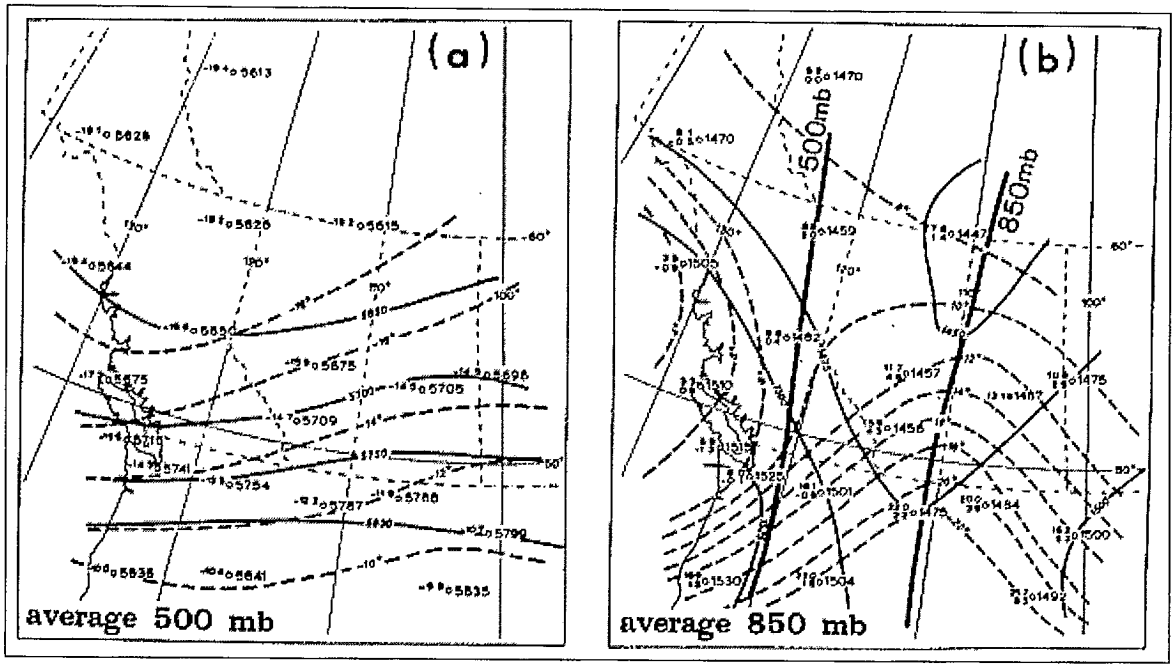

2.4 Example Storm Environment Case Studies

Strong (1981) confirmed that both preferences are not incompatible, and that major Alberta storms tend to occur in "post-cold-frontal" situations, while Saskatchewan can have "cold-frontal" storms on the same day, associated with the same synoptic system. Figure 2.14 is an example of this, with hailstorms in Alberta and Saskatchewan triggered by the same synoptic system on the same day, 21 July 1976 (with Saskatchewan hailswath information compliments of Paul, 1980a). Paul (1991a,b, 1993) documents other such storms, some with hail swaths exceeding 600 km in length. Thus, it is not too surprising that the average flow patterns of Figures 2.12 and 2.13 are quite similar. Because of this, one should avoid classifying convective events, particularly thunderstorms, simply as either frontal or air mass type. Most severe Alberta storms do not fit either classification. A better approach to Alberta storms is to stratify each situation according to the type of synoptic system, with fronts as qualifiers if necessary.

The average climatological patterns of Figures 2.12 and 2.13 can be demonstrated for individual cases. Figure 2.15 shows 500 hPa and surface synoptic charts for (a) the most severe storm days (CDC = +5, or >golf ball size hail), and (b) the most stable non-convective days (CDC = -3) for the three consecutive summers, 1981–83. To summarize these patterns, severe storm days are favourable in central Alberta (AHP operations area, Figure 2.5) when there is an approaching shortwave trough providing a moderate southwest flow aloft and surface cyclogenesis over Alberta, preferably with the low centre south of the storm region giving an easterly upslope ABL flow over AHP. Glickman et al. (1977) confirmed that the effect is enhanced for a negatively tilted upper trough (trough oriented northwest to southeast), partly due to increased coriolis

effect resulting in stronger ascent, and partly because this produces a longer fetch from the south, thereby advecting more moisture from the south. A negatively tilted trough, for example, preceded the Edmonton tornado, and both effects can be seen in figures presented by Bullas and Wallace (1988). For surface conditions, severe Alberta storms are typically post-cold-frontal, that is, the surface cold front (or TROWAL) moves by and thunderstorms form behind it, but in advance of the upper trough. Stable days are favoured with the reverse patterns of an approaching shortwave ridge aloft and an anticylonic surface flow. This type of synoptic *pattern recognition* is extremely valuable for a forecaster, since he/she can make a first guess at a glance, and if the patterns are as clear as these, they are very reliable indicators. The next step after this first guess is to assess atmospheric instability and to estimate how much it will change during the early part of the day.

Figure 2.14 Schematic summary of known Alberta and Saskatchewan hail swaths in relation to the interpolated surface cold front and 500 mb trough at 2100 UTC, 21 July 1976. Arrows indicate hailswath orientations while times are approximate known median hail times for each swath. (After Strong, 1981; Saskatchewan hail swaths were provided by Paul, pers. comm., 1980b).

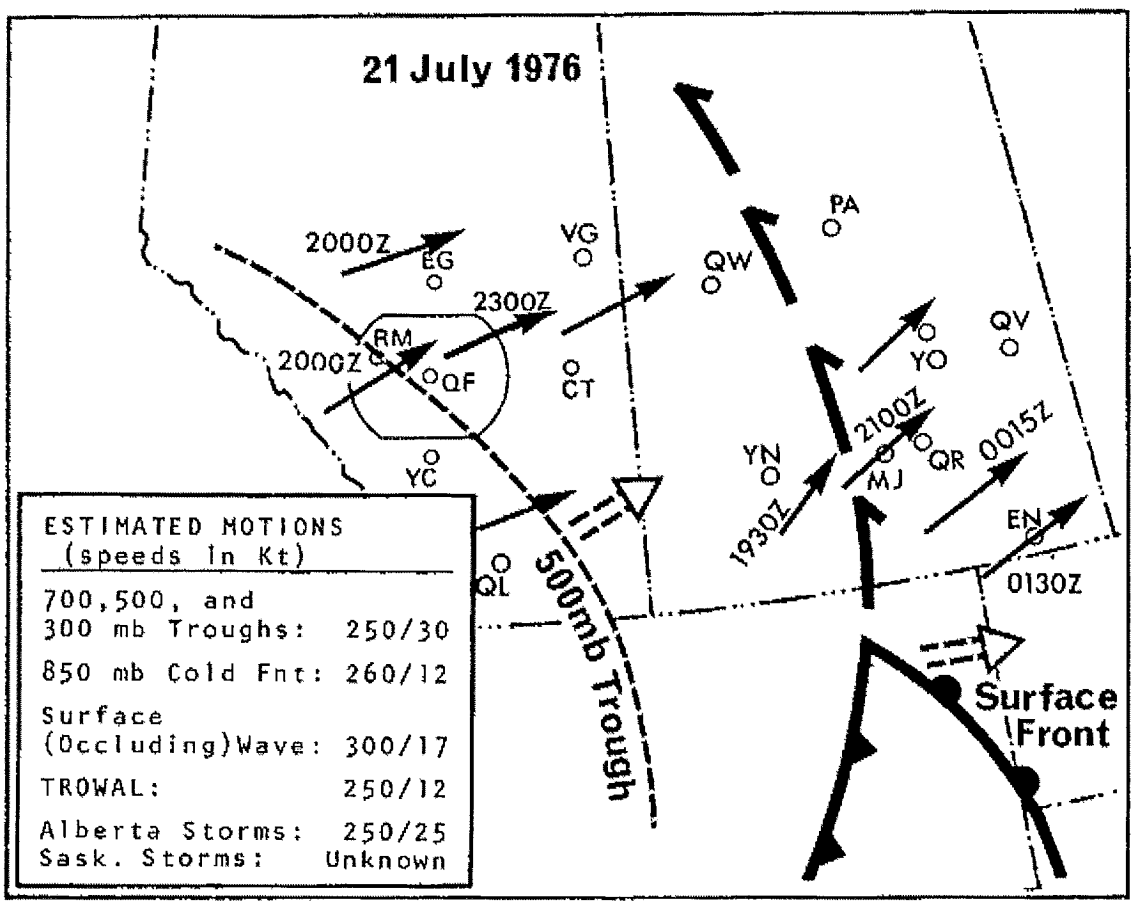

Figure 2.15 500 mb and surface isobaric patterns for (a) most severe hailstorm days, and (b) most stable (non-convective) summer days in central Alberta for 1981, 1982, and 1983.

(a) **(b)**

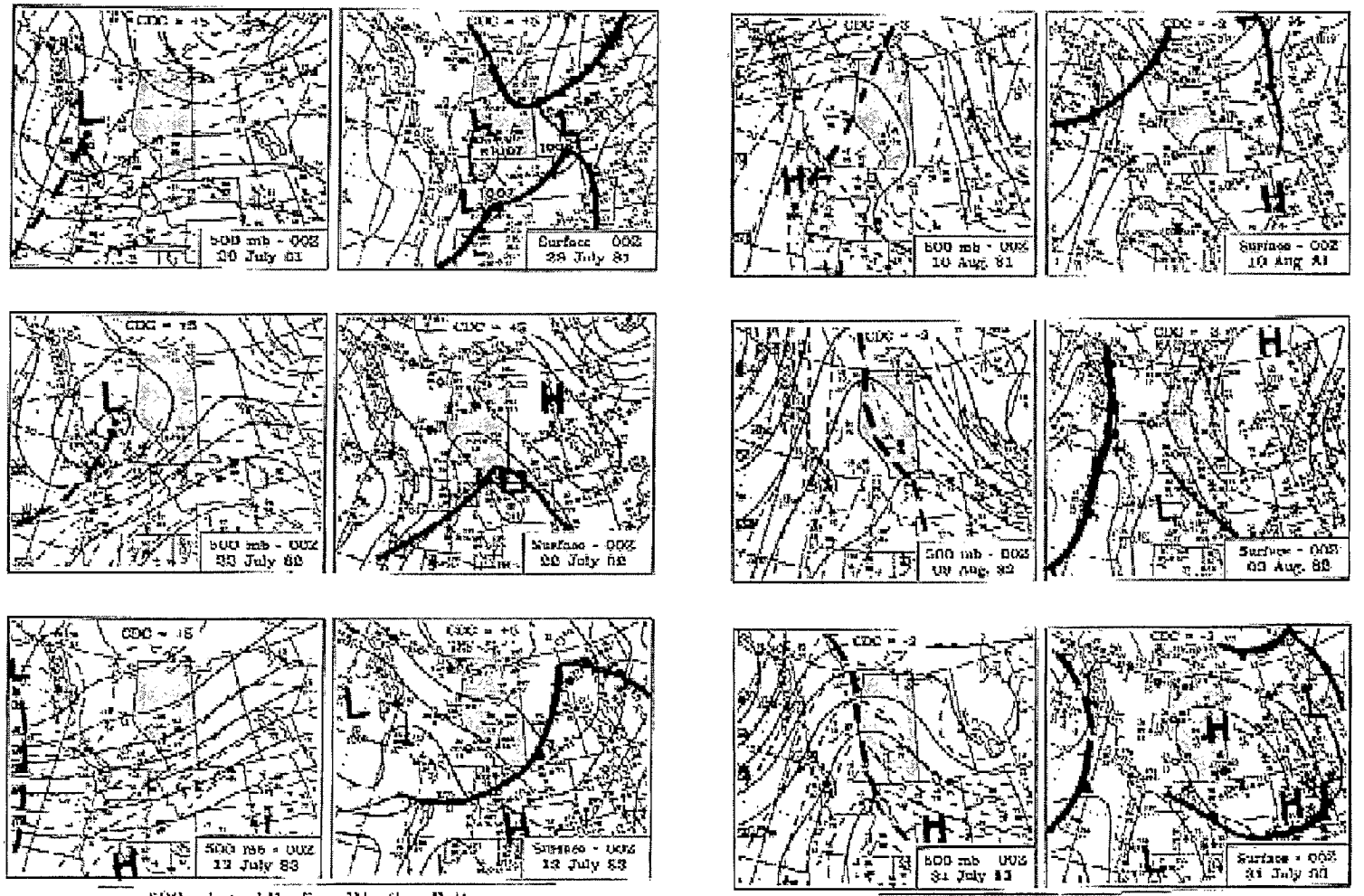

500 mb and Surface Weather Patterns
Severe Convective days (central Alberta)

500 mb and Surface Weather Patterns
Non-Convective days (central Alberta)

Doswell (1980) described similar synoptic patterns for U.S. High Plains severe thunderstorms wherein storms typically form behind the frontal passage but in advance of the upper trough. There are exceptions to all rules, especially when it comes to weather. Occasionally, severe weather occurs in Alberta under rather weak dynamic conditions. Little (1990) documents one such case wherein the main upper feature was an upper ridge building over British Columbia, albeit with a small, weak vorticity maximum superimposed on the ridge. Severe thunderstorms resulted in grape-size hail, heavy rain, and lightning north and west of Edmonton.

Section 2.3 showed climatological average patterns suggesting that a key difference between Saskatchewan and Alberta severe thunderstorms was the tendency for Saskatchewan storms to occur along cold fronts, whereas Alberta more frequently experiences post-cold-frontal storms. Both occur in advance of an upper trough, so that severe storms can occur in both provinces triggered simultaneously by the same upper trough. An example of this was given in Section 2.4 case studies.

2.5 Modification of Thunderstorms

It is not our intention to review the theory and practices of weather modification. Suffice to say, the cloud-seeding hypothesis for hail suppression is based on the cloud microphysical concept of *beneficial competition* (Krauss, 1999). This concept assumes a deficiency of natural ice crystal nuclei in the environment, and that the injection of silver iodide (AgI) will result in the production of a significant number of artificial ice nuclei. The natural and artificial ice nuclei compete for the available super-cooled liquid cloud water within the storm. In this way, hailstones that are formed within the seeded cloud volumes will be smaller and produce less damage if they survive the fall to the surface. Furthermore, if sufficient nuclei are introduced into the new growth region of the storm (see Figure 1.3), then the hailstones will be small enough to melt completely before reaching the ground.

One additional assumption in hail suppression is that the total water vapour available to the storm to form cloud droplets remains a constant. There are some hail suppression opponents who claim that over-seeding can result in significant additional latent heat release in the cloud, which in turn might increase storm dynamics, including the inflow of water vapour to the cloud. That raises the possibility of increasing rather than decreasing hail size, or simply having no net effect. The current Alberta Hail Modification Project, operated by Weather Modification Incorporated (WMI), is funded by private insurance companies under the management of the Weather Modification Society, a non-profit group. While there was no funding allotted for research or evaluation, other than their own examination of hail damage claims, the WMI group are following strict seeding criteria using the very latest information on cloud-seeding practices. Damage claims have reportedly been down overall during the five-year program, 1996–2000, while the insurance companies involved report average loss-to-risk ratios for the first four years of the program, 1996–99, down to 2.4% compared with 4.4% for the previous 18 years – a reduction of 45% (Krauss, 1999). Given that hail damage claims exceed the cost of the seeding program by about two orders of magnitude, a decision to proceed with another five-year program would probably be good insurance in itself.

One area of research that WMI is funding independently is a numerical modeling effort at McGill University that will eventually provide predictions of the size distributions of cloud droplet and ice nuclei in a storm, for seeded or unseeded conditions. If the model can be evaluated successfully, this might provide adequate tools to evaluate the program over shorter timeframes than are traditionally required in a randomized seeding program. Thus, it would be mutually beneficial for any thunderstorm field research in Alberta to collaborate with this program, obtaining cooperative use of their equipment that includes radar, radiosondes, and aircraft data, not to mention on-site expertise of local storms.

2.6 Cloud Photography in Severe Storm Research

Photography has seen limited use in severe thunderstorm research, and may be a forgotten valuable tool. Renick and Douglas (1970) employed stereo-photographic techniques to obtain quantitative measurement of cloud dimensions. Time-lapse photography has been instrumental in validating and documenting the history and lifetimes of new cells that merge into a main thunderstorm from the feeder and shelf cloud zones. Radar still cannot measure returns on as fine a scale as photography allows.

Still cameras and video have been used extensively to document severe storm lifetimes, including that of tornadoes, and these remain the main tools of professional *storm chasers.* Canadian chasers, Arjen and Jerrine Verkaik, have spent their careers doing exactly this, and have produced many important cloud works, including Environment Canada's official "Severe Weather Watcher Handbook" (Verkaik and Verkaik, 2000), and a textbook detailing a survey of two serious tornadoes which struck southern Ontario on 20 April 1996 (Verkaik and Verkaik, 1997), including extensive interviews, photographs, and descriptions of the events. Their collection of fully documented sky photos, with a decided emphasis on severe convective storms and lightning, may be unsurpassed in the world. During the Pine Lake supercell storm (Joe and Dudley, 2000) of 14 July 2000, the Verkaiks happened to be photographing the southwest Saskatchewan storm shown in the GOES infrared satellite image of Figure 1.1. Differences between this storm and the Alberta tornado storm were discussed briefly in Section 1.1. Figure 2.16 shows a visible satellite image of both storm groups, a rear-flank photograph of the Pine Lake supercell with over-shooting top (taken from Olds-Didsbury Airport by Terry Krauss, pers. comm.), and a comparable rear-flank photograph of the decaying Saskatchewan storm, all within one half hour of each other, giving a different perspective on these storms than the larger GOES image of Figure 1.1. Yellow dots (white in grey-scale printing) on the satellite image indicate approximate locations from where the photos were taken.

Figure 2.16 (a) Visible satellite and cloud photos of (b) Pine Lake storm, and (c) southern Saskatchewan storm, 14 July 2000.

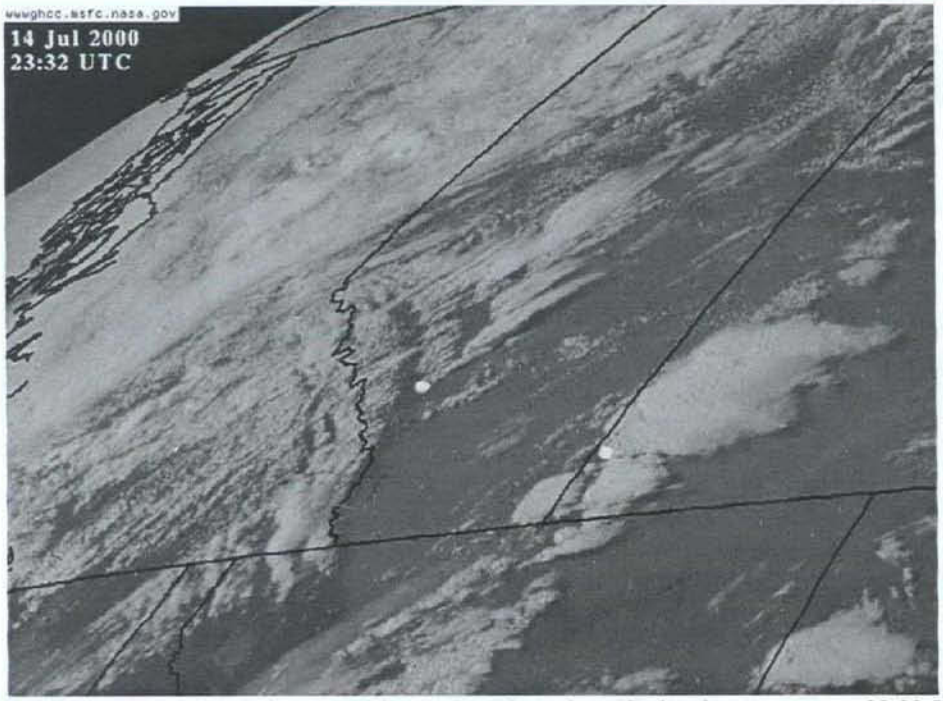

(a) Oblique visible satellite image of central Alberta & and southern Saskatchewan storms, 23:32 UTC, 14 July 2000. Pine Lake tornado storm is the southernmost one over central Alberta; yellow dots (white in grey-scale) indicate locations where (b) and (c) were taken.

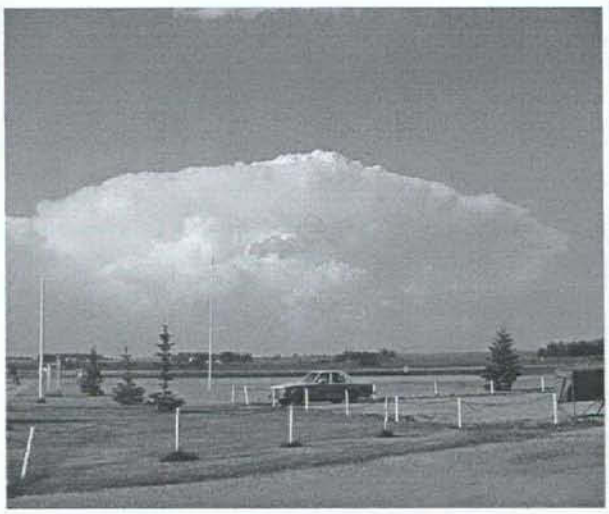

(b) Rear view (from Olds-Didsbury Airport) of Pine Lake Tornado storm, ~24:00 UTC, 14 July 2000 (compliments Dr. Terry Krauss, WMI, Red Deer, AB).

(c) Rear view (from near Maple Creek) of southern Saskatchewan storms, 23:33 UTC, 14 July 2000 (compliments of Arjen Verkaik, SkyArt Productions, Elmwood, ON).

2.7 Summary

Simple conceptual models and climatologies of thunderstorms, related phenomena, and thunderstorm environments were reviewed in this section. Both models and climatologies have great value for thunderstorm forecasting, if only because they provide *pattern recognition* tools for the forecaster – his first line of defence. For example, an approaching shortwave trough and surface low in Alberta during July virtually assures hail-producing thunderstorms. The capping lid, on the other hand, while a critically important feature of most severe multicell and supercell thunderstorms, is not a sufficient condition by itself for such storms. These pattern recognition tools have come about through climatological types of studies such as Longley and Thompson (1965), and through the formulation of various types of conceptual models, many of which we have discussed in this section.

Statistics on severe thunderstorm phenomena such as hail and tornadoes are notoriously inaccurate, since the statistics, especially those on relatively infrequent tornadoes, are often more dependent on population density and "awareness" than they are on actual occurrence. Both of these factors have increased with time in general, although there are many areas of the Prairies, especially in Saskatchewan, where urban populations are increasing at the expense of rural areas. The deadly Edmonton (1987) and Pine Lake (2000) tornadoes have raised awareness of tornadoes tremendously, so that occurrences in that central Alberta corridor are unlikely to go unnoticed.

Some severe thunderstorm climatologies are considered to be both accurate and representative, such as the Alberta Hail Project statistics on hail in central Alberta from 1957–85. Nevertheless, there were regions of AHP in isolated foothill and mountain locations where hail statistics would be unreliable. Remote sensing data on thunderstorms such as radar reflectivity and lightning should provide much more reliable statistics. However, these data, particularly radar, do not yet provide complete coverage of the Prairies, while data are only recently being archived, so that no long-term database exists.

Radar has long been a valuable tool for studying thunderstorm processes. Radar climatologies of prairie storms, together with that of lightning, synoptic surface and upper air data, satellite data, and other sources, should also be valuable for detailing differences and similarities in storm characteristics across the Prairies. It was also pointed out that better use could be made of proxy data sources such as instrumented towers, aircraft data, newer instrumentation systems such as wind profilers and GPS vertical moisture integrators, and finally, of cloud photography. When severe storm research was in its infancy, cloud photography, especially stereo cloud photography and time-lapse photos of storms, were a major tool. There is room for a comeback for this sometimes art form, sometimes valuable scientific evidence.

3.0 Quantitative Atmospheric Processes Research

Big whirls have little whirls
that feed on their velocity,
And little whirls have lesser whirls
and so on to viscosity.
L.F. Richardson (1922)

This above verse by Richardson, who was, in fact, the grandfather of modern-day numerical weather prediction, possibly makes the remainder of this section unnecessary. However, in what follows, we try to provide the theoretical background, less the mathematics, which back these words up.

3.1 Scale Interactions

More than 50 years ago, it was shown that the planetary and synoptic scale processes interact through exchanges of potential and kinetic energy (Starr, 1948; Rossby, 1949). The quote from Rossby (1949) at the start of Section 1.0, regarding the transfer of energy between weather systems, essentially says that you cannot simply model a select portion of the atmosphere, because adjacent weather systems work in tandem. Hence, all numerical weather depiction models have to model at least a hemisphere, and even there, we have errors introduced because of energy exchange across the inter-tropical convergence zone. We find that this energy exchange works between weather entities on different time and space scales as well, including dynamical interactions between synoptic weather systems and mesoscale thunderstorms in their vicinity.

Diagnostic studies since those key works on atmospheric dynamics have confirmed the earlier theories, and have led some scientists, even as early as White and Saltzman (1956), to speculate on possible interactions between the synoptic scale and severe extra-tropical thunderstorm systems. These *scale interactions*, as they have come to be known, include both the downscale and feedback modes of energy in the atmosphere. For example, Sechrist and Dutton (1970) showed that a developing shortwave cyclone, in varying degrees, depending on the weather system, extracts upper level kinetic energy from the mean planetary flow upstream (the *downscale process*), while converting potential energy at low-levels in the atmosphere to kinetic energy of the mean flow at intermediate levels downstream (the *upscale process*).

Apart from several exploratory studies by Kung and his associates at the University of Missouri during the 1970s, diagnostic studies of energetics at the smaller (mesoscale convective) scales have been limited to investigations of energy *feedback* from the severe storm to the mean flow (e.g., Fuelberg and Printy, 1983, 1984). Since frictional dissipation alone cannot account for all of the released latent heat once the storm dies, a feedback of energy to the synoptic scale flow seems reasonable and necessary. However, this does not complete the conceptual model by any means. *Downscale* energy transfers, from synoptic processes to the mesoscale, and especially to the pre-storm environment, were largely ignored until the mid-1980s.

Barnes (1976) reviewed many of the conceptual models of thunderstorms that have evolved over the past century. To a weather forecaster, the most striking similarity in these models is the concentration on the visible, in-cloud processes. There appears to be general agreement that the micro-physical processes involved are essentially the same for the severe storms of Alberta, Colorado, and Oklahoma (Krauss and Marwitz, 1984). However, there was no universal agreement on the relative importance of these processes. Also, models of the kinematics of storm structures and their immediate environmental flow showed marked variations over the important field research period of 1970–85 (e.g., Chisholm and Renick, 1972; Lemon and Doswell, 1979; Krauss and Marwitz, 1984). There was even less agreement on the degree of importance of the larger scale (synoptic) processes in convective storm development.

An important consideration for this review is how scale interactions affect the evolution of convective storms, most critically, how they affect the pre-storm environment of severe thunderstorm systems. To begin, the relative scales of atmospheric motion being considered were already presented and discussed in Section 1.0 (through Table 1.1). The literature review in this section will attempt to show how we arrived at our present level of understanding of scale interactions involving severe storms. This review is necessary background for the conceptual model of scale interactions to be developed in Section 4.0.

3.2 Energetics of Scale Interactions

Long before scale interactions were recognized, it was known that synoptic disturbances, alternately referred to as baroclinic waves or extra-tropical cyclones, experience an increase in kinetic energy as they intensify. Three schools of thought emerged as to how this increase in kinetic energy occurred. The original theory, attributed to Margules (1903), was that the kinetic energy (KE) of a cyclone increased through an *in situ* conversion of available potential energy (APE)[4] by an overturning or readjustment of air masses of different density.

During the 1940s, revelations of the tremendous kinetic energy carried by the upper tropospheric jet streams led to renewed interest in energy conversion processes. Thereafter, Margules' theory ran into trouble when Starr (1948), Rossby (1949), and others showed mathematically that single cyclones cannot be even approximated as closed systems. Rossby explained that this is so because it is impossible to have a KE source in a closed system without also having sinks of KE, *independent of frictional sinks*. Using a scaling argument, he showed that frictional dissipation alone does not account for the total energy sink observed in single cyclones. Rossby's earlier quote and simple observation (beginning of Section 1.0) makes the argument even clearer. Since the same upper winds blow through and around convective clouds and storms of various scales, one may also conclude that similar energy exchanges take place in this instance. Scaling arguments show that the environmental energy flowing into the storm region is of the same order of magnitude as the thermodynamic energy generated by the storm through latent heat release.

[4] Margules (1903) recognized a maximum attainable gain of kinetic energy through the adiabatic redistribution of total potential energy, and called it the *available kinetic energy* (AKE). Lorenz (1955) redefined this as the *available potential energy* (APE), being equal to the maximum amount of the total potential energy available for conversion into kinetic energy under adiabatic redistribution of mass.

Two alternate theories to explain the intensification of cyclones were developed around this time. Charney (1947) and Eady (1949) independently showed that APE of the zonal (planetary mean) flow was converted to (synoptic scale) KE in developing cyclones. But this appeared to be in conflict with Kuo (1949), who demonstrated how the KE of the cyclone could come directly from KE of the planetary mean flow. In one of the earliest diagnostic studies of energetics, Starr (1953) introduced a new complexity. By using hemispheric wind observations, he suggested that the synoptic scale feeds back at least some of its KE to the mean planetary flow, thereby maintaining the latter against frictional dissipation.

These problems were partially resolved by Lorenz (1955), who, by partitioning the APE and KE budget equations into zonal and eddy components, showed that both the Charney/Eady and Kuo theories were possible. Lorenz also emphasized the distinction between frictional and eddy dissipation, by showing that friction alone could not account for the observed energy sink. Consequently, he inferred that there must exist intermediate eddies which hold the balance of energy between the observed synoptic scale and friction. Following the lead of Lorenz (1955, 1960), diagnostic studies of energetics became quite popular, particularly after much of this theoretical controversy had been resolved. The purpose of the diagnostic studies has been to determine the relative importance of the various terms in the energy budget equations. Eliassen (1966) removed any remaining conflict by proving that there were both APE and AKE at both scales (planetary and synoptic) for conversion to perturbation energy of both types, and these could be redistributed either upscale or downscale. Thus, Margules' (1903) original theory was not entirely incorrect either, since synoptic scale APE could presumably be converted to KE at the same scale.

McInnis and Kung (1972) provided the first results showing that these conversions of energy are applicable down to the mesoscale range as well. Thus, at all scales in the atmosphere, one is basically dealing with balances of kinetic and potential energy sources and sinks. In other words, if the winds driven by one scale of motion are *flowing through* some phenomenon at a smaller scale, one can assume that energy exchanges and therefore scale interactions are taking place. This must also be true of severe convective storms, unless one takes the improbable stance that such storms simply float in the atmosphere without any exchange of matter, like a cork on a river.

The Sechrist and Dutton (1970) study diagnosed a case where planetary scale energy was an energy source for a developing synoptic disturbance downstream. The convective studies of Kung and associates suggested similar interactions between synoptic scale flow and downstream convective storms. The Fuelberg studies (Fuelberg and Jedlovec, 1982; Fuelberg and Printy, 1984) demonstrated that a feedback of energy from the storm to the larger scale flow downstream occurs during mature thunderstorms, but they did not investigate downscale effects, perhaps because the Kung group (McInnis and Kung, 1972; Kung and Tsui, 1975; Tsui and Kung, 1977) had run into opposition and controversy on this several years earlier. The Kung results, which indicated that the downscale effect of the larger scale transferring kinetic energy to the convective storm environment might be more significant, at least in the pre-storm environment, are correct. This makes sense since jet stream dissipation at the planetary scale is primarily to synoptic scale eddies.

Irrespective of these studies, both dynamics theory and diagnostic results clearly indicate that thunderstorm activity consumes some energy supplied from the larger scale in addition to that generated through latent heat release. This process is probably most important for the pre-storm environment, while the feedback is probably maximized during the period of maximum convective intensity. These facts will be used in developing the hypothesis for convective storm formation in Section 4.0

3.3 Kinematics and Scale Interactions

3.3.1 Observed Effects of Scale Interactions for Alberta Storm

Thunderstorm kinematics are discussed briefly in Section 2.0 in connection with climatologies and pattern recognition, particularly studies involving the *capping lid* such as Beebe and Bates (1955). We now touch on a few case study examples of kinematics that relate to the current subject of energetics and scale interactions.

Strong and Lozowski (1977, 1980) discussed the fine scale variability of hail impact energy at the ground. These included the pattern of kinetic energy of cumulative hail impacts as measured from the 1973 hailpads. Examples are reproduced in Figure 3.1, showing spatial analyses of impact kinetic energy density on three different scales for a severe hailstorm that hit central Alberta on 16 August 1973 (Figure 3.1a, b) and for a light hailfall in Edmonton on 24 August 1974 (Figure 3.1c). These analyses of impact energy density (in J m^{-2}) are of three different scales for hailpads at (a) 4-km mean spacing, (b) 800-m (½ mile) spacing, and even (c) 0.2-m spacing. Strong and Lozowski (1980) referred to these three different scales of hailfall as *hail swaths*, *hailstripes*, and *hailspots* respectively, although it is possible that the smaller pattern may have resulted from stochastic variations among hailpads.

The intermediate 800-m network, which recorded impact energies of 440 to >2000 J m^{-2} (the latter value being an estimate from a smashed pad) was located within the KE maximum (values >800 J m^{-2}) in the north-central part of the larger 4 km network. To place the impact energies into perspective, Strong and Lozowski (1977) determined from crop insurance statistics, and the damage determined by the insurance adjusters, that the critical value of impact energy that ensured 100% crop loss was 450 J m^{-2}. Beyond this value, damage spreads to buildings, vehicles, and even, in the case of the intermediate network, results in dead livestock. The light hailfall analysis was included to show that maximum *gradients* of impact kinetic energy density in all three analyses are in the range of 5–10 J m^{-2}, (Strong and Lozowski, (1980).

It is not difficult to compute the amount of storm energy dissipated just through hail impact energy alone. The storm had to generate enough energy to create all of this hail and get it up into the clouds. The kinetic energy of impact is one end result by which the storm transfers energy from one scale to another by other than viscous dissipation. The small-scale patterns that we see on these analyses are simply reflections of smaller scale entities within the storm that created the patterns.

Figure 3.1 Impact kinetic energy density (J m^{-2}) for hailpads (a) 4 km mean spacing, (b) 800-m mean spacing, for a severe hailstorm of 16 August 1973 (after Strong and Lozowski, 1977), and 0.2-m mean spacing for a light hailfall in Edmonton, 24 August 1974 (after Strong and Lozowski, 1980). The intermediate 1 mi^2 network (b) was located at the "X" marked within the KE maximum in the north-central part of network (a).

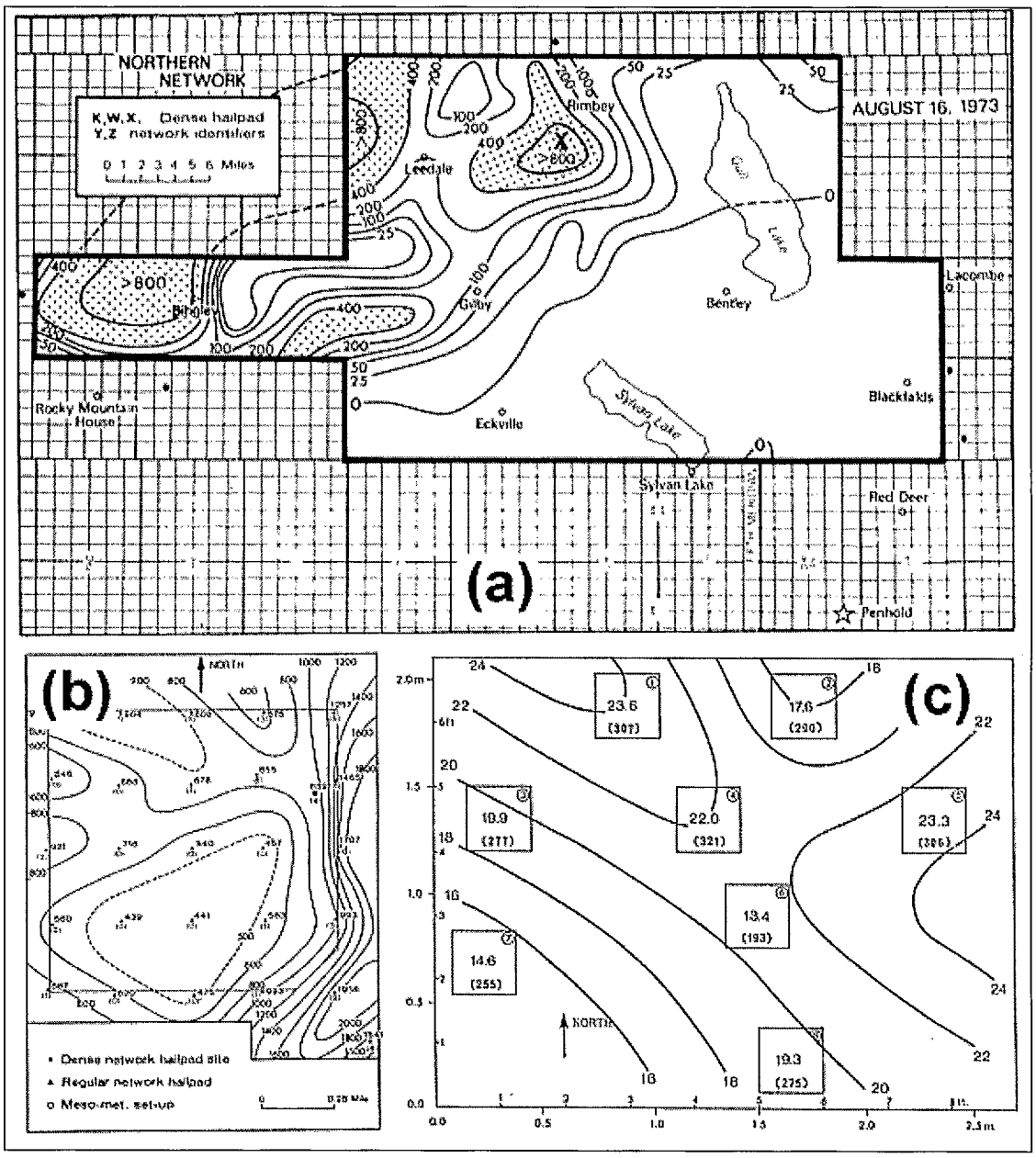

3.3.2 Advection, Convergence and Related Factors

Mesoscale dynamics such as temperature advection, moisture convergence, and ascent have been known to be important to storm formation for at least 50 years (e.g., Miller, 1959). High degrees of air mass instability in the absence of significant dynamics to organize a storm, and to prolong its lifetime, simply results in short-lived cumulus congestus clouds which can create large raindrops, but which fall back in on the cloud, destroying the updraft which created it, and thus ending that convective cycle. This is as close as nature comes to a single-cell storm, which may have a lifetime measured only in minutes, and is typical of tropical convection where often there may be little or no larger dynamics occurring.

Ogura and Chen (1977) documented a severe squall line case with marked capping lid in Oklahoma on 8 June 1966. They found that the lid was raised almost to the lifting condensation level prior to first radar echoes of convection. The process responsible for the lift, and for triggering the severe storms which ensued, was a well-defined band of convergence and lift of about 100 km wide which was present at least 90 minutes before first radar echoes. Furthermore, this was a post-cold-frontal event, similar to the Alberta case documented in Section 2.4.

Chen and& Orville (1980) used a time dependent cloud model to estimate the effects of mesoscale convergence on cloud convection. Their results suggested that to effectively forecast cloud scale convection three to six hours in advance, some knowledge of the mesoscale convergence field was necessary, at least qualitatively if not quantitatively.

Ogura et al. (1982) carried out a detailed mesoscale analysis of severe tornadic thunderstorms developing along a cold front over the Texas-Oklahoma panhandles, which subsequently swept down over the SESAME (Severe Environmental Storms and Mesoscale Experiment) mesoscale radiosonde network on 9 May 1979. This case featured a very prominent and strong capping lid over a wide area, and which they concluded was removed by mesoscale ascent associated with the front. Stobie et al. (1983) studied severe storms on the same day just north of the SESAME network, and concluded that gravity wave trains initiated the convective storms by extracting energy from the synoptic flow through "critical level interaction." Carlson et al. (1983) and Lanicci and Carlson (1983) dealt with this same case and discussed the importance of differential advection, involving mid-level dry air overrunning cool, moist air, in the initiation of severe convective storms in Texas and Oklahoma. Strong (1986) also studied this case and a follow-up SESAME case for 20 May 1979 (detailed in Section 5.0 of this report), focussing on the mesoscale vertical motion fields. He found that both cases were triggered by decaying synoptic systems while the mesoscale systems grew in intensity. This may be an important clue in *scale interaction* considerations.

Honch and Strong (1990) and Brennand (1992) used LIMEX-85 mesoscale upper air data to highlight mesoscale moisture convergence and low-level ascent in the initiation of Alberta storms. Joe et al. (1995) described case studies where Doppler radar data had been used to identify mesocyclones, rear inflow jets, downbursts, gust fronts, and convergence lines associated with multi-cellular thunderstorms in Ontario – all signatures of mesoscale dynamics associated with the storm formation and propagation.

The literature on convective storms over the southern U.S. often associate the *low-level jet* (LLJ) with the top of the capping lid, generally 800–1200 m above ground. Bonner (1968) describes it as primarily a night-time phenomenon, and offered various theories as to its cause, including diurnal oscillations in eddy viscosity, diurnal changes in temperature fields over sloping terrain, and blocking of the large-scale flow by the Rocky Mountains. The LLJ has not been well-documented on the Canadian Prairies, either through lack of data or of occurrences of the phenomena, so that this feature is deferred as a possible important area of future research.

3.3.3 Sensible and Latent Heat Fluxes

Both sensible and latent heat fluxes are essential elements in the development of thunderstorms. Rabin et al. (1990) concluded that the flux of sensible heat, in the absence of significant soil moisture, warms and deepens the atmospheric boundary layer, generally reducing the low-level humidity, and favouring the development of fair-weather cumulus clouds rather than deep convection. Strong (1997), using radiosondes and a 25 km grid mesoscale network in Saskatchewan, estimated evapotranspiration rates from an atmospheric moisture budget technique as high as 10 mm d^{-1} during a period of abnormally high soil moisture during July 1991. It was concluded that regional evapotranspiration from grain crops was a major factor in producing deep convective clouds on the Prairies.

Raddatz (1998) showed that the transformation of vegetation on the Prairies over the past 100 years due to agriculture has resulted in more frequent and probably more severe thunderstorms during the growing season. This is caused by higher evapotranspiration rates over grain crops than over natural prairie grasses. Conversely, convective storms are probably less frequent prior to crop emergence in the early summer, and again during the senescence and post-harvest stages. Raddatz (2000) showed that 25–35% of the total summer rainfall during June to August of 1997–99 was recycled; that is, water that had previously fallen as rain and been recycled through local evapotranspiration. Some of the original precipitation would have been non-convective, while the recycled rain was primarily convective. This suggests that an even greater percentage of convective precipitation may be recycled, so that a major thunderstorm system can greatly influence storms on the following day, contributing to convective outbreak periods.

3.3.4 Drylines

For many years, severe weather forecasters, especially in the United States, have been trained to identify *drylines* as a signature to a severe storm situation. The physics involved was explained by Danielson (1977), who showed that westerly momentum is transported downward rapidly in the deep, dry mixed layer on the west side of the line separating dry hot desert air from moist air moving northward from the Gulf of Mexico, and that this downward westerly momentum can generate severe convective storms.

However, some confusion occasionally arises over what constitutes a dryline for severe convective storms. Fawbush et al. (1951) and Miller (1959) spoke of a distinct "dry tongue" at middle levels, and one rule for predicting the location of severe weather was *where the upper dry tongue crosses over the lower moist wedge.* Carlson and Ludlam (1965), however, clearly define the dryline as *a very rapid transition at screen-level from dew points of 18°C or more in the moist southerly flow to values of 0°C or less on the west side.* Schaefer (1973) described it being

nearly vertical through the lowest 900–1200 m, having a slightly unstable or neutral temperature profile on the dry (west) side, and a low-level inversion or stable layer on the moist (east) side. He also indicated that the dryline exhibits the sharpest moisture discontinuity during the afternoon. Another important point was that the rapid motion of the dryline could not be accounted for by the mean wind across it. McGinley and Sasaki (1975) applied KE and momentum budgets with synoptic data to relate sources and sinks to the occurrence of severe thunderstorms in the vicinity of drylines. They concluded that the process involved on drylines is baroclinic symmetric instability, whereby momentum, assisted by turbulent mixing from surface heating, reaches ground level, increasing surface winds that produce strong local convergence and ascent, favouring thunderstorm development. This process also results in waves or bulges on the dryline, often accompanied by mesoscale surface lows on the dryline and strong westerly wind streaks.

Carlson (1982) emphasized more the effect of differential advection of warm, dry air from the arid elevated Mexican plateau overrunning moist air over Texas and immediate areas. Ogura et al. (1982), describing the SESAME tornadic storm case of 9 May 1979 over the Texas panhandle, observed a well-defined dry line present, but that it did not seem to have contributed directly to the initiation of storms. Studies using satellite imagery frequently refer to the *dry slot* region generally in the southwest quadrant of synoptic cloud systems as regions of potential severe storm formation (e.g., Rockwood and Maddox, 1988). In these cases, the authors are obviously referring to a dryline throughout the troposphere. Parsons et al. (1991) describe the dew point gradient on a west Texas dryline as varying *18°C* or more in distances less than 10 km. Doppler lidar measurements suggested that dryline convergence is intense with maximum ascent rates of 5 m s^{-1}. They observed a retrogressing dryline as hot, dry air overrunning a westward-moving denser, moist flow, with gravity waves observed above the dryline interface.

More recent studies clearly refer to a *surface dryline*, and also relate these to lines of convergence (e.g., Hane et al., 2000). Knott and Taylor (2001) describe an Alberta severe weather outbreak, which they conclude was triggered by a dryline originating in the southwest corner of the province, and then moved northeastward. The ensuing storms spawned three tornadoes: one of F3 intensity, and two of the four severe storms split. Their motivation in this study was to highlight synoptic and mesoscale features that suggest dryline formation, storm genesis, and storm splitting so that forecasters can identify potential severe thunderstorm and tornado hazards.

3.4 Technological Influences on Thunderstorm Research

Severe storm research took major steps forward during the 1970s. While there was a concentration of research on the visible, mature severe storm, two other developments started to direct some focus back to the storm environment, and more recently to the subject of scale interactions. These were the advent of high-resolution satellite imagery, and the operation of several mesoscale upper air networks. Satellite imagery revealed a degree of organization to severe convective storms previously attributed only to synoptic scale features. This included the recognition of large mesoscale convective complexes (Maddox, 1980). When a number of

complexes occur together within a large region, they also show a tendency for synoptic scale organization and influence (as in Figure 1.2 for example).

Mesoscale networks, notably those of the National Severe Storms Laboratory (NSSL – Wilk et al., 1976), SESAME-79 (Hill et al., 1979), CCOPE-81 (Knight, 1982), and LIMEX-85 (Strong, 1989) were designed to study meteorological aspects of the severe storm and its immediate environment, rather than interactions with the synoptic scale specifically. However, they also provided a useful database for scale interaction studies. NSSL data revealed mesoscale organization in the pre-storm environment, which was attributed primarily to convectively-induced surface convergence. Realization of the tremendous amounts of latent heat produced by such storms provoked speculation as to its feedback effect on the larger scale environment. These considerations prompted the design of the SESAME network, which, for the first time, involved simultaneous three-hour releases from the surrounding synoptic as well as the mesoscale network.

Prior to the 1980s, severe storm research was generally directed towards understanding the visible entity, the thunderstorm itself at the cloud (meso-γ) and smaller scales. The pre-storm environment, without any "interesting" clouds, was largely neglected until the 1980s, except by the forecasting community. This trend also influenced technological development for the field, with research emphasis on radars and cloud physics instrumentation with which to measure the visible storm alone, and during the 1980s, Doppler radar and wind profiler systems. Satellite temperature and moisture sounding systems are improving, but still need development work for the critical boundary layer measurements.

More recently, GPS vertical moisture integrators offer the promise of continuous measurements of precipitable water in the atmosphere. Businger et al. (1996) used GPS receivers to detect fluctuations in the dryline and rapid changes in precipitable water consistent with moisture flux convergence. The study also showed that a network of GPS receivers combined with other data sources can be a very valuable tool for short-term forecasting applications. A network of over 40 real-time GPS receivers in the U.S. provides real-time atmospheric remote sensing of integrated water vapour (Ware et al., 2000). This supplemental network, known as the SuomiNet, is expected to contribute significantly to mesoscale diagnostic and modeling research for severe weather forecasting applications, regional climatology, and related areas.

Very little of this new technology has been applied to "prairie" convective storms, with the exception of Doppler radars which are only recently being installed. Some notable studies have been accomplished with older radar technology, such as the reflectivity-rainfall relationships developed from C-Band radar data in Edmonton by Xin et al. (1997).

3.5 Summary

While severe storm researchers for many years concentrated their efforts on the visible, mature severe storm cases for study, forecasters were forced to use basic synoptic scale data sets, yet had to make predictive inferences regarding the mesoscale. At the same time, on a day-to-day basis the forecaster must deal with all ranges of convective weather, not just the exceptional severe storms. As a result, forecasters had accepted the concept of interacting scales more easily and sooner than much of the research community, and carved out a research focus of their own (e.g., Fawbush and Miller, 1953 et al., 1951), albeit perhaps without a deep scientific understanding of the processes involved. Other important contributions to severe storm research from the operational community include the kinematic and climatological studies of Beebe and Bates (1955), Lowe and McKay (1962), Longley and Thompson (1965), Miller (1972), and Maddox (1980). In addition, there have been many useful convective forecasting techniques published, including the various instability indices of Showalter (1953), Galway (1956), Sly (1966), Checkwitch (1971), and Strong (1979), to mention but a few.

Severe thunderstorm research trends finally changed during the 1980s with the recognition of large, sub-synoptic and mesoscale convective complexes (Maddox, 1980). These exhibit organization and circulation patterns not unlike synoptic processes in many instances, and are intricately tied to the latter. Detailed mesoscale analyses of the pre-storm and storm environment are now possible through the use of data sets such as those provided by the 1979 SESAME cases in Okalahoma (Barnes, 1981), CCOPE (Knight, 1982), and the 1980-85 LIMEX data sets of Alberta (Strong, 1989).

There is a great need for research quantifying interactions between the synoptic and mesoscales prior to and during severe convective weather. Such studies have been rare in the past because of the high cost of the necessary radiosonde data at the mesoscale. However, new and emerging technologies such as wind profilers, satellite soundings, and GPS moisture integrators provide means to greatly offset such costs. Scale interaction and related studies required in this area include atmospheric KE, APE, and moisture budgets. The Canadian Prairie situation also calls for field studies to better quantify the roles of local evapotranspiration, drylines, and the low-level jet.

Finally, two issues that have not been emphasized up to this point are (1) *availability of data for research*, and (2) *availability of researchers*. The main point about both of these issues is that there are precious few meteorologists presently conducting research on prairie convective processes; in fact, less than half a dozen in any given year. Some of these are operational forecasters who take the time to write results of a case study or climatological work on storms. Since the demise of the Alberta Hail Project (AHP) in the mid-1980s, there has not been any coordination of research on prairie storms, so that these recent studies tend to be individual efforts, with consequently limited funding. Related to this, access to archived meteorological data, even operational data, is difficult in Canada, so that there is a great need on both these issues to *network* data collection and research efforts, discuss ideas and concepts, avoid duplication of effort, etc. Clearly, current research needs tend towards forecasting applications, stressing the importance of collaborating with MSC regional offices wherever possible. MSC could assist with data access and generating ideas, as well as gaining collaboration for

conducting their own studies, while being direct beneficiaries of research results. Newark (1989) proposed a similar idea, but to our knowledge, nothing has come of that.

Such a network of professional meteorologists focussing on prairie convective processes (or related studies), might best be coordinated through the local Centres of the Canadian Meteorological Society, either through an existing Significant Interest Group (such as the Operational Meteorology SIG), or as a separate prairie entity.

At the same time, there is an urgent need for a coordinated effort to ensure a permanent home for past research data sets, such as those of the long-defunct AHP, which includes the LIMEX mesoscale surface and upper air data. Presently, the AHP data, including LIMEX, aircraft, radar, and hail data, reside at

http://datalib.library.ualberta.ca/AHParchive/

but there are no guarantees of their permanent sanctity. There are other equally valuable research datasets such as SHARP (Paul, 1980a), RES-91 (Strong, 1997), and others that may have no permanent archive. These datasets might best be archived at a permanent centre such as MSC, and might be the subject of discussion for the proposed network, should it come about.

Section 4.0 will describe a multi-scale conceptual model for Alberta thunderstorms, including a hypothesis for the pre-storm creation, breakdown, and role of the capping lid in thunderstorm initiation. This conceptual model was chosen as the focal point for this review. Section 5.0 will present quantitative results of case studies used to test the model, which will be continued into the section on forecasting.

4.0 Multi-Scale Conceptual Model of Alberta Thunderstorms

Before describing the background and hypothesis behind the multi-scale conceptual model of Alberta thunderstorms described in this section, it is necessary to explain some confusion over the source of this model. The model discussed here was initiated in a much earlier article (Strong, 1982), published as part of the author's Ph.D. thesis (Strong, 1986), and again in Strong (2000). The model discussed here was also the subject of a series of field experiments, collectively called the Limestone Mountain Experiment (Strong, 1989), carried out by the senior author in the 1980s while with the Alberta Hail Project. This model borrows heavily from results of several studies of the 1940s to 1980s period; in particular, Byers and Braham (1949), Beebe and Bates (1955), Lowe and McKay (1962), Longley and Thompson (1965), Chisholm and Renick (1972), Kung and Tsui (1975), Lemon and Doswell (1979), Maddox (1980), Carlson et al. (1983), as well as early field tests using radiosondes during LIMEX-80 (Strong, 1982). The confusion arises over a surprisingly similar conceptual model of Alberta thunderstorms published by Smith and Yau (1993b), formulated on the basis of their own analysis of LIMEX-85 data provided by Strong (1989). Since this later model describes few, if any, differences from Strong (1986), we proceed here with background based on our earlier model.

The two previous sections reviewed a wide field of meteorology from planetary scale dynamics down to cloud micro-structures. Until recently, the only links connecting these scales of motion were made through studies concerned with forecasting convective storms. We now recognize the interactions between these scales, but still do not understand the processes involved. A starting point in developing this understanding is to investigate those severe storms where the relation between synoptic scale and mesoscale processes appears most obvious. Some of the possible dynamical interactions between large scale processes and convective storms were addressed in the literature review. Kinematic links are fairly obvious in the conceptual model of Figure 2.11 described in Section 2.3 presented by Beebe and Bates (1955), and in the mesoscale forecasting capability illustrated in Section 2.4. A scale interaction hypothesis for Alberta hailstorm conditions is now presented, supported to some degree by examples from two severe hailstorm cases. These are used along with the foregoing review to formulate a conceptual model of convective storms, linking them more closely with synoptic scale processes. The hypothesis will then be tested on severe storm cases from Oklahoma-Texas and Alberta in Section 6.0.

4.1 Background Research and the *Capping Lid*

4.1.1 Topography

The Alberta Research Council (ARC) Hail Project (AHP) summer operations area of approximately 130 km radius during 1974–85 was described in Figure 2.5, which shows locations of main surface and upper air observing sites, along with schematic topographic contours that locate the major mountain barrier (Rocky Mountains) over the extreme southwest portion of AHP. This barrier runs from south-southeast to north-northwest through Alberta and northern B.C. The foothills region, 40–80 km wide east of this barrier, is generally thickly forested with patches cleared as grazing pasture. It contains numerous smaller mountain peaks, mostly 10–25 km east of the barrier. The plains area east of the foothills consist mostly of grain crops during summer, which transpire copious amounts of water into the atmospheric boundary layer (ABL) at rates varying from 1–10 mm day^{-1} depending on the availability of soil moisture

in the top 10 cm, an important factor in the generation of convective clouds. Thunderstorm activity tapers off on the Prairies when grain crops "head out" and effectively stop transpiring moisture, or when the top layer of soil moisture is depleted, whichever comes first. The effect was noted in the hail day frequency plot shown in Figure 2.6.

The LANDSAT mosaic photo of Figure 4.1 shows the topographical variations across the mountains and foothills region of southwest Alberta, emphasizing the discontinuity between "foothill peaks" such as Limestone Mountain and the main Rocky Mountain barrier. The three photos of Figure 4.2, looking north-northwest, west-southwest, and south-southwest from Limestone Mountain ridge, show much the same thing from a different perspective. Under southwest flow conditions, the barrier leads to a narrow band of strong subsidence, generally between it and the foothill peaks. Storms therefore tend to form on the east slopes of the foothill peaks.

Figure 4.1 LANDSAT view of Alberta mountains and foothills region, including (1) main Rocky Mountain barrier; (2) Limestone Mountain; (3) marks eastern edge of foothill peaks; (4) town of Rocky Mountain House at confluence of North Saskatchewan and Clearwater Rivers.

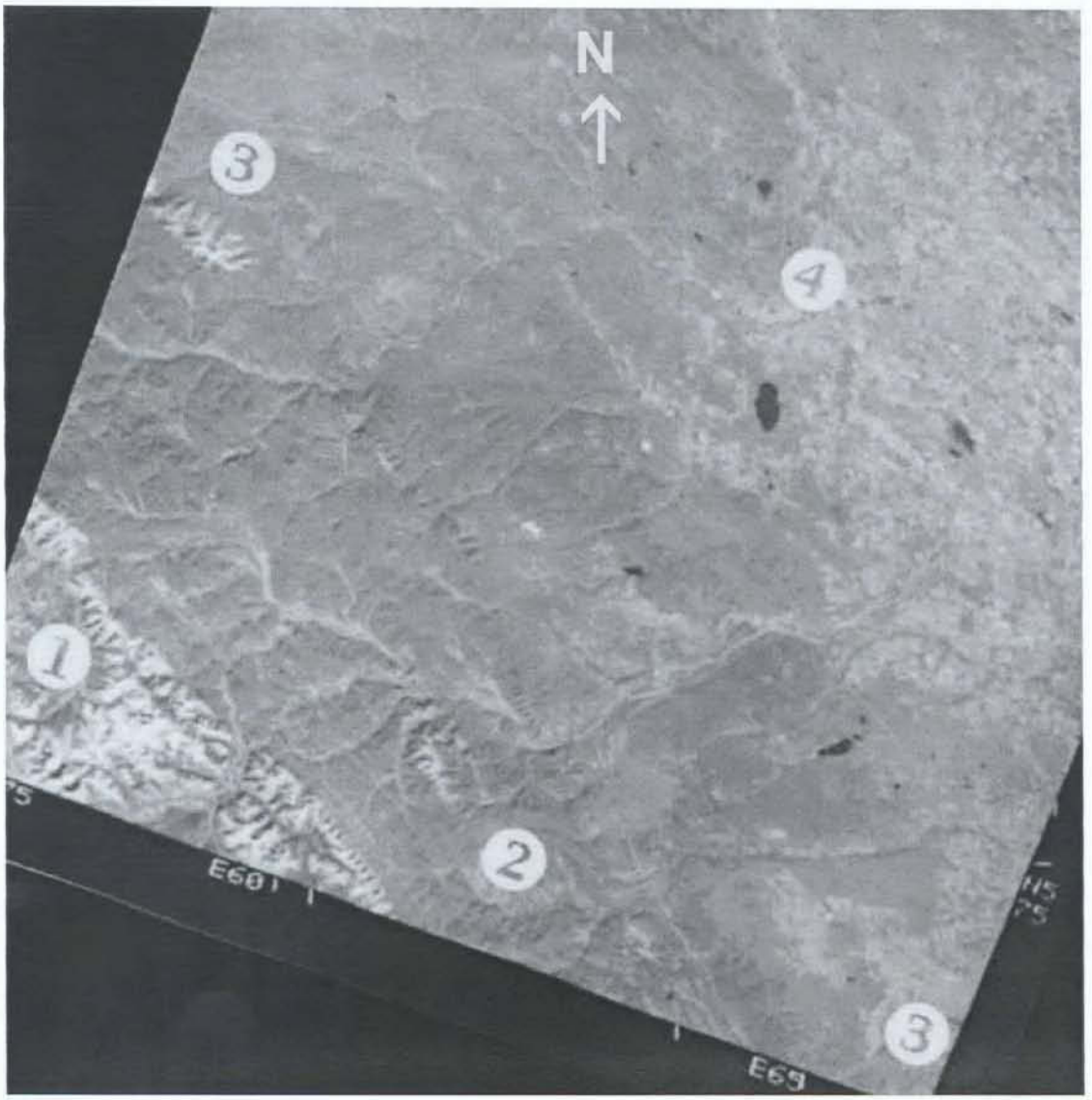

Figure 4.2 Views of main Rocky Mountain barrier from the foothills, in this case, Limestone Mountain ridge looking north-northwest, west-southwest, and south-southwest. Photo location is on the ridge just northwest of number 2 in Figure. 4.1.

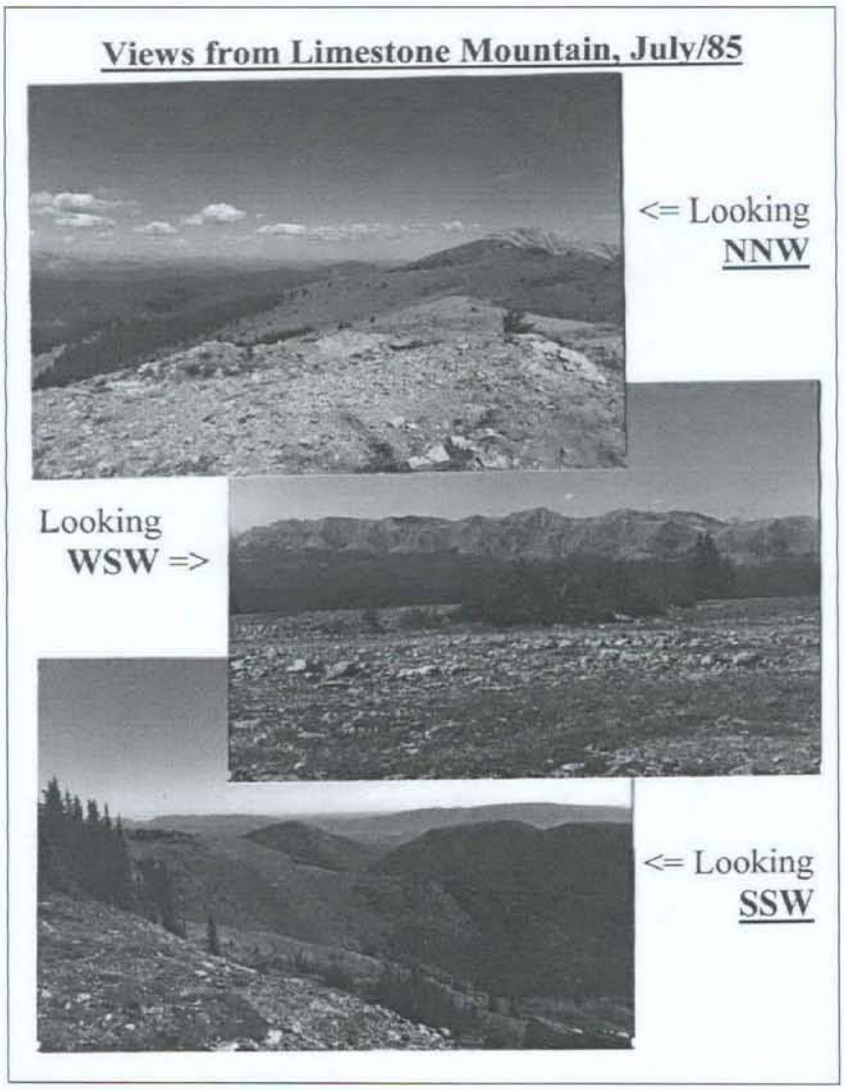

4.1.2 Meso-γ (Cloud) Scale Patterns for Convective Storms

It is worthwhile exploring some important and identifiable patterns at the meso-γ (cloud) scale that will signal either the impending development of a thunderstorm or no significant convection. These cloud patterns, which have theoretical basis in the preceding discussions (such as the synoptic kinematics discussed in Section 2.3.1), are identified here as either positive or negative factors, which are not sufficient alone to predict a storm or no storm, but can be used in conjunction with other factors; a few examples, not meant to be exhaustive, include the following:

Negative – Observations of cirro-stratus (CS) clouds invading the sky from the west.
Positive – Observations of alto-cumulus castellanus (ACC) clouds, especially towards the west or southwest, and especially during morning.
Negative – Observations of alto-cumulus lenticularis (ACSL) clouds, especially towards the west or southwest.
Positive – Morning observations of cumulus congestus (or towering cumulus, TCU) clouds, especially towards the west or southwest.

Cirro-stratus is visual evidence of significant upper-level convergence and probably mid-level subsidence, unfavourable conditions for convective development. CS cloud layers have the additional negating effect of suppressing insolation at ground level. A layer of AC cloud is a clear indication of mid-level ascent. ACC clouds, especially if observed during morning hours, further indicate pre-existing mid-level instability, and if persistent, may not require much surface heating before they grow into a thunderstorm. ACSL clouds are frequently observed over the foothills, and indicate a strong mid-level jet and near-laminar flow conditions, with little ascent at these levels except within the lenticular clouds. The very strong shear associated with this structure also tends to suppress the updrafts vital to organized mesoscale convection. Needless to say, existing TCU clouds are very conducive to a thunderstorm, since very little further surface warming (or cooling aloft) continues to add to the convective intensity. These four cloud patterns are indicated in Figure 4.3.

Positive – Evidence of an unstable air mass; this requires a graphical plot of temperature and humidity versus height or pressure (a tephigram), such as exhibited in Figure 2.11 in Section 2.3.1. There we noted four positive signatures on the capping lid sounding: a moist ABL of 500–1000 m deep, capped by an inversion of temperature (the *lid*), dry air above the lid and a mid-level unstable layer (usually dry adiabatic). The ABL becomes well-mixed with daytime heating, and often gains moisture through evapotranspiration and moisture convergence; i.e., a constant mixing ratio with height develops in the ABL.

Positive – Wind directions veering from light easterly (or northeast) at the surface to southwesterly above the ABL, and increasing speed with height. The reader can refer once more to the schematic wind hodographs of Figure 2.3 for typical multicell and supercell wind profiles.

Positive – In Alberta, there is a strong tendency for storms to form over the foothills, and less frequently over the plains or over the higher mountains west of the foothills. During the Alberta Hail Project (AHP) cloud-seeding operations of the 1970s and 1980s, first radar echoes of the most severe storms were frequently recorded over the foothill peaks such as Limestone Mountain, approximately 110 km west-southwest from Red Deer Airport (Strong, 1986, 1989). This is demonstrated partly by hailswath maps produced by AHP, the last of which (for 1985) was shown in Figure 2.7.

Figure 4.3 Photos (left to right) of cirro-stratus (CS) clouds invading the sky from the west, altocumulus castellanus (ACC) at western (left) edge of receding AC layer, altocumulus standing lenticularis (ACSL) clouds, and tower cumulus (TCU), evidence of negative, positive, negative and positive factors respectively for thunderstorm growth.

(from WMO International Cloud Atlas, 1969)

(from WMO International Cloud Atlas, 1969)

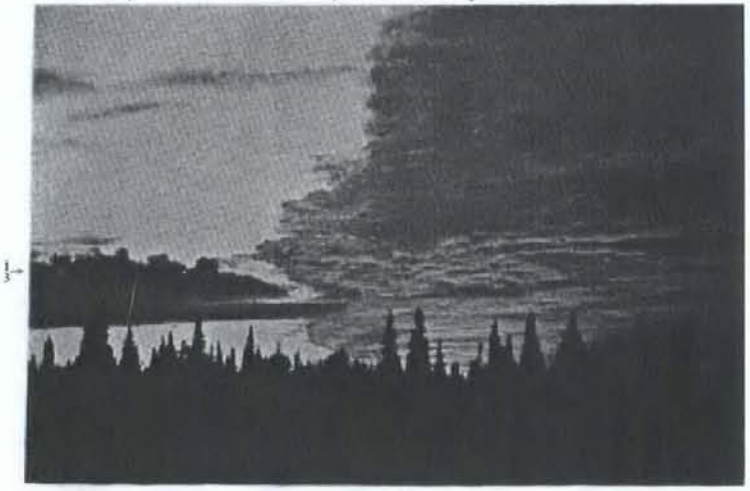

(from WMO International Cloud Atlas, 1969)

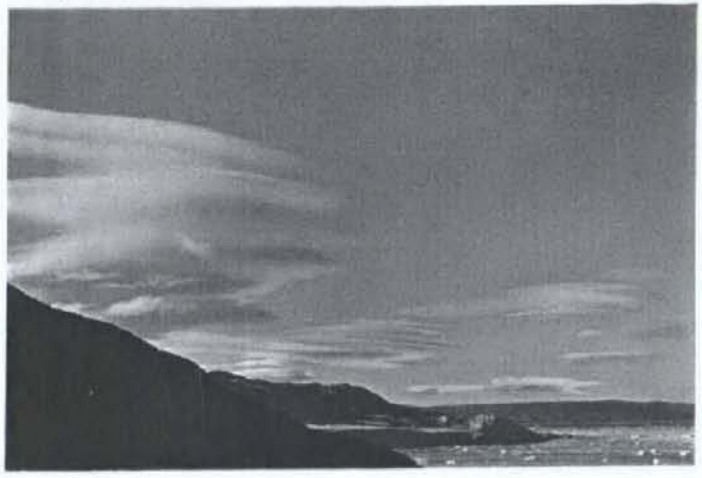

4.1.3 The Capping Lid and a Severe Alberta Hailstorm Example

Figure 4.4 shows late afternoon soundings for two consecutive days, 15–16 August 1973 at Rocky Mountain House (YRM, at location 4 in Figure 4.1). Both soundings indicate distinctive capping inversions around 800 hPa, typical of the pre-storm environment for all High Plains regions, and similar to the average pre-tornado sounding of Figure 2.11. The soundings alone provide no real clue as to why convective weather failed to materialize on the first day (August 15), while a particularly severe hailstorm (with hail as large as baseballs) occurred on the second day (August 16).[5] This storm commenced southwest of the upper air site shortly after the sounding release. The storm-day sounding, in fact, is more stable than that of the first day. For this case, it is clear that the capping lid must be at least partially removed at some time prior to storm initiation.

Figure 4.4 Representative sounding of dry bulb (solid line) and dew point (broken line) temperatures for 2400 UTC, August 15, and 1330 and 2400 UTC, August 16 1973. The curved line is the estimated cloud adiabat (Theta-W); the dotted line for August 16 is the post-storm temperature trace at 1200 UTC the following morning.

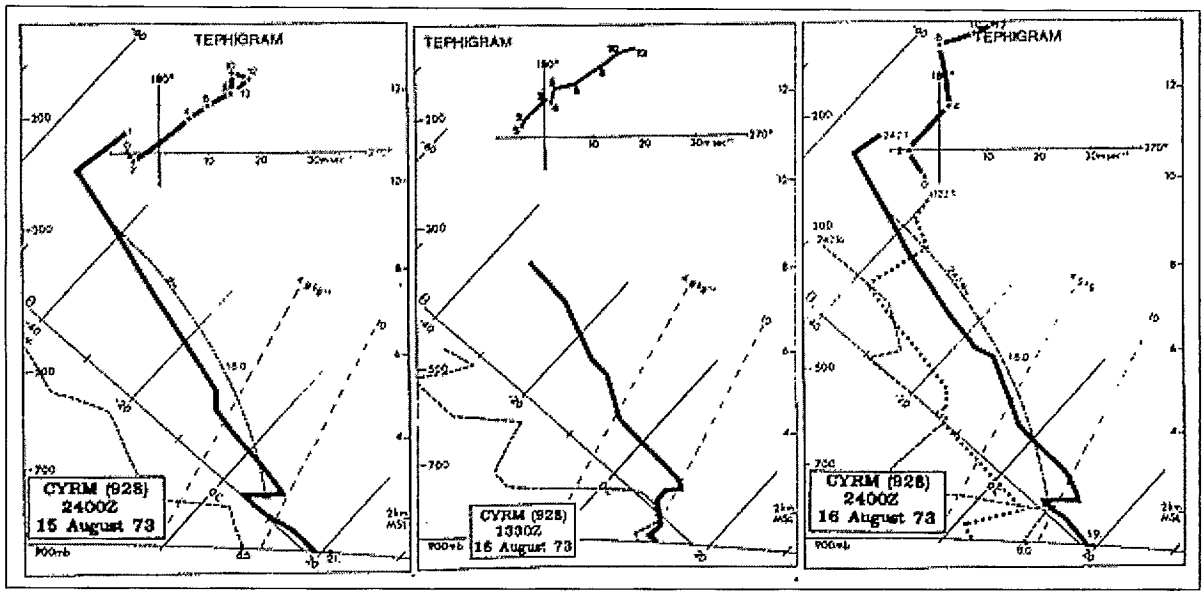

The 500 hPa analyses (Figure 4.5) for these two days do show a clear distinction between the two cases at the synoptic scale, as well as clues to the formation and removal of the capping inversion. On the first day there was a shortwave ridge upstream, with associated subsidence over Alberta, a surface high pressure cell, and generally dry air. The ridge had moved by on the second day, and it was replaced by an approaching shortwave trough, strong PVA (for the time of year), large-scale ascent, surface cyclogenesis, and moist surface air. Note that the trough on August 16 has a significant negative tilt of the type mentioned in Section 2.4, enhancing the

[5] The hailfall severity of this storm has been documented by Strong and Lozowski (1977), synoptic conditions by Strong (1982, 1986).

ascent on the east side of the trough, a requirement for removing the lid in Figure 4.4 prior to storm initiation.

Figure 4.5 500 mb and surface analyses for 2400 UTC, 15–16 August 1973.

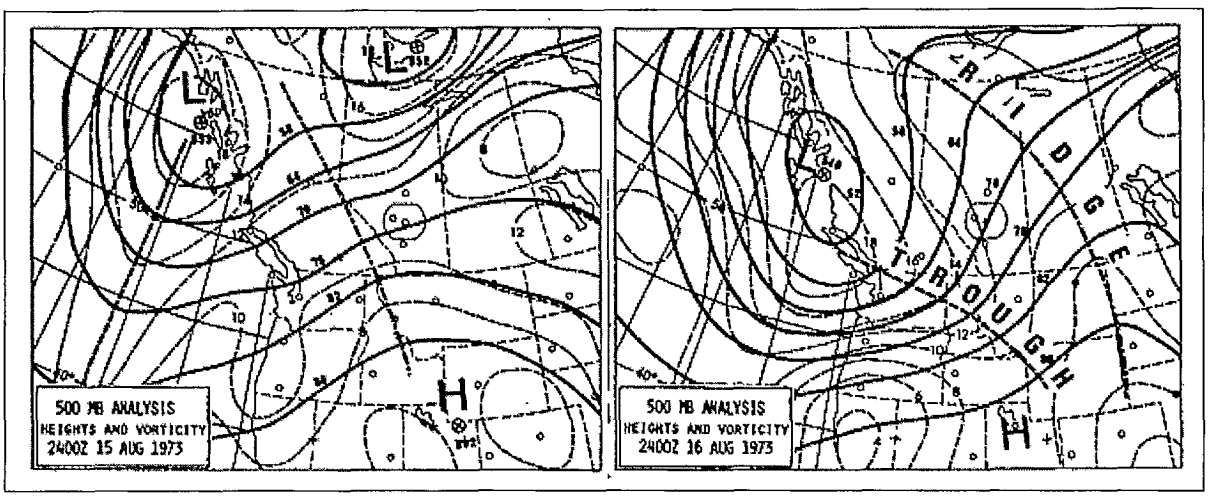

4.2 Hypothesis for the Conceptual Model

Based on the patterns discussed thus far, and supporting material in severe storm literature, a conceptual model of thunderstorms incorporating all scales of atmospheric motion is now presented, with special emphasis on Alberta storms. This is presented as a sequence of events in seven main stages, using hypothetical diagrams of upper air and surface flows patterns (Figure 4.6), and a schematic vertical cross-section of dynamic and thermodynamic features (Figure 4.7).

Stage 1: Early Pre-Storm Lid Preparation

1. The pre-conditions for a severe convective storm are usually prepared a day or two before the storm. An upper shortwave ridge (Figure 4.6a, top) initiates the process at least one day prior to the storm, providing large-scale subsidence warming at middle levels of the atmosphere, while also maintaining anti-cyclonic conditions at the surface (Figure 4.6a, bottom).

2. The subsidence warming at middle levels, combined with cool air in the boundary layer, results in the beginning of the *capping lid* (Figure 4.7, top).

3. As the upper ridge moves over central Alberta overnight, mid-level winds back from northwest into southwest (Figure 4.6b, top), enhancing the subsidence through orographic downslope flow in a relatively narrow band just east of the main mountain barrier, generally over the foothills.

4. Clear skies overnight allow for surface radiation cooling, strengthening the *capping lid* effect. When surface humidities are high, fog patches are a common occurrence near

dawn in these instances (Figure 4.7, top). The fog becomes an additional source of moisture for the later storm.

Stage 2: Late Pre-Storm Lid Formation

5. Clear skies under the surface high later in the morning (Figure 4.6b, bottom) allow surface heating to start warming the boundary layer (Figure 4.7, bottom). The foothills will tend to warm more rapidly through differential heating caused by the angle of sunshine onto the elevated slopes.

6. By mid-day, the next upper shortwave trough is approaching Alberta from the B.C. coast (Figure 4.6c, top), and this initiates surface cyclogenesis (low pressure) over the southern Alberta plains region (Figure 4.6c, bottom), with subsequent ascent in the boundary layer and an increasing easterly component of wind and moisture convergence over the foothills.

7. Meanwhile, orographic subsidence continues close to the main mountain barrier, with subsidence warming often extending down to near ground level close to the mountains (Figure 4.7), while the capping lid can intensify over the foothills during this period due to the beginning of ascent and resulting cooling of the boundary layer.

8. Over the plains region, grain crops, with a shallow root zone (mostly in the upper 10 cm of soil), contribute significant amounts of moisture daily to the atmosphere through evapotranspiration, and this is often a contributing factor in moisture convergence over the foothills.

Stage 3: Pre-Storm Lid Breakdown

9. By early afternoon, this moisture convergence and easterly winds over the eastern slopes of the foothills results in upslope flow along a narrow band (Figure 4.7), with the moisture under running the lid. This enhanced ascent begins to work at breaking down the capping lid over the foothills by gradually cooling the top of the lid through adiabatic lift and cooling, creating "preferred lid weaknesses" at select locations depending on the degrees of ascent and moisture convergence.

10. Below the lid, daytime heating has continued to warm up the boundary layer, and together with continued evapotranspiration and moisture convergence, these increases in sensible and latent heat continue to raise convective instability beneath the lid over the foothills.

Stage 4: Storm Initiation

11. The final breakdown of the lid over the foothills occurs quite rapidly in the more severe convective cases. Storms form within minutes where previously there may have been almost clear skies. Because of the capping lid, convective potential is released suddenly and with great fury, rather than latent heat being dissipated slowly throughout the day.

Figure 4.6 Hypothetical upper air and surface charts leading to the formation and subsequent breakdown of a capping lid over southwest Alberta due to synoptic scale and orographic dynamics, and subsequent severe thunderstorm.

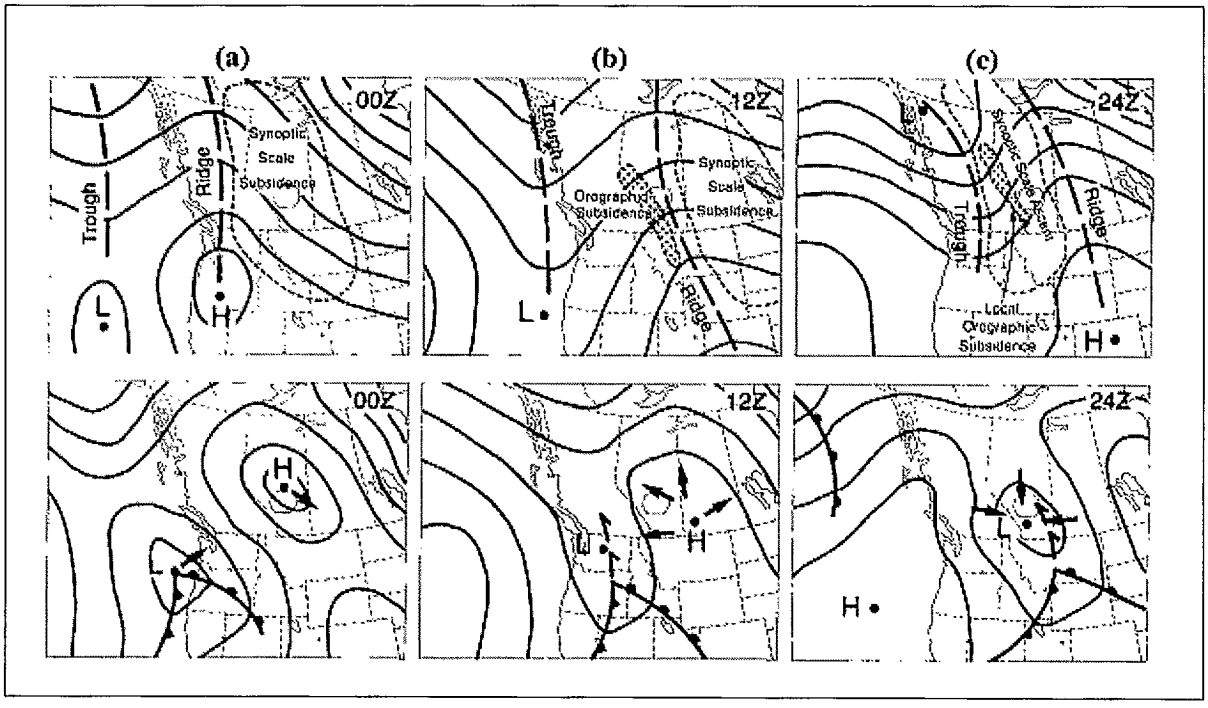

Figure 4.7 Schematic vertical cross-sections illustrating the formation of the capping lid through synoptic scale and orographic subsidence, then breakdown of the lid through boundary layer ascent, followed by rapid development of a severe thunderstorm.

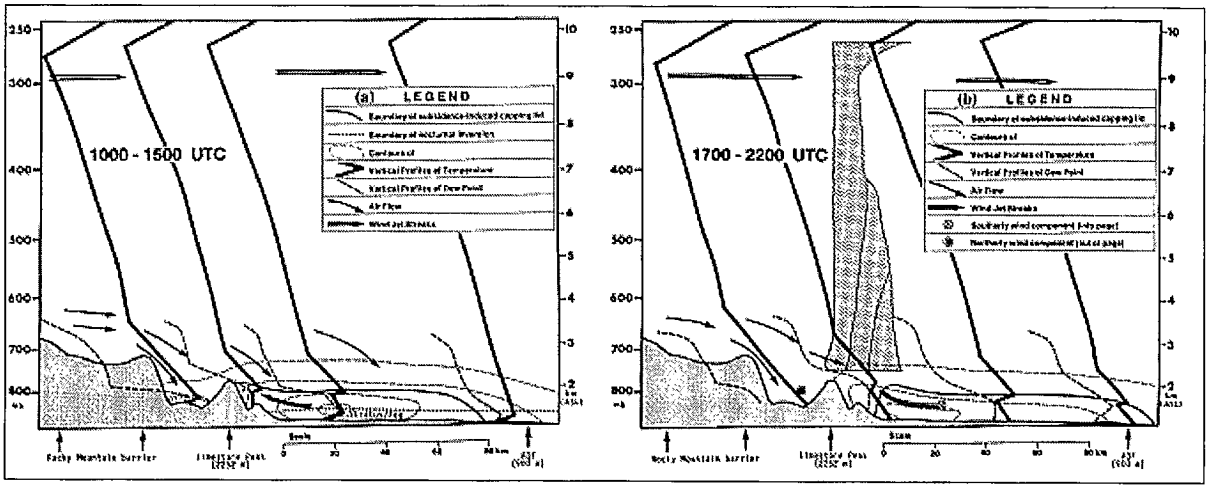

Stage 5: Storm Progression

12. Such thunderstorms, when all of these factors combine, tend to be quite severe with frequent lightning, heavy precipitation, large hail, and long hail swaths; tornadoes are not uncommon in these situations. The major Calgary hailstorm of 28 July 1981 (at that time the most expensive natural disaster in Canadian history), and the Edmonton tornado of 31 July 1987 (which exceeded it in damage) had virtually all of these factors in place.

13. The breakdown of the lid over a narrow band along the foothills effectively explains why Alberta storms tend to form there, and once formed, the propagation of the storm and its hailswath track becomes a vector result of the upper winds and boundary layer moisture convergence. Moisture convergence was so strong to the southeast of the 1981 Calgary hailstorm, that the storm propagated ~90° to the right of the upper-level southwest winds right through Calgary.

14. The role of local evapotranspiration over the grain fields to the east of the foothills has not been fully quantified, but the effect is thought to be significant, and helps explain why Alberta hailstorms drop off rapidly in frequency and severity by mid-August, since grain crops have then "headed out" and no longer draw much soil moisture.

15. Once the storm forms, the southwest flow at middle to upper levels finally becomes coupled with the surface flow, and a return subsiding circulation is enabled immediately in front of the storm or on its right forward flank, completing a vertical circulation and contributing to the continued redevelopment of storm cells in the inflow region as described by Chisholm and Renick (1972) (Figure 2.2).

Stage 6: Storm Decay

16. The storm eventually decays once its source of latent heat (moisture) and sensible heat are curtailed or cut off altogether, and/or the upper shortwave pushes through and is replaced by an approaching ridge. Storm decay destroys the vertical circulation, and with nightfall, clearing skies allow a stable nocturnal inversion to reform.

Stage 7: Post-Storm Effects

17. Finally, following a major thunderstorm, ground moisture left from high precipitation rates often provides the seed for a second storm day in succession, if other environmental conditions are favourable. If a drier and cooler air mass does not following immediately behind the storm, the capping lid can re-establish itself the following morning, allowing a similarly intense storm to develop.

4.3 Summary

This section has offered an explanation for the pre-storm creation, breakdown, and physical role of the *capping lid*, along with large-scale processes, topographic forcing, and local effects of surface heating and evapotranspiration, in triggering severe convective storms in Alberta. The capping lid is a frequent pre-storm thermodynamic condition from Alberta to Texas. The lid by itself is neither a necessary nor sufficient condition to ensure the formation of a severe convective storm, or indeed, of any convective clouds as was demonstrated by the case of 15–16 August 1973 (Figures 4.4, 4.5), yet it still plays the crucial role in such storms. The conceptual model offered here is based on known dynamics and the published results of research covering different scales of atmospheric motion, including mesoscale studies and the forecasting experience of the lead author.

Thunderstorms can be viewed as one of nature's mechanisms that help correct imbalances in the larger scale kinetic energy budget caused by frictional losses. They also provide a means for balancing the atmospheric moisture and surface water budget of the relatively dry Canadian Prairies through the redistribution of water. Energy feedbacks occur at various scales, depending, it seems, on where they are needed most in the atmosphere. The generation of baroclinic waves and of severe thunderstorms are two such major mechanisms for maintaining the global energy balance at different scales. This has potentially important implications with respect to climate change, since a warmed climate would be a more energetic climate. It is therefore quite conceivable that we would experience more frequent and more intense severe storms in a warmer climate.

While the physics of the scale interactions involved are very complex and are still poorly understood, the explanation and hypothesis presented here suggests various ways to test various aspects of this multi-scale model, and to expand on the hypothesis through smaller mesoscale field research experiments and modelling tests. Such field experiments necessitate the most efficient use of existing data sources, including current surface and upper air data networks, satellite, radar, and aircraft data, supplemented by additional surface and upper air instrumentation where possible.

This multi-scale conceptual model of Alberta thunderstorms is thought to be valid throughout the North American plains region in the immediate lee of the Rocky Mountains, and undoubtedly in similar locations in the world in the lee of significant mountain ranges. The remainder of this report is devoted to the evaluation of some of the processes hypothesized here, mostly through process study results (Section 5.0), but also through the use of a statistically-based forecast index, the Synoptic Index of Convection (Sc_4 – Section 6.0). Testing of the main hypothesis is accomplished using mesoscale upper air datasets from Alberta and the Oklahoma/West Texas region. These tests also address factors that may lead to improvements to the hypothesis, and thus contribute to the formulation of a "total" conceptual model of severe to weak convective storms, as well as non-convective cases.

5.0 Tests of the Conceptual Model

The multi-scale conceptual model of Alberta thunderstorms is tested in this section using several datasets. The hypothesis suggests that similar conditions lead to thunderstorms in the immediate lee of the Rocky Mountains from southwestern N.W.T. southward through west Texas; the main difference being generally a deeper and moister boundary layer to the south with consequently larger and more severe thunderstorms. The LIMEX-85 data were not ready for analysis until after the model had been developed. Hence, Strong (1986) used the SESAME-79 (Severe Environmental Storms Area Meteorological Experiment, May, 1979) data of Oklahoma and west Texas for preliminary tests of the model, along with the more limited LIMEX-80 Alberta data.

The conceptual model was presented in Section 4.0 as seven main stages: the *early pre-storm lid preparation, late pre-storm lid formation, pre-storm lid breakdown, storm initiation, storm progression, storm decay,* and *post-storm effects*. The first three of these are of the *pre-storm* period that severe weather forecasters must deal with, covering the creation of the *capping lid* under which latent and sensible heat are initially trapped; this generally occurs anytime within the 24-hour period prior to storm formation. It was these first three stages that LIMEX-80 focused on. Confirmation of the first stage was provided partly in Section 2.0 dealing with synoptic climatology and storm environment cases studies. SESAME-79 and LIMEX-85 data are used to evaluate the remaining phases of the model.

A few words about some technical terms used in the discussion are in order here. We occasionally refer to the following terms: mixing ratio = the absolute humidity, or mass of water vapour present in the air measured in g of water vapour per kg of dry air; divergence = rate at which air is leaving (diverging from) a point, usually quantified in cm s^{-1} units; the opposite term is convergence = negative of divergence; vertical velocity = velocity of ascending air (positive values) or descending air (negative values) when expressed in cm s^{-1} units; sometimes the units $\mu b\ s^{-1}$ are used, in which case the sign is reversed (negative values are then ascent).

A brief description of all LIMEX field experiments and data collected are presented in Appendix A, and in more detail in Strong (1989).

5.1 LIMEX-80 Results

LIMEX-80 was carried out specifically to measure thermodynamic responses to the synoptic scale and orographic subsidence postulated in the first two phases of the model. Radiosondes were released at three-hour intervals, commencing at 1400 UTC on three successive days, 15–17 July 1980, in a 10 km wide valley west of Limestone Mountain peak (LMW, at 1506 m ASL) adjacent to the main mountain barrier, in an attempt to sample the maximum response to orographic subsidence. Radiosondes were also released at three-hour intervals at Rocky Mountain House (YRM, at 988 m ASL), 65 km northeast of the Limestone site, and at Red Deer Airport (AQF, at 900 m ASL), some 110 km east-northeast. There are 36 LIMEX-80 soundings in the LIMEX data archive.

Central Alberta remained under a northwest surface flow with westerly winds aloft throughout

the three-day period. Figure 5.1 shows the 500 hPa and surface analysis for 16 July, along with a Red Deer sounding representative of storms on that day. Several moderate thunderstorms developed over the foothills on July 15, producing up to walnut-size hail (CDC = +3). The most convectively-active day was 16 July as a shortwave trough moved through the region. Larger than golf ball hail (CDC = +5) was reported from a line of storms over central Alberta, as depicted by the AHP Red Deer radar PPIs during its mature stage (Figure 5.2). Most of the hail was produced by the southern storm cell in this line, just west of YRM on Figure 5.2, as it swept southeast just south of Red Deer. Cooler, drier air behind this trough yielded only a few weak storms producing small hail on 17 July.

Figure 5.1 500 hPa analysis, surface analysis, and representative Red Deer sounding (for thunderstorm) 2400 UTC, 16 July 1980 (LIMEX-80) (after Strong et al., 1984).

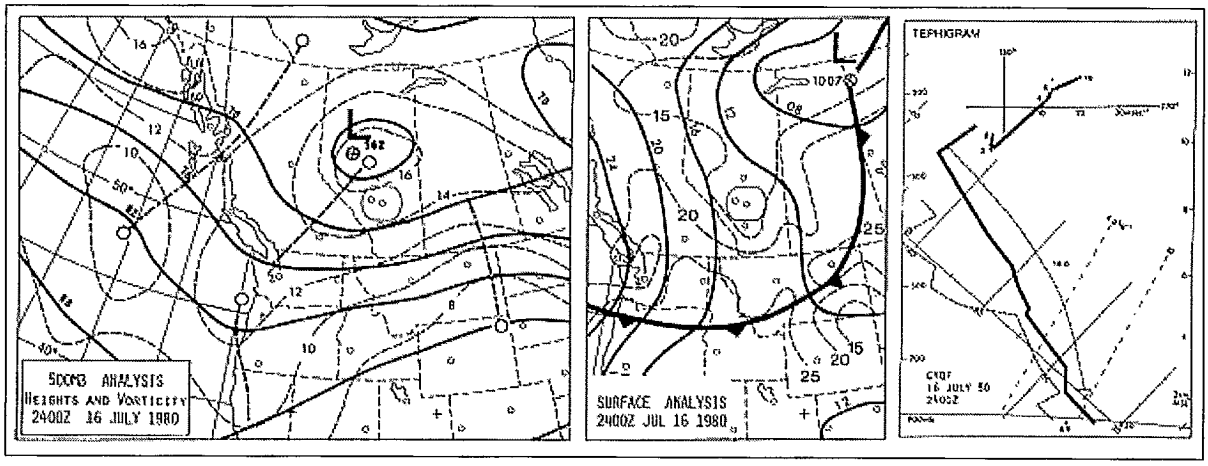

Figure 5.3 shows the average of four daily soundings at the Limestone Mountain West site (LMW), situated between the foothill peak and the main Rocky Mountain barrier (see Figure 4.1), and at Rocky Mountain House (YRM). Strong orographic subsidence was detected on all three days at LMW close to the mountain barrier, as evidenced by the dry adiabatic temperature traces (heavy solid lines) from 700–850 hPa (surface) on all three sounding averages.

These LIMEX-80 results confirm the first two stages (of seven) of the conceptual model without any major revision.

Figure 5.2 Hourly sequence of S-band radar PPIs during the mature storm stage, 2115–0014 UTC, 15–17 July 1980 (LIMEX-80). The locations of special soundings at Limestone Mountain West (LMW) and Rocky Mountain House (YRM) are indicated by the stars in (a) (from Strong et al., 1984).

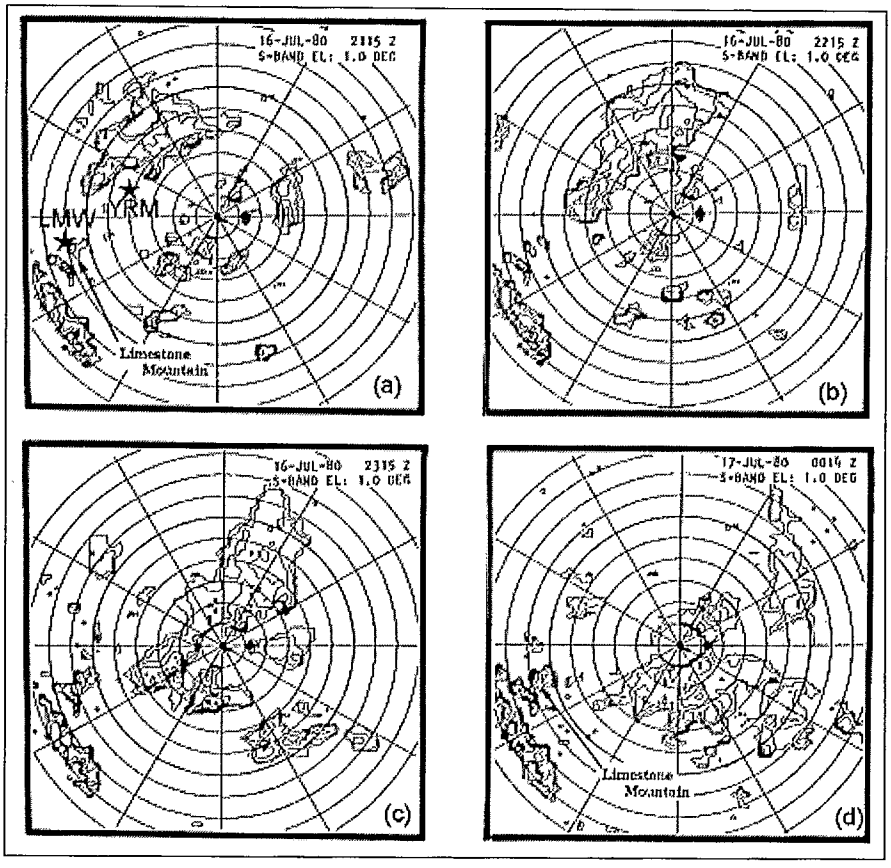

Figure 5.3 Average of four daily soundings for Limestone Mountain West (LMW) and Rocky Mountain House (YRM) for 15–17 July 1980 (LIMEX-80) (from Strong, 1986).

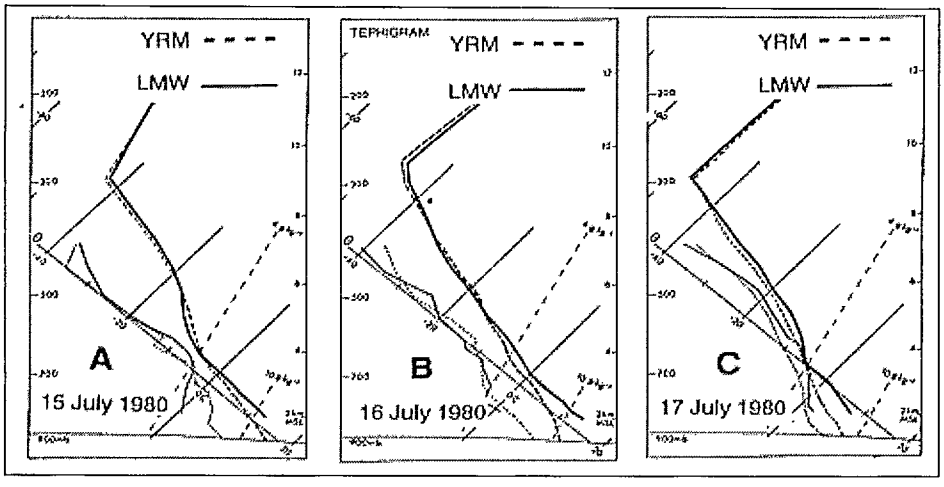

5.2 SESAME-79 Tests

One of the limiting factors in mesoscale process studies of severe thunderstorms is the lack of datasets with sufficient temporal and spatial resolution. In order to carry out a thorough analysis of such storms, which typically have horizontal dimensions of 20–200 km and lifetimes of one to12 hours, data of meso-β scale resolution (refer to Table 1.1) are required, and preferably at the lower end of the meso-β range. To be statistically suitable for three-dimensional analysis, one needs a minimal network of six or more sites (Panofsky & and Brier, 1963). Until LIMEX-85, the 1979 SESAME data set from Oklahoma and west Texas was one of the very mesoscale upper air data sets focussing on severe storms. The SESAME data meet requirements for both synoptic and mesoscale analysis. The SESAME mesoscale radiosonde network shown in Figure 5.4 consisted of 20 sites (open circles) at 80 km mean spacing. These, plus the surrounding regular synoptic network sites (solid circles) at 450 km mean spacing, released soundings at 1.5 to 3 hour intervals for several select severe storm case studies. We present one such case in this section, for 20–21 May 1979 (from Strong, 1986), which demonstrates many of the features of the *pre-storm lid breakdown, storm initiation, storm progression,* and *storm decay* phases of the conceptual model described in Section 4.0.

Figure 5.4 SESAME mesoscale radiosonde network over Oklahoma and west Texas during Case IV, 20–21 May 1979. Open circles are locations of special mesoscale network sites, solid circles are regular synoptic operational sites (from Strong, 1986).

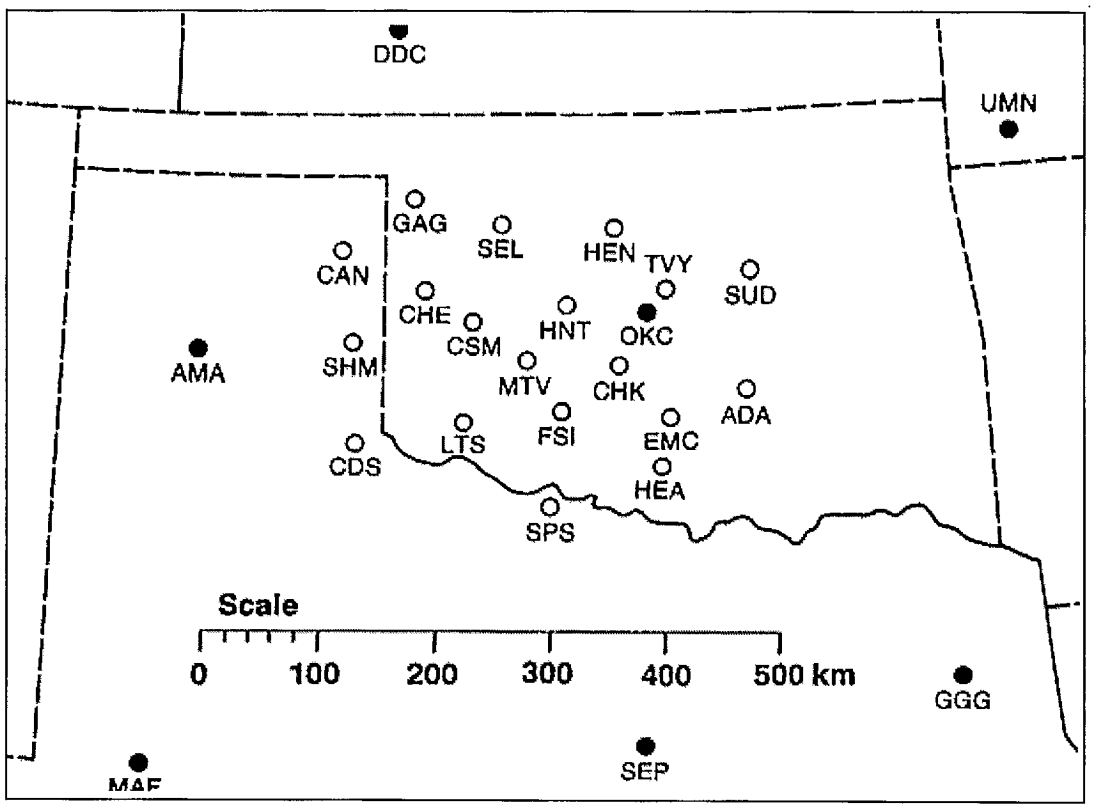

5.2.1 Synoptic Situation of 20 May 1979 and Early Pre-Storm Lid Preparation

The main weather system was an upper closed low over northwest Mexico at 0000 UTC (Figure 5.5), with a shortwave trough extending eastward into southern Texas and rotating northward around the low. A surface low associated with this remains near the Texas-Mexico border, with a quasi-stationary front lying through north Texas and southern Oklahoma. The front is well defined with temperatures in the mid-teens and dew points 10–15°C under northeast winds on the north side, contrasted with temperatures in the mid-20s and dew points 15–20°C under southerly winds south of the front. This combination resulted in moisture convergence over the foothills of the Texas Panhandle with an upslope component, and all along this front as well.

The visible GOES satellite images for 1831 UTC in Figure 5.6 shows cloud along this frontal convergence zone, all along the east slopes of the Rockies through the Texas Panhandle, New Mexico, Colorado, and Wyoming. Upslope convergence was occurring in the cooler air mass, and through much of Texas south of the front, where warm moist air was being lifted by the low pressure system as it moved inland from the Gulf of Mexico. Initial convective clouds developed simultaneously at 1830 UTC just southwest of southwestern Oklahoma, over the Texas Panhandle, and near Midland (MAF on Figure 5.4), Texas as indicated by the arrows. The former becomes the major storm of the day with a line of cells forming all along the front through southern Oklahoma, which together with blow-off from the storm tops, virtually cover Oklahoma with a mesoscale convective complex (MCC – Maddox, 1980). Both the Oklahoma and Midland storms spawned small tornadoes and large hail.

Figure 5.5 500 hPa and surface synoptic scale analyses for 1200–0000 UTC, 20–21 May 1979 (from Strong, 1986).

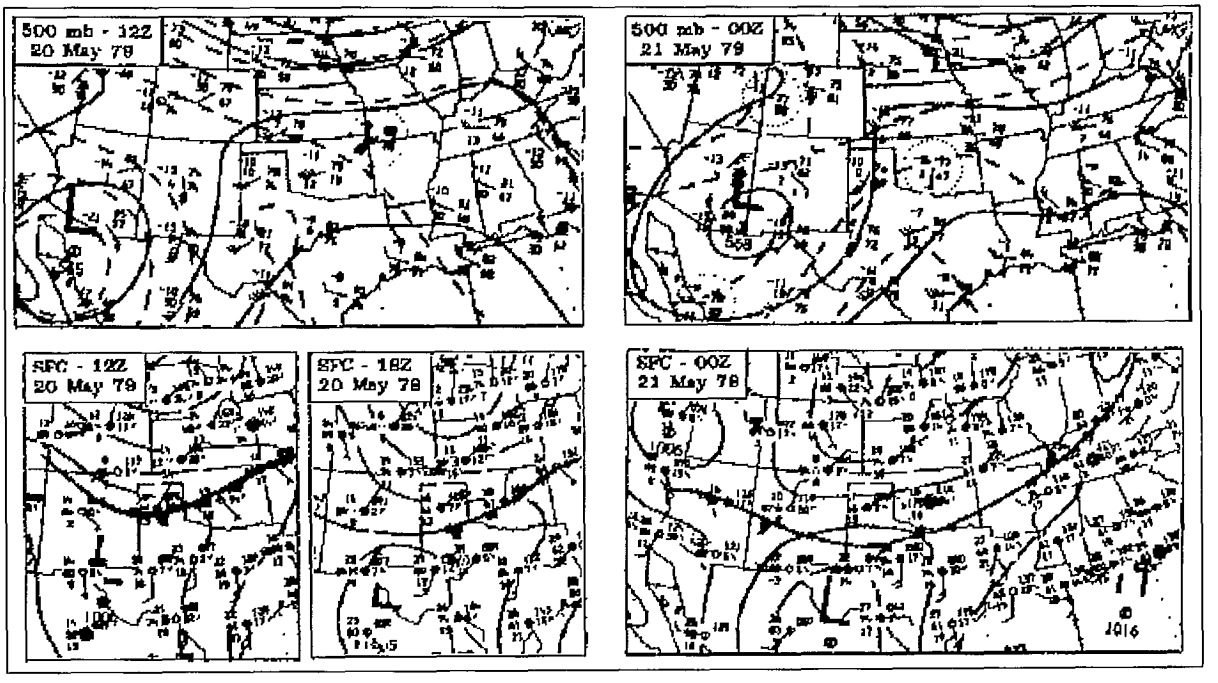

Figure 5.6 GOES visible satellite images at 1831 and 2131 UTC, 20 May 1979 (from Strong, 1986).

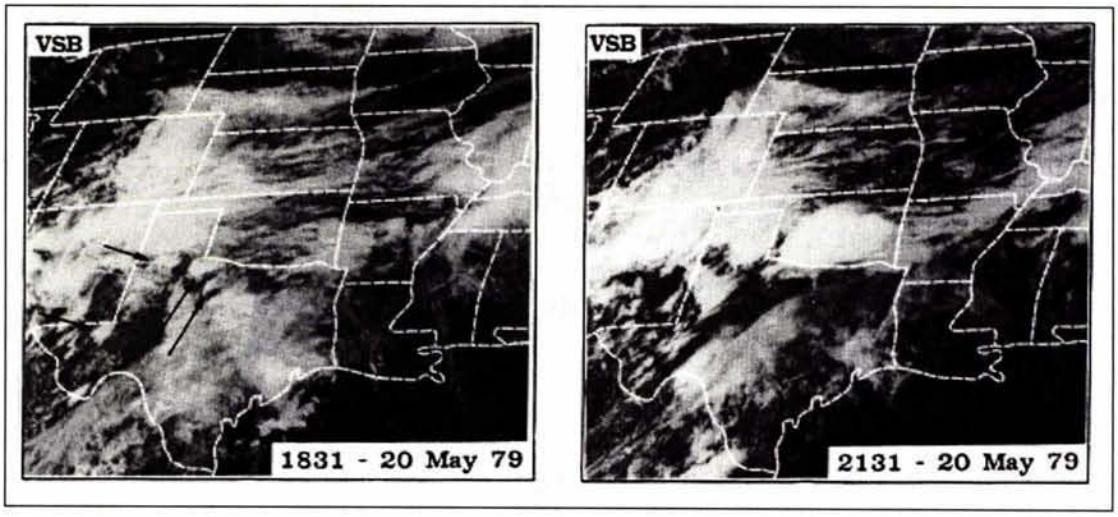

5.2.2 Pre-Storm Lid Breakdown

Sequential soundings for Childress (CDS), Texas are shown in Figure 5.7. These illustrate the rapid breakdown of a strong *capping lid* prior to the initial development of storm cells close to CDS, as indicated by the double arrows in the 1831 UTC visible image of Figure 5.6.

Figure 5.7 Sequential soundings released at Childress (CDS), Texas, at 1415, 1710, and 2001 UTC, 20 May 1979, illustrating the breakdown of the capping lid (from Strong, 1986).

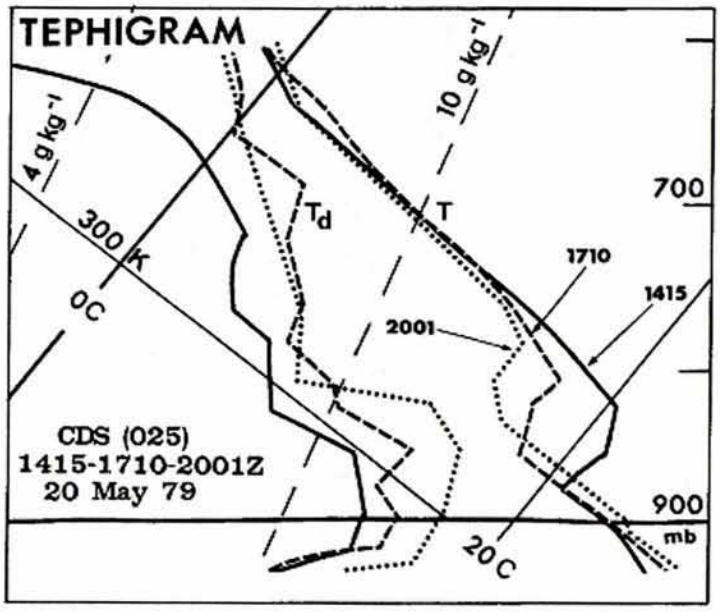

To examine the cause of the lid breakdown, Figure 5.8 depicts the ABL (800 hPa) and mid-level (700 hPa) vertical velocity fields computed from the mixed mesoscale and synoptic radiosonde data at 1230 UTC, and surface divergence field computed from surface data at 1400 UTC. In these analyses, vertical motion was computed using the adiabatic method (Strong, 1986), which is based on changes in the temperature and moisture fields. These adiabatic computations should be relatively unaffected by mesoscale thunderstorms, since radiosonde operations specifically avoid penetrations into thunderstorms. Hence, the adiabatic computations of vertical motion should, in theory, be sensing the synoptic scale *environmental* (or extra-storm) field, with vertical velocities generally less than 10 cm s^{-1}. On the other hand, the more common kinematic method of computing vertical motion utilizes the wind fields, which are strongly influenced by thunderstorm systems (as was shown in Figure 2.4), such that the vertical motion becomes quickly swamped by mesoscale thunderstorm-induced ascent (in tens of m s^{-1}). Both techniques are discussed in most dynamics texts (e.g., see Holton, 1979).

Figure 5.8 Vertical velocity fields at 700 and 800 hPa at 1230 UTC and visible satellite image at 1301 UTC (from Strong, 1986), and surface divergence field at 1400 UTC, 20 May 1979 (from Sikdar and Fox, 1983).

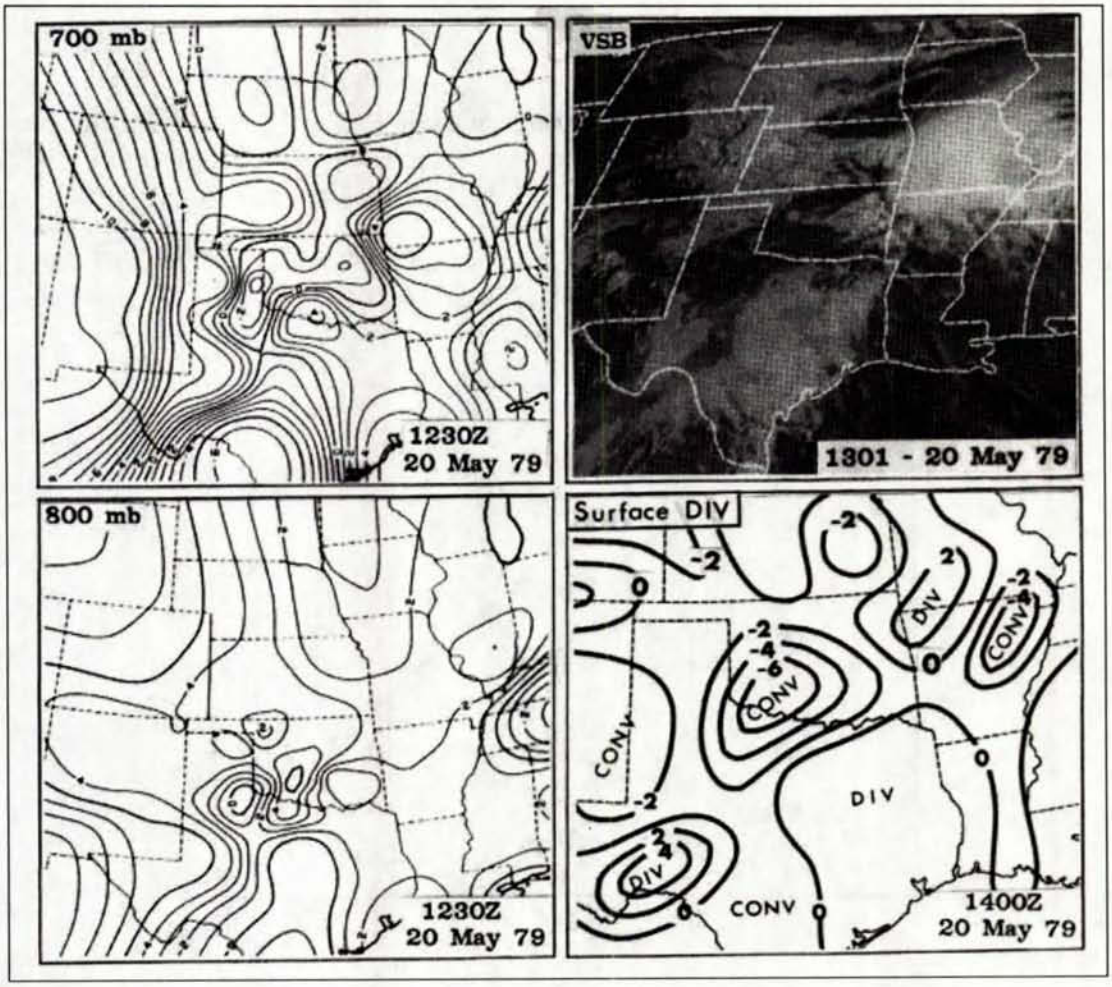

In the latter case, one can theoretically examine changes in the soundings caused by synoptic scale vertical motion. Thus, at 1230 UTC, we note a region of ascent over south-central Oklahoma with maximum ascent of 4 cm s^{-1} and an adjacent region of subsidence to the west with maximum descent of 2 cm s^{-1}. The region of ascent was advecting slowly westward and was associated with the thunderstorm formation some six hours later. It can be shown by a simple computation of adiabatic cooling that the rates of ascent indicated in Figure 5.8 result in the degree of cooling and lifting of the lid exhibited in Figure 5.7 for CDS. The visible satellite image at 1301 UTC indicates how well the major regions of cloud (clear air) correspond with the mid-level (700 hPa) regions of ascent (descent). The surface divergence field in Figure 5.8 (from Sikdar and Fox, 1983), computed from an independent database (surface wind field), corresponds well with the vertical motion (convergence → ascent). The surface convergence over Oklahoma approximates the shape of the convective complex several hours later (Figure 5.6, 2131 UTC).

Figure 5.9 provides a larger scale view of the region affected by the capping lid in this instance. The area affected includes virtually all of Oklahoma, and all but the western part of Texas – a synoptic scale region of approximately 1 M km^2. This aspect diverges from the Alberta situation where the region of capping lid tends to affect a much smaller region west-east, but can extend many hundreds of kilometres north-south. One other interesting aspect of Figure 5.9 is that the storm that formed near MAF, for example, did so without the benefit of a lid to temporarily trap latent heat and moisture, once again reminding us that the capping lid is neither a necessary nor sufficient condition for severe thunderstorms.

Figure 5.9 Region encompassed by a capping lid on 20 May 1979. Open circles represent radiosonde sites of the SESAME mesoscale radiosonde network. (From Strong, 1986).

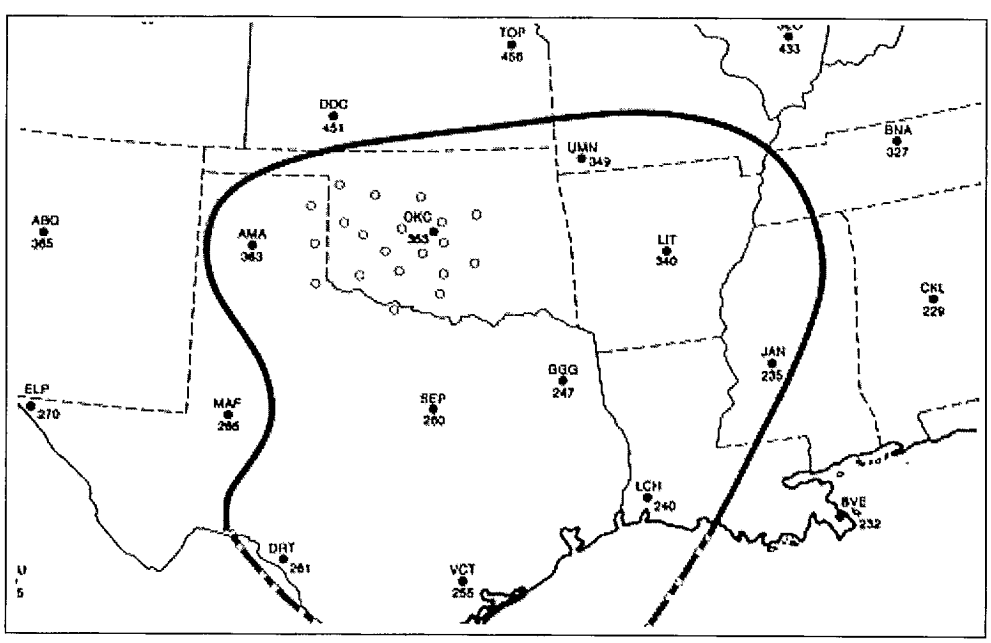

Figure 5.10 provides regional analyses of two components of the lid: the *depth* of the lid, or more correctly, of the ABL (in hPa, from ground level to the top of the lid); and the *strength* of the lid, defined simply as the change in temperature from the base to the top of the lid. In this instance, the ABL varied from 80–200 hPa deep (approximately 800–2000 m), and was 150 hPa (or 1500 m) deep at the time and location of storm initiation (indicated by the solid black diamonds in Figure 5.10 (c, d). Typical ABL depth for Alberta storms is 500–1000 m.

Figure 5.10 Capping lid strength, defined by the difference in dry bulb temperature between the lid base and top at 1400 and 1700 UTC, 20 May 1979. Arrows (in (c) indicate positions of the low-level jet on the 1200 UTC 850 hPa analysis. (From Strong, 1986)

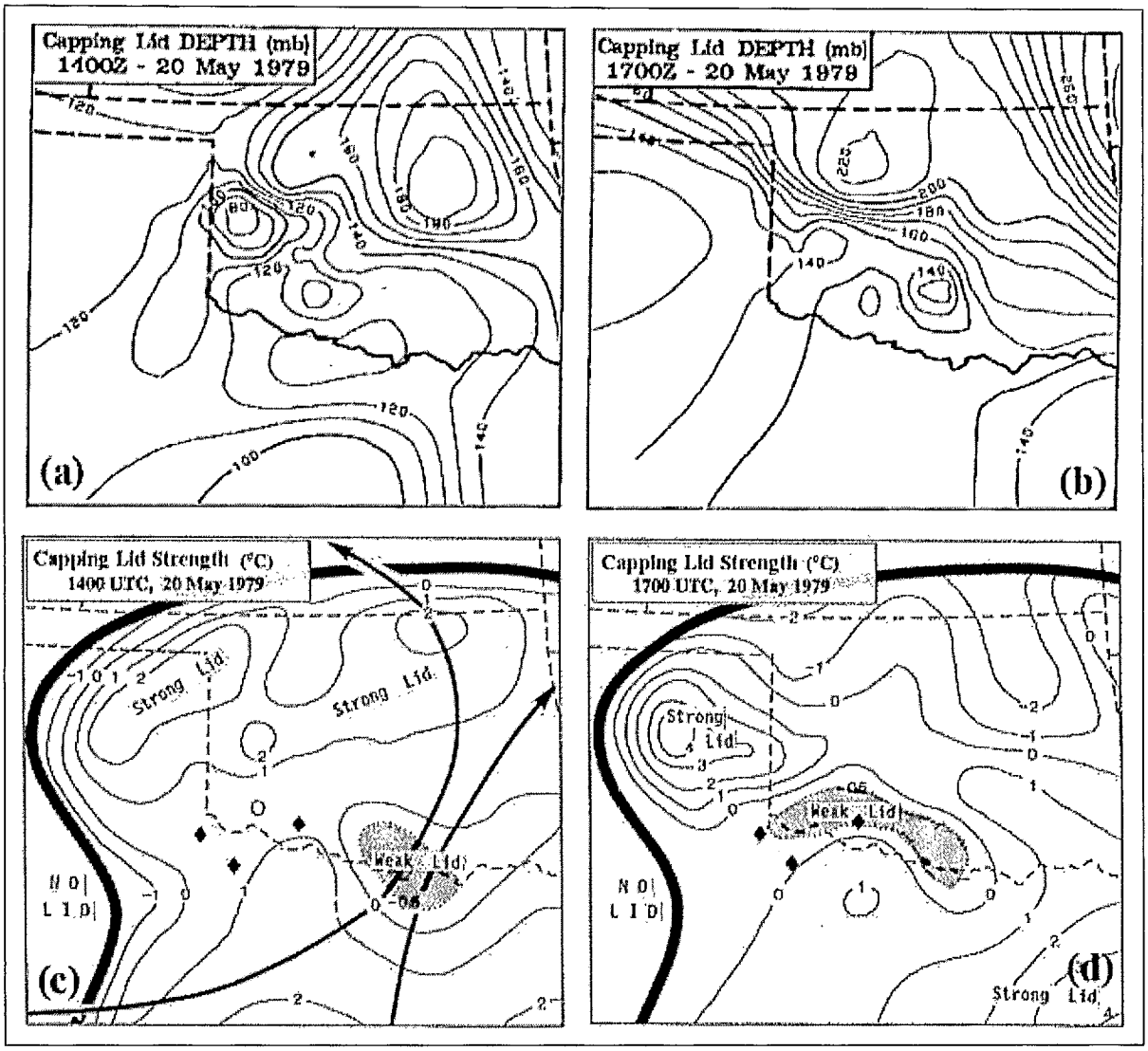

Of more interest dynamically is the lid strength, and how it evolved in the few hours before storm initiation. Note that a lid is defined as an inversion of *potential temperature*, so that an

isothermal layer (i.e., constant dry bulb temperature with height) such as all three evolutions of the CDS lid in Figure 5.7, still constitutes a capping lid since potential temperature is still increasing with height. Thus, the small area of negative lid strength index in Figure 5.10 (c, d) is still within the lid area. The weak lid area at 1400 UTC corresponds with the strongest region of 800 hPa ascent and of surface convergence over south-central Oklahoma (Figure 5.8). The lid has weakened here *because* of adiabatic ascent and cooling. The weak-lid region moves further west by 1700 UTC, and extrapolation would place this region right over the storm initiation at 1830 UTC. The very strong lid formation centred over the northeastern Texas Panhandle at 1700 UTC corresponds roughly to the dry slot region shown on the earlier satellite image for 1831 UTC (Figure 5.6a).

During the late-morning period, 1400–1700 UTC, maximum surface heating occurred over southwest Oklahoma where temperatures rose by 5°C to 30–32°C in the initiation region (Figure 5.11a,b). Surface mixing ratios during the same period remained static at about 13 g kg^{-1}, but increased by 1–2 g kg^{-1} outside the eventual storm area in the vicinity of southwest Oklahoma. This suggests the well-mixed nature of the ABL throughout the morning period in the storm region, with any additional moisture from local evapotranspiration being dispersed through the weak lid into the free atmosphere. Regions with a stronger lid could trap more moisture; hence the moderate increases in mixing ratio outside the weak-lid region. These inferences are supported by the soundings for those areas.

Figure 5.11 Analyses of surface temperature change, 1400–1700 UTC and of temperature at 1700 UTC, and surface mixing ratios at 1400 and 1700 UTC, 20 May 1979 (from Strong, 1986).

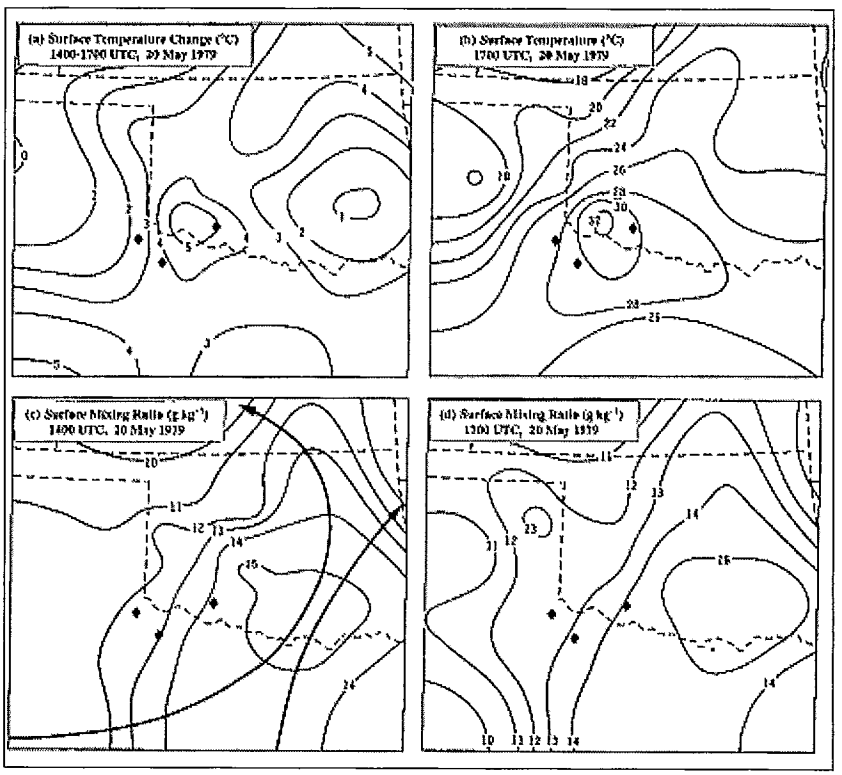

5.2.3 Storm Initiation and Progression

It has already been noted that the major storm which formed near southwest Oklahoma at 1830 UTC covered most of Oklahoma with its cloud shield by mid-afternoon (satellite image in Figure. 5.6b). Figure 5.12 is an area-averaged time-height cross-section of *environmental* vertical motion for the 20 mesoscale radiosonde sites for the 24-hour period 1200–1200 UTC, 20–21 May 1979. During the early period as the upper shortwave is slowly approaching, we note ascent within the boundary layer (average 4 cm s^{-1}) and at upper levels (500–300 hPa), with subsidence at mid-levels (-2 cm s^{-1} at 700 hPa). The depth and magnitude of environmental ascent start to increase around the time of storm formation, reaching a maximum of over six at 2130 UTC, with ascent extending above 500 hPa.

Figure 5.12 Area-averaged time-height cross-section for the 20 SESAME mesoscale radiosonde sites for the 24-hour period 1200–1200 UTC, 20–21 May 1979.

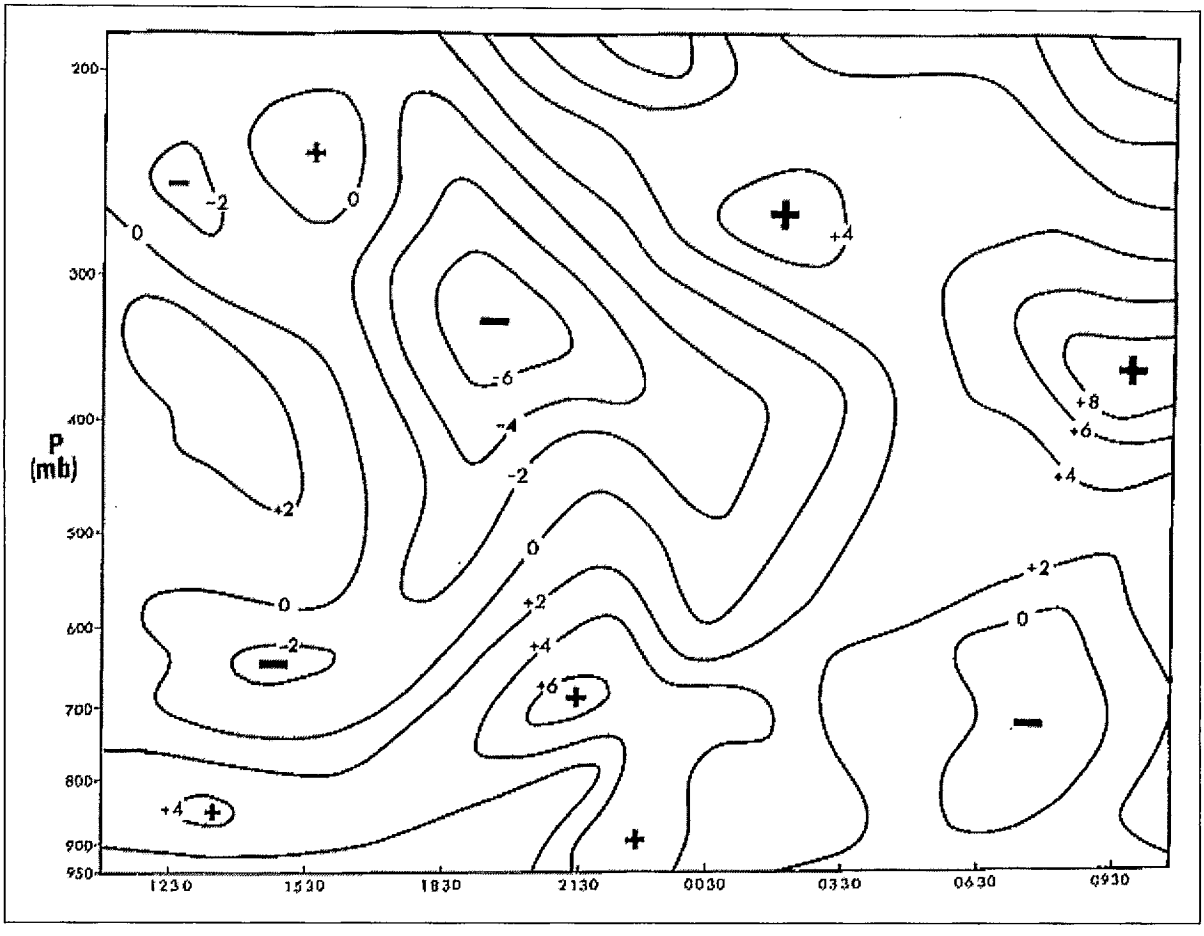

Adiabatic computations of vertical velocity theoretically sense primarily the environmental fields. However, the computation includes an advective term which involves wind, so that in reality, especially with so much convective cloud as was present over Oklahoma during the storm peak, it is reasonable to suspect that mesoscale storm ascent probably creeps into this field as well. For comparison, Figure 5.13 is an analysis of the mesoscale (storm) *kinematic* vertical

motion field computed by Fuelberg and Printy (1983) for this same case. (Note that the vertical velocity units are in μb s^{-1}, so that negative values are ascent, and visa versa, and that -1 μb s^{-1} ≈ +1 cm s^{-1}.) The area-average vertical motion field peaks around the same time (2130 UTC) as in Figure 5.12, but as one should expect, maximum values are of storm-scale ascent of -20 μb s^{-1} at 400 hPa, virtually a full order of magnitude greater than environmental values of Figure 5.12. The space-height cross-section runs northwest to southeast across Oklahoma and the mature storm at 2130 UTC, and peaks at 400 hPa with a maximum of -60 μb s^{-1}, 10 times the environmental (extra-storm) values. Obviously, the environmental vertical motion is negligible when the storm is super-imposed on it, but is absolutely critical in *preparing the atmosphere* prior to storm initiation. These two methods of computation are not incompatible; rather, one estimates motion outside the (storm) clouds, while the other measures the higher velocities within convective clouds. In the absence of clouds, both should provide comparable estimates of the environmental vertical motion field.

Figure 5.13 Kinematic computation of (a) time-height cross-section of area-averaged vertical velocity (μb s^{-1}) over SESAME mesoscale network, 20–21 May 1979, and (b) space-height (SEL-EMC) cross-section of vertical velocity at 2130 UTC, 20 May 1979 (reproduced from Fuelberg and Printy, 1983).

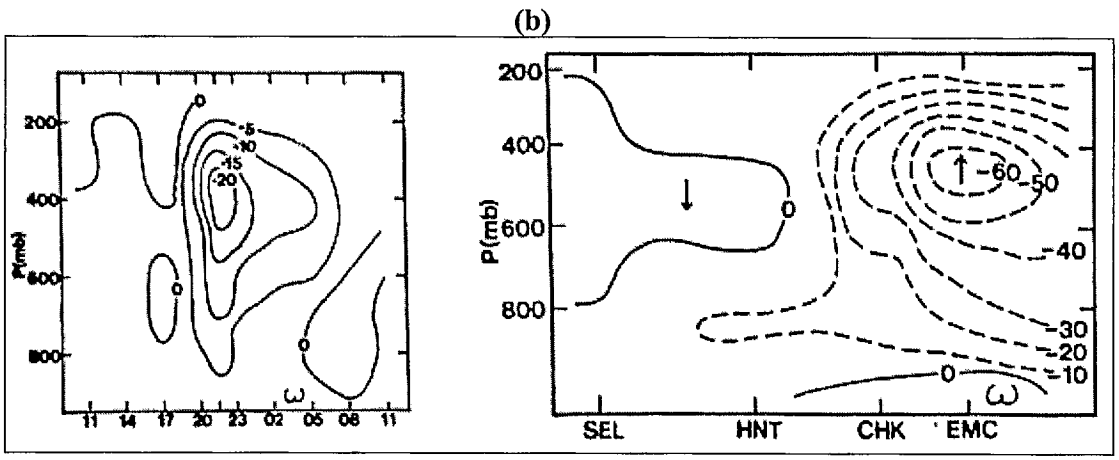

5.2.4 Storm Decay

Radar PPIs for this storm (not shown) indicate that the storm started to decay after 0300 UTC. This is commensurate with subsidence setting into the lower levels after that time on both Figures 5.12 and 5.13. This has several negative effects on convection: it limits ABL moisture from entering the storm, hence cuts off its supply of latent heat; it destroys the vertical circulation between the storm and the environment; this in turn, decouples the ABL from the free atmosphere once more.

Stages 2 to 6 (of seven) of the multi-scale conceptual model hypothesized in Section 4.0 have been demonstrated with the results from this one SESAME severe storm case. However, a complete model validation would require several more cases and types of convective storms. Most importantly, the model requires some validation with Alberta mesoscale radiosonde data,

which did not exist at the time of the SESAME analysis. We can now accomplish some of that validation using LIMEX-85 data.

5.3 LIMEX-85 Tests

Where LIMEX-80 focussed on the *pre-storm lid preparation* and *formation* stages, LIMEX-85 concentrated on the *late pre-storm lid formation, pre-storm lid breakdown,* and *storm initiation* stages. The LIMEX-85 mesoscale radiosonde network shown in Figure 5.14 consisted of nine sites (solid stars) at 60 km mean spacing in a semi-triangular grid. Eight automatic weather stations recording half-hourly surface data filled some of the gaps between soundings sites. A total of 11 operational days were conducted during 8–23 July 1985, with soundings released at two-hour intervals from 1200 or 1400 UTC, with a decision at 1800 UTC on whether to continue for the day. More details of the field data are provided in Appendix A. For this report, we focus on one main storm day of the LIMEX-85 period: 11 July 1985.

Figure 5.14 Topographic chart showing Limestone Mountain and adjacent regions, and special upper air and automatic surface sites during LIMEX-85, 8–23 July 1985.

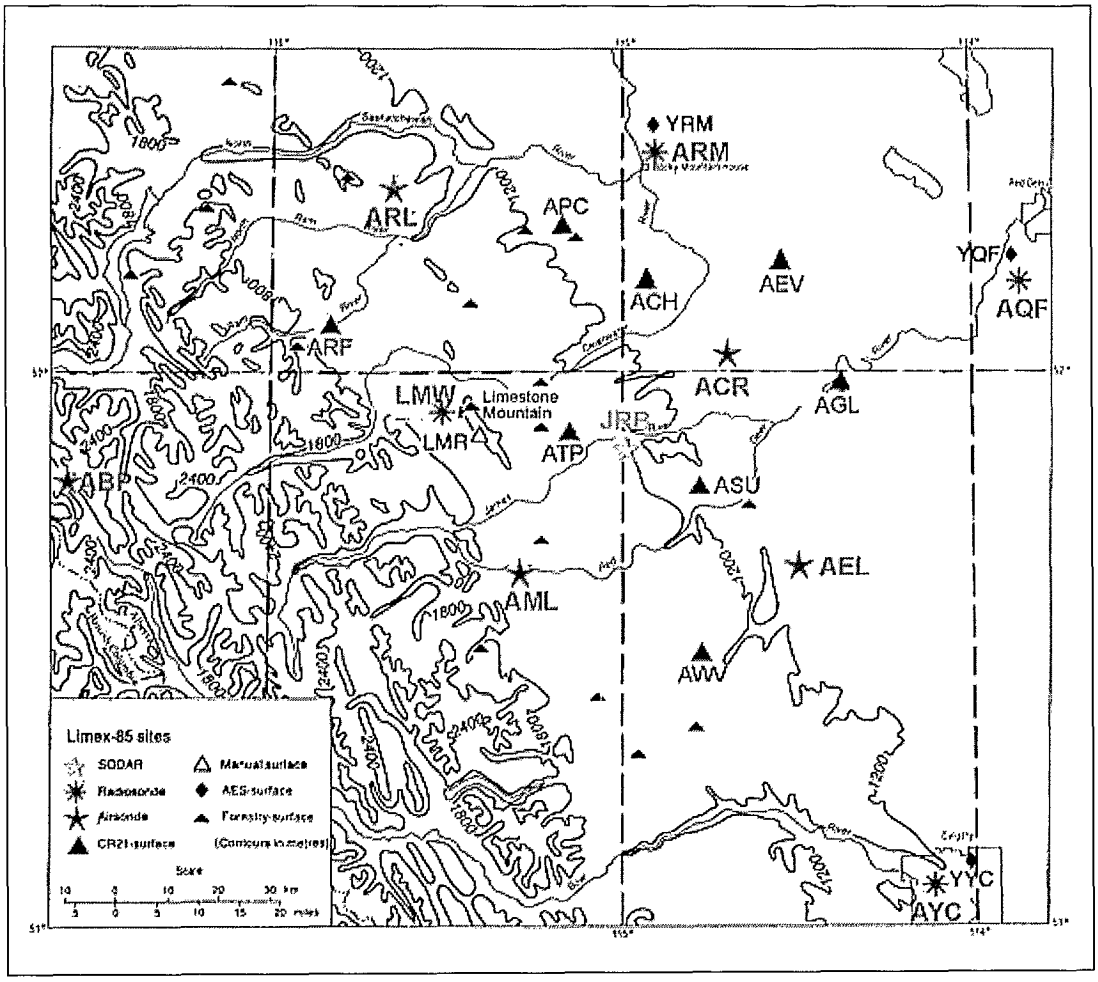

5.3.1 Synoptic Conditions and Weather on 11 July 1985

Synoptic scale influences in this case are depicted in Figure 5.15, showing 500 hPa, surface, and representative sounding analyses for late afternoon of July 11. An upper ridge had passed through central Alberta the previous evening, and was being displaced on July 11 by a trough approaching from the west coast. A weak surface trough extended northwest from a low in southern Saskatchewan to central Alberta. Several lines of severe thunderstorms formed northwest of Rocky Mountain House, the first starting around 2200 UTC, and resulted in numerous reports of golf ball- and walnut-sized size hail as the storms tracked east-southeast through central Alberta, just on the northern edge of the LIMEX-85 network. Several small, weak thunderstorms also developed within the ARM-LMW-ACR triangle, producing showers and some small hail. Figures 5.16a,b show two PPI images of the main storms over the northern half of the AHP operations area at 0100 and 0300 UTC, along with the noted small storms over the LIMEX network. The latter storms are depicted in the photo collage of Figure 5.16c, taken from Limestone Mountain ridge at 0300 UTC.

Figure 5.15 500 hPa, surface, and representative sounding analyses for 11 July 1985 during LIMEX-85.

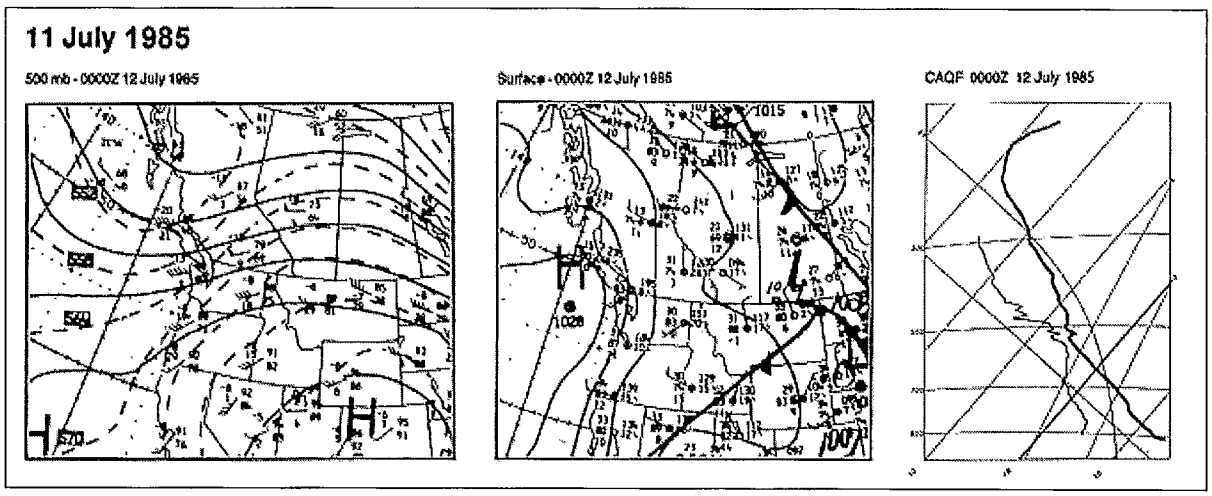

Figure 5.16 AHP S-band radar PPIs at (a) 0100 and (b) 0300 UTC, plus photo collage of storms from Limestone Mountain Ridge at 0300 UTC, 12 July 1985 during LIMEX-85. Radar range rings are at 20 km intervals and reflectivities are contoured at 10 dBz intervals starting at 20 dBz in these images. Radar elevation angle was approximately 1.5°.

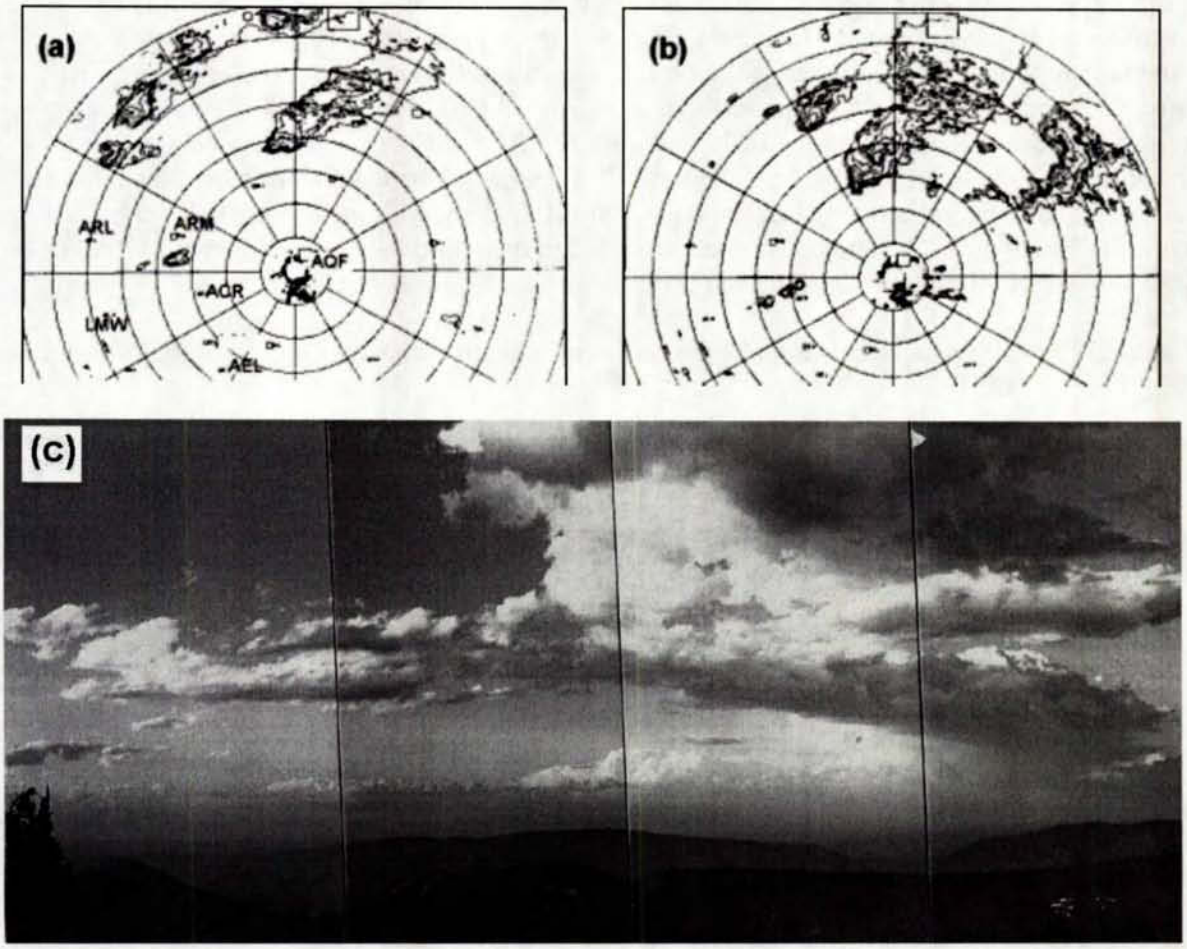

5.3.2 The Pre-Storm Capping Lid

An example of the final rapid *lid formation* and *breakdown* are demonstrated in Figure 5.17, a tephigram of five sequential soundings of temperature and dew point at two-hour intervals at Caroline (ACR) on 11 July 1985. The 1404 UTC (08:04 MDT) sounding shows only a nocturnal inversion, and while the surface dew point temperature is 10°C, it drops to 1°C a mere 150 m above ground, and to 0°C at 225 m. Just two hours later, the ABL has been transformed upward into a well-mixed 525 m depth (with constant mixing ratio of 9 g kg^{-1}), with a capping lid top at 665 m AG. Total moisture added to the ABL (in precipitable water) was 2 mm in just two hours.

The ABL depth increased still further to 720 m AG at 1801 UTC, while the capping lid reached an 855 m depth, with a further 1.5 mm of water added to the ABL. By 2001 UTC, the ABL had

attained total mixing of moisture and sensible heat, with the boundary layer depth then at 1090 m AG, but less well-defined. Surface heating and possibly low-level ascent had virtually erased the capping lid, and with this change, ABL moisture was now mixing upward into the free atmosphere. These fluxes balanced additional moisture increases in the ABL, but a further 2 mm was added to the surface-600 hPa layer.

Figure 5.17 Daytime evolution and breakdown of the capping lid (example from LIMEX-85, 11 July 1985).

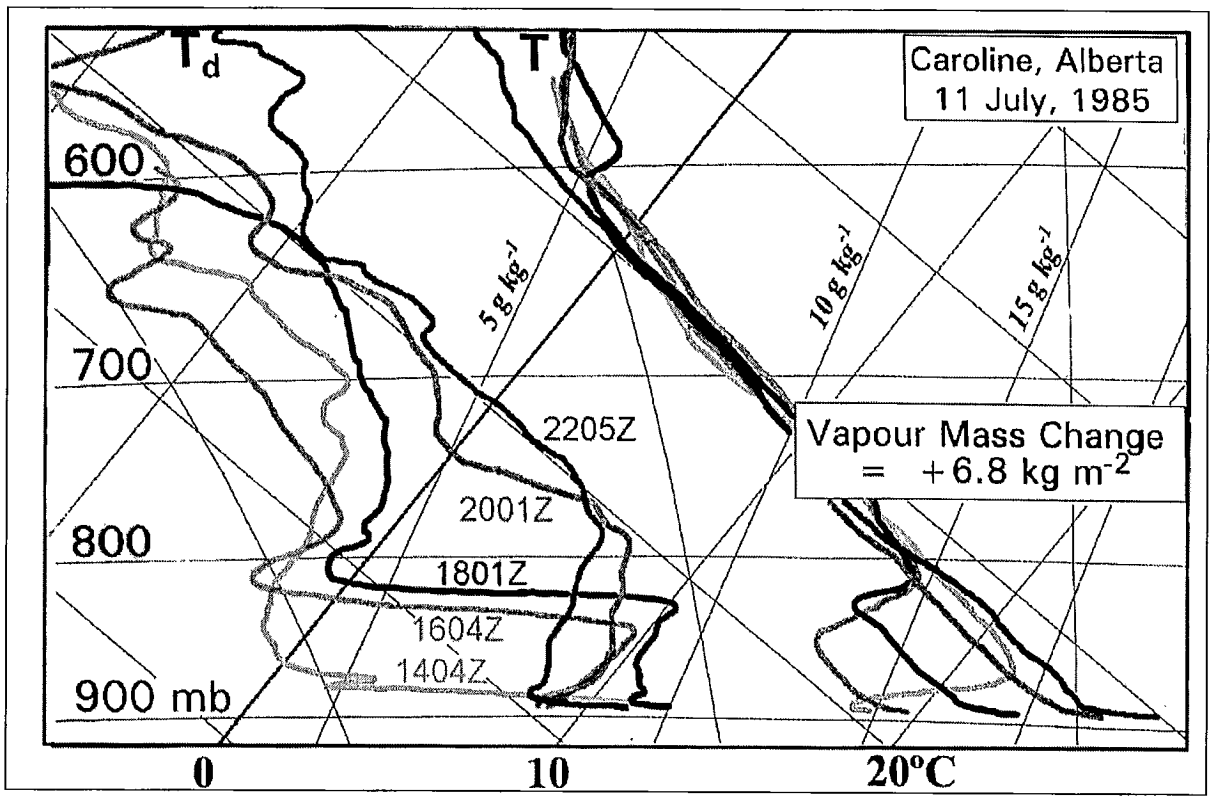

5.3.3 Mesoscale Dynamics during Pre-Storm Lid Formation and Breakdown

ABL winds at all sounding sites were light and variable during late-morning, initially suggesting minimal moisture advection. However, surface divergence computations by Honch (1989), using the complete LIMEX-85 surface and upper air dataset, shows that strong mesoscale surface *convergence* had formed over the foothills parallel to the mountains by 1900 UTC (Figure 5.18a), with a comparable region of ascent at 800 hPa (displaced slightly eastward) with values as high as 5 cm s^{-1} (Figure. 5.18b), peaking near 750 hPa at ~10 cm s^{-1}. Brennand (1992), using the same LIMEX database, confirmed these and additionally showed a line of *moisture convergence* through AYC-AML-ARL by 1800 UTC, with weaker convergence earlier in the morning.

Figure 5.18 (a) Mesoscale surface divergence field, with line of convergence (negative values) over foothills parallel to mountains, and (b) mesoscale (adiabatic) vertical velocity field (positive values are ascent) for the same region, at 1900 UTC, 11 July 1985 during LIMEX-85. (Reproduced by permission from Honch, 1989).

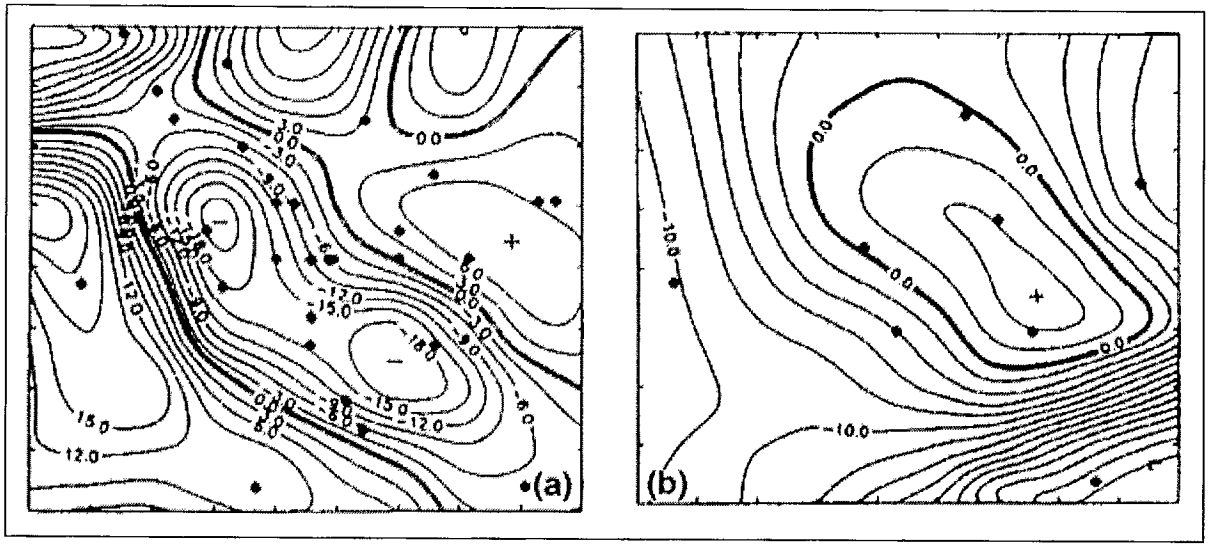

5.3.4 Sensible and Latent Heat Fluxes

Figure 5.19 compares the evolution of moisture at individual sounding sites, using profiles of mixing ratio in transects (EL-CR-RM) parallel and (QF-CR-MW) normal to the mountains as shown in the accompanying map, with Caroline (CR) as the common focal point, as in Figure 5.17. These transects are approximately 90 and 115 km in length respectively.

For the EL-CR-RM transect, Caroline is noticeably drier at 1400 UTC than either Elkton (EL) or Rocky Mountain House (RM) immediately above the surface, with the latter showing an increase in mixing ratio near the top of the ABL (~1500 m AG). However, two hours later this changed, with Caroline showing a large increase in moisture as previously observed on the tephigram soundings of Figure 5.17. This increase corresponds to an increase of 2 mm in precipitable water in two hours within the ABL (see Figure 5.21). Such rates almost certainly involve significant local evapotranspiration, as well as strong localized moisture convergence in the Caroline vicinity. Brennand's (1992) analysis indicated moisture (mixing ratio) convergence of 0.2 g kg^{-1} hr^{-1} at 1400 and 1600 UTC at Caroline, while the average ABL increase in mixing ratio was close to 3.0 g kg^{-1} in two hours, lending credence to high values of evapotranspiration. The latter is not surprising, given that the land around Caroline, especially to the east, is heavily dedicated to grain crops, which can contribute regional evapotranspiration rates as high as 10 mm d^{-1} (Strong, 1997).

Figure 5.19 LIMEX-85 mixing ratio profile trends along (a) intersecting transects parallel to and normal to the mountains for (b) Elkton – Caroline – Rocky Mountain House (EL-CR-RM), and (c) Red Deer – Caroline – Limestone Mountain West (QF-CR-MW), 11 July 1985.

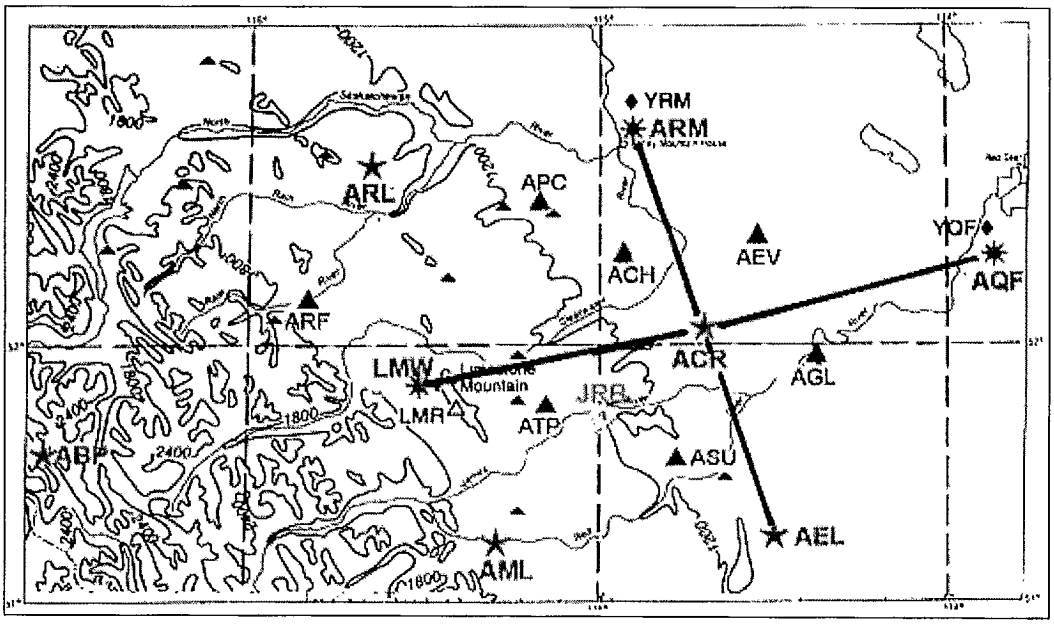

(a)

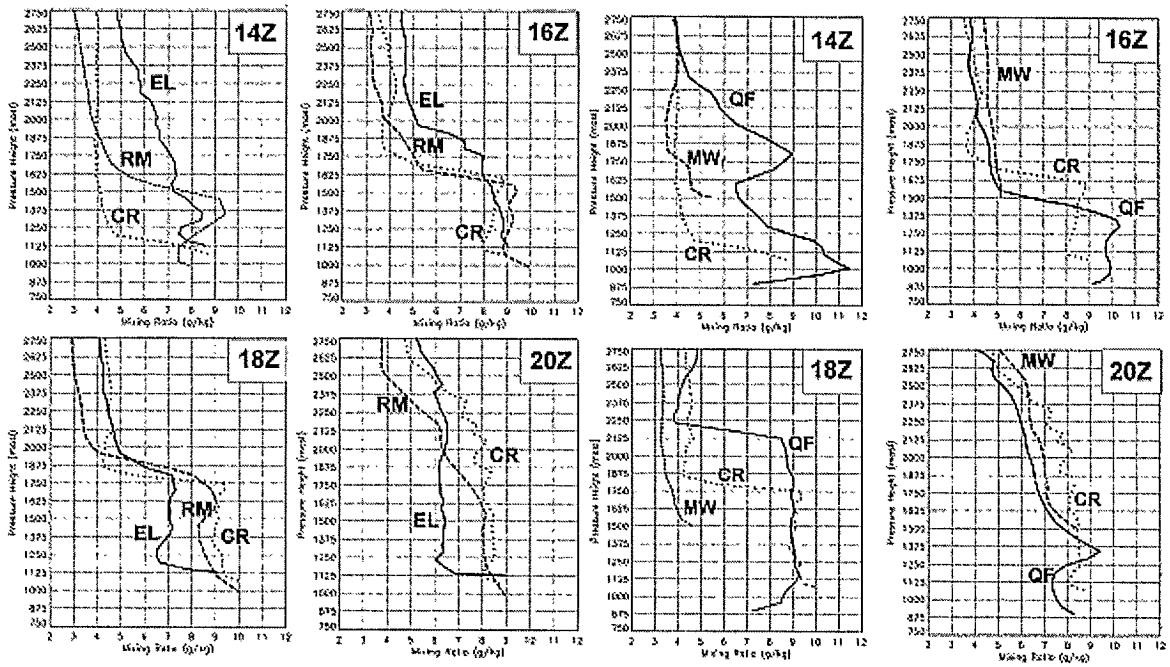

(b) (c)

The QF-CR-MW transect (Figure 5.19(c)) shows the ABL over QF increasing in depth between 1600 and 1800 UTC, but precipitable water decreased thereafter (Figure 5.21), which follows from the surface divergence indicated over the eastern LIMEX network in Figure 5.18(a).

Comparable QF-CR-MW transect profiles of potential temperature (Θ, Figure. 5.20 (a)–(c)) show that each sounding site simultaneously attained a fully mixed ABL by 1800 UTC (just as the Caroline soundings in Figure 5.17 suggest). The south-north EL-CR-RM transects are similar (only 1800 UTC shown in Figure 5.20(d)). The implication here is that temperature becomes well-mixed more uniformly over a fairly wide area (transects encompass 90 km x 115 km) than moisture. It is obvious that latent heat fluxes (evapotranspiration) play an important role in the process of *preparing* the ABL and the *capping lid* for thunderstorm formation. One might also assume from these analyses that the combined vertical and horizontal moisture fluxes (evapotranspiration and moisture convergence) have more spatial and temporal variability than temperature fluxes. However, more data would be required to confirm these deductions than are available in the LIMEX data. The two main factors determining evapotranspiration are the spatial variations in both land cover and topography.

Figure 5.20 LIMEX-85 profile trends of potential temperature along intersecting transects parallel to and normal to the mountains for Red Deer – Caroline – Limestone Mountain West (QF-CR-MW) at (a) 1400, (b) 1600, and (c) 1800 UTC, and for Elkton – Caroline – Rocky Mountain House (EL-CR-RM) at (d) 1800 UTC, 11 July 1985.

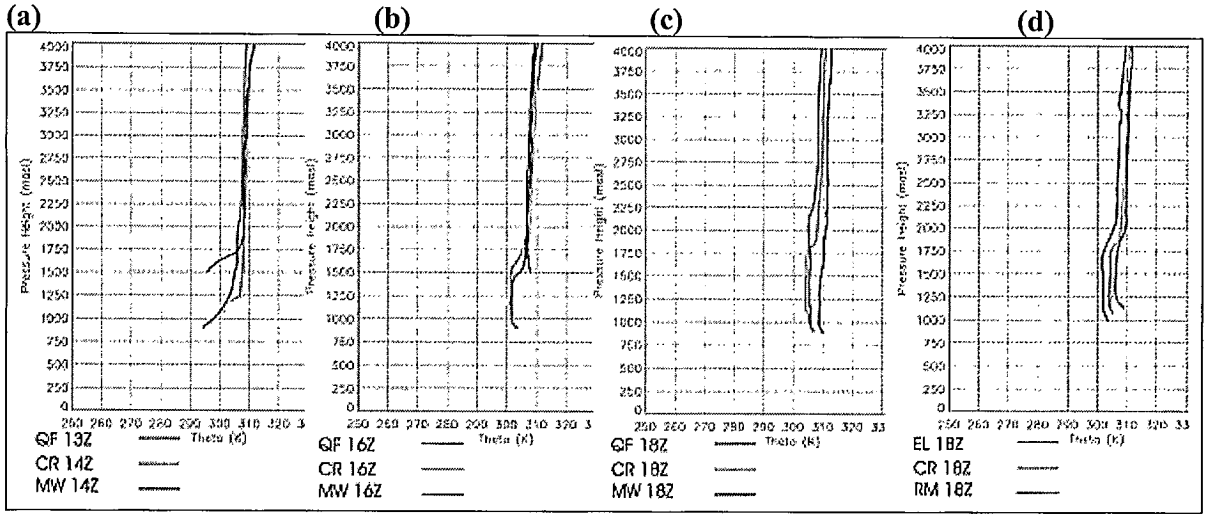

Figure 5.21 shows the diurnal trends in vertically-integrated precipitable water for the surface-800 hPa layer (ABL) at four foothill sounding locations, plus spot values at Stony Plain (WSE) near Edmonton. Most notable in the ABL integrations (Figure 5.21) are the rapid diurnal increases at AQF on July 10, and at ACR on July 11. Often, as in this case, the build-up of ABL moisture due to evapotranspiration and local moisture convergence commences on the day before (July 10) a severe storm (July 11). However, as is evident here, the increases are not widespread, but occur over mesoscale regions due to mesoscale variations in topography, land cover, and dynamics (convergence, vertical motion, etc.). In this series, small storms had formed

and remained over the foothills on July 10. Precipitable water decreased during the day at ACR over the foothills, but increased rapidly during the morning at AQF over the agricultural plains, then remained at a steady level, possibly due to local evapotranspiration from surrounding grain crops, with only a weak wind field to ventilate the moisture (Figure. 5.16). Strong evapotranspiration and mesoscale convergence over the foothills lead to the rapid increase in precipitable water at ACR on July 11, while the ABL in the vicinity of AQF had remained moisture-loaded and was probably feeding moisture to the more severe storms sweeping across the northern half of the AHP operations area. This is inferred from the PPIs of Figure 5.16, and the divergence (of ABL moisture) occurring at AQF in Figure 5.18a. The 12-hour WSE soundings north of these storms indicate even higher moisture content (solid diamonds in Figure 5.21), but it is not known from this analysis just how this may have affected the storms.

Figure 5.21 Diurnal trend in precipitable water (mm), surface to 800 hPa layer at Caroline, Red Deer, Rocky Mountain House, and Limestone Mountain West, with spot values at 1200 and 0000 UTC at Stony Plain (WSE) for 10–12 July 1985 during LIMEX-85.

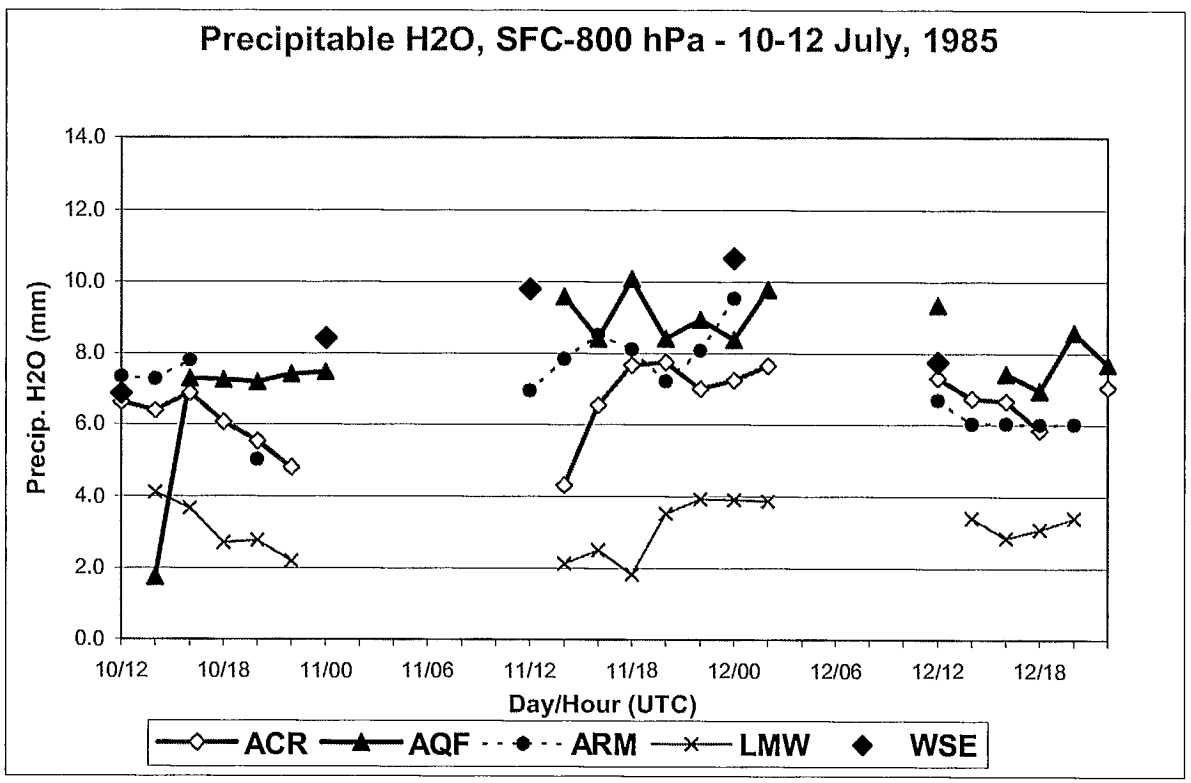

The surface-to-600 hPa vertically-integrated totals of precipitable water are included to demonstrate that ABL eventually overloads with moisture in these storm situations, moisture flux into the *free atmosphere* then occurs at the expense of the ABL moisture once the capping lid is removed through mesoscale ascent and adiabatic cooling. For example, we note that the ABL precipitable water stopped increasing at the three mesoscale network sites ACR, AQF, and ARM between 1700 and 1800 UTC on July 11 (Figure 5.21). However, the surface-to-600 hPa moisture increases continue at a steady pace until late in the day (Figure 5.22). This is the time

(17–1800 UTC) when convection broke through the capping lid allowing ABL moisture flux into the free atmosphere, shortly after which deep convection and severe thunderstorms can occur.

Figure 5.22 Diurnal trend in precipitable water (mm), surface to 600 hPa layer at Caroline, Red Deer, Rocky Mountain House, and Limestone Mountain West, with spot values at 1200 and 0000 UTC at Stony Plain (WSE) for 10–12 July 1985 during LIMEX-85.

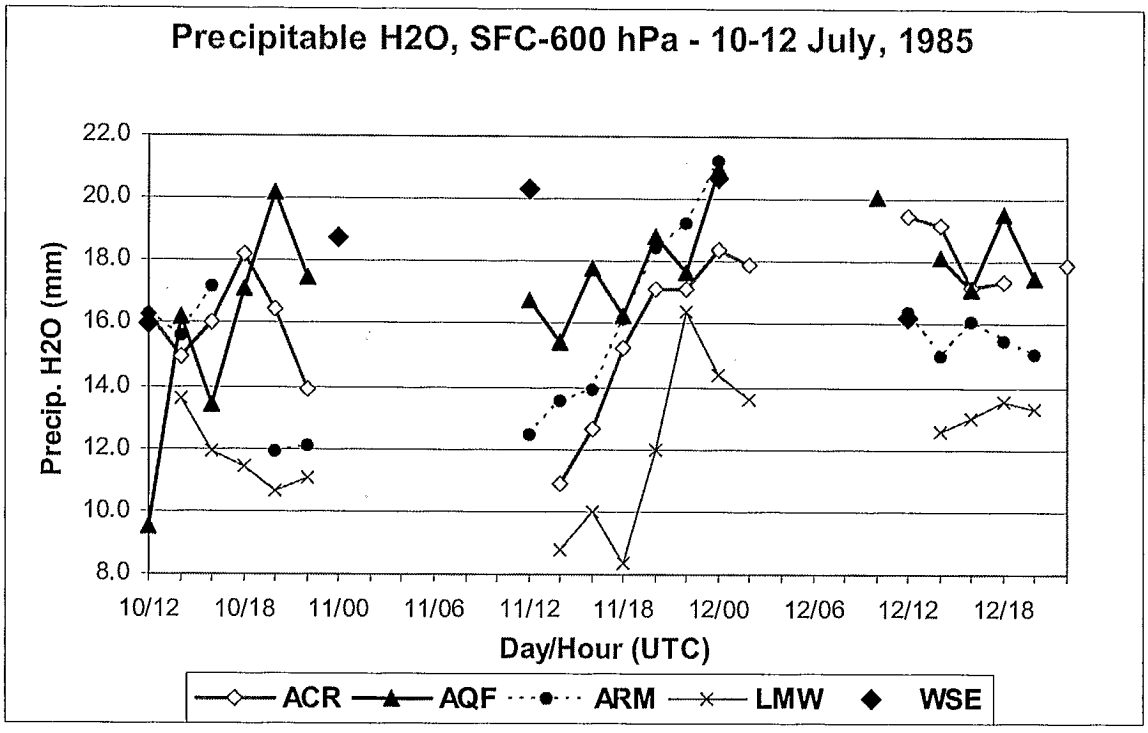

The high values of ABL precipitable water on July 11 were not depleted by July 12, despite a drying westerly flow. Widespread thunderstorms formed again on the 12th, producing up to walnut-sized hail (Deibert, 1985). Heavy precipitation from the previous day's storms is thought to be a contributing factor, although this is admittedly a qualitative observation. This LIMEX-85 case study has thus provided some confirmatory evidence for Stages 2–7 of the multi-scale conceptual model presented in Section 4.0.

5.4 The Pine Lake Tornado Storm, 14 July 2000

The Pine Lake tornado case of 14 July 2000 was introduced in Section 1.0 as an example of how Alberta thunderstorms tend to have different (generally smaller scale) characteristics from storms in Saskatchewan or Manitoba. This storm was mentioned briefly again in Section 2.0 as an example of cloud photography (Figure 2.16) in severe storm research. The Pine Lake tornadic storm is now examined in more detail, using available operational synoptic data as well as proxy data sources, to determine how well it fits the conceptual model hypothesized in Section 4.0, and also to examine storm characteristics and differences in more detail.

Figure 5.23 provides 500 hPa and surface analyses for 1200 and 0000 UTC, along with the observed 0000 UTC sounding for Stony Plain (WSE, near Edmonton), and GEM-model simulated soundings for Red Deer Airport at 1200 and 0000 UTC, 14–15 July 2000. These synoptic analyses, together with the satellite image shown previously in Figure 2.16, confirm that the Pine Lake storm and the storms over southwest Saskatchewan were triggered by the same synoptic shortwave moving in from the west coast. The Pine Lake storm was clearly a post-cold-frontal thunderstorm type, with the front along the Alberta-Saskatchewan border by 0000 UTC, and the synoptic patterns were typical for severe Alberta storms.

The Stony Plain sounding exhibited a capping lid, even at 0000 UTC, but is too far from the source region and storm track to be considered fully representative of the storm. The time of simulated soundings for Red Deer straddle the typical period of most important changes in the ABL (1400–2000 UTC), but even so, the simulated instability is very high on the 0000 UTC sounding.

Figure 5.23 (**a, b**) 500 hPa and (**c, d**) surface analyses (with fronts super-imposed) for Pine Lake tornado storm, 1200–0000 UTC; (**e**) observed Skew-T sounding for Stony Plain (WSE), 0000 UTC; model-simulated tephigram soundings for Red Deer Airport (AQF) at (**f**) 1200 and (**g**) 0000 UTC, 14-15 July 2000.

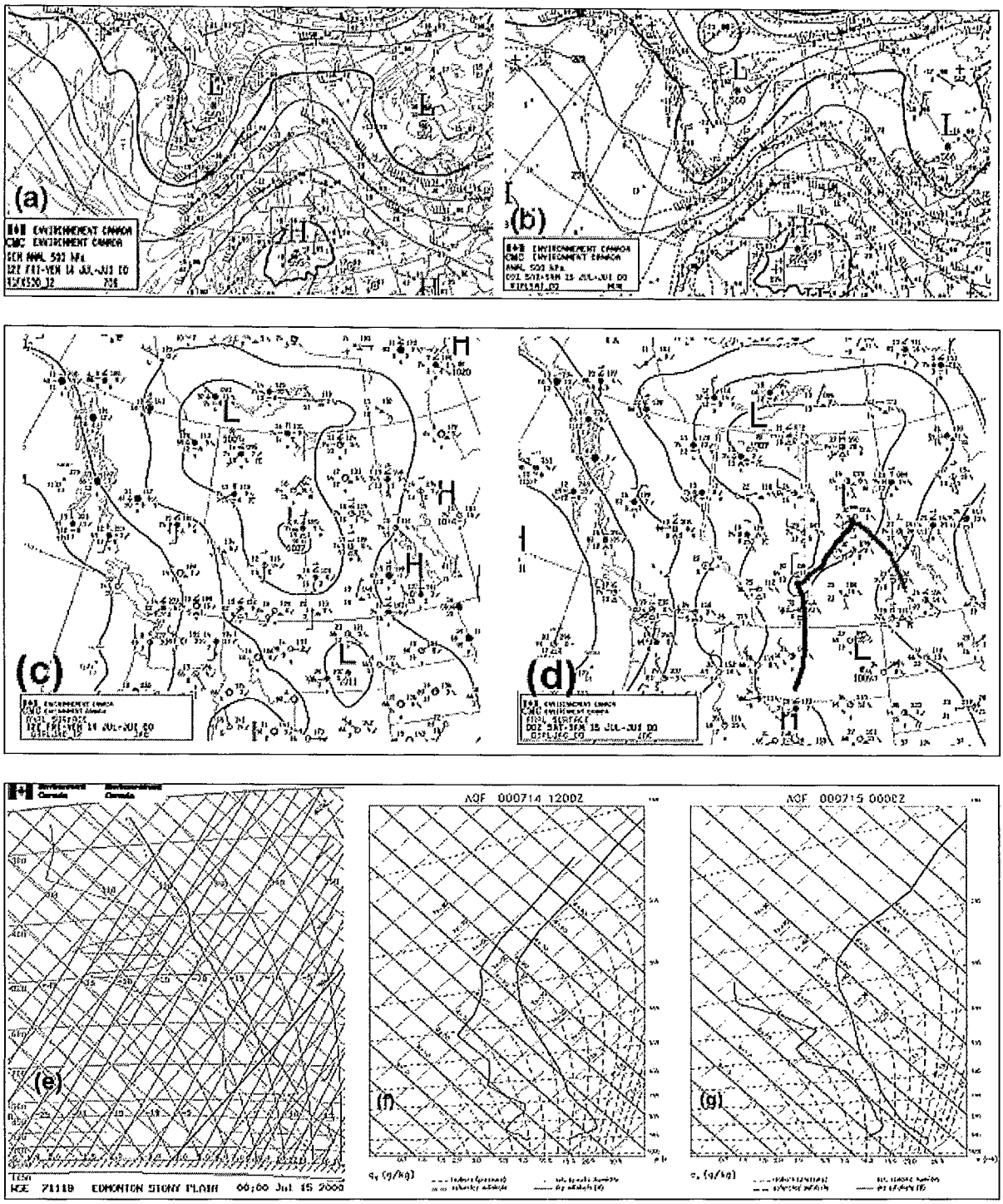

Figure 5.24 shows that this storm originated over the foothills close to Limestone Mountain shortly after 2000 UTC, the southernmost and most severe of a line of such storms parallel to the mountains (2224 UTC). The storm dropped hail up to golf ball-size all along its path as it tracked due east to south of the city of Red Deer by 0013 UTC. At this point, the storm expanded in size and intensity, developing a "hook" echo, and spawned a tornado that touched down west of Pine Lake at 0045 UTC. Severe thunderstorms had been forecast for central Alberta, and a "storm watch" was issued at 2330 UTC, which was upgraded to a "weather warning" at 0018 UTC. Although it was classed as only F1 intensity, the tornado had a 25 km track (Joe and Dudley, 2000), and had a devastating effect on a campground trailer park at Pine Lake while taking 12 lives. The storm prompted Phillips (2001) to label it as *the number one weather event of 2000*, being ranked as Canada's fifth deadliest tornado and the deadliest in North America in 2000.

Using Run-0 initialized GEM MOLTS (MOdel Location Time Series) model data, 12-hour changes in vertical profiles of potential temperature and mixing ratio are produced in Figure 5.25 for the six simulated sounding sites. The three sites closest to the storm track (ARM, ACR, and AQF) suggest a very clear signal; that is, the ABL is warmed through the input of sensible heat flux, but cooled above the ABL, likely through a change in air mass (cooling). The mixing ratio profiles exhibit equally important severe storm signatures. The most obvious signature is that (simulated) soundings for central Alberta show an increase in the absolute humidity at all levels. These increases are maximum at the top of the ABL (between 850 and 800 hPa) in this instance, with the greatest increases at Red Deer, Caroline, and Rocky Mountain House (in that order), or along the storm track.

Diurnal increases in the vertically-integrated vapour mass (or precipitable water) in Figure 5.26 were maximum along the storm track, with both Red Deer and Caroline experiencing increases of 10 g kg^{-1} or more between 1200 and 1400 UTC. The coarse surface analysis of mixing ratio at 0000 UTC (Figure 5.27) suggests that the storm at this time (00:13 in Figure 5.24) was drawing on moisture to the southeast and possibly northeast.

Figure 5.24 Selected Olds-Didsbury Airport radar CAPPIs of Pine Lake tornadic storm, 14 July 2000. (Provided by T. Krauss, WMI.)

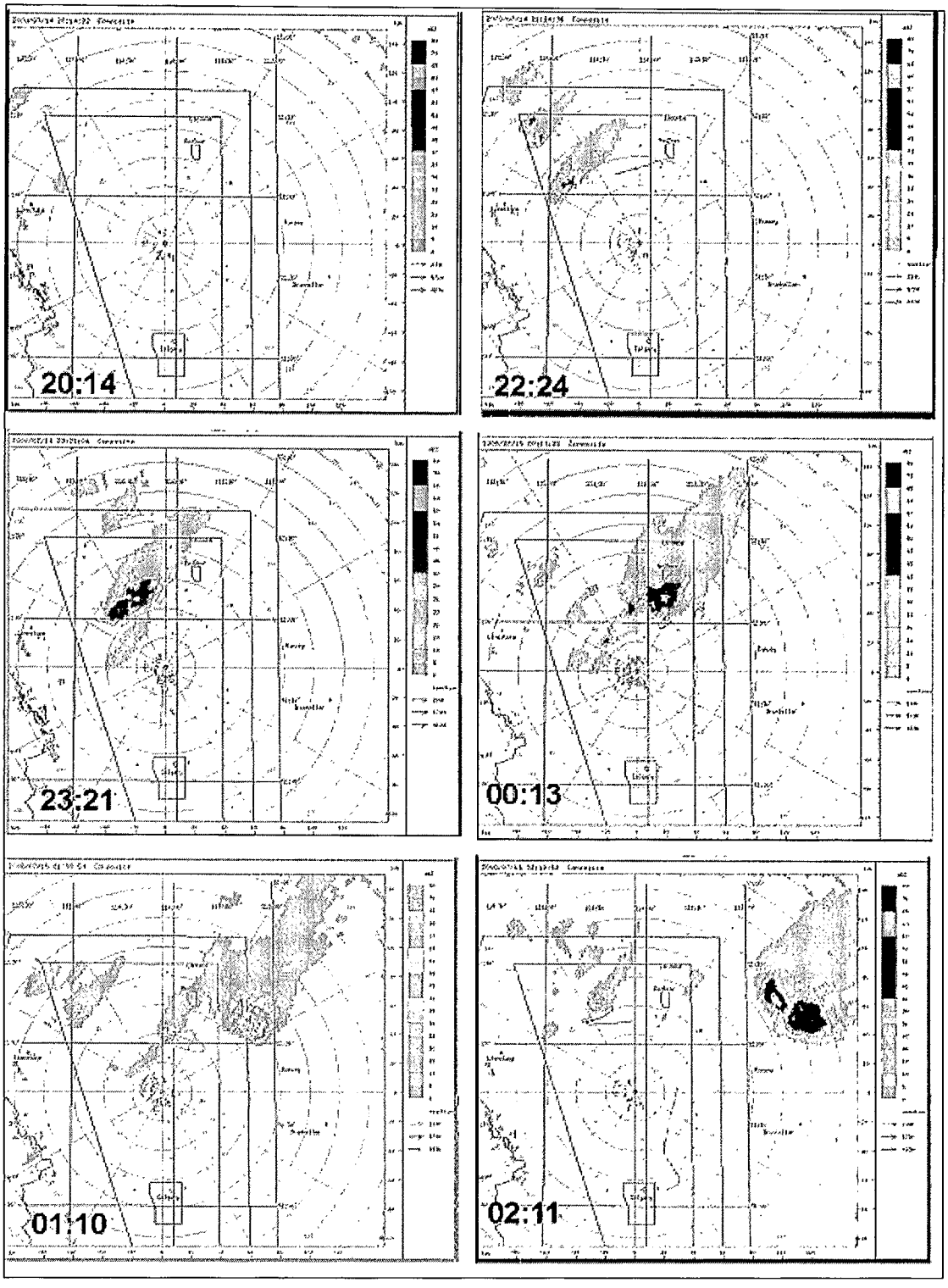

Figure 5.25 12-hour changes in potential temperature and mixing ratio at selected locations, 1200 to 2400 UTC, 14 July 2000, using GEM-model Run-0 output data.

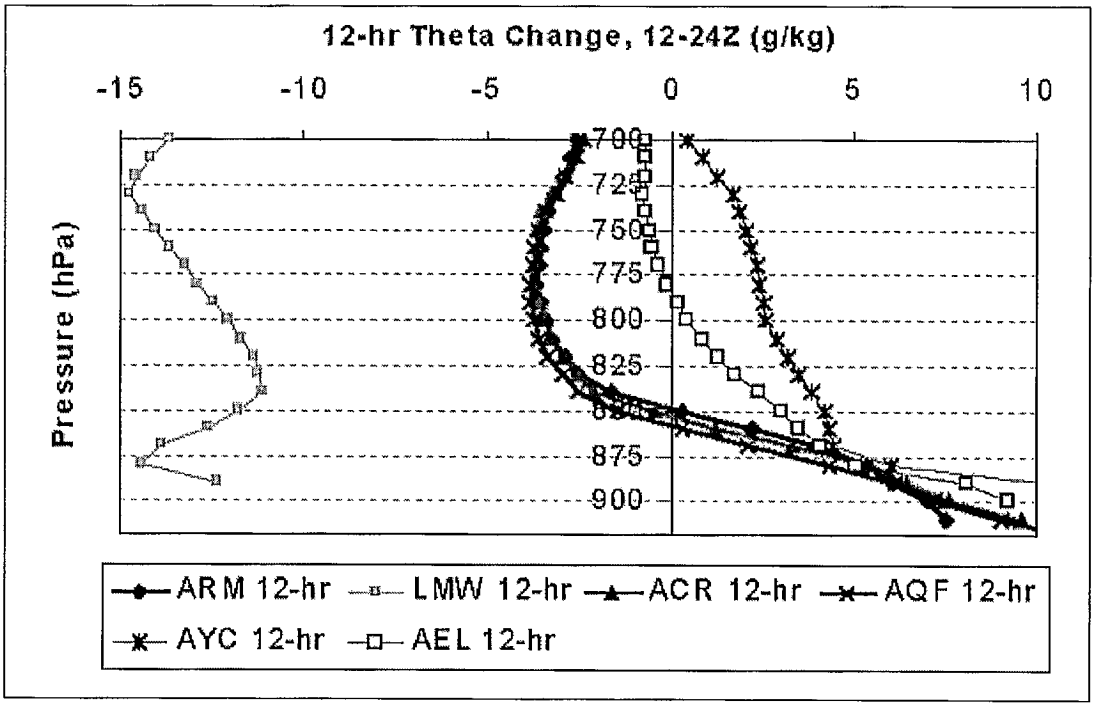

Figure 5.26 Precipitable water at 2400 UTC, 14 July 2000, using GEM-model Run-0 output data.

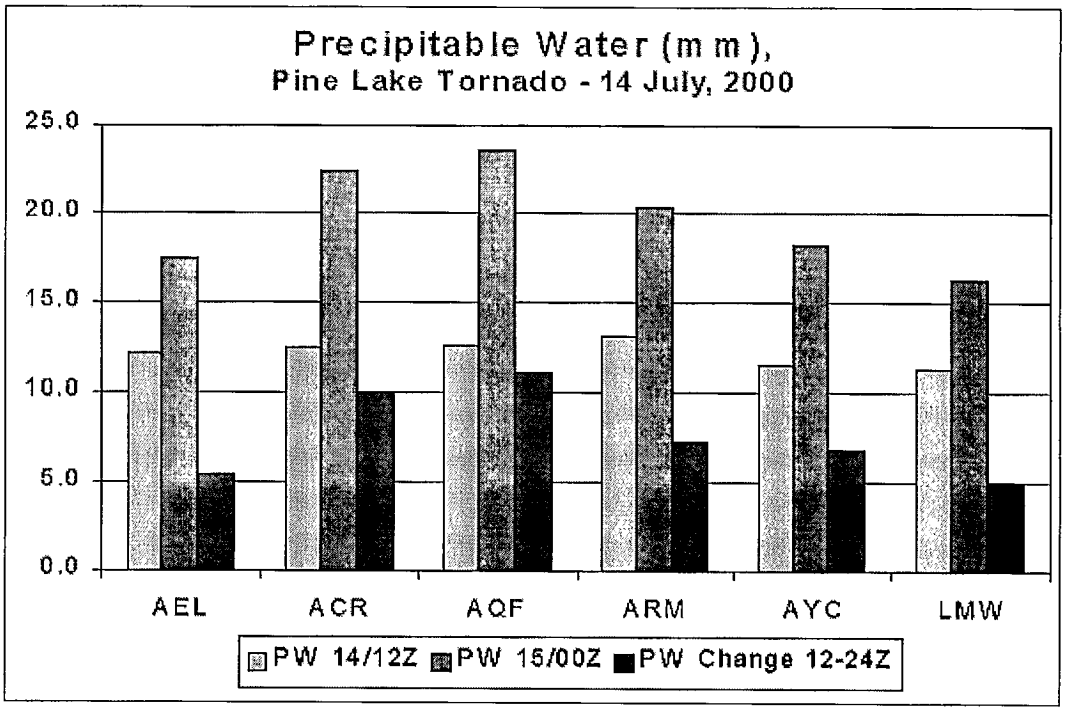

Figure 5.27 Surface analysis of mixing ratios (g kg^{-1}) at 0000 UTC, 15 July 2000.

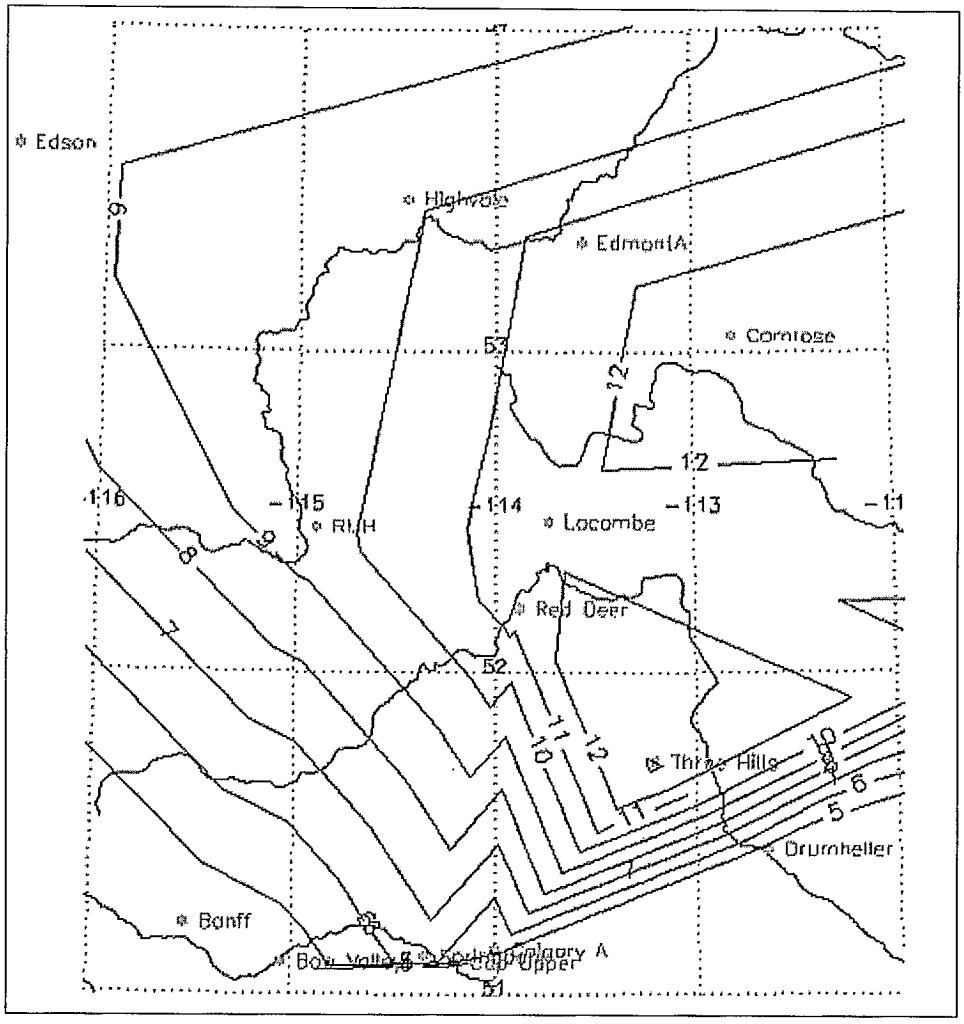

5.5 Summary

We have drawn on three major case studies (LIMEX-80, SESAME-79, and LIMEX-85) with mesoscale surface and upper air data to test most aspects of a multi-scale conceptual model of thunderstorms proposed by Strong (1982, 1986, 2000). A fourth test of the model was carried out on the recent Pine Lake tornadic storm, using synoptic scale surface and upper air data, together with mesoscale model (GEM) output and radar analyses. These four test cases have confirmed in varying degrees all seven stages of the conceptual model. However, it is recognized that several more detailed mesoscale case studies, utilizing special surface and radiosonde data, combined with radar, satellite and other proxy data, are necessary to fully quantify this model, and to adapt its use to Prairie regions beyond western Alberta.

Some marked *differences* in the characteristics of storms west-east across the Prairies have been noted, particularly scale characteristics. This makes the *similarities* between "lee-of-the-

mountains" storms from Alberta south to west Texas all the more intriguing. We note that Texas-Oklahoma storms tend to peak during May, while Alberta storms peak in July. The mean 700 hPa patterns of Figure 5.28 for May 1979 over Oklahoma, and for July 1979 over Alberta suggest a starting point for further investigation of this. Both regions indicate upper air patterns similar to those identified with severe convective storms as discussed in Sections 2.3 and 2.4; that is, an upper ridge just gone by the region with an upper shortwave trough approaching. Even the closest mean height contour through both regions are is the same (3090 m) for their peak storm months, despite there being some 20° latitude difference between the two regions.

Figure 5.28 Mean monthly 700 hPa contours (dam) during peak severe convective weather months for (a) Oklahoma – May 1979 (from Dickson, 1979); (b) Alberta – July 1979 (from Wagner, 1979).

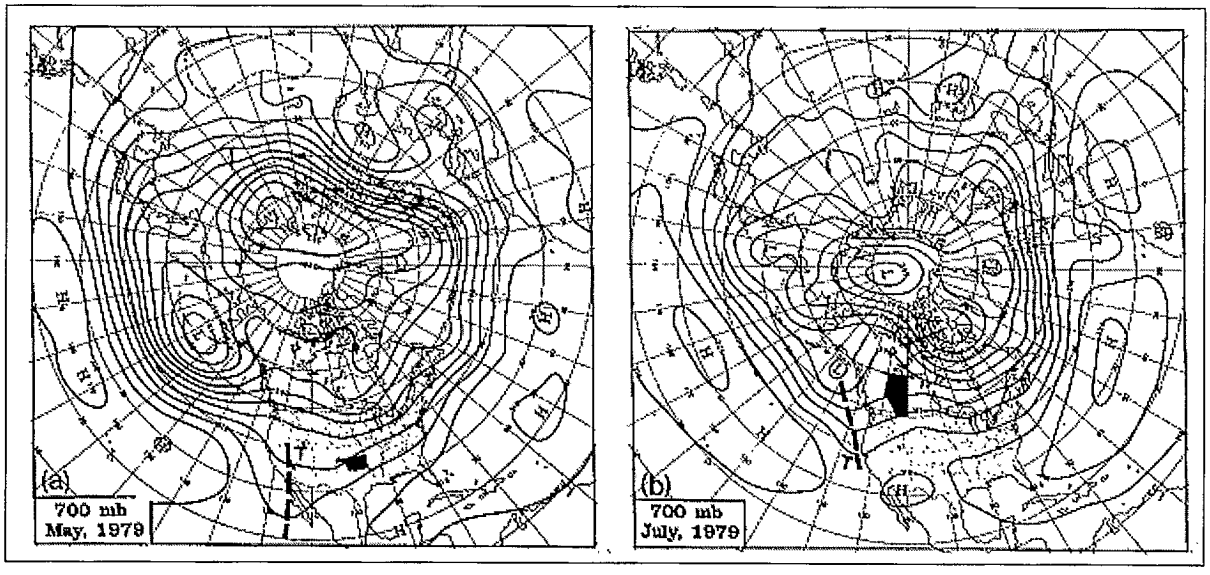

The upper air patterns identified with severe convective storms are revisited a number of times in the forecasting case studies to be discussed in Section 6.0 to follow.

6.0 Forecasting Convective Weather

The science of weather forecasting uses a combination of *pattern recognition* techniques, numerical weather prediction (NWP) models based on physics and mathematics, statistical models or model output statistics, and sometimes a combination of all of the above in artificial intelligence (AI) models such as METEOR (Elio et al., 1987; Strong, 1988). Pattern recognition techniques are the first approach of all forecasters for predicting convective (and other types of) weather, and include recognition of persistent synoptic patterns, derived originally from climatological averages and extremes, and case studies, or from various types of weather observations such as cloud types. While this approach is mostly *qualitative*, it remains in very successful use today. NWP and MOS models attempt to provide a *quantitative* forecast of events. Ideally, one would like NWP models to give an exact, quantitative forecast of thunderstorm location, severity, hail size, any tornado occurrence, and all the other associated parameters. While great strides have been made towards this end in the last ten years, the science is still rather inexact for predicting small mesoscale dynamic features. We will review both of these approaches, qualitative and quantitative, in this section.

6.1 Pattern Recognition – Qualitative Techniques

6.1.1 Necessary and Sufficient Conditions for Thunderstorms

Based on the preceding sections, we are able to summarize the "necessary" conditions for severe thunderstorms in Alberta and elsewhere. We list three prime conditions:

1. unstable air of sufficient depth;
2. relatively high humidity near ground level; and
3. a lifting agency (trigger) to start the air in vertical motion.

6.1.2 Favourable Conditions for Thunderstorms

We can expand on those necessary conditions to include the "favourable" conditions for Alberta storms by exploiting pattern recognition techniques discussed throughout this report and apply these to thunderstorm forecasting. The result is 14 favourable, though not all essential, conditions for severe storm formation, as shown in Table 6.1. These conditions are particularly relevant to severe Alberta hail or tornado-producing thunderstorms. They are organized into four groups that correspond approximately to the order in which a forecaster might review data and maps available to him or her when composing a forecast for the day, and are also prioritized in three levels of importance using F = favourable, F+ = more favourable, F++ = most favourable conditions. The reader is cautioned that this list is simply a guide, and that the prioritizations are quite subjective, since some of the conditions are somewhat relative; e.g., a capping lid can be so strong that ascent does not weaken it to the point of releasing convection, or the surface low pressure could be a "cold low" with massive cloud formations to suppress deep convection. Moreover, one can easily add other favourable conditions to this list. Forecasters are encouraged to use their own ratings based on their own experience and that of their peers.

Table 6.1 Subjective list of conditions favourable to thunderstorms in Alberta. Each is given a subjective level of importance according to F = favourable, F+ = more favourable, F++ = a most favourable condition.

#	Imp.	Condition and Grouping
		I. Morning Skies – *a forecaster's first (and last) indicator*
1	F	Generally sunny skies, or at the least, no significant high-level (cirrus) clouds, ground fog or broken mid-level (AC) clouds are NOT deterrents for convective storms.
2	F	Observations of ACC (alto-cumulus castellanus) clouds during morning (often a location for a later storm), as observed in Figure 4.3.
		II. Low-Level T/RH – *most important thermal structure for the ABL*
3	F	Early morning surface temperatures of 10–20°C, increasing to the mid-20s by mid-afternoon.
4	F+	High humidities in the lowest 500–1000 m, the ABL; often accompanied by morning "ground fog patches" over the region.
5	F+	An inversion of temperature capping the top of the ABL, generally at 500–1000 m above ground (the *capping lid*), acting as a trap until convection is suddenly realized.
		III. Middle-Level T/RH – *thermal structure above the ABL*
6	F	Dry air above the *capping lid* and ABL (also illustrated in Figure 6.1; dew point temperature trace is the broken line on the LHS).
7	F	Pre-existing instability at mid-levels (generally confirmed by a dry adiabatic[6] lapse rate within the layer from 500–850 hPa), and/or the appearance of ACC or towering cumulus (TCU) clouds.
		IV. Dynamics – *the important dynamic triggers*
8	F++	Surface low-pressure system south of the region.
9	F	Light easterly wind component (southeast – northeast winds) at low-levels (in the ABL) initially, with moisture advection.
10	F+	Ascending air within the ABL.
11	F++	An approaching upper shortwave trough over B.C. (the storm "trigger"), most especially if the trough has negative tilt (oriented NW to SE).
12	F	A moderate southwest flow at middle-levels (700–500 hPa) in advance of the shortwave trough, with cooling temperatures at these levels.
13	F+	Evidence of ascent and cooling aloft (850–500 hPa) slightly UPSTREAM (west to southwest) of the storm development area.
14	F	A jet stream aloft, where storm development will be favoured under the left exit region of a cyclonically-curved jet, or under the right entrance of an anticyclonically-curved jet.

[6] The dry adiabatic lapse rate refers to the atmosphere cooling with height at a rate of 9.8°C km^{-1}. In Figure 6.1, the line running from lower-right to upper-left connecting the 20 and 0°C isotherms is a "dry adiabat" (or potential temperature line). A temperature trace parallel to this is dry adiabatic.

Apart from simple cloud observations, a forecaster's first assessment of severe storm potential for the day should be the synoptic to mesoscale dynamics. When all five of the dynamic conditions above are present during June through August, a day similar to the Pine Lake tornado storm (14 July 2000) should be initially anticipated. Only *then* should the forecaster assess existing thermodynamic instability, but with the awareness that a 1200 UTC sounding, especially the ABL, is very likely not representative of what will happen in the three to six hours following the sounding time. For Alberta, initial storm formation is favoured (but not limited) to the foothills regions. For this same reason, the Stony Plain sounding does not always reflect the ABL conditions over the foothills.

There are three main questions that the forecaster must assess regarding the morning ABL, which are partly addressed in the example sounding of Figure 6.1, for 1200 UTC, 16 August 1973, at Rocky Mountain House: (1) How will the ABL temperature profile change with surface heating and temperature advection?; (2) This one is really critical, *and* difficult to assess – how will the ABL moisture profile change with evapotranspiration and moisture advection?; (3) How will the environment temperature and moisture adjust with mesoscale vertical motion? For example, at what point may surface moisture flux be dispersed into the free atmosphere above the capping lid (if one is present)?

Figure 6.1 Illustration of diurnal heating of the boundary layer of an actual capping lid sounding based on recorded surface temperatures at Rocky Mountain House, 1200–2200 UTC, 16 August 1973 (reproduced from Strong, 1986).

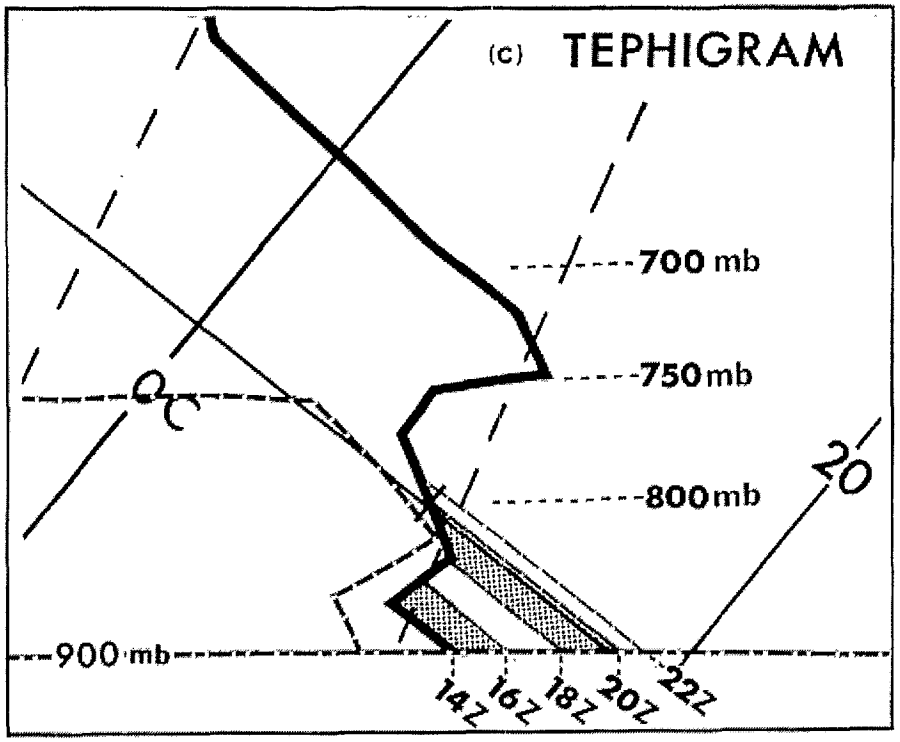

The sounding shown above is also included in Figure 4.4, for a day on which a supercell formed a few kilometres south of Rocky and resulted in a devastating hailstorm as illustrated in Figure 3.1.

6.1.3 Composite Analyses for Forecasting Severe Thunderstorms

Most of these conditions and pattern recognition techniques have been used qualitatively to forecast severe convective thunderstorms. Various *composite analyses* have been used, the most familiar of which were those developed by Fawbush et al. (1951), and Fawbush and Miller (1953, 1954). This was an empirical method of forecasting tornado development using composite analyses of synoptic charts and instability analyses such as temperature lapse rate above and below the capping lid, moisture above and below the lid, wind shear, Showalter Index, and warm frontal zones. These are still in use today by forecasters worldwide, having been automated into computer simulations.

6.2 Quantitative Operational Techniques

Various attempts have been made to come up with a single objective number that would predict convective intensity in one form or another. While no universal system has been derived, various simple convective instability indices have been in use for the past half-century. The most famous of these indices was the Showalter Index (Showalter, 1953). Various modifications of this have been developed for specific areas or uses, including the Lifted Index (Galway, 1956), and a couple of Canadian versions, the SlyDex (Sly, 1966; Braun, 1968), and the EGDEX (Checkwitch, 1971). All of these basically lift a surface parcel dry adiabatically until saturation is attained, then moist adiabatically up to the 500 hPa level. The difference between the parcel temperature and the environmental (radiosonde sounding) temperature is the value of the index. Positive instability is indicated when the parcel temperature is warmer, and visa versa. Some versions of the technique average the dew point (or mixing ratio) within the boundary layer, and then lift it as above. The EGDEX is a surface parcel lifted index adjusted to account for the climatological increase in surface moisture due to evapotranspiration, stratified by wind direction.

Other sounding-derived indices attempt to combine thermodynamic instability with dynamics variables such as the storm relative helicity (Moller et al., 1994), convective available potential energy (CAPE, Moncrief and Green, 1972), and the Bulk Richardson Number (Weisman and Klemp, 1986). Strong (1979) used both the EGDEX and a surface parcel lifted index as two of 10 predictors in a MOS technique called the Synoptic Index of Convection.

6.3 Numerical Models

6.3.1 Synoptic Scale NWP Models

The Canadian Meteorological Centre (CMC) in Dorval, Québec currently runs the GEM (Global Environmental Multiscale) Numerical Weather Prediction (NWP) model. The model assimilates radiosonde, surface, and other data from around the globe four times daily at 0000, 0600, 1200,

and 1800 UTC. An initialization run outputs the analysis (Run-0), then 12, 24, 36, and so on to 240-hour forecast runs. The model uses previous six- and 12-hour prognostic runs to fill in where there are nil or missing data. In general, the model now produces forecasts of pressure height, temperature, humidity, winds and a host of other variables, including simulated radiosonde soundings for several hundred sites, for various pressure levels (1000, 925, 850, 700, 500, etc. hPa). Currently the model outputs data on an approximate 25 km grid with 28 vertical levels.

While the general features of weather systems are forecast quite accurately, the accuracy at a single point is highly variable, especially over mountainous terrain such as the Rockies or the foothills. This is evident in the initialized (Run-0) and forecast MOLTS (MOdel Location Time Series) soundings output by the GEM model. Figure 6.2 is an example comparison sounding showing the observed (radiosonde levels, solid lines), Run-0 (initialized model 0-hour forecast at observation time, dotted lines), and previous Run-12 (12-hour forecast, dashed lines) soundings for Fort Smith, N.W.T., all valid at 1200 UTC, 25 July 1998.

Figure 6.2 Comparative example of observed and modelled atmospheric profile. The solid line represents the observed radiosonde profile, while the dotted/dashed lines represent profiles from the initialized model run and 12-hour forecast respectively, all valid for 1200 UTC, 25 July 1998 at Fort Smith, N.W.T.

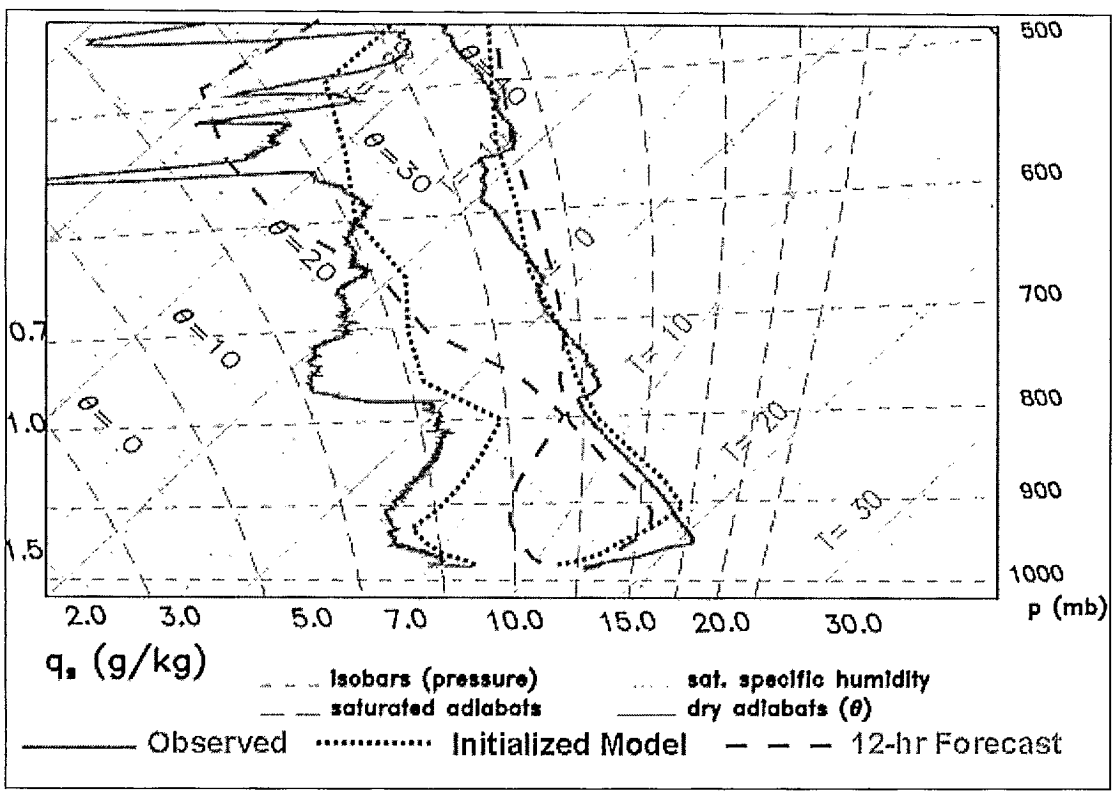

The Run-0 should technically be very close to the observed data, but such is not the case. The initialized data are not *just* an objective analysis and gridding procedure. The temperature trend is reproduced well, but not the mesoscale details – *particularly* the ABL features, including the observed capping lid just above the 800 hPa level. The initialized (Run-0) dew point trend is too

moist throughout the sounding. The 12-hour forecast sounding (Run-12) from the previous forecast run is considerably poorer than the Run-0 of course, most especially the ABL moisture, where mixing ratios are about 3 g kg^{-1} too high in the boundary layer, while temperatures are predicted somewhat on the cool side. These biases are typical of similar problems found in other MOLTS sounding data for the Mackenzie GEWEX Study (Strong et al., 2001). Additionally, the GEM model was unable to simulate the summertime diurnal cycle in moisture due to evapotranspiration. Since the ABL is the key to a good convective forecast, the MOLTS soundings are presently not very useful for summer convective forecasts. It is important that the modellers obtain feedback on any field validation of these data to see if these numerical prediction problems can be rectified.

While the above comparison is almost two years old at this writing, we have not had cause to believe that the ABL forecast profiles have improved since then. Details of the GEM model, output data, verification, and actual analyses and forecasts can be found at

http://www.msc-smc.ec.gc.ca/cmc/index_e.html

6.3.2 Mesoscale Models

Mesoscale models, initialized with pre-storm environmental data, have three important potential uses. First, they provide one method of testing scientific hypotheses concerning interactions with the mesoscale environment. Second, if one can successfully simulate convective environmental conditions using mesoscale data for initialization and for ground-truthing, then the model input could be varied to simulate other conditions for which one lacks the necessary mesoscale data. Assuming that the model performs well for these applications, the third use, as a real-time forecasting tool, is rather obvious. Pielke (1984) provides an excellent overview of some mesoscale models, many of which are fast approaching forecasting potential.

6.3.3 Cloud Physics Models

Cloud physics numerical models have been in use for many years in a variety of applications, including prediction of rainfall amounts, maximum hail size, cloud liquid water content, storm updraft velocity, and downdraft/outflow velocities. These have varied in complexity from the one-dimensional steady state loaded moist adiabatic model (LMA) of Chisholm (1973) to complex, time-dependent three-dimensional hail models such as Kubesh et al. (1988) for both diagnostic studies and forecasting applications. One of the more recent one-dimensional models is HAILCAST, comprised of a 1-D steady-state cloud model and a time-dependent hail growth model (Brimelow, 2001). Diagnostic tests using three summers (1983–85) of AHP sounding data, including LIMEX-85, yielded forecast accuracies on hail size as high as 95%. The Alberta Hail Modification Project plans to test-run the model during 2001 as both a forecast aid and a possible tool for evaluating cloud-seeding results.

6.4 The Synoptic Index of Convection

The urgent need for forecast products sometimes obscured useful scientific results. For example, Longley and Thompson (1965) stated that "*among the variables examined, no necessary and sufficient conditions were isolated by which one could distinguish a day with severe hail from days with either minor or no hail.*" They saw little forecasting significance in the patterns of Figures 2.12 and 2.13. Still, forecast techniques such as the composite analysis methods of Miller (1972), evolved from similar types of synoptic studies, and with moderate success. During the 1970s, more objective statistical applications of these concepts were developed. One fairly successful example is the Synoptic Index of Convection (Sc_{10}), developed by Strong (1979) as a single predictor of maximum storm severity over a 130 km radius area (the AHP operations area). This later evolved into an *areal* predictor, the Sc_4, using only four or three predictor variables, and its use was extended to other areas (Strong and Wilson, 1983).

Ideally, one would like NWP models to give an exact, quantitative forecast of thunderstorm location, severity, hail size, any tornado occurrence, and all the other associated parameters. In the absence of such models, model output statistics (MOS) techniques combine model output with statistical relations to improve the forecast as well as make it more specific; that is, for a specific variable or specific region. MOS was therefore used to develop a *daily quantitative* index of thunderstorm severity for the AHP cloud-seeding project carried out from 1974–85. However, before attempting to develop a quantitative forecasting technique, one must first define some sort of quantitative index of thunderstorm severity. In this regard, we will refer to the terms *predictand*, the quantity that we would like to predict, and *predictor variable*, referring to variables used in the prediction technique.

6.4.1 Convective Day Category (CDC)

The required *predictand* was developed first, using AHP *maximum hail size* reports as an indicator of storm severity, and the distribution was deliberately constrained so as to fit a *normal*-type statistical distribution (i.e., to fit a bell-type distribution curve). This constraint was imposed in order to obtain the best possible statistical correlations with the *predictor* variables to be used, which all fit a *normal*-type distribution; e.g., Figure 6.3(a) shows the distribution of 12-hour (1200–2400 UTC) 400 hPa temperature change for 1975–77 summers at Red Deer just as an example of typically normally distributed predictor variables. If one grouped all no-hail days in one category along with the distribution of maximum hail size, an exponential-type distribution results, as shown in Figure 6.3(b). To force this into a normal distribution, it was necessary to devise several *no-hail* categories. The result was a predictand called *Convective Day Category* (CDC), defined for nine categories of convective intensity, ranging from no convection to hailstones larger than golf ball-size (Strong, 1979, 1986). These are shown in Table 6.2.

Figure 6.3 Example of (a) normal distribution of most predictor variables – 12-hour 400 hPa temperature change at Red Deer, AB, 1975–77 summers; (b) exponential distribution of AHP maximum hail size categories using one category for NO HAIL.

(a)

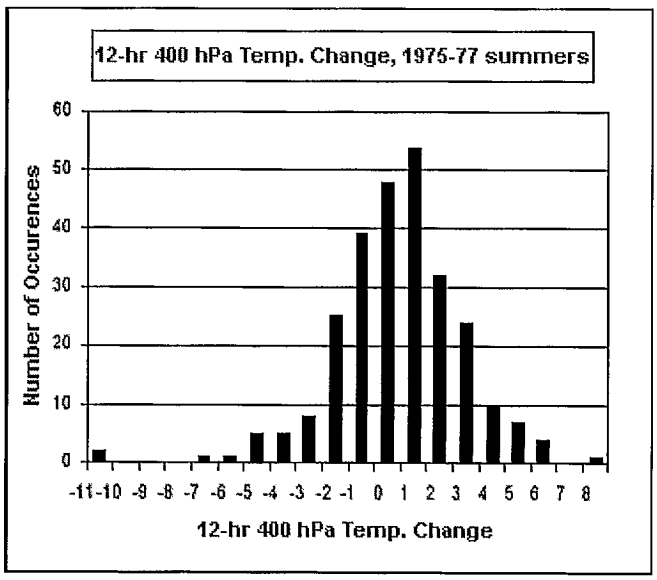

(b)

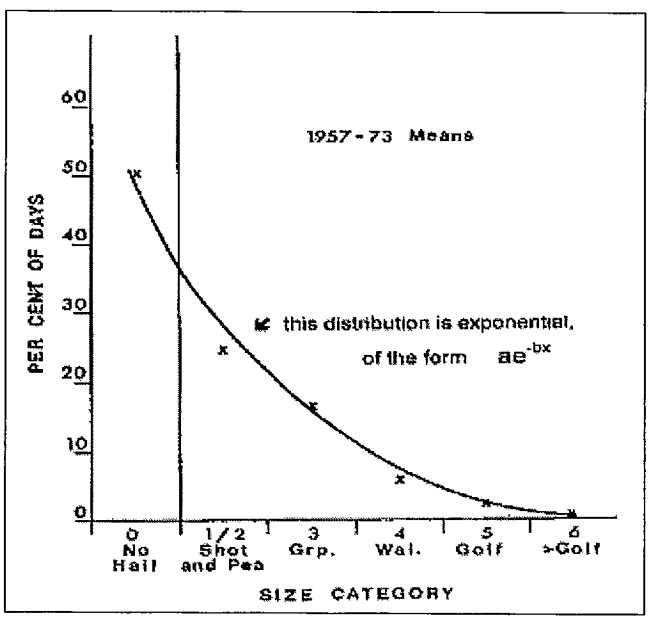

6.4.2 Single-Valued Synoptic Index of Convection

Daily values of CDC were initially determined for three summers of data, 1975–77, and new statistics were thereafter added with each successive summer of data. These were then compared statistically with various *predictor* variables. Potential *predictor* variables were chosen primarily by using the list of most favourable conditions for Alberta thunderstorms shown in Section 6.1. Initially, 10 predictors were chosen (for the Sc_{10}), prioritized on the basis of linear correlation with CDC. Later, it was found that using only the four highest correlating variables produced almost as good a result (the Sc_4). Table 6.3 shows linear correlation statistics for the four-variable Synoptic Index of Convection (Sc_4) with the predictand CDC.

Table 6.2 Definitions of Convective Day Category (CDC) for the AHP operations area 130 km radius from Red Deer Airport, AB (after Strong, 1979).

CDC	DEFINITIONS	
+5	LARGER THAN GOLF BALL	> 52 mm diameter HAIL
+4	GOLFBALL	33–52 mm hail reported
+3	WALNUT	21–32 mm hail reported
+2	GRAPE	13–20 mm hail reported
+1	PEA or SHOT	< 13 mm hail reported
0	WIDESPREAD SHOWERS throughout most of the AHP area, or the occurrence of THUNDERSHOWER, but NO HAIL	
-1	SCATTERED SHOWERS (over less than half the area), NO HAIL or THUNDERSHOWER	
-2	SIGNIFICANT CONVECTION (ACC, TCU or CB clouds), but NO SHOWERS	
-3	NO DEEP CONVECTION reported (no ACC, TCU, or CB clouds)	

Notes: At least two hail reports are required to qualify for CDC>0. All categories are determined from the period 1700 through 1200 UTC. See Strong (1979), Strong et Wilson (1983a) for other qualifiying remarks on these categories.

Table 6.3 Correlations, and weighting statistics for Sc_4 predictor variables with CDC, based on 1975–77 statistics (after Strong and Wilson, 1983).

	Predictor Variable	Correlation with CDC	Weighting Coefficient
1.	EGDEX	0.577	0.288
2.	24-hr. 700 hPa Temperature Change (1200–1200 UTC)	- 0.492	0.246
3.	24-hr. 1000–500 hPa Thickness Change (1200–1200 UTC)	- 0.479	0.239
4.	Surface Parcel Lifted Index	0.456	0.227

The weighting coefficients of Table 6.3, based again on the degree of correlation, are used to formulate a normalized equation for Sc_4:

$$Sc_4 = \sum_{k=1}^{n} W_k (a_k p_k + b_k) \quad (1)$$

where $\sum_{k=1}^{n} W_k = 1.000$, $W_k = |\rho_k| \; / \sum_{k=1}^{n} |\rho_k|$ and the ρ_k and W_k are the correlation and weighting coefficients respectively in the table; "n" normally = 4 (for the four predictors in the table), but has been used successfully with only three predictors (e.g., EGDEX values have not been determined for locations beyond the Canadian Prairies).

6.4.3 Evaluation of Single-Valued Sc_4

The Sc_4 is based on predictors that are routinely output by NWP products, so that computation of the index was fully automatic. However, since the individual forecaster had the final say in the actual forecast, using additional data sources, he applied a more subjective interpretation and issued a *forecast CDC*. Figure 6.4 evaluates forecast CDC values against observed CDC for eight summers of data (619 days in total). The forecast CDC was the forecaster's subjective modification to the objective forecast Sc_4 (i.e., after the forecaster had seen the forecast Sc_4). Figure 6.5 shows average values of forecast Sc_4, revised forecast CDC, and observed CDC, and linear correlation coefficients between observed/forecast CDC, and observed CDC/forecast Sc_4. This suggests that the forecaster could add a small degree of value through his subjective interpretation skills, improving the correlation by about 0.05 – the "human" element. The linear correlation of observed CDC with forecast CDC was 0.68, and with forecast Sc_4 is 0.63, with individual years ranging from 0.61 (1983) to 0.82 (1980).

Figure 6.4 Evaluation of forecast CDC (after forecaster had seen the forecast Sc_4) with observed CDC, eight summers (619 days), 1978–85.

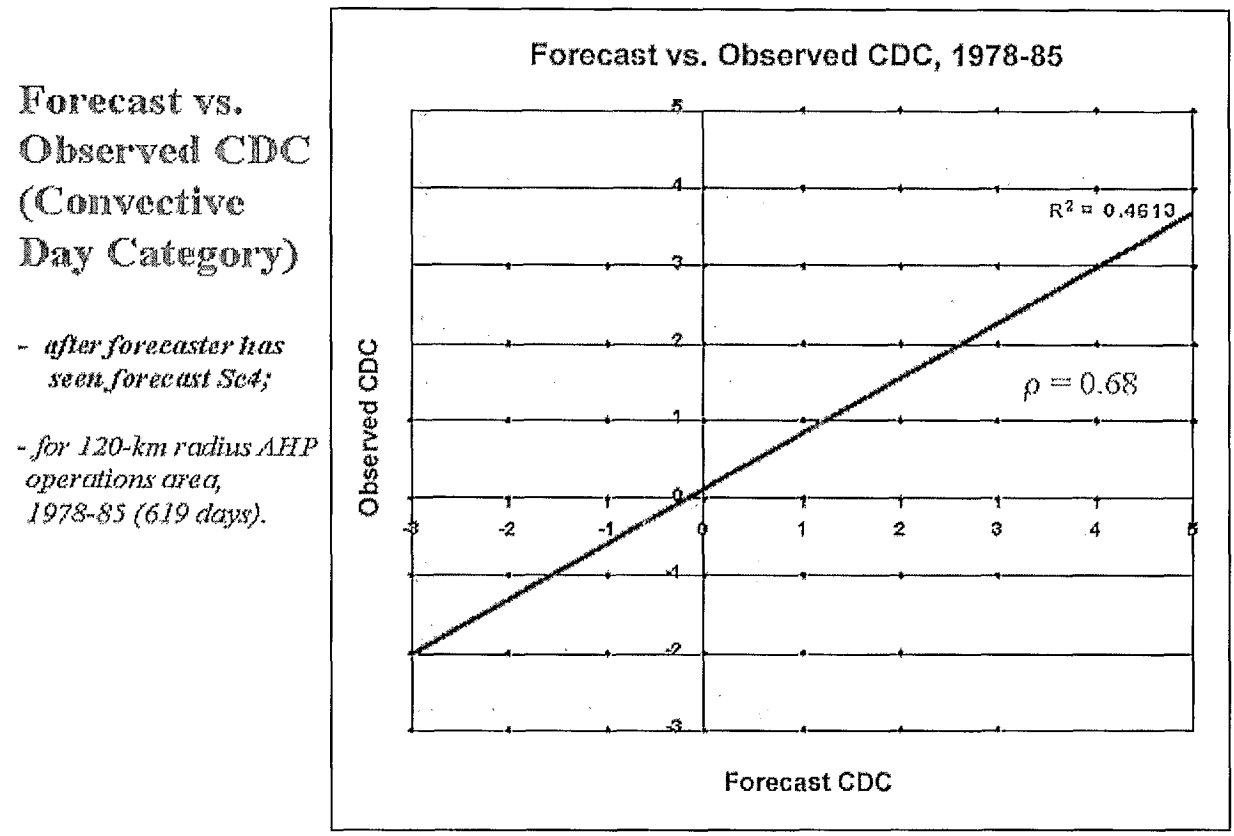

The value-added degree of accuracy results in the forecast evaluation (by CDC category) shown in Figure 6.6, and in the hail/no-hail forecast evaluation of Figure 6.7 for the eight-year period, 1978–85. While forecasts of exact CDC category appear to be only 31% accurate, the *reporting* of hail size by untrained observers is itself a rather inaccurate measure, so that the forecast evaluation within one, and even two CDC categories is more relevant, where the accuracy improves to 72% and 89% respectively. Evaluation on a *hail/no-hail* basis is less relevant still, since a day is classified as a hail day whether only two observations of pea-size hail or several hundred larger than golf ball are reported. Nevertheless, the forecaster was accurate 76% of the time on HAIL/NO-HAIL forecasts during these eight summer periods.

Evaluations of forecast CDC categories and HAIL/NO-HAIL by year are included in Appendix B of this report.

Figure 6.5 Average values of forecast Sc_4, revised forecast CDC, and observed CDC, and linear correlation coefficients between observed/forecast CDC, and observed CDC/forecast Sc_4, eight summers (619 days), 1978–1985.

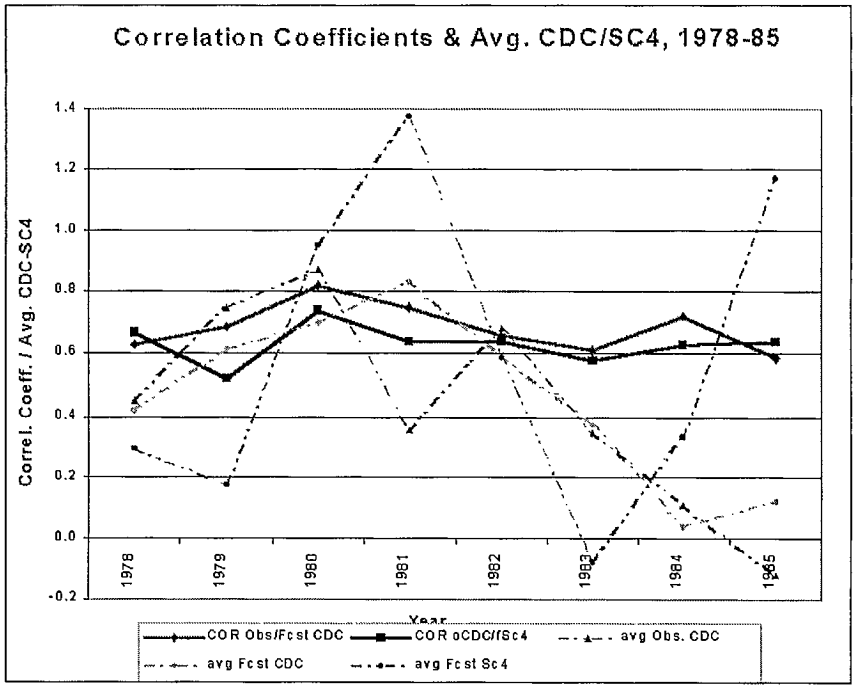

Figure 6.6 AHP Forecast accuracy on CDC categories, 1978–85.

AHP Forecast Accuracy (CDC Categories), 1978-85

		Forecast Convective Day Category										
		-3	-2	-1	0	+1	+2	+3	+4	+5	Totals	%
Observed	-3	26	15	11	1	1	1	1	0	0	56	8.7
	-2	12	21	13	11	8	5	0	0	0	70	10.9
Convective	-1	2	14	26	16	10	1	3	0	0	71	11.0
	0	3	6	29	39	25	14	5	3	0	124	19.2
Day	+1	1	5	10	29	37	31	8	4	1	126	19.5
	+2	0	1	5	13	29	31	16	4	2	101	15.7
Category	+3	0	1	2	6	8	22	12	4	1	56	8.7
	+4	0	0	0	4	2	7	10	6	3	32	5.0
(CDC)	+5	0	0	0	0	1	2	4	1	1	9	1.4
	Totals	44	63	96	118	121	114	59	22	8	645	100.0
	%	6.8	9.8	14.9	18.3	18.8	17.7	9.1	3.4	1.2	100.0	

Forecast Category Accuracy:

Correct Category:	199 days	30.9 %
Correct within one Category:	467 days	72.4 %
Correct within two Categories:	576 days	89.3 %

Figure 6.7 AHP Forecast accuracy on HAIL/NO-HAIL, 1978–85.

AHP Forecast Accuracy (HAIL/NO-HAIL), 1978-85

OBSERVED	Forecast: NO HAIL	Forecast: HAIL
NO HAIL	244	77
HAIL	77	247

HAIL/NO-HAIL Accuracy:

No. hail days in period:	324 days	50.2 %
No. 'severe' hail days in period:	97 days	15.0 %
Correct HAIL days forecast:	247 days	76.2 %
Correct NO HAIL days forecast:	244 days	76.0 %

The distribution of CDC for the 1978–85 period is shown in Figure 6.8, and it can be seen to be approximately normal, similar to that of the predictor variables (compared with the example in Figure 6.3a). The left-skewed distribution in this figure suggests that one additional no-hail (negative CDC) category would be useful, and might provide improved correlations over what was observed in Figure 6.5. Note also that approximately 50% of the summer days (mid-June through early-September) in central Alberta have hail, and 15% of these days can be classified as severe; that is, when walnut or larger size hail (CDC ≥+3) occurs.

Figure 6.8 Distribution of observed Convective Day Category, 1978–85.

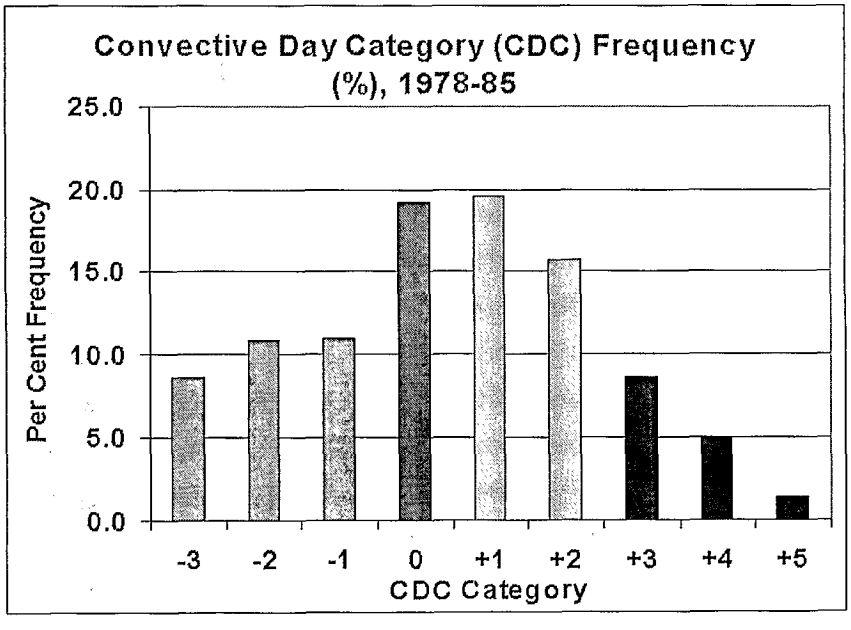

- for 120-km radius AHP operations area, central Alberta

6.5 The "Areal" Version of the Synoptic Index of Convection (Sc_4 and Sc_3)

The Synoptic Index was originally designed to provide a single forecast value for the whole of the 120 km radius AHP cloud-seeding operations area. It was desirable to have an *areal* index, which would provide a contoured map of maximum thunderstorm severity. The Sc_4 was easily adapted for this, and used for the very first time on a very noteworthy storm: the Calgary hailstorm of 28 July 1981. At the time, this was the most expensive storm in Canadian history, resulting in insurance claims and pay-outs well in excess of $100M (Strong, 1982).

6.5.1 The Calgary Hailstorm, 28 July 1981

Figure 6.9 gives a brief summary of the synoptic conditions (500 hPa and surface patterns), the Sc_4 prediction, CDC evaluation, and satellite enhanced infrared pictures showing the storm in its early stages (northwest of Calgary at 2101 UTC, 1501 MDT), and in the dissipation stages following its track through Calgary (southeast of the city at 0202 UTC, 2002 MDT). This case very much fits the multi-scale conceptual model described earlier, with the upper shortwave trough approaching Alberta, cyclogenesis south of the AHP area, easterly flow within a *capped* boundary layer, etc. The storm also exhibited virtually all of the 14 most favourable conditions outlined in Table 6.1. It is noteworthy that this storm propagated southeastward, 90° to the right of the upper flow (500 hPa analysis). In presenting the weather briefing on the morning of July 28, the forecaster correctly suggested that the storm might propagate southeast because of an existing supply of moisture to the east of Calgary with an easterly ABL flow. The Sc_4 alone correctly predicted the storm formation region (highest values over the southwest quadrant of AHP), maximum intensity (values exceeding +4, suggesting >golf ball size hail), and provided some hint of storm propagation (ridge of higher Sc_4 values southeast through Calgary).

Figure 6.9 First test of *areal* version of Sc_4, on the Calgary hailstorm of 28 July 1981. Included are 500 hPa and surface analyses, contoured map of forecast Sc_4, observed convective weather composite, and infrared NOAA satellite images at 2101 UTC and 0202 UTC, 28–29 July 1981 (reproduced from Strong, 1986).

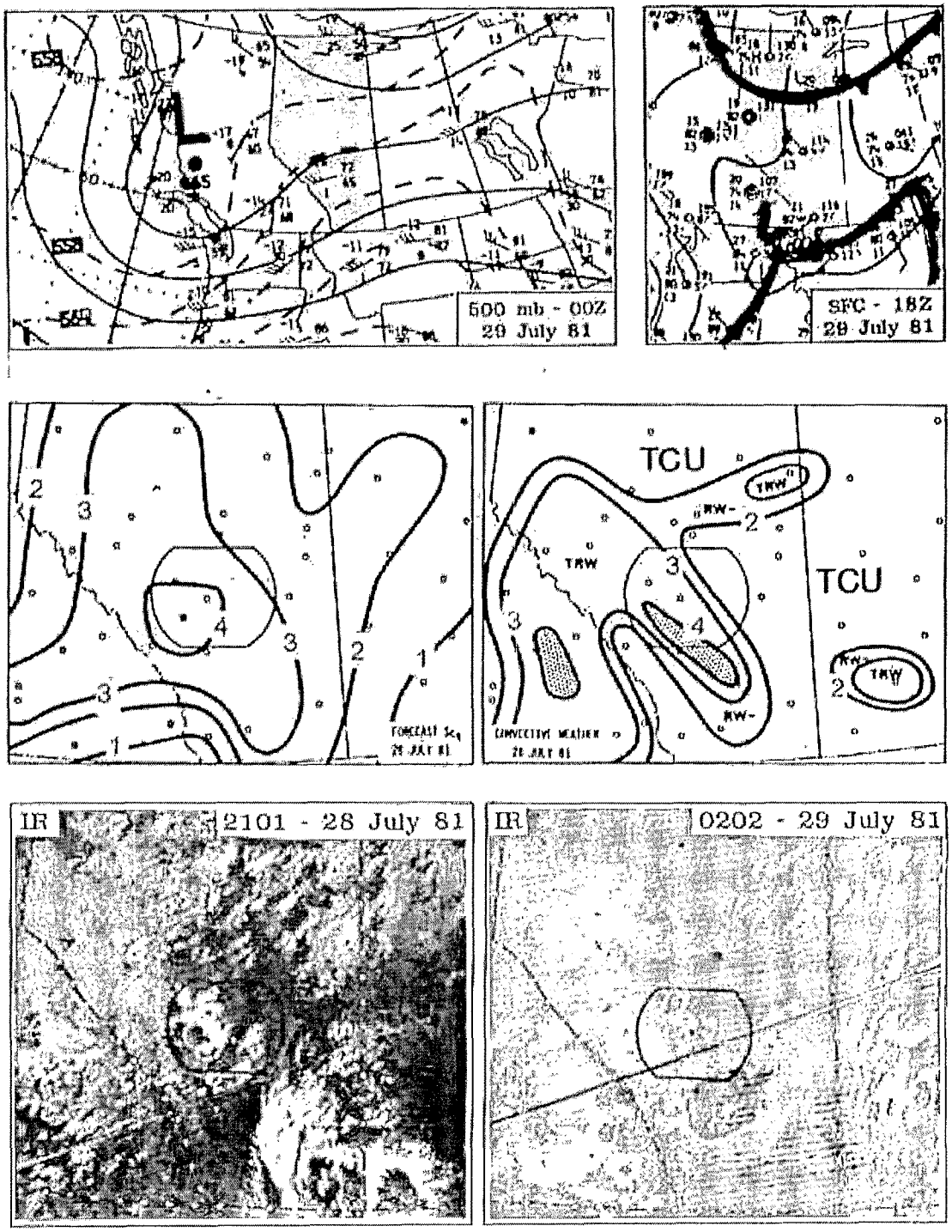

6.5.2 Weak Alberta Convective Case, 7 September 1982

Further daily experiments using this *areal* version of the Sc_4 in real time confirmed its value for predicting maximum thunderstorm intensity, but also provided a coarse estimate of where storms would form and their direction of propagation. The index works equally well for non-convective cases, as the example in Figure 6.10 demonstrates. Only scattered cumulus congestus (TCU) clouds (Sc_4 = -2) were predicted (and observed) over central Alberta for this case. Not too surprisingly, there is an upper ridge (not shown) approaching Alberta in this instance.

Figure 6.10 Test of *areal* version of Sc_{C4} on weak convective case (CDC=-1), 7 September 1982 (reproduced from Strong, 1986).

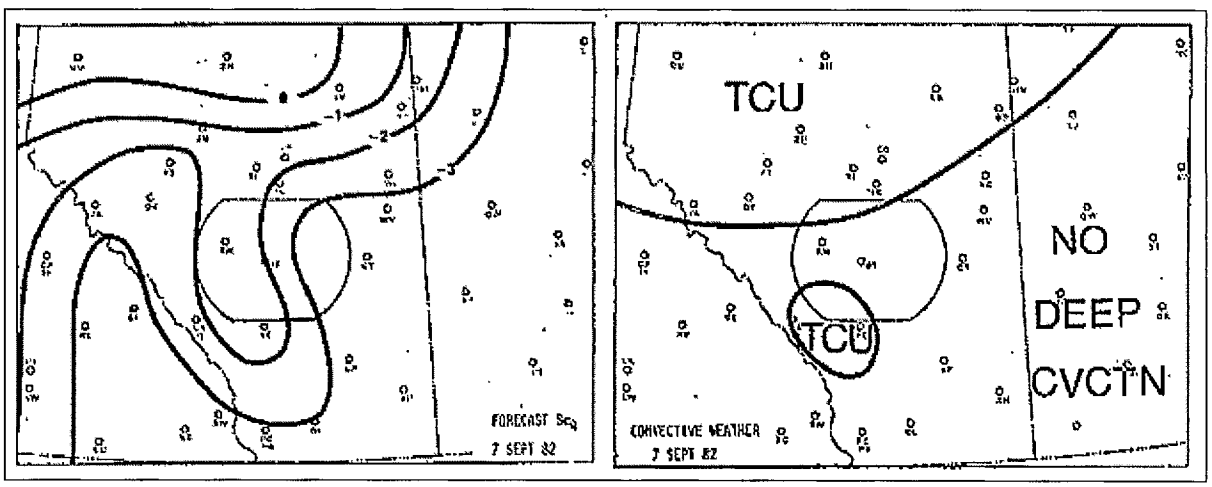

6.5.3 Small, Intense Storm Test, 17 July 1984

Occasionally, small-scale severe storms form that are often difficult for forecasters to predict. Figure 6.11, showing the 500 hPa and Red Deer sounding analyses, 1600 UTC forecast Sc_4 and observed θ_e (equivalent potential temperature) fields, and early-evening visible satellite image, demonstrates a case where primarily synoptic scale data input to the Sc_4, along with sub-synoptic scale surface data (spatial resolution 130 km over Alberta, upper meso-β scale), correctly predicted a meso-γ scale multicell thunderstorm.

During 1984, the forecast procedure started taking into account observed θ_e analyses, and the *areal* forecast became based on the intersection of the Sc_4 and θ_e advection fields (advected by 850 hPa wind field), using maximum Sc_4 within the intersected fields as the forecast storm maximum intensity. Synoptic conditions were somewhat benign, with a west-coast trough and near-zonal flow across western Canada, possibly with embedded small-scale shortwaves. While the new procedure somewhat over-predicted the maximum intensity of the storm, the degree of accuracy on the details are quite surprising, including correctly predicting the second convective complex northwest of the AHP area, as well as the relatively unknown convective complex in northeast Alberta. AHP radar indicated that the storm over the northern half of the AHP area on the satellite image was only 25 km across. While the storm barely reached a CDC = +3 category (two reports of walnut-size hail), this 1600 UTC forecast (Sc_4 and θ_e are actual operational output

for the day) demonstrates an ability to make the most efficient use possible of available data through the use of MOS (model output statistics).

Figure 6.11 Test of new Sc_4/θ_e forecast procedure on a meso-γ scale severe storm over central Alberta, 17 July 1984 (reproduced from Strong, 1986).

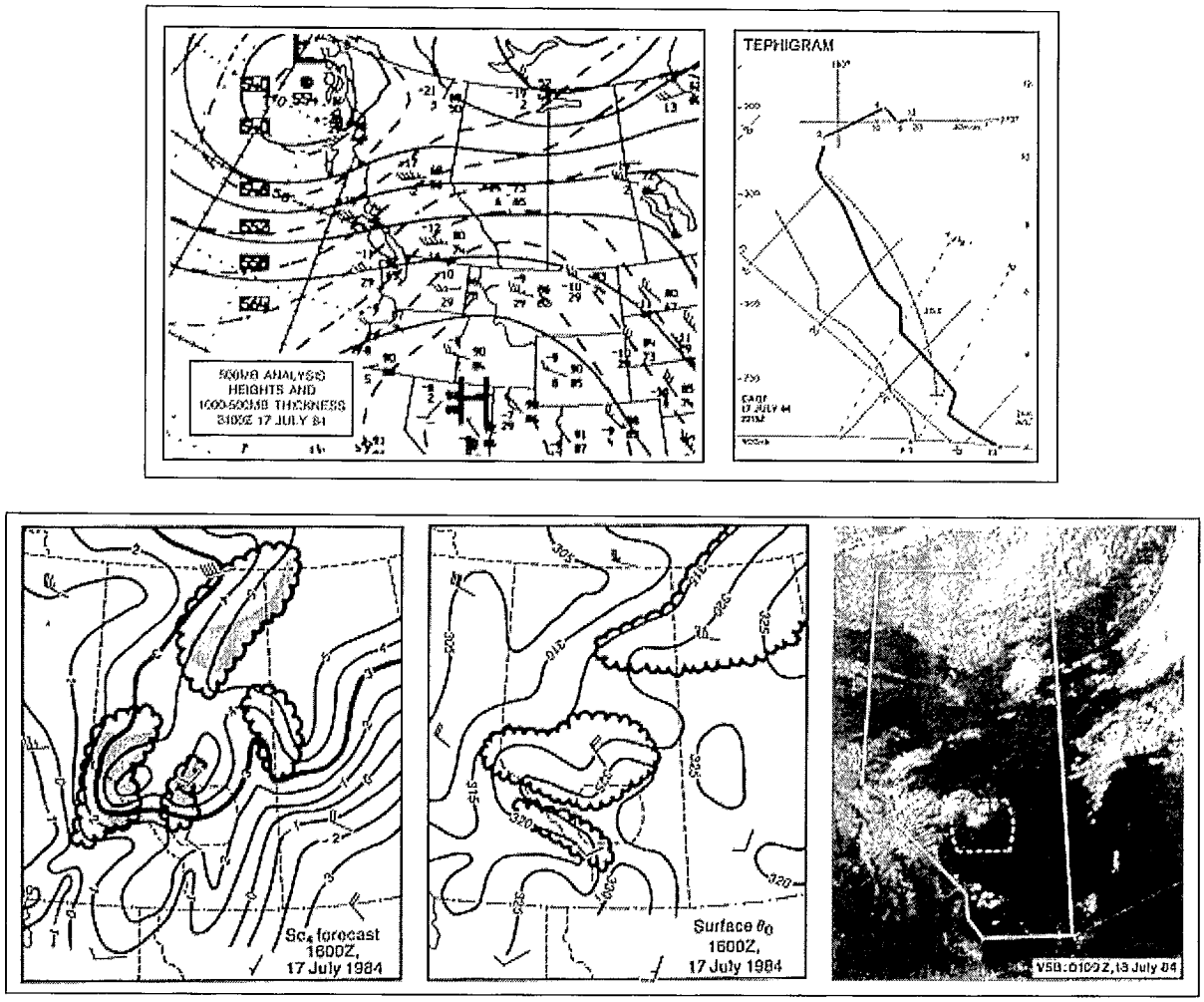

6.5.4 An "Unpredictable" Colorado Hailstorm, 30 July 1979

While developing the *areal* version of the Sc_4/θ_e forecast procedure, tests were made to see how well the index, based on Alberta statistics, might perform on non-Alberta storms. The first external test was applied to a severe storm which formed over southeast Wyoming on 31 July 1979, then propagated due southward (about 50° to the right of the upper flow) to hit Fort Collins, Colorado with "grapefruit" size hail (CDC = +5). The case was chosen simply because it was reported in the literature as being unpredictable (Fritsch and Rodgers, 1981), but refuted in this case by Strong and Wilson (1983). Applying the procedure of predicting storms based on the

intersection of *negative forecast Sc_3*[7] *advection* and *negative diagnostic θ_e advection* fields (for 1500 UTC in this case), weak, moderate, and severe storms (labelled as W, M, or S on the Sc_3 map and visible satellite image in Figure 6.12). The *negative* advection quantities are used because one wants to know foremost, where the storm will develop, after which it moves to some location where it reaches maximum intensity (the predictand on which the index is based).

Figure 6.12 First external test of new Sc_4/θ_e forecast procedure on an "unpredictable" severe hailstorm over Wyoming-Colorado, 29 July 1979 (reproduced from Strong and Wilson, 1983).

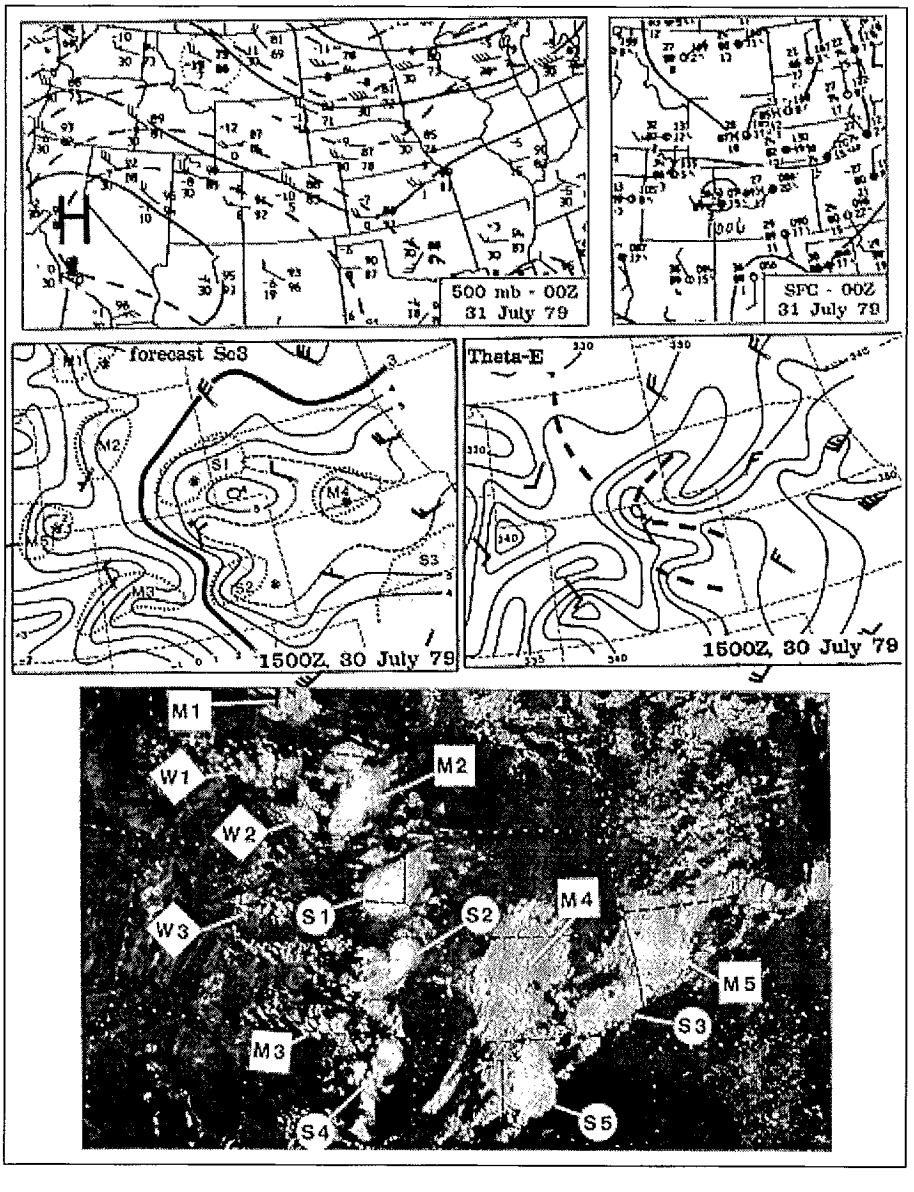

[7] The main predictor variable input to the Sc_4, the EGDEX, was not available outside the prairies simply because the diurnal change statistics used in its computation (diurnal increase in surface θ_w) were not readily available. When one variable is missing, the technique uses an Sc_3, re-weighting the statistics shown in Table 6.3.

Qualitatively, the evaluation of this case has to be considered quite good compared with other available techniques, even almost 20 years later in 2001. Fritsch and Rodgers (1981) stated that *as convective systems grow larger, their impact on their environment significantly increases, and in some instances these systems even appear to detach themselves from any discernible travelling wave or synoptic forcing that may have initiated and supported them.* Others have expressed this opinion, and while such events may be possible, it is obviously not so in this instance, since the forecast is based on 1500 UTC data, several hours before the storms formed. In this case, the storm formed due to predictable synoptic scale processes and the sub-synoptic scale moisture field measured during the pre-storm period. For a short period, the storm's motion was controlled mainly by this low-level moisture field, which itself was organized predominantly by the synoptic scale, with mesoscale concentrations of moisture due to convergence within river valleys or other sub-mesoscale topographic features. In this case at least, the Sc_3 forecast and θ_e analysis would have proven Fritsch and Rodgers incorrect on the non-predictability of the storm formation, intensity, and motion. One must wonder if such is the case for other severe storms where the analyst has detected no other logical predictive capability. It raises questions concerning how well we make use of existing data.

For storm motion, experience with the Sc_4 (or Sc_3) has shown that severe storms, once formed, tend to move towards the line of maximum Sc_4. In this respect, the Fort Collins (S1) storm might have moved either east or south, since higher values of Sc_3 lie in both directions, while the region directly southeast contains a minimum. However, for short-term (one to six hours) forecasts once a storm is in progress, new convective cells will form where thermodynamic instability is greatest and where there is a supply of moisture. A good measure of this instability and moisture is surface equivalent potential temperature (θ_e, Figure 6.12d). In this case, 1500 UTC θ_e values are <335K to the east, but are some 15K higher to the south, with a maximum value (350K) near Fort Collins. Based on this, new cells would be expected to form rapidly on the south side of the main storm, producing the apparent southward propagation of the whole complex. θ_e analyses have proven valuable for such short term forecasts in Alberta.

Forecasting techniques such as the Synoptic Index rely on synoptic and sub-synoptic scale measurements, which are basically unaffected by later convective events. There remain many in severe storm research who doubt any current predictive skill for mesoscale convective events. However, the success shown by the Synoptic Index in predicting such events may well be a demonstration of the importance of downscale effects on the pre-storm environment. Further, it raises the question as to whether we are making the best possible use of existing data sources.

Clusters of convective storms tend to deflect to the right of the mean environmental winds because of the systematic pattern of new cell formation on the upwind side (Newton and Fankhauser, 1975). The degree of this deflection seems to be in direct proportion to the storm's intensity and its rate of development, both being functions of the degree of conditional instability present and the balance of supply and demand for water vapour. These factors are pre-set by synoptic processes acting on the mesoscale in conjunction with local topography. Thus, net storm motion is such as to intercept the required supply of water vapour. The above applications of the Sc_4/Sc_3 to the extreme, right-deflecting Calgary and Fort Collins storms are important because they illustrate that these mesoscale processes are deterministic; that the formation and motion of severe convective complexes can be predicted, even, to a large degree, from existing

synoptic and sub-synoptic scale data. This demonstrates as well that such storms do not behave independently of the larger scale processes.

6.5.5 Oklahoma Tornadic Storm, 20 May 1979

This next non-Alberta Sc_3 forecast test case is the SESAME (Severe Environmental Storms Area Meteorological Experiment) Case IV, 20–21 May 1979 for Oklahoma, which has already been discussed in detail in Section 5.2 in connection with our conceptual model tests. This case is covered extensively in published literature, including the lead author's Ph.D. thesis (Strong, 1986).

The weather situation involved a shortwave trough moving northeast from Mexico that triggered severe convective storms over western parts of Texas and southwest Oklahoma. These storms produced large hail and several small tornadoes, the most severe storm being one which formed over the southwest corner of Oklahoma. Figure 6.13 shows the 1500 UTC forecast Sc_3 with predicted storm initiation regions (hatched areas), 1500 UTC equivalent potential temperature (θ_e) analysis, the GOES visible satellite image for 2131 UTC, and radar and storm top composite summary. The forecast procedure is as described for Section 6.5.4 for the Colorado storm, predicting storm initiation based on the negative advection of Sc_3 and negative advection of θ_e, with storm formations predicted based on the intersection of these two negative advection fields, that is, the storms should form somewhere upstream from where they will reach maximum intensity.

Thunderstorms materialized for all of the predicted locations of Figure 6.13a. The satellite and radar images approximate the +3 Sc_3 contour (thicker broken contour) that encompasses regions of severe storms (defined as CDC $\geq$ +3). This includes the main storm covering most of Oklahoma at 2131 UTC, a smaller but intense thunderstorm which formed near Midland, west Texas (near southeast New Mexico), and weaker thunderstorms along the Texas-Mexico border, over the Texas panhandle, and throughout New Mexico and eastern Colorado. The prediction even does a credible job on the generally clear areas (edge defined by the –3 contour). An older storm complex (left over from the previous day) just disappearing off the eastern edge of the analysis, is also predicted.

Figure 6.13 (a) 1500 UTC forecast with predicted storm initiation regions (hatched areas); (b) 1500 UTC θ_e analysis; (c) 2131 UTC GOES visible image; and (d) 2135 UTC radar and storm top composite during SESAME, 20 May, 1979 (reproduced from Strong, 1986).

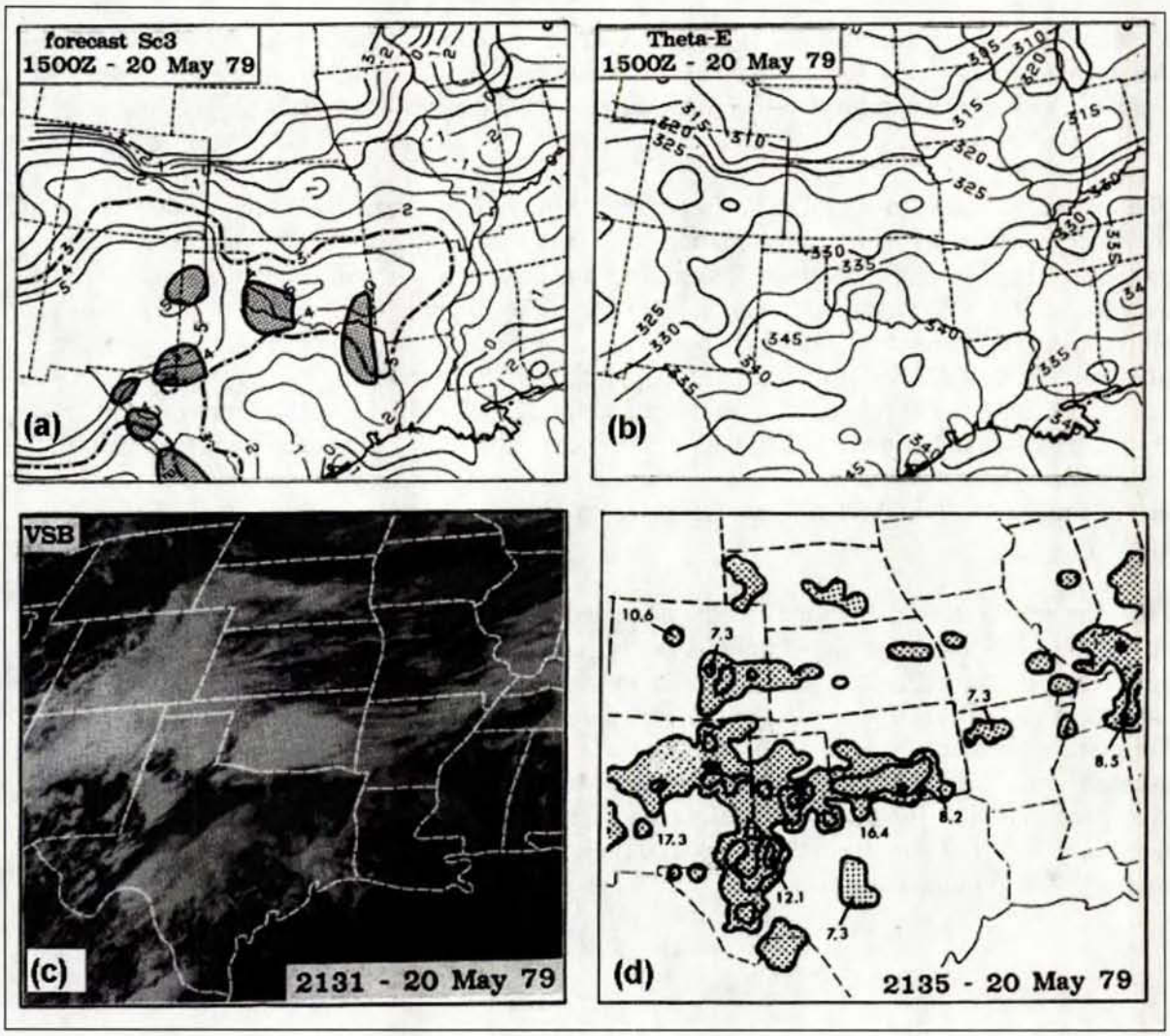

6.6 Artificial Intelligence (AI) Applications: METEOR and SWIFT

The Synoptic Index proved quite successful for predicting the maximum intensity of Alberta convective weather during the early 1980s. The discussion around Figure 6.5 indicated that experienced forecasters, with access to additional data and techniques, particularly *pattern recognition*, provided a small margin of value-added accuracy in predicting maximum intensity using the single-valued index. They also provided an advantage in terms of determining where storms might initiate and their general motion. This suggested that the Synoptic Index, combined with the human interpretation of other information, might make an ideal candidate for artificial

intelligence (AI) applications. A preliminary AI model simply called METEOR was developed and given an 11-day test period during the summer of 1985. METEOR correctly predicted 10 of the 11 days, including the most severe hailstorm of the summer (3 August 1985), a +5 category storm. A description and test results are given by Elio et al. (1987). It was not possible to conduct further tests of METEOR because of the demise of the AHP in early 1986.

6.6.1 Edmonton Tornadic Storm, 31 July 1987

A later collaborative project between ARC, MSC, and McDonald Detwiler Associates upgraded METEOR into SWIFT (Severe Weather Intelligent Forecast Terminal), with updated rules, but still based on the Sc_4 forecast technique. Figure 6.14 is an example post facto forecast (a *hindcast*) of the *Edmonton tornado* based on 1500 UTC data. Figure 6.14(a) is a prediction of main storm *initiation threat* regions, 6.14(b) is the predicted total severe storm maximum intensity threat region (where $Sc_4 > +3$), and 6.14(c) is the θ_e analysis, which is used in helping to predict storm motion as well as initiation regions (intersection of negative Sc_4 advection and negative θ_e advection). Thus, in the absence of other information (such as synoptic charts, soundings, etc.), SWIFT would predict storms to initiate over southwestern Alberta, propagating east and northeast towards the centres of maximum Sc_4 and θ_e advection.

Figure 6.14 SWIFT's morning forecast of the *Edmonton Tornado* storm of 31 July 1987; (a) predicted region of storm initiation; (b) forecast Sc_4 and severe storm threat region; (c) θ_e advection (positive values indicate heat/moisture convergence). Edmonton is indicated by the "star" (reproduced from Strong, 1988).

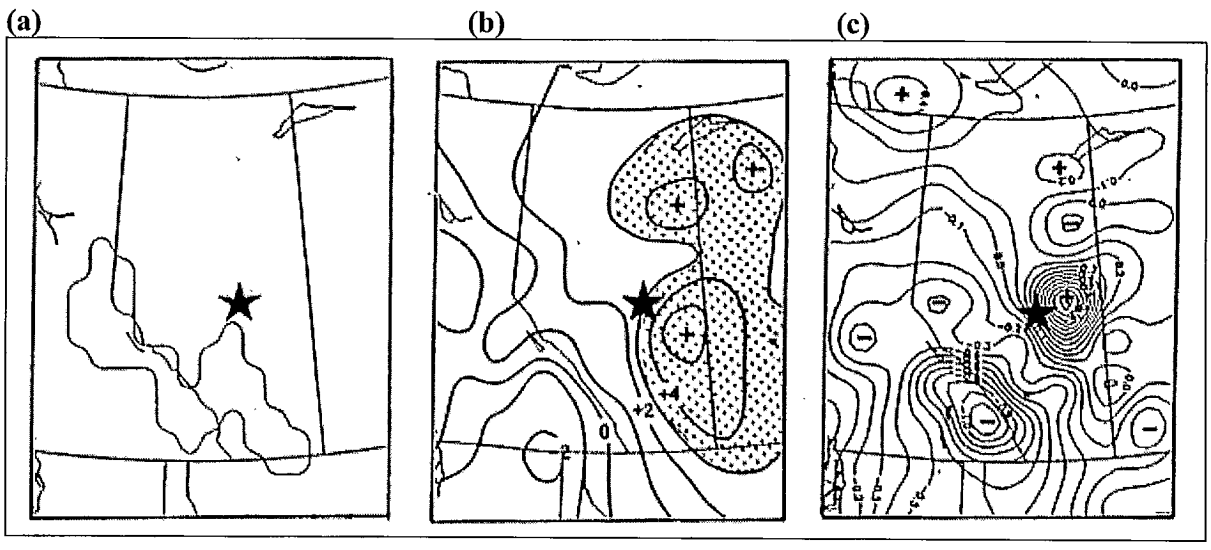

Without any further AHP operations for testing, SWIFT had to be abandoned as a prototype. It was far from being an *expert system*, but was a good first attempt at simulating human reasoning in automated forecast products. There are many areas where it could have been improved, but even with its limited rulebase, SWIFT showed significant success in predicting severe convective weather situations.

After a flurry of activity in AI forecasting applications during the late 1980s, including two major conferences (Moninger et al., 1987; Dyer and Moninger, 1988), interest seemed to recede, partly because of the difficulties of programming the human forecaster element into an expert system. Given new advances in neurological science and related areas and technology over the past 10 years, the time seems ripe to reactivate weather applications. The degree of subjective interpretation involved in forecasting severe convective storms makes this application an appealing candidate.

6.7 Summary

Section 6.0 has provided some insight into the most favourable conditions for Alberta thunderstorms, based on visual evidence, thermodynamic, and dynamic properties at a range of atmospheric scales of motion. More importantly, it has provided examples of how we can make the efficient use of available data, as opposed to demanding more data than we might otherwise be able to assimilate and use to our advantage.

While the output resolution and accuracy of numerical weather prediction models have improved immensely in the 20 years since the development of the Synoptic Index, this simple statistical technique can still provide value-added accuracy to forecasts of convective storms, excelling in the more severe cases. It is still in use for special projects requiring accuracy at the scale of thunderstorm processes, including cloud-seeding projects in Alberta, Greece, and Argentina, but no further development or updated statistics have been applied to it since the last AHP operational year, 1985.

MOS techniques such as described for the Synoptic Index can be improved considerably yet, without even exploring some of the new data sets (e.g., Doppler radar data, lightning, GPS moisture integrator data, etc.) which have come on line since this technique was developed and used in the early 1980s. In the absence of remarkable breakthroughs in NWP of these phenomena, new MOS predictand and predictor variables should be explored. The utility of Artificial Intelligence techniques also has not been fully explored. The technique described above and used in METEOR/SWIFT utilized only a small portion of the data and forecasting techniques available during the early 1980s. This is one area that begs more work.

For operational meteorology, there is a great need for new and improved forecasting techniques, for which we have made some recommendations above. Forecasters want and need better resolution and accuracy of the ABL, both in terms of observed data (soundings), and of NWP output (the CMC GEM model in Canada). Mesoscale models that can receive output from the larger scale models may eventually provide automated forecasts. Continued work on models at all scales needs to be supported. Regionally, given the decidedly different and smaller spatial scale of Alberta storms in general, Alberta forecasters see a renewed need for an operational severe weather desk specifically for Alberta, since the Prairies are simply too large an area to be covered by one forecast desk.

Finally, we need to recognize that significant progress has been made in severe weather prediction. Ostby (1999) reviewed rapid progress in improving accuracy of severe weather

forecasting over the past 25 years in the U.S. He pointed out that the 10-year death toll from tornadoes across the U.S. has improved from 972 in 1961–70, to 590 in 1971–80, and fell to 430 for the 10 years ending in 1996. He attributes this reduction to improvements in both forecasting skill and in communications, including warning and preparedness efforts, volunteer spotters, ham radio operators, and the media. All of these areas have also been addressed and improved in Canada over the past 10 years by MSC and the various agencies involved.

7.0 Conclusions: Synthesis of Review and Consultations

Meteorologists are the first to admit that their science is far from perfect. The atmospheric system is very complex and requires much more research effort to increase our understanding. Thus the impetus for this study was initiated with *three main objectives*, namely to: (1) *provide a review of our knowledge of and predictive capabilities for severe prairie thunderstorms and related phenomena;* (2) *identify gaps in our science and data systems;* and (3) *provide recommendations to alleviate such gaps.*

The main body of this document deals with the first objective. In this review, we have attempted to emphasize the importance of severe prairie thunderstorms inboth sociological and scientific contexts. Precipitation and lightning from convective showers and thundershowers are essential to maintaining uniformity of moisture and nutrients to the prairie and boreal forest climates. A large percentage of growing season precipitation on the Prairies results from convective storms. Without these systems, agriculture would not be possible in its present form, since in the absence of convective processes, weak summertime ocean-originated weather systems remain essentially decoupled from the ABL once they cross the mountains – hence the importance of convective storms to all systems and activities requiring warm season precipitation, especially to human activities. However, less beneficial consequences of severe convective storms include large hail, flooding from heavy precipitation, strong winds, and tornadoes. These can result in large financial losses and threats to human and animal life. This makes understanding and predicting these systems essential.

As part of this project, consultation meetings were held during August and November 2000 with regional MSC operational forecasters, atmospheric scientists at university, provincial and federal research organizations, and representatives of the weather modification industry in Alberta in Red Deer and Olds-Didsbury Airport. Discussions focused on the following issues: forecasting severe convective storms, gaps in our observational and modelled data, technology and techniques, training and education, communications, and research needs to alleviate gaps in the science. A complete set of discussion notes appears in Appendix C. Section 7.1 below is a synopsis of the highest priority issues discussed. Taking these discussions into consideration as well as the other findings of this project, the remaining sections of this report will summarize objectives (2) and (3).

7.1 Feedback from Consultations

Since available resources and time did not allow an extensive survey of all prairie meteorologists, we attempted to consult with those most closely associated with forecasting or conducting research or exploratory operations (such as hail suppression) on severe weather systems, although not all individuals were available at the selected times. The same limitations also excluded any thorough prioritization of issues raised, although some attempt was made to do this based on emphasis of issues by more than one individual. It is important to emphasize at this point that ***opinions expressed during these discussions were solely those of the individuals involved, and should not be assumed to represent the opinions of their respective parent organizations.***

Forecasting

Operational forecasters at both the Alberta and Manitoba Weather Centres of MSC in Edmonton and Winnipeg were invited to discuss forecasting issues. It was pointed out that severe weather forecasters relied heavily on specific forecasting techniques and environmental indicators in predicting severe weather. These include the Fawbush-Miller techniques of composite analyses, mid-level lapse rates, instability indices such as EGDEX, and the presence of dry air at mid-levels. A high priority was also put on large-scale dynamics and boundary layer processes such as moisture flux convergence. A system called WADS (Weather Analysis Display System) is an invaluable tool used to interpret large amounts of information available to the forecaster. The atmospheric researchers also felt that high priority should be put upon large-scale dynamics.

Data Gaps

The forecast community discussed the relative importance of having a greater spatial resolution in atmospheric soundings, especially over the Alberta foothills. Researchers consulted felt that this should have a very high priority.

Technology and Techniques

Discussions dealing with this issue were focused on operational forecasting model issues, and the availability of new technologies in the production of severe weather forecasts and severe weather research. Forecasters place a high priority on the utilization of the GEM model for prediction of large-scale dynamics, but pointed out weaknesses in the model in simulating the ABL. They also discussed the potential advantages of wind profiler systems in determining the nature of developing storms. Researchers put high priority on increased use of Doppler radar in storm analysis.

Training and Education

The forecasters pointed out that annual severe weather workshops are very useful for disseminating information on severe weather forecasting and upgrading skills. This practice should be continued in the future. They also expressed the potential usefulness of an on-line database of 50 or more severe storm cases that could be used for training and reference. Making WADS available as a training and research tool at selected institutions would be very valuable. Researchers felt that this system would make a very powerful research tool, especially for graduate students in meteorology.

Communications

Forecasters expressed the general consensus that there was an under-estimation of the role of the "Watch" mode in severe weather forecasting. A greater emphasis on this forecasting mode needs to be communicated to the public. It was felt that the dissemination of severe weather forecasts and warning was still a major concern of the public. The effectiveness of these forecasts and warnings may be improved on by improved technologies and continued public education efforts.

Research

Research priorities were discussed with both the forecasting and research communities. Table 7.1 highlights the priorities given to each issue discussed. "H" refers to high priority, "M" to medium priority, "L" to low priority, and "D" refers to the fact that an issue was discussed but not assigned a priority.

Table 7.1 Prioritized research issues discussed in consultation with forecasters (FCST) and atmospheric researchers (RES). Priorities: H–high, M–medium, L–low, D–not prioritized, blank–not discussed.

#	RESEARCH ISSUES	FCST	RES
1.	Techniques to distinguish large/small/soft hail using radar	H	H
2.	Techniques to predict "storm initiation regions"	H	
3.	Techniques to predict "nocturnal" storm development	M	
4.	Techniques to predict "no-storm" cases and "non-severe" storms	H	
5.	Techniques to predict storm decay	H	
6.	Processes and role of coupling of upper and lower jets	H	
7.	Processes, role of, and importance of dry lines	H	
8.	Role of ABL processes – regional evapotranspiration, moisture convergence, especially over Alberta foothills	H	H
9.	Similarities and differences in storm characteristics across the Prairies	M	H
10.	Cloud physics research of rain/hail processes	L	H
11.	Cloud physics modeling (use existing models)		H
12.	Mesoscale modeling of storms (use existing models)	M	H
13.	Predictors to forecast/identify tornadic situations	H	M
14.	Radar and synoptic climatology of summer storms for prairies		H
15.	Emphasizing important features using radar and lightning data	H	H
16.	How storm frequency and severity is affected by climate change		M
17.	Synoptic Control processes	H	H
18.	Research on public dissemination of forecasts/warnings	M	D
19.	Identification of tornado vorticity centeres	M	H
20.	Identification of splitting/merging storms with radar/satellite		M

#	RESEARCH ISSUES	FCST	RES
21.	Flood forecasting through improved QPFs		M
22.	Identification of high forest fire (lightning) threat cases		M
23.	Cloud photography – time lapse, microscale and mesoscale features		M

7.2 Objective 1: Status of Scientific Knowledge and Forecasting Capabilities

Key scientific results, as well as their implications, have been discussed in greater detail in earlier sections of this report. In order to address each of the three objectives of this review, we have chosen to identify and group various knowns and unknowns (using the scales of motion defined in Section 1.4) under six key areas as follows:

1. *Synoptic Forcing*: starting at the synoptic scale and working down into the mesoscale.
2. *Spatial/Temporal Characteristics of Storms*: starting at the meso-β scale, but also including the meso-γ (cloud-) scale.
3. *Atmospheric Boundary Layer* processes: primarily in the meso-β and meso-γ scale range.
4. *Forecasting* the full range of convective weather at the mesoscales.
5. *Numerical Modelling* at all scales of motion.
6. *Climate, Data Systems*, and *Communications*.

It is tempting to include a seventh category covering cloud micro-physics (meso-γ and smaller scales), but cloud physics issues were only very briefly addressed in this report, and while they are certainly relevant to the problems discussed, the areas to cover would raise more issues than solutions, and would require a complete review in itself, which the authors do not feel qualified to carry out at this time without a further extensive review of the literature.

The rest of this section is devoted to providing a table (7.2) of important examples of partly or fully quantified *science theories/facts*, *science and data gaps*, and *recommendations* to overcome the gaps under each of the above categories. The prioritized research issues obtained through consultations, and indicated in Table 7.1, are clearly related to some of the recommendations outlined in Table 7.2. The list simply raises issues that have come up in the context of the review and consultations, and is by no means an exhaustive one. Other issues and recommendations can be added later.

Table 7.2 Summary of Key Results and Recommendations

Science Theories/Facts Partly or Fully Quantified	Gaps in Science and Data	Recommendation(s)
1. Synoptic Scale Influences		
1.K1. Development of severe convective storms can be predicted based on recognition of particular synoptic pattern types.	**1.U1.** Synoptic pattern recognition leaves a synoptic scale region for the forecaster to narrow down to the mesoscale.	**1.R1.** See recommendations under 4.R. Continued climatological studies to confirm and assist in 2.R.1.
1.K2. Approaching upper S/W *troughs* during June–August signal impending thunderstorms.	**1.U2.** Forecaster must still assess PVA, tilt of trough, cloud systems, ABL, etc.	**1.R2.** Consider existing map-typing schemes to categorize severe storm situations.
1.K3. Approaching upper S/W *ridges* during June–August signal fair weather or just non-severe convective showers.	**1.U3.** Occasionally small scale disturbances super-imposed over ridges, can trigger small but intense thunderstorm.	
1.K4. Alberta thunderstorms tend to post-cold-frontal (unlike Sask./Man. storms), so storms frequently occur on the same day over Alberta and Sask.	**1.U4.** Cold fronts/trowals not always easy to identify in summer.	
2. Spatial/Temporal Characteristics of Prairie Thunderstorms		
2.K1. Severe Alberta thunderstorms may be more similar to other locations in immediate *lee of Rockies* than with Sask. or Man. storms.	**2.U1.** Differences in storm characteristics W–E across prairies have not been adequately quantified.	**2.R1.** Carry out climatologies of synoptic, radar, and lightning data as first step in defining W–E characteristics of prairie storms.
2.K2. Differences in storm intensity N–S in lee of mountains are primarily a function of ABL depth and moisture content.	**2.U2.** ABL depth (and other factors) not well-quantified over central and eastern Prairies.	**2.R2.** Quantify W–E and N–S similarities AND differences in storm characteristics.
2.K3. Evapotranspiration significantly exceeds precipitation over the Prairies during summer, feeds directly into ABL; sometimes may be the critical factor between showery weather and a severe storm.	**2.U3.** Sources and sinks of energy and moisture not well quantified on the Prairies.	**2.R3.** Synoptic to mesoscale diagnostic studies of atmospheric energy and moisture budgets across the Prairies, similar to Mackenzie GEWEX Study (MAGS) →SAGE.
3. Atmospheric Boundary Layer		
3.K1. ABL undergoes rapid pre-storm changes on severe storm days over Alberta foothills.	**3.U1.** Rapid changes only partially quantified and require confirmatory results.	**3.R1.** Design fieldwork with focus on soundings plus supporting data.
3.K2. *Capping lid* one of most important signatures for severe storms, but neither necessary nor sufficient for a severe storm.	**3.U2.** Final pre-storm lid enhancement and breakdown usually take place during late-morning **between** operational soundings.	**3.R2.** As above; requires foothills soundings at 15 and 18Z, especially during pre-identified severe storm days.
3.K3. Lid is created by combination of mid-level warm advection and subsidence warming, overrunning cool moist ABL air, enhanced by orographic subsidence; starts as nocturnal inversion, ABL ascent initially enhances lid.	**3.U3.** Lid is often either confined to or most prominent over foothills where there are currently no sounding information; can go undetected with only Stony Plain sounding.	**3.R3.** At least one additional operational sounding site required over foothills, even if only one (morning) sounding per day, augmented with a GPS vertical moisture integrator and possibly wind profiler.

Science Theories/Facts Partly or Fully Quantified	Gaps in Our Science and Data	Recommendation(s)
3.K4. Lid breaks down due to ABL ascent lifting and cooling, enhanced by orographic forcing.	**3.U4**. Areal extent of capping lid over central and eastern Prairies not quantified.	**3.R4**. Research to improve parameterization for GEM model to improve prediction of the ABL for the Prairies.
3.K5. Lid parallels mountains east of foothill peaks, extends 50–100 km E in storm situation.	**3.U5.** Virtually no quantification of LLJ over the Canadian Prairies due to lack of data.	**3.R5.** Improved radiosonde network, addition of wind profiler network.
3.K6. LLJ and perturbations in *drylines* signal downward transfer of momentum and possible severe storm signature as in the U.S. High Plains.	**3.U6.** Quantification and understanding of processes w.r.t. drylines over Canadian Prairies is currently weak.	**3.R6.** Improved radiosonde network, testing and addition of GPS moisture integrators.
3.K7. *Multi-scale conceptual model of thunderstorms* appears valid following various diagnostic tests using SESAME and LIMEX data.	**3.U7.** *Conceptual model* requires more extensive mesoscale data to validate, refine, and adapt to other prairie locations.	**3.R7.** Design and implement multi-scale field research focused on prairie thunderstorms.
4. Forecasting		
4.K1. Near perfect numerical forecasts are theoretically possible given more detailed information on synoptic and mesoscale dynamics, topography, surface heating, and regional evapotranspiration.	**4.U1.** Key variables essential for model improvement are either not measured or poorly estimated, including regional evapotranspiration and precipitation.	**4.R1.** Improve observational datasets and make available to research community for feedback of results.
4.K2. Forecasters use pattern recognition as first guess. Four groups: synoptics, ABL and mid-level thermodynamics, and morning sky conditions.	**4.U2.** Detailed forecasts (location/timing) require detailed information on diurnally-varying temperature, humidity, and winds especially in the ABL.	**4.R2.** Development of on-line database of severe weather events to assist in pattern recognition. Make database available to research community for further improvements.
4.K3. General severe thunderstorm forecasts and warnings currently adequate given limitations on forecasters, data, and modeling output	**4.U3.** Prediction of specific information unreliable; e.g., location of storm initiation, motion, intensity (hail size, precipitation amount, wind speeds, or tornado occurrence).	**4.R3.** Increase key observational data (e.g., soundings), improve display systems (e.g., WADS) to increase time for forecasters to assess all information available.
4.K4. MOS techniques showed relative high degree of accuracy in 1980s (e.g. Sc_4 with AHP).	**4.U4.** MOS models developed for one region are not always applicable to others; hence, do not get widespread use.	**4.R4.** Field-test various MOS models and adapt for local use.
4.K5. Artificial Intelligence models such as SWIFT proved successful with minimal rulebase.	**4.U5.** Forecasters have limited experience with AI model use.	**4.R5.** Combine improved AI rulebase with current technology to improve AI models.
		4.R6. Develop and encourage the use of more regional forecasting techniques adapted to results of above.
		4.R7. Continue/improve training/refresher workshops.

Science Theories/Facts Partly or Fully Quantified	Gaps in Our Science and Data	Recommendation(s)
5. Modelling		
5.K1. NWP models (e.g., Can. GEM) currently adequate at predicting synoptic scale processes, and with proper interpretation, help determine storm threats for meso-β spatial/temporal scales.	**5.U1.** NWP models do not currently model critical ABL parameters well (e.g., *capping lid*) for severe storm situations; hence, MOLTS soundings poorly represent convective situations at present.	**5.R1.** Collaborate with CMC modellers in recommended fieldwork in 3.R1.–3.R7. above with feedback to improve ABL parameterization, especially for GEM simulated MOLTS soundings.
5.K2. Mesoscale models, when initialized with adequate data, can simulate storm morphology.	**5.U2.** Mesoscale models currently too computational-intensive for operational use.	**5.R2.** Continue efforts to adapt Mesoscale models to operational use, increase data observations available for initialization.
6. Climatology, Data, and Communications		
6.K1. Severe Alberta storms tend to form over the foothills, where hail has highest frequency in Canada.	**6.U1.** Very little Alberta hail climatology since demise of AHP in 1985.	**6.R1.** Initially focus attention on this region, valuable knowledge here will benefit research and forecasting efforts in other regions of the Prairies
6.K2. Southern ¼ of Sask. also a hotbed for summertime thunderstorm activity.	**6.U2.** Saskatchewan severe storm climatology poorly quantified, and not at all without case study work by A. Paul.	**6.R2.** See Recommendations of 2.
6.K3. Tornado frequencies difficult to quantify, but known maximum in Red River Valley of Manitoba, highest frequency on the Prairies.	**6.U3.** Manitoba severe storm climatology and risk assessment is poorly quantified.	**6.R3.** Continue public education efforts, develop and implement new technologies to disseminate severe weather "*Watches*" and "*Warnings.*"
6.K4. Recent data archive improvements include addition of radar and lightning data.	**6.U4.** Current severe storm climatologies (especially tornadoes) are as much dependent on population density as actual occurrence).	**6.R4.** Develop new severe storm climatology variables with uniform coverage of radar and lightning data.
6.K5. MSC forecasters are knowledgeable, dedicated, and quick to react to threatening weather situations. Recent innovative storm reporting and forecast dissemination include using ham radios, cellular phones, etc.	**6.U5.** Dissemination (or rather reception) of forecasts (especially *Watches* and *Warnings*) are still inadequate and often not well understood by the general public.	**6.R5.** Increase media and public awareness of the implementation and implication of *Watch* mode of severe weather forecasting. Consider alternate means (automated cell phone calls to threat areas, etc.) of delivering warnings.
6.K6. Public awareness of the hazards to property and human life from severe prairie storms is at an all-time high, ironically due in part to two devastating tornadoes (Edmonton, 1987; Pine Lake, 2000).	**6.U6.** Exact statistics such as severe storm return probabilities are lacking due to lack of data in low population density areas on the Prairies.	**6.R6.** Fund socio-economic studies to assess risk factors. Coordinate with other agencies, possibly through ICLR (Institute for Catastrophic Loss Reduction, London, Ont.).

7.3 Objective 2: Gaps in Our Knowledge and Data

The *second objective* of this project was to identify gaps in the science and data collection networks for severe prairie thunderstorms. We elaborate here on some of the gaps as identified in Table 7.2.

Science Gaps

1. More detailed mesoscale ABL information is required to validate the *multi-scale conceptual model of Alberta thunderstorm formation*. Critical to this is quantification of the pre-storm creation and breakdown of the capping lid, mapping its areal extent and depth, moisture sources (both advection and local evapotranspiration), moisture convergence over the foothills, and identifying "hot spots" of sensible heating. The conceptual model should also be refined and its use extended to other prairie locations.

2. Perturbations in drylines and low-level jets (LLJs) are also considered to be signals for storm initiation over the U.S. Mid-West, but have not been as well quantified on the Canadian Prairies. Both are dynamically linked to the capping lid in some way, and are coupled to the free atmosphere (and upper jet) once deep convection begins. For example, the LLJ has a maximum occurrence at the capping lid level. Both the LLJ and drylines "tend" to peak near the western edge of the capping lid, where lids tend to weaken first and allow first convection, and where the dryline is, in effect, a dry front.

3. Quantitative analyses of the temporal and spatial characteristics of prairie storms are required to assess similarities and differences west-east across the Prairies and north-south into the U.S. High Plains. In particular, there appear to be fundamental differences between Alberta storms and those of the central and eastern Prairies.

4. Techniques to provide accurate objective forecasts of storm formation areas and time, movement, maximum intensity and time, storm decay and time, are all lacking.

5. NWP and mesoscale models cannot yet accurately simulate the ABL changes (noted in Section 6.0 above) in the absence of high spatial and temporal resolution radiosonde data.

Data Gaps

6. Forecasters have no operational radiosonde soundings available over the critical Alberta foothills area, while model output soundings lack necessary details for the ABL, and do not adequately simulate diurnal changes in soundings. Given cost restraints, further effort can be put into developing sources of proxy data and continued improvement of operational and research models.

7. Severe weather reports and climatologies, especially of tornadoes, are inaccurate, incomplete, and may be more dependent on population density than on actual occurrence (i.e., many go unreported in rural areas). New data sources for severe storm signatures need to be developed, including the obvious radar and lightning data.

8. There are too few datasets available on the capping lid for the central and eastern Prairies to make any generalizations.

9. Accurate regional estimates of evapotranspiration, a significant factor in convective storm development, are not available.

10. There is a need for a severe storm data archive (of all data types available) specifically tailored to case study analysis, as opposed to standard climatic data. Related to this, special field research datasets have a tendency to be lost. There is a need for a permanent central location for research data sets on prairie convective storms and their documentation. Examples might be the AHP data, much of which has already been lost forever, and the SHARP (Saskatchewan Hail Research Project) data. Remaining AHP data presently reside on a University of Alberta web site at http://datalib.library.ualberta.ca/AHParchive/, but there is no guarantee that these data will be safe indefinitely.

While many other examples of science and data gaps could easily be identified, these 10 best represent gaps indicated in this review and brought out in consultations with local experts.

11. However, there is one other gap that needs to be highlighted and discussed which does not directly involve either science or data. It is a two-fork gap involving *researchers* and available *funds* as follows. There is at present no coordinated effort to conduct research of severe convective storms on the Canadian Prairies. Efforts of the past five years, for example, have been carried out by a small number of individuals, with theses and papers such as Xin et al. (1997), Etkin and Brun (1999), Taylor (1999), Raddatz (2000), Strong (2000), and Brimelow (2001). There have also been a number of commendable shorter-term studies in support of forecasting by operational (MSC) forecasters such as Vickers (1996), Joe and Dudley (2000), Cummine and Noonan (2001), and Knott and Taylor (2001), to mention a few, but clearly our total research effort is small compared with that of our American colleagues. Individual research efforts receive little funding, which in turn tends to discourage collaboration, which in turn does not attract new researchers, and the cycle repeats itself.

7.4 Objective 3: Recommendations

Our *third objective* in this review was to provide specific recommendations to alleviate some or all of the identified gaps. Some were identified in Table 7.2. These are now linked into a more cohesive set of recommendations. We will begin with the last two identified gaps (#11 and 10), for it is fruitless to discuss research objectives without researchers, data, and funding.

7.4.1 Form a Prairie Convective Weather Network (R1)

The limited list of recent contributors mentioned in number 11 above suggests that research on prairie convective processes is a minimal effort carried out by a very few individuals with very minimal funding, the result being no collective strength in the efforts. Because the quantities of researchers and available funds are small, all such research of the past 15 years has been individual efforts without any coordinated infrastructure or network. This prairie research

situation has steadily deteriorated ever since the demise of the Alberta Hail Project following their final 1985 field season, and it is still on that downward trend. We have to be realistic about this. We cannot re-build an institutional infrastructure such as the AHP provided, and certainly not a Canadian version of NCAR (the National Center for Atmospheric Research in Boulder, Colorado), at least not in the near future. However, the growth of Internet facilities, and the research needs we have identified, makes the formation of a *network* of research and operational meteorologists a viable, and possibly necessary, starting point. Such a network would provide a valuable forum for research and operational meteorologists (and researchers in related fields) interested in prairie convective processes and forecasting, to discuss ideas, present results, and obtain feedback. Because many of the issues have weather forecasting objectives or certainly impacts, it is our opinion that such a network cannot succeed without some involvement by the regional prairie offices of MSC and those staff interested. Direct collaborative efforts are essential to make the most efficient use of resources, to enhance focus, and to provide mutual access to data. A network might be coordinated through the Canadian Meteorological and Oceanographic Society (CMOS) regional Centres (in Winnipeg, Saskatoon, and Edmonton) as a "Prairie Convective Weather Network." In this way, planning meetings and presentations of advance results could be coordinated through these centres, and, if interest warrants it, a special session could be arranged at future CMOS annual Congresses.

7.4.2 Create a Permanent Home to Archive Prairie Research Datasets (R2)

Data gap #10 above suggests the creation of a permanent home to archive prairie convective research datasets. The location for such an archive is uncertain, but an obvious choice would be one of the prairie MSC offices, considering their degree of permanency, personnel with data archiving skills and resources, facilities to provide ready access to the research data, plus potential access to additional national climatic data resources, assuming that network security issues can be circumvented. The latter is mentioned because it would be essential that researchers anywhere in Canada could gain access to the research database.

7.4.3 Create New Part-time Summer Operational Sounding Sites (R3)

To alleviate identified Data Gaps 6 and 8, as well as some of the data requirements for all Science Gaps 1 to 5, resources for new part-time summer sounding sites should be considered. The first priority would be at least one sounding site over the critical foothills storm formation region of central Alberta. The second would be to provide similar sounding capability for the south-central Saskatchewan storm generation area; and third, a system in the vicinity of the Red River Valley tornadogenesis area of Manitoba.

Suggested Primary Siting Priorities, in order of priority are:

1.) Sundre to Cremona, AB area;
2.) Swift Current, SK area or south (nearest operational site is Glasgow, about 200 km SSW);
3.) 50–100 km south to southwest of Winnipeg.

Secondary Sitings, possibly on a temporary research basis, would be:

4.) Rocky Mountain House (a former operational site in the 1970s);
5.) In the foothills region northwest of Edmonton.

Operational Priorities should be to have 1330 and 1730 UTC daily sounding releases from mid-June through mid-August. Times might be varied by up to one hour depending on forecast priorities. These could be operated either by a part-time contract, or as fully automated sites such as MSC has had at Whitehorse, Yukon Territory. From an operational perspective, a 0000 UTC sounding at these locations is not necessary.

7.4.4 New Data Systems and Proxy Data Sources (R4)

Most other issues identified in the Data Gaps could be alleviated through a combination of wind profilers (to quantify the LLJ), GPS vertical moisture integrators (e.g., to sense the diurnal cycle in atmospheric moisture caused by local evapotranspiration, dryline signatures, etc.), instrumented towers, temperature-humidity profiles from aircraft on ascent/descent at major airports, new automatic weather stations, particularly in known severe storm regions (such as Alberta foothills, southern Saskatchewan, etc.), and tethered balloon systems. Cellular phone companies such as Telus maintain towers up to 300 m, which, if instrumented at several levels on one datalogger, could provide valuable information on the lower boundary layer. These proxy data provide alternative means to map the ABL over large areas, provided there is at least one radiosonde system nearby.

7.4.5 Develop Severe Weather Predictands Based on Radar/Lightning Data (R5)

Forecast operations are encouraged to develop new severe weather predictands based on radar, lightning, and possibly satellite data. It would be difficult to obtain the data resolution required for an accurate tornado or hail climatology right across the Prairies. Various criteria in these data could be used to relate to actual hail size and possibly tornado F-scale by those severe weather reports which are presently available to fine-tune the radar and lightning data. These new severe weather databases should also be employed to develop new MOS objective forecast techniques.

7.4.6 Compute Atmospheric Moisture and Energy Budgets for Sources and Sinks (R6)

Existing radiosonde data are rather sparse across the Prairies. With the addition of a few new sites as described above, it becomes possible to carry out atmospheric moisture and energy budget studies to delineate moisture source and sink regions, as well as contributing to resolving the temporal and spatial characteristics of storms across the Prairies. Large convective complexes in particular, cycle tremendous amounts of moisture and energy, which during the mature storm phase should create signatures in such budget studies. This study would require collaboration with hydrologists to carry out a surface water balance using streamflow measurements, and particularly hydrologic modellers to estimate the monthly surface water storage changes (at the time of writing, this is only done by the University of Waterloo WATFLOOD model).

7.4.7 Design/Implement a Field Research Experiment to Map Atmospheric Boundary Layer Processes (R7)

The remaining science issues demand special research datasets, and a series of field experiments therefore needs to be designed to tackle these issues. We recommend, at the very least, two summer programs of sequential soundings over the central Alberta foothills using a minimum of three temporary sounding sites. Sequential soundings at two-hour intervals from 1200–0000 UTC are desirable, 1400–1800 UTC essential. This needs to be combined with a collection of other datasets, including surface, radar, satellite, lightning, instrumented towers, aircraft, and one or more wind profilers and GPS moisture integrators each.

Some suggestions for sounding site transect lines are shown on the map of Figure 7.1. Such a field experiment could be conducted during July of 2002 and/or 2003.

7.4.8 Develop and Field-Test New MOS Forecast Techniques Using Radar and Lightning Data (R8)

It is recommended that resources be acquired to develop new MOS forecasting techniques using new datasets, specifically radar and/or lightning data as predictands. If successful, these could be combined with an artificial intelligence (AI) expert system to provide automated forecasts of storm formation area, time, movement, maximum intensity, and decay. These techniques could be tested with higher resolution data in the proposed field research experiments.

Figure 7.1 Proposed radiosonde transect sites field experiment to map atmospheric boundary layer processes.

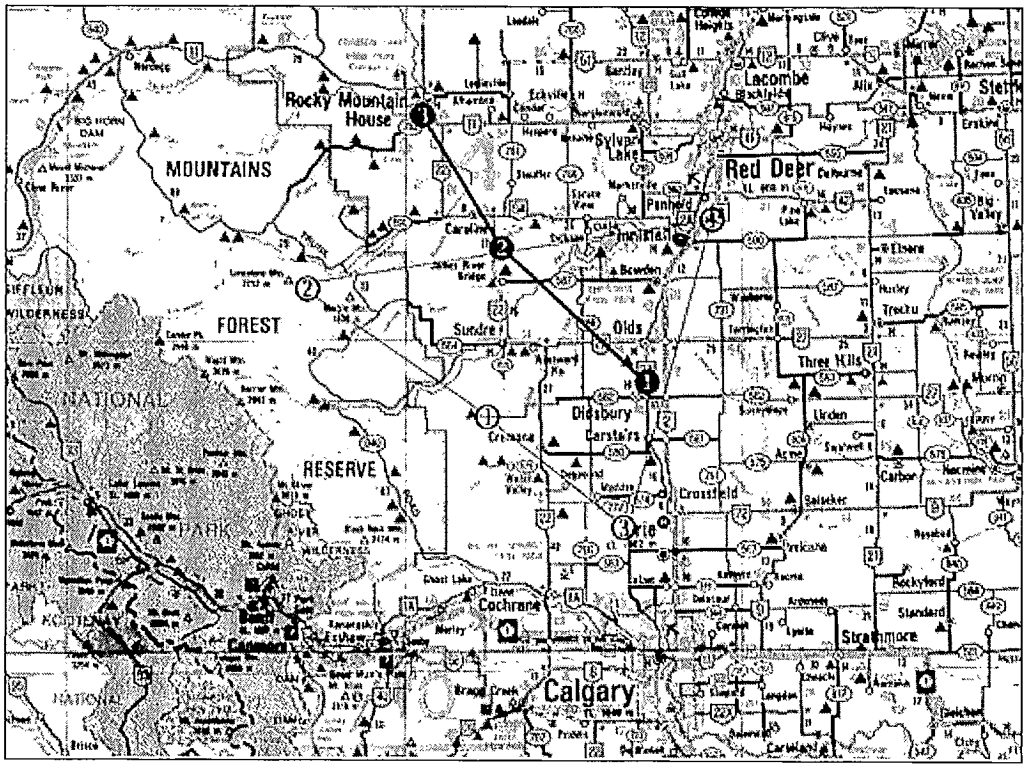

7.5 Relevance of Review and Closing Remarks

The comments and suggestions obtained from consultations with operational and research meteorologists in this study were revealing with their overall consistency of opinions. On the research side, there is a great need for further field study and analysis of ABL processes, particularly over storm formation areas such as the Alberta foothills, and studies to resolve similarities and differences in storm characteristics across the Prairies. The latter requires climatological analyses of synoptic, radar, lightning, cloud, and satellite data in particular, together with regional atmospheric moisture and kinetic energy budget analyses over the Prairies to determine sources and sinks. Results from these studies will have direct input to the development and improvement of new and existing forecasting techniques, and to improved parameterizations for numerical weather prediction models.

7.5.1 Relevance

What is the relevance of this review? In summary, this study identified gaps in our science and data systems, and where research efforts on convective storms need to be directed. It also captured the essence of forecasting problems, and it identified the means to merge research and forecasting needs into common goals. Specific recommendations required to make that merger successful were made.

Along the way, we have barely touched on some climate change questions. For example, what would be the impact of a warmed climate on prairie convective storms? Our best estimate is *more frequent* and *more severe*, although the final answer must come from the modelling community. In terms of mitigation of storms, the only severe storm effect that may have any chance of success for mitigation appears to be hail suppression. In terms of mitigating disasters and preparing for potential severe storm disasters that inevitably must occur, the answer lies partly on improvements to forecasting capabilities. This in turn depends on funding for research, and partly on public education and awareness, which we leave to Environment Canada, Emergency Preparedness Canada (now the Office of Critical Infrastructure Protection and Emergency Preparedness), other federal-provincial departments, and institutes such as the Institute for Catastrophic Loss Reduction (ICLR).

8.0 Bibliography

Anderson, K., 2000. Predicting convective rainfall amounts from lightning flash density. Preprints 20th AMS Conf. Sev. Loc. Storms, Orlando, FL., Sept. 2000: 166–168.

Atchison, G., 1988: Forecaster tells Edmonton tornado story. Chinook, Winter 1988: 8–14.

Barge, B.L., and F. Bergwall, 1976. Fine scale structure of convective storms associated with hail production. Proc. 2nd W.M.O. Sci. Conf. on Wea. Mod., Boulder, Col., 2–6 Aug. 1976: 341–348.

Barnes, S.L., 1976. Severe local storms: concepts and understanding. Bull. Amer. Meteor. Soc., 57: 412–419.

Barnes, S.L., ed., 1981. *Project SESAME 1979 Data Users Guide.* Boulder, Col.: NOAA, ERL, Feb. 1981, 236 pp.

Beebe, R.G., and F.C. Bates, 1955. A mechanism for assisting in the release of convective instability. Mon. Wea. Rev., 83: 1–10.

Bonner, W.D., 1968. Climatology of the low level jet. Mon. Wea. Rev., 96: 833–850.

Bosart, L.F. 1984. The Texas coastal rainstorm of 17–21 September 1979: an example of synoptic-mesoscale interaction. Mon. Wea. Rev., 112: 1108–1133.

Bosart, L.F., and F. Sanders, 1981. The Johnstown flood of July 1977: A long-lived convective system. J. Atmos. Sci., 38, 1616–1642.

Braun, O., 1968. Overlay scale to determine Sly Index directly from tephigram. Tech. Memorandum #702, Dept. of Trans., Meteor. Br., Toronto, 17 Dec. 1968, 4 pp.

Brennand, M.P., 1992. *Convective storms and moisture fields in LIMEX-85: A case study.* M.Sc. thesis, University of Alberta, Edmonton, 136 pp.

Brimelow, J.C., 2001. Numerical modeling of hailstone growth in Alberta storms. Submitted to J. Hydrometeor.

Brooks, H.E., 2000. The climatology of severe thunderstorms: What we can know. Preprints 20th AMS Conf. Sev. Loc. Storms, Orlando, FlL., Sept. 2000: 126–129.

Bullas, J.M., and A.F. Wallace, 1988. The Edmonton tornado, 31 July 1987. Preprints 15th AMS Conf. Sev. Loc. Storms, Baltimore, MarylandD, Feb. 1988: 437–443.

Burrows, W.R., P. King, P.J. Lewis, B. Kochtubadja, B. Snyder, and V. Turcotte, 2001. Lightning occurrence patterns over Canada and adjacent United States from lightning detection network observations, Atmos.-Ocean (submitted 2 March 2001).

Businger, S., S.R. Chiswell, M. Bevis, J. Duan, R.A. Anthes, C. Rocken, R.H. Ware, M. Exner, T. VanHove, and F.S. Solheim, 1996. The promise of GPS in atmospheric monitoring. Bull. Amer. Meteor. Soc., 77(1): 5–18.

Byers, H.R., and R.R. Braham, 1949. *The Thunderstorm.* Final Rep., Chicago, Ill., 287 pp. Dept. Meteor., Univ. Chicago.

Carlson, T.N., 1982. The role of the lid in severe storm formation: Some synoptic examples from SESAME. Preprints 12th Conf. Sev. Loc. Storms, San Antonio, Amer. Meteor. Soc., Jan. 1982: 221–224.

Carlson, T.N., S.G. Benjamin, G.S. Forbes, and Y.-F. Li, 1983. Elevated mixed layers in the regional severe storm environment: conceptual model and case studies. Mon. Wea. Rev., 111: 1453–1473.

Charlton, R.B., M.K. Bradley, and L Wojtiw, 1998. The Edmonton tornado and hailstorm: a decade of research. CMOS Bull. SCMO, 26, spec. issue, Aug. 1998, 56 pp.

Checkwitch, S.M., 1971. *A short-range forecast technique for summer precipitation forecasting in the Edmonton area.* Unpub. int. AES manuscript by Alberta Weather Centre, Edmonton, AB, 32 pp.

Chen, C.-H., & H.D. Orville, 1980. Effects of mesoscale convergence on cloud convection. J. Appl. Meteor., 19: 256–274.

Chisholm, A.J., 1973. Alberta hailstorms, Part I: Radar case studies and airflow models. Meteor. Monogr., 14, No. 36, Amer. Meteor. Soc., Boston, Mass.: 1–36.

Chisholm, A.J., and J.H. Renick, 1972. Supercell and multicell Alberta hailstorms. Proc. Int. Cloud Phys. Conf., London, Eng., Aug. 1972: 1–8.

Cummine, J., and M. Noonan, 2001. Tornado-day climatology of Manitoba 1980–1999. CMOS Bull. SCMO, 29: 3–8.

Danielson, E.F., 1977. *A conceptual theory of tornadogenesis. Part I: Large-scale generation of severe storm potentials*. Meteor. Monogr., Amer. Meteor. Soc.

Darkow, G.L., 1969. An analysis of over sixty tornado proximity soundings. Preprints 6th AMS Conf. Sev. Loc. Storms, Apr. 1969, Chicago, IL: 218–221.

Deibert, R.J., ed., 1982. Alberta Hail Project Field Program 1982, Atmospheric Sciences. Edmonton: Alta. Res. Coun., 58 pp.

Deibert, R.J., ed., 1985. *Field Program 1985, Atmospheric Sciences*. Alta. Res. Coun., Edmonton, 70 pp.

Dickson, R.R., 1979. Weather and Circulation of May 1979. Mon. Wea. Rev., 107: 1087–1092.

Doneaud, A.A., J.R. Miller, D.L. Priegnitz, and L. Viswanath, 1983. Surface mesoscale features as potential storm predictors in the northern Great Plains – two case studies. Mon. Wea. Rev., 111: 273–292.

Doswell, C.A., 1980. Synoptic-scale environments associated with High Plains severe thunderstorms. Bull. Amer. Meteor. Soc., 61: 1388–1400.

Douglas, R.H., 1959. *Alberta Hail, 1958 and Related Studies, Parts I and II.* Stormy Weather Research Group, Sci. Rep. MW-30, McGill U., July 1959 pp.

Douglas, R.H., and W. Hitschfeld, 1959. Patterns of hailstorms in Alberta. Q.J.R.M.S., 85: 105–119.

Dyer, R., and W. Moninger, 1988. Summary Report on the Second Workshop on Artificial Intelligence Research in Environmental Sciences (AIRIES), 15–17 September 1987, Boulder, Colorado. Bull. Amer. Meteor. Soc., 69: 508–514.

Elio, R., J. deHaan, and G. Strong, 1987. METEOR: An artificial intelligence system for convective storm forecasting. J. Atmos. and Oc. Tech., 4: 19–28.

Etkin, D., and S.E. Brun, 1999. A note on Canada's hail climatology: 1977–1993. Int. J. Clim., 19: 1357–1373.

Etkin, D., and M. Leduc, 1994. A non-tornadic severe storm climatology of southern Ontario adjusted for population bias: Some surprising results. CMOS Bull. SCMO, 22, #3: 4–8.

Fawbush, E.J., and R.C. Miller, 1953. A method of for forecasting hailstone size at the Earth's surface. Bull. Amer. Meteor. Soc., 34: 235–244.

Fawbush, E.J., R.C. Miller, and L.G. Starrett, 1951. An empirical method of forecasting tornado development. Bull. Amer. Meteor. Soc., 32: 1–9.

Fawbush, E.J., and R.C. Miller, 1954. The types of airmasses in which North American tornadoes form. Bull. Amer. Meteor. Soc., 35: 154–165.

Fritsch, J.M., and D.M. Rodgers, 1981. The Ft. Collins hailstorm – an example of the short-term forecast enigma. Bull. Amer. Meteor. Soc., 62: 1560–1569.

Fuelberg, H.E., and G.J. Jedlovec, 1982. A subsynoptic-scale kinetic energy analysis of the Red River Valley tornado outbreak (AVE-SESAME I). Mon. Wea. Rev., 110: 2005–2024.

Fuelberg, H.E., and M.F. Printy, 1983. Meso beta-scale thunderstorm environment interactions during AVE-SESAME V (20–21 May 1979). Bull. Amer. Meteor. Soc., 64: 1144–1156.

Fuelberg, H.E., and M.F. Printy, 1984. A kinetic energy analysis of the meso beta-scale severe storm environment. J. Atmos. Sci., 41: 3212–3226.

Fujita, T.T., 1971. Tornadoes and downbursts in the context of generalized planetary scales. J. Atmos. Sci., 38: 1511–1534.

Galway, J.G., 1956. The lifted index as a predictor of latent instability. Bull. Amer. Meteor. Soc., 37: 528–529.

Glickman, T.S., N.J. Macdonald, and F. Sanders., 1977. New findings on the apparent relationship between convective activity and the shape of 500 mb troughs. Mon. Wea. Rev., 105: 1060–1061.

Hage, K.D., 1987a. *Review of the Weather Warning System Associated with the Edmonton Tornado of July 31, 1987*. 85 pp plus apps. Edmonton: Government of Canada, Environment Canada.

Hage, K.D., 1987b. A comparative study of tornadoes and other destructive windstorms in Alberta and Saskatchewan. Proc. Sym. On the Impact of Clim. Variability and Change on the Can. Prairies, Edmonton, Sept. 1987: 351–377.

Hage, K.D., 1994. *Alberta tornadoes, other destructive windstorms and lightning fatalities, 1879–1984*. Pub. By Keith D. Hage, Spruce Grove, AB, 67 pp.

Hage, K.D., 2000. "Probability of tornado strikes has increased with population settlement." Letter to ed., *Devon Dispatch News*, 25 Aug. 2000: p.3.

Hane, C.E., R.M. Rabin, T.M. Crawford, H.B. Bluestein, and M.E. Baldwin, 2000. Severe thunderstorm initiation along the dryline: A mesoscale case study. Proc. 20th Conf. Sev. Loc. Storms, Orlando, FL, Sept. 2000. Amer. Meteor. Soc.: 80–83.

Hill, K., G.S. Wilson, and R.E. Turner, 1979. NASA'S Participation in the AVE-SESAME 79 Program (SESAME News). Bull. Amer. Meteor. Soc., 60: 1323–1329.

Holton, J.R., 1979. *An Introduction to Dynamic Meteorology*. New York: Academic Press.

Honch, R.W., 1989. *Mesoscale vertical velocity fields in the lee of the Alberta Rockies: A case study*. M.Sc. thesis, Univ. of Alberta, 125 pp.

Honch, R.W., and G.S. Strong, 1990. Mesoscale dynamics associated with convection during LIMEX-85. 16th Conf. Sev. Loc. Storms, Kananaskis Park, AB, 22–26 Oct. 1990, Amer. Meteor. Soc., Boston: 681–686.

Holton, J.R., 1979. An Introduction to Dynamic Meteorology. Academic Press, New York, 391 pp.

Joe, P., and D. Dudley, 2000. A quick look at the Pine Lake storm. CMOS Bull. SCMO, 28, #6: 172–180.

King, P.W.S., and W.R. Burrows, 2000. Some mesoscale features in Canadian lightning data. Preprints 20th AMS Conf. Sev. Loc. Storms, Orlando, FL, Sept. 2000: 122–125.

Knight, C.A., ed., 1982. The Cooperative Convective Precipitation Experiment (CCOPE), 18 May – 7 August 1981. Bull. Amer. Meteor. Soc., 63: 386–398.

Knott, S.R.J., and N.M. Taylor, 2001. Operational Aspects of the Alberta Severe Weather Outbreak of 29 July 1993. Accepted for publication in National Weather Digest.

Krauss, T.W., and J.D. Marwitz, 1984. Precipitation processes within an Alberta supercell hailstorm. J. Atmos. Sci., 41, 1025–1034.

Krauss, T.W., ed., 1999. *Alberta Hail Suppression Project Final Report 1999*. Fargo, North Dakota: Weather Modification Inc., 79 pp.

Krauss, T.W., and J.D. Marwitz, 1984. Precipitation processes within an Alberta supercell hailstorm. J. Atmos. Sci., 41: 1025–1034.

Kubesh, R.J., D.J. Musil, R.D. Farley, and H.D. Orville, 1988. The 1 August CCOPE Storm: Observations and modeling results. J. Appl. Meteor., 27: 216–243.

Kung, E.C., 1967. Diurnal and long-term variations of the kinetic energy generation and dissipation for a five-year period. Mon. Wea. Rev., 95: 593–606.

Kung, E.C., 1969. Further study on the kinetic energy balance. Mon. Wea. Rev., 97: 573–581.

Kung, E.C., and T.L. Tsui, 1975. Subsynoptic-scale kinetic energy balance in the storm area. J. Atmos. Sci., 32: 729–740.

LaDochy, S., 1985. *The Synoptic Climatology of Severe Thunderstorms in Manitoba.* Ph.D. thesis, Univ. Manitoba, Winnipeg, pp.

Lanicci, J.M., and T.N. Carlson, 1983. Three-dimensional numerical simulations of dryline and elevated mixed layer evolution as related to soil moisture distribution. Preprints AMS 13th Conf. Sev. Loc. Storms, Tulsa, Okla., 17–20 Oct., 1983: 328–331.

Lanken, D., 2000. Struck by lightning. Can. Geog., July/August, 2000, Ottawa: 20–32.

Lawford, R.G., 1970. The Behavior of Thunderstorms over Alberta Forests. M.Sc. thesis, University of Alberta, Edmonton, Alberta, 176 pp.

Lemon, L.R., and C.A. Doswell, 1979. Severe thunderstorm evolution and mesocyclone structure as related to tornadogenesis. Mon. Wea. Rev., 107: 1184–1197.

Little, K., 1990. A case of summer severe weather over Alberta under weak supporting dynamics. Western Region Tech. Note 90-N-095, Edmonton: Alta. Wea. Cen., Sept., 1990, 10 pp.

Longley, R.W., and C.E. Thompson, 1965. A study of the causes of hail. J. Appl. Meteor., 4: 69–82.

Lorenz, E.N., 1955. Available potential energy and the maintenance of the general circulation. Tellus, 7: 157–167.

Lorenz, E.N., 1960. Energy and numerical weather prediction. Tellus, 12: 364–373.

Lowe, A.B., and G.A. McKay, 1962. Tornado composite charts for the Canadian Prairies. J. Appl. Meteor., 1: 157–162.

Maddox, R.A., 1980. Mesoscale convective complexes. Bull. Amer. Meteor. Soc., 61: 1374–1387.

Maddox, R.A., 1983. Large-scale meteorological conditions associated with midlatitude, mesoscale convective complexes. Mon. Wea. Rev., 111: 1475–1493.

Margules, M., 1903. Über die Energie der Stürme. Jahrb. kais-kon Zent. für Met., Vienna. Translation by C. Abbe in Smithson. Inst. Misc. Coll., 51: 1910.

McCarthy, P.J., A. Erfani, and D. Patrick, 2000. Multiple bounded weak echo regions in the 16 July 1996 Winnipeg, Manitoba, Canada, hailstorm supercell. Preprints 20th AMS Conf. Sev. Loc. Storms, Orlando, FL, Sept. 2000: 481–484.

McGinley, J.A., and Y.K. Sasaki, 1975. The role of symmetric instabilities in thunderstorm development on drylines. Preprints 9th Conf. Sev. Loc. Storms, Norman, OK Amer. Meteor. Soc., Oct. 1975: 173–180.

McInnis, D.H., and E.C. Kung, 1972. A study of subsynoptic scale energy transformations. Mon. Wea. Rev.: 126–132.

Miller, R.C., 1959. Tornado-producing synoptic patterns. Bull. Amer. Meteor. Soc., 40: 465–472.

Miller, R.C., 1972. *Notes on analysis and severe-storm forecasting procedures of the Air Force Global Weather Central.* Tech. Rep. 200.Offut, Nebraska: Air Weather Service (MAC), USAF, May 1972, 102 pp.

Moller, A. R., C. A. Doswell, M. P. Foster, and G. R. Woodall, 1994. The operational recognition of supercell thunderstorm environments and storm structures. Wea. Forecasting, 9: 327–347.

Moncrief, M.W., and J.S.A. Green, 1972. The propagation and transfer properties of steady convective overturning in shear. Quart. J. Roy. Meteor. Soc., 98: 336–352.

Moninger, W.T., D.F. Cote, J. Davis, R. Dyer, R. Kittredge, R. McArthur, A.H. Murphy, and I.R. Racer, 1987. Summary of the First Conference on Artificial Intelligence Research in Environmental Sciences (AIRIES). Bull. Amer. Meteor. Soc., 68: 793–800.

National Oceanic and Atmospheric Administration, 1979. Storm Data, Envir. Data and Info. Serv., Nat. Clim. Cen., Asheville, North Carolina, 21, No. 5, 23 pp.

Newark, M.J., 1984. Canadian Tornadoes, 1950–1979. Atmos.-Ocean, 22(3): 343–353.

Newark, M.J., 1989. Understanding the severe local storm hazard in Canada: Where do we go from here? Clim. Bull., 23(1): 15–23.

Newton, C.W., 1967. Severe Convective Storms. Adv. in Geophys., 12: 257–308.

Newton, C.W., and J.C. Fankhauser, 1975. Movement and propagation of multicellular convective storms. Pageoph, 113: 747–764.

Ogura, Y., and Y.-L. Chen, 1977. A life history of an intense convective storm in Oklahoma. J. Atmos. Sci., 34: 1458–1476.

Orlanski, I., 1975. A rational subdivision of scales for atmospheric processes. Bull. Amer. Meteor. Soc., 56: 527–530.

Ostby, F.P., 1999. Improved accuracy in severe storm forecasting by the severe local storms unit during the last 25 years: Then versus now. Wea. and Forecasting, 14: 526–543.

Panofsky, H.A., and G.W. Brier, 1963. *Some Applications of Statistics to Meteorology.* University Park, PennA, 224 pp.: Penn. State Univ.

Parsons, D.B., M.A. Shapiro, R.M. Hardesty, R.J. Zamora, and J.M. Intrieri, 1991. The finescale structure of a west Texas dryline. Mon. Wea. Rev., 119: 1242–1258.

Paruk, B.J., and S.R. Blackwell, 1993. *A severe thunderstorm climatology for Alberta.* Alberta Wea. Cent. Tech. Note 93-01, Mar. 1993, 7 pp.

Paul, A.H., 1967. *Hailfall in Central Alberta.* M.Sc. thesis, University of Alberta, Edmonton, Alberta, 124 pp.

Paul, A.H., 1980a. Hailstorms in southern Saskatchewan. J. Appl. Meteor., 19: 305–314.

Paul, A.H., 1980b. Personal communication on storms of 21 July 1976.

Paul, A.H., 1991a. A comment on hailswath lengths. Clim. Bull., 25(2): 125–127.

Paul, A.H., 1991b. Studies of long-lived hailstorms in Saskatchewan, Canada from crop insurance data. Nat. Hazards, 4: 345–352.

Paul, A.H., 1993. The thunderstorms of 8 July 1989 in the northern Great Plains. Clim. Bull., 27, #3: 170–178.

Phillips, D., 2001. The top ten weather stories of 2000. CMOS Bull. SCMO, 29: 18–19.

Pielke, R.A., 1984. *Mesoscale Meteorological Modeling.* Orlando, FL, 612 pp.: Academic Press.

Rabin, R.M., S. Stadler, P.J. Wetzel, D.J. Stensrud, and M. Gregory, 1990. Observed effects of landscape variability on convective clouds. B.A.M.S., 71: 272–280.

Raddatz, R.L., 1998. Anthropogenic vegetation transformation and the potential for deep convection on the Canadian Prairies. Can. J. Soil Sci., 78: 657–666.

Raddatz, R.L., 2000. Summer rainfall recycling for an agricultural region of the Canadian Prairies. Can. J. Soil Sci., 80: 367–373.

Raddatz, R.L., and J.M. Hanesiak, 1991. Climatology of tornado days 1960–1989 for Manitoba and Saskatchewan. Clim. Bull., 25(1): 47–59.

Reap, Ronald M., 1993. The use of network lightning data to detect thunderstorms near surface reporting stations. Mon. Wea. Rev., 121: 464–469.

Reinelt, E.R., 1970. On the variation of the 500-mb wind and its effect on the release of instability in the lee of the Alberta Rockies. Atmosphere, 8: 119–127.

Renick, J.H., ed., 1970. *Alberta Hail Studies Field Program 1970.* Hail Studies Report 70-1. Edmonton: Alberta Research Council, 49 pp.

Rockwood, A.A., and R.A. Maddox, 1988. Mesoscale and synoptic scale interactions leading to intense convection: the case of 7 June 1982. Wea. Forecasting, 3: 51–68.

Rossby, C.-G., 1949. On a mechanism for the release of potential energy in the atmosphere. J. Meteor., 6: 163–180.

Sackiw, C., F.E. Robitaille, and E.P. Lozowski, 1979. Large Funnel Cloud Latitude 52N. Preprints 11th AMS Conf. Sev. Loc. Storms, Kansas City, Mo., Oct. 1979.

Sackiw, C.M., and G.S. Strong, 1983. The spatial/temporal resolution study (STRESS) of upper air data. Presented at 17th Ann. Congr. Can. Meteor. and Oc. Soc., Banff, AB, 3–5 May, 1983, published by Alta. Res. Coun., Edmonton, 13–25.

Sackiw, C.M., 1986. *Examination of Upper-Air Data Resolution using Stability Indices.* M.Sc. thesis, Univ. of Alberta, Edmonton, 82 pp.

Schaefer, J.T., 1973. The motion of the dryline. Preprints 8th Conf. Sev. Loc.cl Storms, Denver, CO, Amer. Meteor. Soc., Oct. 1973: 104–107.

Scorer, R., and A. Verkaik, 1989. *Spacious Skies*. Devon: David and Charles Publishers pp.

Sechrist, F.S., and J.A. Dutton, 1970. Energy conversions in a developing cyclone. Mon. Wea. Rev., 98: 354–362.

Showalter, A.K., 1953. A stability index for thunderstorm forecasting. Bull. Amer. Meteor. Soc., 34: 250–252.

Sikdar, D.N., and D. Fox, 1983. An evolving severe storm complex during SESAME: Its large scale environment and momentum budget. Preprints 13th AMS Conf. Sev. Loc. Storms, Tulsa, Okla., 17–20 Oct. 1983: 312–315.

Sly, W.K., 1966. A convective index as an indicator of cumulonimbus development. J. Appl. Met., 5: 839–846.

Smith, P.J., 1969. On the contributions of a limited region to the global energy budget. Tellus, 21: 202–207.

Smith, S.B., and M.K. Yau, 1993a. The causes of severe convective outbreaks in Alberta. Part I: A comparison of a severe outbreak with two non-severe events. Mon. Wea. Rev., 121: 1099–1125.

Smith, S.B., and M.K. Yau, 1993b. The causes of severe convective outbreaks in Alberta. Part II: Conceptual Model and statistical analysis. Mon. Wea. Rev., 121: 1126–1134.

Starr, V.P., 1948. On the production of kinetic energy in the atmosphere. J. Meteor., 5: 193–196.

Starr, V.P., 1953. Note concerning the nature of the large-scale eddies in the atmosphere. Tellus, 5: 494–498.

Strong, G.S., 1979. Convective Weather prediction based on synoptic parameters. Preprints 11th AMS Conf. Sev. Loc. Storms, Kansas City, Mo., Oct. 1979, 608–615.

Strong, G.S., 1974. *The Objective Measurement of Alberta Hailfall.* M.Sc. thesis, Univ. of Alberta, Edmonton, Alberta, 182 pp.

Strong, G.S. 1979. *Convective Weather prediction based on synoptic parameters*. Preprints 11th AMS Conf. Sev. Loc. Storms, Kansas City, Mo., Oct. 1979: 608–615.

Strong, G.S., 1981. *Severe Alberta thunderstorms: a post-cold-frontal type*. Presented at 15th Ann. Congr. Can. Meteor. and Oc. Soc., Saskatoon, Sask., 27–29 May 1981, 22 pp (avail. from author).

Strong, G.S., 1982. Hailstorms! – Why Alberta? Chinook, Winter/Spring: 21–23.

Strong, G.S., 1986. *Synoptic to Mesoscale Dynamics of Severe Thunderstorm Environments: A Diagnostic Study with Forecasting Applications*. Ph.D. thesis, University of Alberta, Edmonton, 346 pp.

Strong, G.S., 1988. *The Prediction of Meteorological Hazards using Artificial Intelligence Techniques*. Proc. ISCORD '88, International Symposium on Cold Region Development, Harbin, China, 8–13 Aug. 1988, 4: 324–333.

Strong, G.S., 1989. LIMEX-85: 1. Processing of data sets from an Alberta mesoscale upper-air experiment. Clim. Bull., 23: 98–118.

Strong, G.S., 1997. Atmospheric Moisture Budget Estimates of Regional Evapotranspiration from RES-91. Atmos.-Ocean, 35: 29–63.

Strong, G.S., 2000. A multi-scale conceptual model of severe thunderstorms. CMOS Bull., 28, No. 2, April, 2000: 45–54.

Strong, G.S., and E.P. Lozowski, 1980. Hailpad wind measurements and hailfall sampling errors. Pres. at 14th Ann. Congress, Can. Meteor. & Oc. Soc., Toronto, May 1980, 28 pp (paper available from Strong).

Strong, G.S., and W.D. Wilson, 1981. *The Synoptic (instability) Index: 1978–80 tests and new versions*. Presented at 15th Ann. Congr. Can. Meteor. and Oc. Soc., Saskatoon, Sask., 27–29 May, 1981: 17 pp (avail. from author).

Strong, G.S., and W.D. Wilson. 1983a. *The Synoptic Index of Convection: Part I. Evaluation of the single-valued index, 1978–82*. Presented at 17th Ann. Congr. Can. Meteor. and Oc. Soc., Banff, AB, 3–5 May 1983, published by Alta. Res. Coun., Edmonton: 27–37.

Strong, G.S., and W.D. Wilson, 1983b. *The Synoptic Index of Convection: Part II. Applications to regional forecasts of convective complexes*. Presented at 17th Ann. Congr. Can. Meteor. and Oc. Soc., Banff, AB, 3–5 May 1983, published by Alta. Res. Coun., Edmonton: 39–53.

Strong, G.S., and W.D. Wilson, 1983c. *The Synoptic Index of Convection: Application to the Fort Collins hailstorm of 30 July 1979*. Preprints 13th AMS Conf. Sev. Loc. Storms, 17–20 Oct. 1983, Tulsa, Okla.: 300–303.

Strong, G.S., and E.P. Lozowski, 1977. An Alberta study to objectively measure hailfall intensity. Atmosphere, 15: 33–53.

Strong, G.S., L.D. Stovel, W.D. Wilson, J. Ramsden, and R.G. Humphries, 1984. *Combining GOES satellite, radar, synoptic, and mesoscale data to analyze convective weather over the Canadian Prairies*. Final Rep. to Atmos. Envir. Serv. RAINSAT-II Proj. by Atmos. Sci. Dept., Alta. Res. Coun., Edmonton, AB, Mar. 1984, 122 pp.

Strong, G.S., B. Proctor, M. Wang, R. Soulis, C.D. Smith, Frank Seglenieks, and K. Snelgrove, 2001. Closing the Mackenzie Basin Water Balance, Water-Years 1994/95 through 1996/97. In rev. for Atmos.-Oc., 2001.

Summers, P.W., and A.H. Paul, 1967. Some climatological characteristics of hailfall in central Alberta. Proc. 5th AMS Conf. Sev. Loc. Storms, St. Louis, Missouri: 17–26.

Taylor, N.M., 1999. *Climatology of sounding parameters identifying the potential for convective storm development over central Alberta*. M.Sc. thesis, University of Alberta, Edmonton, 121 pp.

Tennekes, H., 1978. Turbulent flow in two and three dimensions. Bull. Amer. Meteor. Soc., 59: 22–28.

Tsui, T.L., and E.C. Kung, 1977. Subsynoptic-scale energy transformations in various severe storm situations. J. Atmos. Sci., 34: 98–110.

Uccellini, L.W., and D.R. Johnson, 1979. The coupling of upper and lower tropospheric jet streaks and implications for the development of severe convective storms. Mon. Wea. Rev., 107: 682–703.

Verkaik, A., and J. Verkaik, 1997. *Under the Whirlwind*. Elmwood, ON, Whirlwind Books pp.

Verkaik, A., and J. Verkaik, 2000. *Severe Weather Watcher Handbook*. Ottawa, ON, 48 pp.: Minister of Supply and Services.

Vickers, G., 1996. *1996 Summer Severe Weather Report, Central and Northern Alberta*. Edmonton: Environment Canada, 37 pp.

Wagner, A.J., 1979. Weather and Circulation of July 1979. Mon. Wea. Rev., 107: 1414–1421.

Ware, R.H., D.W. Fulker, S.A. Stein, D.N. Anderson, S.K. Avery, R.D. Clark, K.K. Droegemeier, J.P. Kuettner, J.B. Minster, and S. Sorooshian, 2000. SuomiNet: A real-time national GPS network for atmospheric research and education. Bull. Amer. Meteor. Soc., 81(4): 677–694.

Weisman, M.L., and J.B. Klemp, 1986. Characteristics of Isolated Storms. In Mesoscale Meteorology and Forecasting, P.S. Ray, ed., Amer. Meteor. Soc.: 331–357.

White, R.M., and B. Saltzman, 1956. On conversions between potential and kinetic energy in the atmosphere. Tellus, 8: 357–363.

Wilk, K., K. Gray, C. Clark, D. Sirmans, J. Dooley, J. Carter, and W. Bumgarner, 1976. *Objectives and accomplishments of the NSSL 1975 Spring Program.* Norman, Okla.: NOAA Tech. Memo ERL NSSL-78K, 47 pp.

Williams, E.R., M.E.; Weber, M. E., and R.E. Orville, 1989. The relationship between lightning type and convective state of thunderclouds. J. Geophys. Res., 94(D11) 13: 213–13, 220.

Wojtiw, L., 1975. *Climatic summaries of hailfall in central Alberta (1957–1973).* Alberta Research Atmospheric Science Report 75-1, Edmonton, AB.

World Meteorological Organization (WMO), 1969. *International Cloud Atlas.* Reprint of 1956 version by WMO, Geneva, Switzerland.

Xin, L., G. Reuter, and B. Larochelle, 1997. Reflectivity-rain relationships for convective rainshowers in Edmonton. Atmos.-Ocean, 35: 513–521.

Appendix A – Brief Descriptions of the Limestone Mountain Experiments

The LIMEX experiments were part of a larger study by the lead author dealing with interactions between synoptic, mesoscale, and fixed orographic processes which lead to convective storms. The overall goal of LIMEX was to improve forecasting capabilities during the DAY-1 forecast period. Therefore, unlike most other convective studies, data collection was not concentrated solely on the mature storm period, nor was it confined to cases of the most severe storms, although the latter type typically provide the best data sets for describing physical processes. These experiments, in fact, focussed primarily on the pre-storm period, and specifically on the pre-storm formation and breakdown of the *capping lid.* This lid is characterized by a moist boundary layer capped by a stable inversion of potential temperature during the pre-storm period. The lid is usually present prior to the formation of a "severe" storm, often 24 hours or more before, and is common in the pre-storm environment of storms which form in the lee of the Rockies from Alberta southward to western Texas. The lid weakens over the potential storm region one to six hours in advance of the storm. The lid is not always detected with "synoptic network" soundings because often, though not always, it is confined to the immediate *region of influence* of the potential storm, and for Alberta storms, is most prevalent over the foothills.

Several LIMEX field experiments were planned (Strong, 1985a) with primary and secondary technical goals as follows:

1. To obtain accurate surface and upper air data of high spatial and temporal resolution over the Alberta foothills during days exhibiting a capping lid; and

2. To test existing forecasting techniques, including the Synoptic Index of Convection (Strong, 1979, 1986; Strong and Wilson, 1983), with high resolution surface and upper air data.

Three main and several smaller LIMEX field experiments were carried out during 1980–85 with the above objectives in mind. All were conducted over the foothills and mountains of southwestern Alberta in the region immediately around Limestone Mountain, the focal point of these experiments. The region was shown visually in Figures 4.1 and 4.2. The three primary experiments are now described briefly. A more detailed description can be found in Strong (1989).

A.1 LIMEX-80

LIMEX-80 was a three-day experiment carried out on 15–17 July 1980. The specific goal was to measure thermodynamic responses to orographic subsidence near the main mountain barrier and over the foothills of southwest Alberta. Subsidence warming was thought to combine with large (synoptic) scale subsidence in creating and maintaining the capping lid.

During LIMEX-80, radiosondes were released at three-hour intervals, commencing at 1400 UTC (Universal Coordinated Time, or 0800 MDT), 15–17 July 1980, in a 10 km wide valley west of Limestone Mountain West (LMW, at 1506 m ASL) adjacent to the main mountain barrier, in

order to measure the maximum response to orographic subsidence. Radiosondes were also released at three-hour intervals at Rocky Mountain House (YRM, at 988 m ASL) 65 km northeast of the Limestone site, and at Red Deer Airport (AQF, at 900 m ASL), some 110 km east-northeast, in an attempt to detect the creation and pre-storm breakdown of any lid.

A.2 STRESS-81

The Spatial and Temporal Resolution Study of upper air data was designed to determine the optimum spatial and temporal resolution of soundings for resolving mesoscale circulations associated with convective weather; soundings were released at 1½-hour intervals at five sites spaced 40 km apart in straight lines over central Alberta, in order that maximum information on gradients could be obtained. Results were discussed by Sackiw and Strong (1983) and Sackiw (1986).

A.3 CIS-82

The Capping Inversion Study field experiment of 1–29 July 1982 (CIS-82) was designed to measure the sequence of low-level thermodynamic changes near an *existing* capping lid prior to the formation and/or approach of a severe storm complex. CIS-82 involved three *mobile* sounding units (airsondes) directed by radio to various sites during an operational day, as well as serial radiosonde releases from fixed sites at Red Deer Airport and Calgary.

In all, 124 airsonde and 43 radiosonde soundings were collected during 16 operational days of CIS-82. A complete listing is provided in ARC (1982). Excellent storm data were obtained during three severe hailstorm days, July 14, 21, and 29. However, it was found that mobile soundings were, at best, difficult to deploy to the most favourable locations (usually the right flank of a storm), and during particularly busy days, mobile personnel often discovered that the storm of interest had passed by them and they were unable to catch up.

A.4 LIMEX-83

LIMEX-83 was conducted on 7–8 July 1983, primarily to test field logistics and sounding frequency interference. This fieldwork included three airsonde systems in the vicinity of Limestone Mountain, plus six radiosonde releases from Rocky Mountain House.

A.5 LIMEX-84

LIMEX-84, conducted on 19–20 July 1984, involved a total of 20 releases from three airsonde sites in the vicinity of Limestone Mountain and from the Rocky Mountain House radiosonde.

A.6 LIMEX-85

LIMEX-85 was by far the most intense data collection phase of the LIMEX experiments. This field study involved nine fixed upper air sites in a semi-triangular grid of average 60 km spacing, along with several eight automatic weather stations recording half-hourly data, and one SODAR sounding unit. Radiosonde operations were conducted on 11 days only during 8–12, 15–18, and 22–23 July 1985. Soundings were released each operational day at two-hour intervals commencing at either 1200 or 1400 UTC, with a decision to continue or not at 1800 UTC. Station information and the types of data collected at each of the upper air and special surface data sites are provided in Table A.1. The LIMEX data archive also includes additional surface data provided by the AES and Alberta Forestry networks of the period. The special data networks are indicated in Figure 5.14, together with a schematic map of the topography involved.

Table A.1 Upper Air and Surface Data Sites Used During LIMEX-85, 8–23 July 1985.

Legend of Observations Types

uR – upper air, Rawinsonde
uA – upper air, Airsonde
SD – SODAR
sM – surface observations, Manual
sC – surface observations, CR-21 autostations
ph – still and/or time lapse photography
XX– alternate site, not used or used just briefly

Balloon Sounding and SODAR Sites:

Stn ID	Stn No.	DLS Land Location	Lat. (degs.)	Long. (degs.)	Elev. (m MSL)	Station Name	Type Obs.
AQF	718781	SW13-37-28-4	52.18	113.90	900	Red Deer A. (home base)	uR,sM
ARM	719281	SE14-40-07-5	52.43	114.92	988	Rocky Mtn House	uR,ph
AYC	718771	NW36-24-02-5	51.08	114.13	1114	Calgary U of C	uR
LMW	99301	SW27-34-11-5	51.95	115.48	1506	Limestone Mtn W	uR,sM,ph
WSE	71119	NW05-53-01-5	53.55	114.10	766	Edm. Stony Plain	uR (00, 12Z)
ABP	99331	NE02-33-19-5	51.81	116.58	1710	Bow Pass	uA,sM,ph
ACR	99320	SE06-36-05-5	52.03	114.42	1068	Caroline	uA,sM,ph
AEL	99317	SW16-31-04-5	51.66	114.51	1130	Elkton	uA,sM,ph
AML	99328	SW13-31-10-5	51.66	115.29	1441	Mountainaire Ldg.	uA,sM,ph
ARL	99329	SW27-34-11-5	52.34	115.65	1294	Ram Lookout East	uA,sM,ph
JRR	99232	NE01-34-08-5	51.89	115.00	1198	James River Ranger	SD

Special Surface Data Sites:

Stn ID	Stn No.	DLS Land Location	Lat. (degs.)	Long. (degs.)	Elev. (m MSL)	Station Name	Type Obs.
JRB	99231	NE01-34-08-5	51.89	115.00	1204	James River Bridge	XX
AEV	99331	SE31-37-04-5	52.22	114.55	1009	Evergreen	sC
AGL	99327	SW09-35-03-5	51.99	114.38	1012	Glennifer Lake	sC
APC	99319	NE16-37-10-5	52.18	115.36	1406	Prairie Creek	sSC
ARF	99500	SW18-36-13-5	52.09	115.85	1618	Ram Falls Ranger	sSC
ASU	99325	NE33-32-06-5	51.79	114.79	1167	Sundre West	SsC
ATP	99313	SE11-34-09-5	51.90	115.16	1380	Tee-Pee Pole Creek	SsC
AWV	99326	NE21-29-05-5	51.50	114.64	1313	Water Valley	SsC
BCH	99322	NW11-37-07-5	52.17	114.90	1090	Cheddarville, WB	sC
ACH	99321	SE15-37-07-5	52.18	114.91	1088	Cheddarville, WK	XX
LMR	99304	SE07-34-10-5	51.90	115.40	2121	Limestone Mtn Ridge (field base)	sM ,ph

Appendix B – Annual Alberta Hail Project (AHP) Forecast Evaluation Tables

(a) Forecast CDC Evaluation Tables and (b) Observed CDC Frequency Graphs, 1978–85.

1978		Forecast Convective Day Category									
		-3	-2	-1	0	+1	+2	+3	+4	+5	Totals
Observed	-3	4	2	1	0	0	0	1	0	0	8
	-2	0	1	1	1	1	0	0	0	0	4
Convective	-1	0	4	7	4	0	0	1	0	0	16
	0	0	1	3	10	4	1	0	1	0	20
Day	+1	0	0	2	3	5	4	0	1	0	15
	+2	0	0	0	3	6	3	2	0	0	14
Category	+3	0	1	0	2	1	4	1	1	1	11
	+4	0	0	0	0	0	1	0	1	0	2
(CDC)	+5	0	0	0	0	0	0	1	0	0	1
	Totals	4	9	14	23	17	13	6	4	1	91

Forecast Category Accuracy:

Correct Category:	32 days	35.2 %
Correct within one Category:	70 days	76.9 %
Correct within two Categories:	83 days	91.2 %

OBSERVED	19 78	Forecast	
		NO HAIL	HAIL
	NO HAIL	39	9
	HAIL	11	32

HAIL/NO-HAIL Accuracy:

No. hail days in period:	43 days	47.3 %
No. 'severe' hail days in period:	14 days	15.4 %
Correct HAIL days forecast:	32 days	74.4 %
Correct NO HAIL days forecast:	39 days	81.3 %

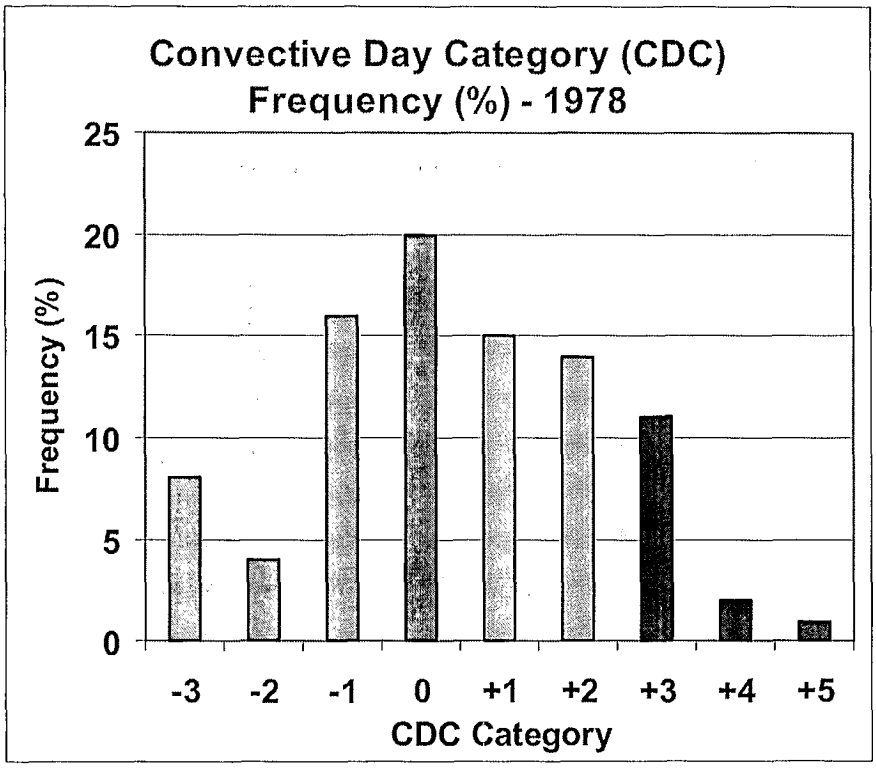
Convective Day Category (CDC)
Frequency (%) - 1978
Frequency (%)
25
20
15
10
5
0
-3
-2
-1
0
+1
+2
+3
+4
+5
CDC Category

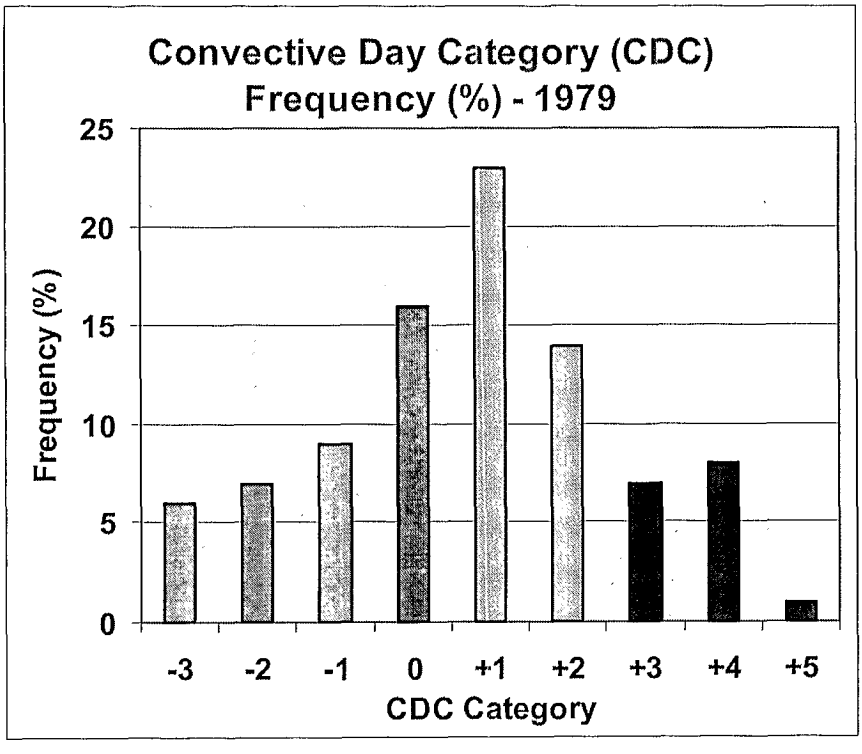
Convective Day Category (CDC)
Frequency (%) - 1979
Frequency (%)
25
20
15
10
5
0
-3
-2
-1
0
+1
+2
+3
+4
+5
CDC Category

1979		Forecast Convective Day Category									
		-3	-2	-1	0	+1	+2	+3	+4	+5	Totals
Observed	-3	3	3	0	0	0	0	0	0	0	6
	-2	0	5	0	1	0	1	0	0	0	7
Convective	-1	0	2	4	1	1	0	1	0	0	9
	0	0	0	5	2	8	1	0	0	0	16
Day	+1	0	0	3	5	4	8	2	1	0	23
	+2	0	0	1	4	4	3	2	0	0	14
Category	+3	0	0	1	1	2	1	1	1	0	7
	+4	0	0	0	0	2	2	2	1	1	8
(CDC)	+5	0	0	0	0	0	0	0	0	1	1
	Totals	3	10	14	14	21	16	8	3	2	91

Forecast Category Accuracy:

Correct Category:	24 days	26.4 %
Correct within one Category:	67 days	73.6 %
Correct within two Categories:	83 days	91.2 %

OBSERVED	19 79	Forecast	
		NO HAIL	HAIL
	NO HAIL	26	12
	HAIL	15	38

HAIL/NO-HAIL Accuracy:

No. hail days in period:	53 days	58.2 %
No. 'severe' hail days in period:	16 days	17.6 %
Correct HAIL days forecast:	38 days	71.7 %
Correct NO HAIL days forecast:	26 days	68.4 %

1980		Forecast Convective Day Category									
		-3	-2	-1	0	+1	+2	+3	+4	+5	Totals
Observed	-3	6	0	0	0	0	0	0	0	0	6
	-2	2	0	4	1	2	0	0	0	0	9
Convective	-1	0	2	3	0	1	0	0	0	0	6
	0	0	0	4	3	4	2	0	0	0	13
Day	+1	0	0	1	7	8	4	0	0	0	20
	+2	0	0	0	0	3	5	4	0	0	12
Category	+3	0	0	1	1	0	6	2	1	0	11
	+4	0	0	0	1	0	3	2	2	1	9
(CDC)	+5	0	0	0	0	0	0	1	0	0	1
	Totals	8	2	13	13	18	20	9	3	1	87

Forecast Category Accuracy:

Correct Category:	29 days	33.3 %
Correct within one Category:	73 days	83.9 %
Correct within two Categories:	82 days	94.3 %

OBSERVED	19 80	Forecast	
		NO HAIL	HAIL
	NO HAIL	25	9
	HAIL	11	42

HAIL/NO-HAIL Accuracy:

No. hail days in period:	53 days	60.9 %
No. 'severe' hail days in period:	21 days	24.1 %
Correct HAIL days forecast:	42 days	79.2 %
Correct NO HAIL days forecast:	25 days	73.5 %

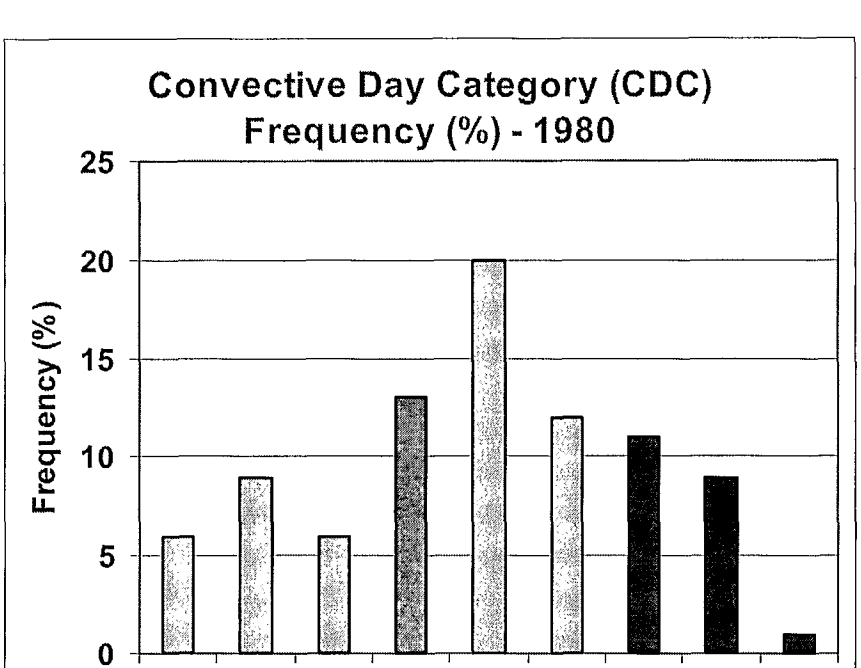
Convective Day Category (CDC)
Frequency (%) - 1980
Frequency (%)
25
20
15
10
5
0
-3
-2
-1
0
+1
+2
+3
+4
+5
CDC Category

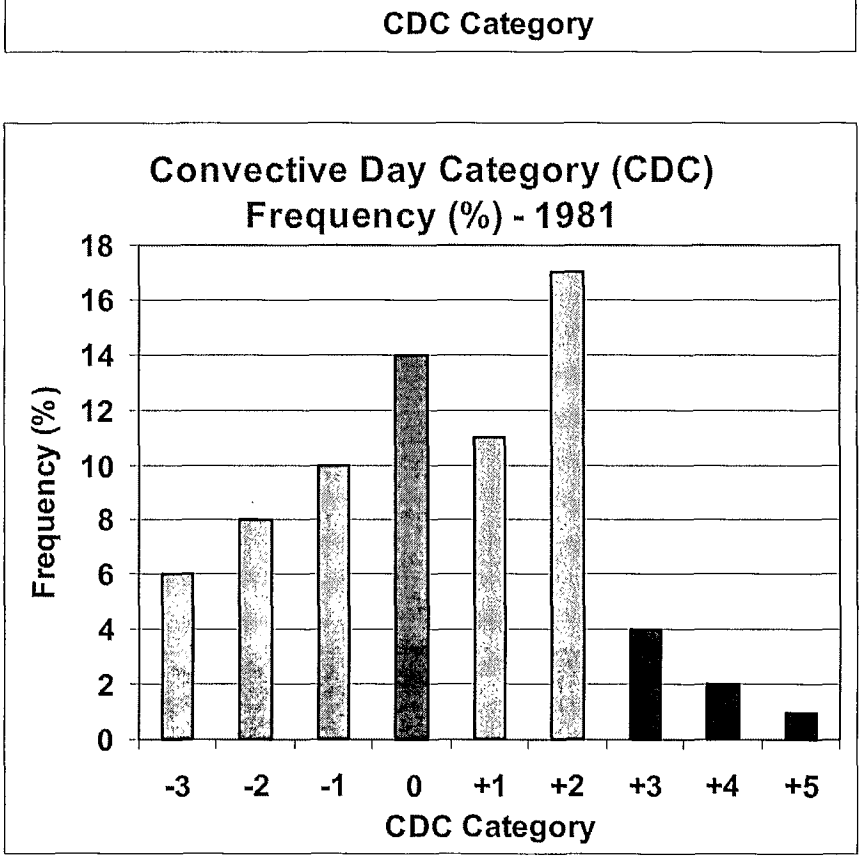
Convective Day Category (CDC)
Frequency (%) - 1981
Frequency (%)
18
16
14
12
10
8
6
4
2
0
-3
-2
-1
0
+1
+2
+3
+4
+5
CDC Category

1981		Forecast Convective Day Category									
		-3	-2	-1	0	+1	+2	+3	+4	+5	Totals
Observed	-3	2	2	2	0	0	0	0	0	0	6
	-2	2	2	2	0	1	1	0	0	0	8
Convective	-1	0	2	3	3	1	0	1	0	0	10
	0	0	1	1	7	1	1	2	1	0	14
Day	+1	0	2	0	0	4	2	2	0	1	11
	+2	0	0	0	0	3	9	2	3	0	17
Category	+3	0	0	0	0	0	2	2	0	0	4
	+4	0	0	0	0	0	0	0	2	0	2
(CDC)	+5	0	0	0	0	0	0	1	0	0	1
	Totals	4	9	8	10	10	15	10	6	1	73

Forecast Category Accuracy:

Correct Category:	31 days	42.5 %
Correct within one Category:	53 days	72.6 %
Correct within two Categories:	64 days	87.7 %

OBSERVED	19 81	Forecast	
		NO HAIL	HAIL
	NO HAIL	29	9
	HAIL	2	33

HAIL/NO-HAIL Accuracy:

No. hail days in period:	35 days	47.9 %
No. 'severe' hail days in period:	7 days	9.6 %
Correct HAIL days forecast:	33 days	94.3 %
Correct NO HAIL days forecast:	29 days	76.3 %

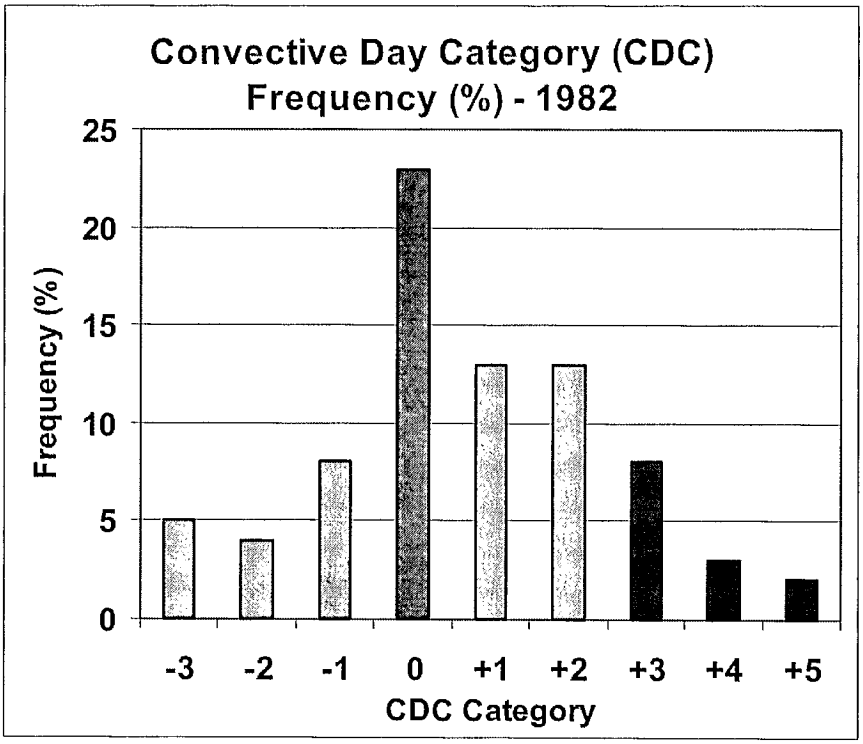
Convective Day Category (CDC)
Frequency (%) - 1982
Frequency (%)
25
20
15
10
5
0
-3
-2
-1
0
+1
+2
+3
+4
+5
CDC Category

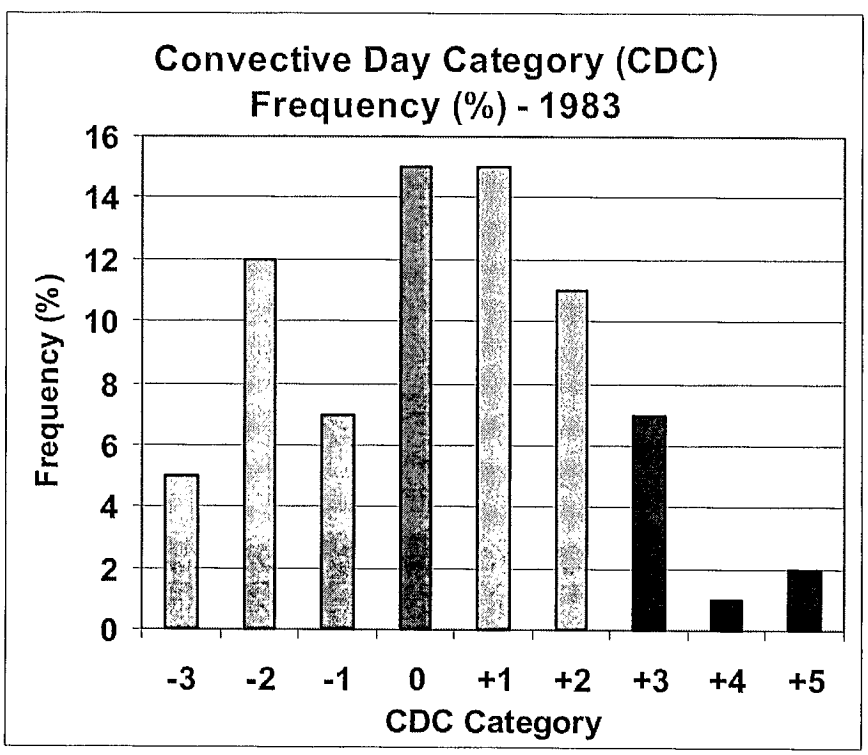
Convective Day Category (CDC)
Frequency (%) - 1983
Frequency (%)
16
14
12
10
8
6
4
2
0
-3
-2
-1
0
+1
+2
+3
+4
+5
CDC Category

1982		Forecast Convective Day Category									
		-3	-2	-1	0	+1	+2	+3	+4	+5	Totals
Observed	-3	1	0	4	0	0	0	0	0	0	5
	-2	2	1	0	1	0	0	0	0	0	4
Convective	-1	1	0	4	1	2	0	0	0	0	8
	0	1	1	4	6	5	4	1	1	0	23
Day	+1	0	1	2	0	5	4	1	0	0	13
	+2	0	0	2	2	4	3	2	0	0	13
Category	+3	0	0	0	0	1	3	4	0	0	8
	+4	0	0	0	1	0	1	1	0	0	3
(CDC)	+5	0	0	0	0	0	1	0	1	0	2
	Totals	5	3	16	11	17	16	9	2	0	79

Forecast Category Accuracy:

Correct Category:	24 days	30.4 %
Correct within one Category:	51 days	64.6 %
Correct within two Categories:	71 days	89.9 %

OBSERVED	19 82	Forecast	
		NO HAIL	HAIL
	NO HAIL	27	13
	HAIL	8	31

HAIL/NO-HAIL Accuracy:

No. hail days in period:	39 days	49.4 %
No. 'severe' hail days in period:	13 days	16.5 %
Correct HAIL days forecast:	31 days	79.5 %
Correct NO HAIL days forecast:	27 days	67.5 %

1983		Forecast Convective Day Category									
		-3	-2	-1	0	+1	+2	+3	+4	+5	Totals
Observed	-3	2	2	1	0	0	0	0	0	0	5
	-2	0	7	2	1	1	1	0	0	0	12
Convective	-1	1	1	1	1	2	1	0	0	0	7
	0	1	1	4	4	1	3	1	0	0	15
Day	+1	0	1	1	4	4	3	1	1	0	15
	+2	0	0	2	0	3	2	2	1	1	11
Category	+3	0	0	0	1	1	2	2	1	0	7
	+4	0	0	0	1	0	0	0	0	0	1
(CDC)	+5	0	0	0	0	1	0	1	0	0	2
	Totals	4	12	11	12	13	12	7	3	1	75

Forecast Category Accuracy:

Correct Category:	22 days	29.3 %
Correct within one Category:	48 days	64.0 %
Correct within two Categories:	62 days	82.7 %

OBSERVED	19 83	Forecast	
		NO HAIL	HAIL
	NO HAIL	29	10
	HAIL	10	26

HAIL/NO-HAIL Accuracy:

No. hail days in period:	36 days	48.0 %
No. 'severe' hail days in period:	10 days	13.3 %
Correct HAIL days forecast:	26 days	72.2 %
Correct NO HAIL days forecast:	29 days	74.4 %

1984		Forecast Convective Day Category									
		-3	-2	-1	0	+1	+2	+3	+4	+5	Totals
Observed	-3	3	5	1	0	0	0	0	0	0	9
	-2	3	2	4	3	0	1	0	0	0	13
Convective	-1	0	2	3	2	0	0	0	0	0	7
	0	0	1	5	3	1	2	0	0	0	12
Day	+1	1	0	0	3	3	2	2	0	0	11
	+2	0	1	0	1	3	4	2	0	1	12
Category	+3	0	0	0	0	2	2	0	0	0	4
	+4	0	0	0	1	0	0	3	0	0	4
(CDC)	+5	0	0	0	0	0	1	0	0	0	1
	Totals	7	11	13	13	9	12	7	0	1	73

Forecast Category Accuracy:

Correct Category:	18 days	24.7 %
Correct within one Category:	55 days	75.3 %
Correct within two Categories:	67 days	91.8 %

OBSERVED	19 84	Forecast	
		NO HAIL	HAIL
	NO HAIL	37	4
	HAIL	7	25

HAIL/NO-HAIL Accuracy:

No. hail days in period:	32 days	43.8 %
No. 'severe' hail days in period:	9 days	12.3 %
Correct HAIL days forecast:	25 days	78.1 %
Correct NO HAIL days forecast:	37 days	90.2 %

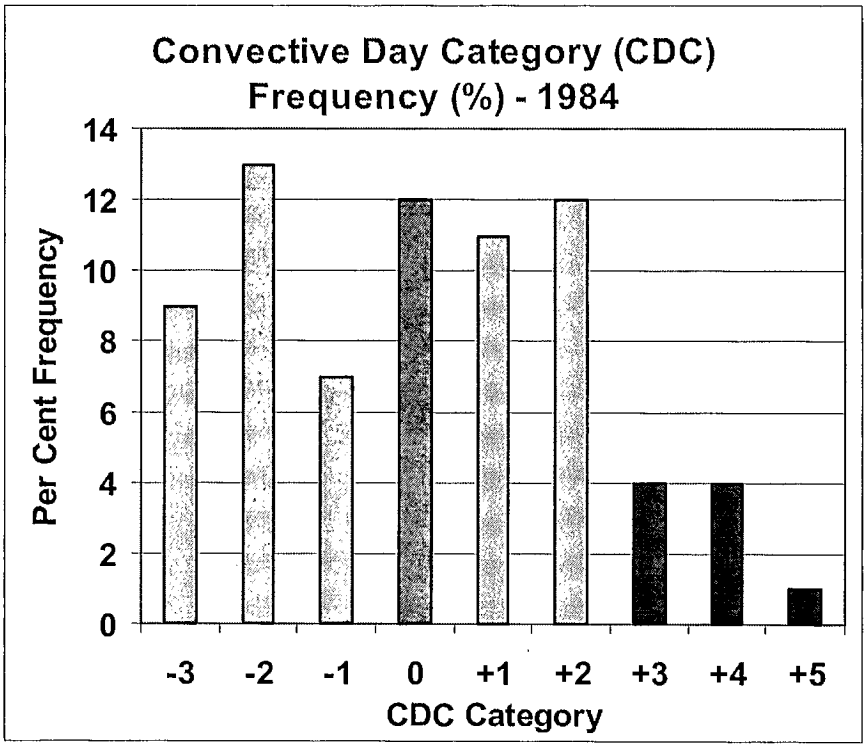
Convective Day Category (CDC)
Frequency (%) - 1984
Per Cent Frequency
14
12
10
8
6
4
2
0
-3
-2
-1
0
+1
+2
+3
+4
+5
CDC Category

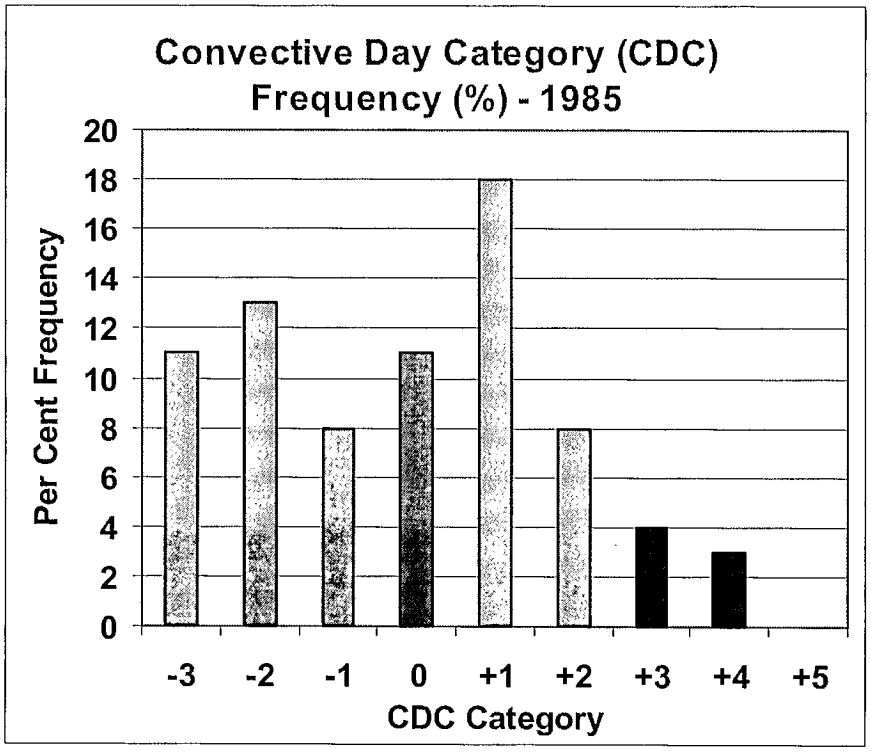
Convective Day Category (CDC)
Frequency (%) - 1985
Per Cent Frequency
20
18
16
14
12
10
8
6
4
2
0
-3
-2
-1
0
+1
+2
+3
+4
+5
CDC Category

1985		Forecast Convective Day Category									
		-3	-2	-1	0	+1	+2	+3	+4	+5	Totals
Observed	-3	5	1	2	1	1	1	0	0	0	11
	-2	3	3	0	3	3	1	0	0	0	13
Convective	-1	0	1	1	3	3	0	0	0	0	8
	0	1	1	3	4	1	0	1	0	0	11
Day	+1	0	1	1	7	4	4	0	1	0	18
	+2	0	0	0	3	3	2	0	0	0	8
Category	+3	0	0	0	1	1	2	0	0	0	4
	+4	0	0	0	0	0	0	2	0	1	3
(CDC)	+5	0	0	0	0	0	0	0	0	0	0
	Totals	9	7	7	22	16	10	3	1	1	76

Forecast Category Accuracy:

Correct Category:	19 days	25.0 %
Correct within one Category:	50 days	65.8 %
Correct within two Categories:	64 days	84.2 %

OBSERVED	19 85	Forecast	
		NO HAIL	HAIL
	NO HAIL	32	11
	HAIL	13	20

HAIL/NO-HAIL Accuracy:

No. hail days in period:	33 days	43.4 %
No. 'severe' hail days in period:	7 days	9.2 %
Correct HAIL days forecast:	20 days	60.6 %
Correct NO HAIL days forecast:	32 days	74.4 %

Appendix C – Non-Research Issues

Following the literature review, some new data analyses (of LIMEX-85 data and of the Pine Lake Tornado storm in Sections 5.0 and 6.0), and consultations with forecasting and research experts, we can highlight some non-research issues resulting from this review. However, *forecast accuracy* is not an issue. *Forecast and warning dissemination* from the source (the forecast office) is not an issue. The real issues are:

1. Providing the forecaster with the latest results of research, and upgrade training to enable him/her to use these results effectively;
2. Providing the forecaster with the best possible datasets from which to assimilate forecasts;
3. Providing the forecaster with the best possible NWP support;
4. Providing the forecaster with the best possible data assimilation, analysis, and display systems; these are simply replacements for what used to be essential human technical support and expertise;
5. Promoting effective media and public education to ensure awareness of the potential risk to life and property of severe storms, and how to make efficient use of forecast information; and
6. Partnering with communications technology experts to ensure the most efficient means of disseminating forecast and warning information to its objective *once it leaves the source.*

These issues have all been addressed in this report to varying degrees, and, we hasten to add, it is clear that all have been addressed to some degree by MSC. However, there is *always* room for improvement on all issues. We are certainly qualified to address issue number one above, since this appears to be one of the first bottlenecks. It was found that research on prairie convective processes are a minimal effort carried out by a very few individuals with very minimal funding, the result being no collective strength in the efforts. Because the quantities of researchers and available funds are small, all such research of the past 15 years haves been individual efforts without any coordinated infrastructure or network. This situation has steadily deteriorated ever since the demise of the Alberta Hail Project following their 1985 field season, and is still on that downward trend. We therefore proposed a *Prairie Convective Processes Network* as one means of addressing this situation in the presence of no new funding at the moment. However, we are hopeful that a collaborative group as proposed might have enough combined strength to attract new funding sources. A key part of this is to develop a research data archive with relatively easy access.

20 October 2000.